

**GROUNDWATER MODELLING AROUND
WETLAND PATCHES IN
GURUPURA SUB-BASIN, KARNATAKA,
INDIA**

Thesis

Submitted in partial fulfillment of the requirement for the degree of

DOCTOR OF PHILOSOPHY

by

SUBRAHMANYA KUNDAPURA

Under the guidance of

Dr. AMAI MAHESHA

Professor



**DEPARTMENT OF APPLIED MECHANICS AND
HYDRAULICS**

**NATIONAL INSTITUTE OF TECHNOLOGY KARNATAKA
SURATHKAL, MANGALURU- 575 025**

JUNE 2017

D E C L A R A T I O N

By the Ph.D. Research Scholar

I hereby *declare* that the Research Thesis entitled **“GROUNDWATER MODELLING AROUND WETLAND PATCHES IN GURUPURA SUB-BASIN, KARNATAKA, INDIA”**, which is being submitted to the **National Institute of Technology Karnataka, Surathkal** in partial fulfilment of the requirements for the award of the **Degree of Doctor of Philosophy in Applied Mechanics and Hydraulics Department** is a *bonafide report of the research work* carried out by me. The material contained in this Research synopsis has not been submitted to any University or Institution for the award of any degree.

100525AM10P05, SUBRAHMANYA KUNDAPURA

Department of Applied Mechanics and Hydraulics
National Institute of Technology Karnataka, India

Place: NITK-Surathkal
Date : 31-05-2017

C E R T I F I C A T E

This is to *certify* that the Research Thesis entitled “**GROUNDWATER MODELLING AROUND WETLAND PATCHES IN GURUPURA SUB-BASIN, KARNATAKA, INDIA**”, submitted by **SUBRAHMANYA KUNDAPURA** (Register Number:100525AM10P05) as the record of the research work carried out by him, is *accepted as the Research synopsis submission* in partial fulfilment of the requirements for the award of degree of **Doctor of Philosophy**.

Dr. AMAI MAHESHA

Professor

Research Guide

(Name and Signature with Date and Seal)

Chairman - DRPC

(Signature with Date and Seal)

Department of Applied Mechanics and Hydraulics
National Institute of Technology Karnataka, India.

ACKNOWLEDGEMENTS

I express my deep sense of gratitude to my supervisor, Dr. A Mahesha, Professor, Department of Applied Mechanics and Hydraulics, NITK for his kind help and valuable suggestions provided, throughout my research work. I also thank him for his in-time assessment and expert guidance in preparing the thesis and technical papers.

I thank the anonymous referees, both Foreign and Indian, for evaluating my thesis.

I am grateful to Research Progress Assessment Committee members, Prof. H. Suresh Hebbar and Prof. Arkal Vittal Hegde, for their critical evaluation and useful suggestions during the progress of the work.

My sincere thanks to anonymous members of my Doctoral Thesis Assessment Committee.

I thank the Director of the NITK, Surathkal, Prof. K. N. Lokesh, for granting me the permission to use the institutional infrastructure facilities, for the research work.

I am greatly indebted to Prof. Katta Venakataramana, Dean Academic, NITK, for his constant support and encouragement.

I sincerely thank all my colleagues from Department of Applied Mechanics and Hydraulics, for the help rendered throughout my research work.

I thank all the non-teaching staff of Department of Applied Mechanics and Hydraulics for their help.

I sincerely acknowledge the assistance offered by technical support staff at support@aquaveo.com regarding the GMS software. I also thank Mr. S.K. Chaurasia, Mr. Sachin M. Patil, from Aditi Infotech, Nagpur for their timely help and service, while working with the GMS software.

I wish to thank the reviewers of technical papers, for the valuable and expert suggestions, which helped me in improving the presentation of my research findings.

Special thanks to my wife Sumitra Subrahmanya, for her moral support. Thanks to my sons Master Ashray and Master Akshay, for their love and care.

My heartfelt thanks to Dr. Pruthviraj U., for his timely help and support.

I thank Shri. Balakrishna for helping me during my research work.

I thank Dr. Amba Shetty for providing me constant support.

I am grateful to Dr. K. Vadivuchezhian, for his spiritual support, encouragement and enthusiasm provided throughout my research work.

Thanks for the blessings of my parents from heaven.

Finally, thanks to the almighty God for blessing me with good health and ability to work.

Subrahmanya Kundapura

ABSTRACT

Numerical groundwater flow models solve the distribution of hydraulic head and describe flow whereas numerical transport models solve the distribution of solute concentration due to advection, dispersion and chemical reactions. In the present study an attempt is made to formulate groundwater flow and transport modelling in and around wetlands of Gurupura basin in Karnataka state of India. The study intended to simulate the response of an unconfined, shallow, tropical coastal aquifer comprising of wetlands using SEAWAT. The numerical simulation of groundwater flow was carried out by building a MODFLOW model of the basin and the transport parameters are assigned to execute the MT3DMS model. Finally, the SEAWAT model which is a coupled version of MODFLOW and MT3DMS designed to simulate three dimensional, variability density groundwater flow and multi-species transport, is developed. The model is calibrated from August 2011 to August 2013 using observed groundwater heads and TDS data obtained from 27 observation wells. The data from VES (Vertical Electrical Sounding) and pumping tests conducted in the study area are used for aquifer characterization. The model is validated for 2013-2015. The model performance is encouraging except for monsoon months (June to September), while evaluating with three techniques R^2 , RMSE and NSE. Overall, the model performance is satisfactory with $NSE \geq 0.5$. The spatial distribution of simulated groundwater map shows presence of groundwater at a higher level in the areas around wetlands in the study area, even during peak summer months (April and May). The sensitivity analysis conducted shows that the aquifer is sensitive to specific yield, hydraulic conductivity and recharge rate. The simulations of solute transport model reveals the presence of TDS concentrations in and around the wetland regions during winter and summer seasons, but within safe range. The groundwater budget was estimated for the aquifer using groundwater mass balance simulation package 'ZONEBUDGET'. This analysis shows that during the period of maximum potential position (August), the component of groundwater contributing to wetland is 4.5% of total outflow. During dry season with minimum potential head, the groundwater contribution to wetland is 1.4% of total outflow. Rest of the outflow contributes to river discharge and pumping of wells. Hence, the presence of water in the wetland during the non-monsoon months is established by the contribution of only groundwater, in the study area. The prognostic simulations conducted for 20 years period (2015-2035) confirms the safety of aquifer, both from quantity and quality perspective.

Keywords: SEAWAT, MODFLOW, Solute transport, Groundwater modelling, Freshwater, Aquifer characterization.

CONTENTS

ABSTRACT	i
CONTENTS	ii
LIST OF FIGURES	v
LIST OF TABLES	viii
CHAPTER 1 INTRODUCTION	1
1.1 General	1
1.2 Wetlands	3
1.3 Wetlands and Groundwater Interaction	5
1.4 Groundwater Modelling	6
1.5 Scope of the work	8
1.6 Research Objectives	10
1.7 Overview of the Groundwater Modelling Methodology Adopted	10
1.8 Organization of the Thesis	12
CHAPTER 2 LITERATURE REVIEW	13
2.1 General	13
2.2 Characterization of Aquifer	13
2.3 Groundwater Modelling	15
2.4 Groundwater Flow Modelling and Wetland Environment	15
2.5 Solute Transport Model	21
2.5.1 General	21
2.5.2 The numerical transport models	22
2.6 Literature Gap	29
CHAPTER 3 THE STUDY AREA AND AQUIFER CHARACTERIZATION	30
3.1 General	30
3.2 Features of The Study Area	32
3.2.1 Topography	32
3.2.2 Climate	34
3.2.3 Soil	34
3.2.4 Land use and land cover of the Study Area	36
3.3 Hydrogeology of the Study Area	38
3.3.1 Bore - log information	38
3.3.2 Lithology map	38
3.3.3 Vertical Electrical Sounding (VES)	40
3.4 Pumping Tests	43
3.4.1 General	43
3.4.2 Pumping Test methodology	44
3.4.3 Analysis of pumping test data	50

3.4.4	Results and discussion	55
3.4.5	Evaluation of aquifer parameters	57
3.5	Closure	59
	CHAPTER 4 GROUNDWATER FLOW MODELLING	60
4.1	General	60
4.2	Program Structure	61
4.3	Governing Equation	64
4.4	Modelling Approach	67
4.4.1	Data	67
4.4.2	Discretization of the basin	67
4.4.3	Hydrologic sources and sinks	68
4.4.4	Boundary conditions	71
4.4.5	Initial conditions	73
4.5	Model Calibration	74
4.5.1	Groundwater levels using observation wells	75
4.5.2	Steady state calibration	83
4.5.3	Transient calibration	85
4.6	Validation of Flow Model	96
4.7	Application of Flow Model	97
4.7.1	The water balance	97
4.8	Sensitivity Analysis	100
4.8.1	General	100
4.8.2	Methodology of Sensitivity Analysis	100
4.8.3	Results and discussion	101
4.9	Closure	105
	CHAPTER 5 SOLUTE TRANSPORT MODELLING	107
5.1	General	107
5.2	Basic Principles and Concepts of SEAWAT	108
5.2.1	Description of the Model	108
5.2.2	The SEAWAT Program Structure	110
5.2.3	Equivalent fresh water head concept	111
5.2.4	The Governing Equation	113
5.3	Application to the Study Area	115
5.3.1	General	115
5.3.2	The Boundary Conditions	115
5.3.3	The Initial Conditions	116
5.3.4	Density and Transport Parameters	116
5.4	Model Calibration	117
5.4.1	Calibration of flow parameters	117
5.4.2	Calibration of Transport Parameters	120
5.4.3	Transient Calibration	120
5.5	Validation of SEAWAT Model	129
5.6	Sensitivity Analysis of Solute Transport Model	134
5.7	Closure	138

CHAPTER 6 PROGNOSTIC SIMULATIONS	140
6.1 General	140
6.2 Description of Different Scenarios	141
6.3 Results and Discussion	142
6.3.1 Spatial effect on the aquifer	142
6.3.2 The temporal effects of scenario on the aquifer	154
6.5 Closure	161
CHAPTER 7 SUMMARY AND CONCLUSIONS	162
REFERENCES	168
APPENDIX	198
PUBLICATIONS	223
BIODATA	224

LIST OF FIGURES

Figure 1.1 Functions of Wetland	3
Figure 1.2 Freshwater wetland	4
Figure 1.1 Flowchart of Methodology	11
Figure 3.1 Location of the Study Area	31
Figure 3.2 Topography of the Study Area	33
Figure 3.3 Monthly rainfall observed at Meteorological Office	34
Figure 3.4 Soil map of the study area	35
Figure 3.5 Land Use / Land Cover map of the study area	37
Figure 3.6 Bore log details	38
Figure 3.7 Lithology map of the study area	39
Figure 3.8 VES locations in the study area	41
Figure 3.9 Snap shots of conduct of VES survey in the study area	42
Figure 3.10 Aquifer profile as per VES	43
Figure 3.11 Locations of Pumping Test Wells	44
Figure 3.12 Photograph of pumping well no. 4	45
Figure 3.13 Photograph of pumping well no. 5	45
Figure 3.14 Photograph of pumping well no. 6	45
Figure 3.15 (a) Measurements for determining the discharge with horizontal pipe	46
Figure 3.15 (b) Measurements for determining the discharge with inclined pipe	47
Figure 3.16 Curves for determining C and F for estimation of flow through inclined and horizontal pipes	48
Figure 3.17 Type curves for fully penetrating wells (Neuman, 1975)	53
Figure 3.18 Graph of drawdown, recovery versus time for pumping well no. 6	56
Figure 3.19 Time–drawdown graph of well no. 6 by Neuman(1974) method	57
Figure 3.20 Aquifer property zonation map	58
Figure 4.1 Flow chart for the program structure of MODFLOW	62
Figure 4.2 Finite difference grid (Harbaugh et al., 2000)	66
Figure 4.3 Village map of study area	71
Figure 4.4 Dirichlet boundary condition applied to study area	72
Figure 4.5 Neumann boundary condition applied to the study area.	73
Figure 4.6 The study area with well numberings	77
Figure 4.7.a Photographs of well no. 1 to well no. 8	78
Figure 4.7.b Photographs of well no. 9 to well no. 16	79
Figure 4.7.c Photographs of well no. 10 to well no. 24	80
Figure 4.7.d Photographs of well no. 25 to well no. 31	81
Figure 4.8 Scatter plot for steady state calibration	84
Figure 4.9 Scatter plots of Simulated and observed groundwater heads	86
Figure 4.10 a Simulated and observed groundwater heads during the calibration	87
Figure 4.10 b Simulated and observed groundwater heads during the calibration	88
Figure 4.11 Groundwater flow contours for November 2012	90

Figure 4.12 Groundwater flow contours for December 2012	91
Figure 4.13 Groundwater flow contours for January 2013	92
Figure 4.14 Groundwater flow contours for February 2013	93
Figure 4.15 Groundwater flow contours for March 2013	94
Figure 4.16 Groundwater flow contours for April 2013	95
Figure 4.17 Groundwater flow contours for May 2013	96
Figure 4.18 Scatter plots of simulated and observed groundwater heads	97
Figure 4.19 Schematic representation of water budget of the aquifer	99
Figure 5.1 Flow chart of SEAWAT module (Guo and Langevin, 2002)	111
Figure 5.2 Concept of equivalent freshwater head (Guo and Langevin, 2002)	112
Figure 5.3 MODFLOW Simulated groundwater heads at the end of transient calibration.	118
Figure 5.4 SEAWAT Simulated groundwater heads at the end of transient calibration	119
Figure 5.5 Simulated and observed TDS values (2011-13) during (A) monsoon and (B) post-monsoon respectively.	122
Figure 5.5 Simulated and observed TDS values (2011-13) during (C) winter and (D) summer respectively.	122
Figure 5.6 Simulated TDS distribution for Year 2012 (July – September)	123
Figure 5.7 Simulated TDS distribution for Year 2012 (October – November)	124
Figure 5.8 Simulated TDS distribution for December 2012– March 2013	125
Figure 5.9 Simulated TDS distribution for Year 2013 (April – June)	126
Figure 5.10 The EPA, USPHS and AWWA recommended TDS limits for classes of water	128
Figure 5.11 Specific Predictive Trend Analyser for TDS by SEAWAT	128
Figure 5.12 Scatter plots of simulated and observed TDS values (2013-15) for seasons (A) monsoon (B) post-monsoon respectively	130
Figure 5.12 Scatter plots of simulated and observed TDS values (2013-15) for seasons (C) winter (D) summer respectively	130
Figure 5.13 Validated TDS distribution for Year 2014 (July – September)	131
Figure 5.14 Validated TDS distribution for Year 2014 (October – November)	132
Figure 5.15 Validated TDS distribution for December 2014 – March 2105	133
Figure 5.16 Validated TDS distribution for Year 2015 (April – June)	134
Figure 5.17 (A) Spatial distribution of TDS concentration as simulated by SEAWAT during the year 2013 for increase of the longitudinal dispersivity by 25%	136
Figure 5.17 (B) Spatial distribution of TDS concentration as simulated by SEAWAT during the year 2013 for increase of the longitudinal dispersivity by 50%	137
Figure 5.17 (C) Spatial distribution of TDS concentration as simulated by SEAWAT during the year 2013 for increase of the longitudinal dispersivity by 75%	138

Figure 6.1 Spatial distribution of groundwater table for (A) Scenario 1	145
Figure 6.1 Spatial distribution of groundwater table for (B) Scenario 2 by the end of 20 year simulation (Year 2035)	146
Figure 6.1 Spatial distribution of groundwater table for (C) Scenario 3 (Case 3) by the end of 20 year simulation (Year 2035)	147
Figure 6.1 Spatial distribution of groundwater table for (D) Scenario 4 (Case 3) by the end of 20 year simulation (Year 2035)	148
Figure 6.2 Spatial distribution of TDS for (A) Scenario 1	151
Figure 6.2 Spatial distribution of TDS for (B) Scenario 2	152
Figure 6.2 Spatial distribution of TDS for Scenario 3 (Case 3)	153
Figure 6.2 Spatial distribution of TDS for (D) Scenario 4 (Case 3)	154
Figure 6.3 Location for studying temporal effects of various scenarios	155
Figure 6.4 Status of Groundwater table over 20 year period during the month of May.	157
Figure 6.5 Status of Groundwater table over 20 year period during the month of September.	158
Figure 6.6 Status of TDS over 20 year period.	159

LIST OF TABLES

Table 3.1 Soil type and Description	36
Table 3.2 Details of the pumping wells	46
Table. 3.3 Range of initial aquifer parameters	58
Table. 4.1 The MODFLOW packages used for simulation of groundwater flow	63
Table 4.2 Availability of water level and TDS data in the study area	67
Table 4.3 Spatial discretization of basin model.	68
Table 4.4. Village-wise details of pumping rates	70
Table 4.5 Details of observation wells in the study area	82
Table. 4.6 Optimal parameter values obtained after seasonal calibration	85
Table. 4.7 The calibrated aquifer parameters obtained for different zones	85
Table 4.8 Monthly model efficiency values for flow model during 2011-13	86
Table.4.9 Groundwater flow model performance during the period 2013-15	97
Table 4.10 Aquifer volumetric groundwater budget	99
Table 4.11 Sensitivity Index (SI) and Nature of Class (Lenhart et al., 2002)	101
Table 4.12 Sensitivity classification of wells for specific yield	102
Table 4.13 Sensitivity classification of wells for hydraulic conductivity	103
Table 4.14 Sensitivity classification of wells for recharge rate	104
Table. 5.1 The MT3DMS packages used for solute transport modelling	109
Table 5.2 Calibrated Solute Transport Parameters	120
Table 5.3 Monthly SEAWAT Efficiency Values during 2013-2015	121
Table 5.4 Groundwater solute transport model performance during the period 2013-15	129
Table 6.1 Groundwater table elevation (with respect to mean sea level) during end of simulation year (2035)	144
Table 6.2 TDS distribution (mg/ltr) for end of simulation year (2035)	149

CHAPTER 1

INTRODUCTION

1.1 GENERAL

Water demand for industrial, agricultural and domestic uses is continuously increasing and freshwater resources are shrinking. Against this backdrop, groundwater management has become critical issue for current and future generations. Ground water systems are affected by natural processes and human activity, and require targeted and ongoing management to maintain the condition of ground water resources within acceptable limits, while providing desired economic and social benefits. Ground water management and policy decisions must be based on knowledge of the past and present behaviour of the ground water system, the likely response to future changes and the understanding of the uncertainty in those responses. The location, timing and magnitude of hydrologic responses of groundwater systems to natural or human-induced events depend on a wide range of factors such as, the nature and duration of the event that is impacting ground water, the subsurface properties and the connection with surface water features such as rivers, oceans and presence of wetlands.

About one-third of the world's freshwater consumption is met by groundwater. However, overdraft is affecting the natural recharge-discharge equilibrium and resulting in declining groundwater levels leading to freshwater scarcity, contamination, saltwater intrusion and land subsidence. The World Health Organisation (WHO) guidelines for drinking water quality suggests 1% of seawater (approximately 250 mg/ltr), renders freshwater unsuitable for drinking purpose (Adrian et al., 2012). If the current trend continues, it is estimated that by 2025 about two-thirds of global population will face moderate to severe water stress. The Ministry of Water Resources, Government of India opines that, the groundwater level in the 16 states of India has

dropped to more than 4 m during the 1981–2000 period. The state of Karnataka is one among those. In order to avoid such consequences of overdraft, it is important to understand the behaviour of an aquifer system subjected to artificial interventions.

The quality and quantity of groundwater in the coastal regions is of greater concern because of the fact that more than 60% of the world population lives within 30 km stretch of shorelines. In India, about 20% (205 million people) of the population lives along coastal region (INCCA, 2010). The coastal groundwater systems are sensitive to impacts such as reduced recharge, contamination from natural and manmade sources and over-exploitation (Essink, 2001). The coastal regions are often densely populated, especially the river deltas, where good soil and abundant water availability have been able to support large inhabitations (Volker, 1983). It is observed that, exploitation of groundwater has resulted in saltwater intrusion, among places up to a distance of 15 km inland (Geyh and Soefner, 1996). Hence, there is a fair possibility that, this may even affect the aquifer system existing in the close proximity of the affected areas.

The groundwater quality degradation by salinization is the most serious threat to coastal fresh groundwater resources, which constitute a major part of supply for human usage in the coastal areas (Custodio and Galofre, 1992). Saltwater intrusion occurs in many of the coastal aquifers around the globe (Amer, 1995) due to over-exploitation of groundwater. The salt water intrusion occurs when the hydrostatic balance that exists between the saline water and freshwater along the coastal tract is disturbed due to various reasons such as overdraft, land reclamation, climate changes, sea level rise etc. The phenomenon may lead to entire coastal aquifer system being subjected to continuous threat of saline contamination. This can significantly disturb the quality of fresh groundwater over a long term and may affect the use of groundwater for drinking and agricultural use. A good understanding of the coastal dynamics and detailed knowledge of the variability of their parameters is necessary to carryout studies on coastal aquifers (Carrera et al., 2010). This also draws major attention of researchers to manage quality concerns of coastal aquifers.

1.2 WETLANDS

Wetlands can be defined as the areas of marsh, fen, peat land or water. The water present in the wetland ecosystems can be static or flowing, permanent or temporary. Wetlands, being a substantial component of regional ecosystems, have many functional services. They have the dual capacity of being the water providers and water users. The functions that a wetland serves is shown in figure 1.1

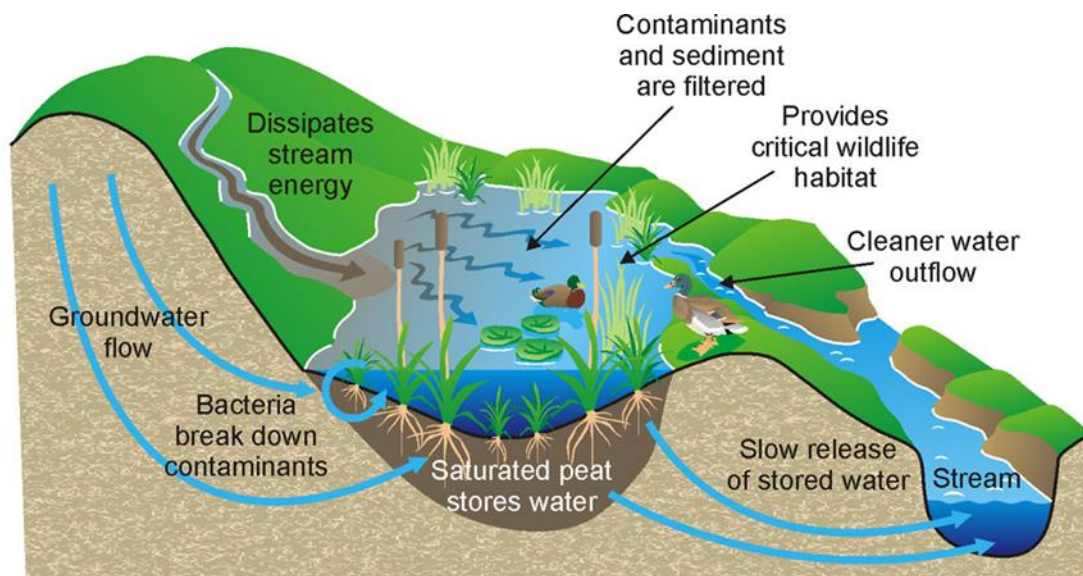


Figure 1.1 Functions of Wetland (Courtesy: <https://sandrp.wordpress.com>)

Globalization has prevented rural communities from developing trading initiatives to market wetland products. Promoting sustainable trade in wetland products is a way to alleviate poverty and conserve wetland. The hydrologic and hydraulic characteristics of a wetland influence all wetland functions and consequently should be an initial focus of a wetland evaluation. Water is introduced to a wetland through direct precipitation, overland flow, channel and overbank flow, groundwater discharge and tidal flow. Temporary storage includes channel, overbank, basin and groundwater recharge. Groundwater table is very important for wetland as this differentiates wetland from a dry land. For a wetland to be called so, the groundwater table should remain very close to the surface, unlike dry land where the ground water table is deep below the surface.

Wetlands have gained greater importance in the last two decades, since they have an important impact on water supply and water quality control. Treatment wetlands have

recently been used as a best management practice to decrease the storm water runoff peaks and to improve storm water runoff water quality. Therefore, efforts have been made toward a better understanding of both wetland hydrology and wetland water quality. A typical location of a fresh water wetland is shown in figure 1.2

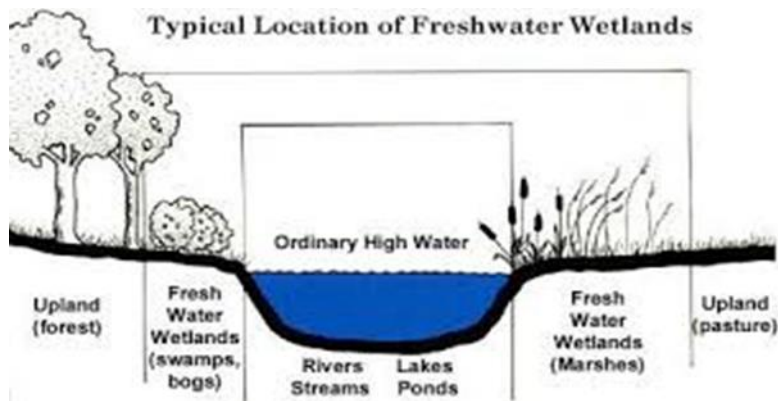


Figure 1.2 Freshwater wetland (Courtesy: <http://more-sky.net/word/plants-in-wetlands>)

There are many definitions of wetlands and their main difference is the broadness. According to the Ramsar Convention, wetlands are defined as, “areas of marsh, fen, peat land or water, whether natural or artificial, permanent or temporary, with water that is static or flowing, fresh, brackish or salt, including areas of marine water, the depth of which at low tide does not exceed six meters”. Wetland includes both riparian and coastal zones and islands or marine water bodies deeper than six meters, lying within the wetlands at low tide. As per the Ramsar Convention definition, most of the natural water bodies (such as rivers, lakes, coastal lagoons, mangroves, peat land, coral reefs) and man-made wetlands (such as ponds, farm ponds, irrigated fields, sacred groves, salt pans, reservoirs, gravel pits, sewage farms and canals) in India, constitute the wetland ecosystem. Only 26 of these numerous wetlands have been designated as Ramsar Sites (Jaimini Sarkar, 2011). However, many other wetlands which perform potentially valuable functions are continued to be ignored in the policy process. As a result many freshwater wetlands ecosystems are threatened and many are already degraded and lost due to urbanization, population growth, and increased economic activities.

Wetlands exist as the interface between truly terrestrial ecosystems and aquatic system, making them inherently different from each other, yet highly dependent on both. Also surface/ground water interactions play an important role in wetlands. These processes affect the dynamics of wetland hydrology.

The present study is about the behaviour of groundwater around wetlands in the Gurupura sub-basin, which is getting destroyed due to human activities, urbanization, industrialization, extraction of groundwater etc. During pre-monsoon season i.e. January to May, as very less or no rainfall occurs, so the availability of surface water becomes a great problem in the region. At this period groundwater becomes one of the major source of fresh water. Over exploitation of the groundwater has been one of the major factors in this region. The decline in fresh water head due to ground water extraction has also resulted in salt water intrusion in the region. Therefore it is essential to make the optimal and effective utilization of the ground water in the region. Wetlands existing in the Gurupura sub-basin are also at a risk of depletion due to infrastructural development, sewage and solid waste disposal in recent years. Salinity also has a strong influence on wetland hydro-chemistry which is regulated by the interactions between surface and ground water influenced by human activity. In order to implement suitable management strategies, study on behaviour of groundwater around wetlands are to be carried out effectively.

1.3 WETLANDS AND GROUNDWATER INTERACTION

Wetlands are found in flat vegetated areas, lakes and along coastlines. Coastal and estuarine wetlands receive water from precipitation, surface runoff, tides and groundwater. Rapid population growth, pollution from pesticides and fertilizers and industrial effluent, all contribute to coastal water stress. Much of the coastal wetland loss is effectively irreversible particularly, where major urban and industrial development is in place (Hegde and Nyamathi, 2005).

Wetlands receiving inflow from groundwater are known as discharging wetlands because water flows or discharges from the groundwater to the wetland. The soil, groundwater level and the surface contour, affect the water storage capacity of the wetland. Wetlands generally occur in natural depressions in the landscape where

geologic or soil layers restrict drainage. The surface contours act to collect precipitation and runoff water and feed it to the depressed area. Groundwater recharge can take place if the soil is not already saturated and the surface contours of the basin hold the water in place long enough for it to percolate into the soil.

The groundwater flow in the vicinity of wetland and groundwater –wetland interaction requires considerable amount of expensive instrumentation and several years of monitoring. Alternatively, numerical models offer a cost effective and rapid means obtaining insight into groundwater-wetland interaction. Specific applications of numerical models include analysis of complex systems (geology, hydrology, geometry, boundary conditions etc.), quantifying groundwater-wetland mechanisms and processes occurring at a site, and assessing long-term impacts due to natural and human induced stresses (Crowe et al. 2004).

1.4 GROUNDWATER MODELLING

Groundwater models are powerful management and prediction tool which combines the appropriate physical laws in a self-consistent mathematical model with the available hydrogeological data, to understand the response to externally applied stress and its behavior and properties of the system. Numerical groundwater models are computer based representation of the characteristics of a real hydrogeological system that uses the laws of science and mathematics. Groundwater modeling in recent years has become one of the major part of many projects dealing with groundwater exploitation, remediation and protection. Groundwater models, which replicate the groundwater flow process at the region of interest, can be used to complement monitoring studies in evaluating and forecasting groundwater flow and transport. Nevertheless, reliable groundwater model is based on accurate field data and decent prior knowledge of the region. The groundwater models are used to integrate hydrogeological understanding with the available data and to develop a prognostic tool for evaluating groundwater systems, subject to assumptions and limitations. Hence, it is essential to interpret the results obtained from the groundwater model, understanding its limitations.

The mathematical model of groundwater system consists of differential equations developed from analyzing groundwater flow or solute transport in groundwater. These models are known to govern the physics of flow and transport in porous media.

Mathematical models of groundwater flow are being used since the late 19th century. The understanding, accuracy and reliability of model predictions depends on how well the model approximates the actual situation of the region under consideration. The field situation will usually be too complicated to be simulated exactly. Hence, simplifying assumption must be made in order to construct a model. Normally, the assumptions necessary to solve a mathematical model analytically are very restrictive. For instance, many analytical solutions are developed for homogeneous, isotropic, and infinite geological formations, where, flow is also steady state (hydraulic head and groundwater velocity do not change with time). In order to deal with the more realistic situations (e.g., heterogeneous and anisotropic aquifer, in which, groundwater flow is transient), the mathematical model is commonly solved approximately using numerical techniques.

In the cases where the complexities involved in the model make it difficult to solve the equations analytically, numerical methods become handy, where the domain of interest is discretized into distinctive cells. The numerical approximations of the governing partial differential equation leads to obtain the solution, in both the space and time.

The finite difference method and finite element methods are widely used numerical solution techniques in groundwater modelling. The approach in finite difference method, is to discretise the computational domain by rectangular or quadrilateral elements. The unknown value is defined at the nodes, which are placed at centre of the cells or at the intersection points of cell boundaries. The groundwater heads or concentrations are calculated at these nodes. The finite element model differs from the finite difference model by approximating the flow equation by integration rather than differentiation.

The difficulties involved in modelling density dependent groundwater flow and transport are overcome by computer modelling techniques. And also these models have emerged as an effective tool for understanding and investigating the groundwater hydrology of coastal aquifers in the recent years. Among the coastal aquifers, saltwater intrusion is one such subsurface flow and transport processes, which can be addressed to get amicable solutions, using the computer models.

1.5 SCOPE OF THE WORK

This coastal stretch of Karnataka state is developing with its industries, commercial complexes and academic institutions, at a faster rate. The Dakshina Kannada is one of the most industrialized districts in the coastal region of Karnataka. Information Technology (IT) sector is also gaining momentum in the district. The coastal region is considered as the largest centres for fisheries.

The economic survey of Karnataka 2010-11 highlights that, the Dakshina Kannada is recognised as the third largest contributor to the state's economy (4.6%). The coastal region of Karnataka state has population of 200 people / km² (INCCA, 2010). The prominent source of water supply is groundwater in the study area, accounting to about 40% of domestic and agricultural water use. The open wells are catering to these usages. The thrust would be on groundwater resources, even though the requirement is partially met by surface water supply, during periods of peak summer. The water demand of Mangaluru city in the year 2026 is estimated to be about 0.25 Million m³/day. The present supply level is less than 0.09 Mm³ per day and the demand has already exceeded to 0.1 Mm³ per day. This discrepancy is causing severe stress on the existing scenario of water supply system (Shetkar and Mahesha, 2011). In order to meet the demand, the thrust will be envisaged on groundwater sources by over-extraction. This would, in turn, attract saline contamination of groundwater, since the aquifer system is in the closer proximity of sea and presence of tidal rivers having backwater effects. The slump in the quantity and quality deterioration of groundwater, which is the only dependable source for domestic, irrigation and industrial purposes during the summer months, may have a great impact on human livelihood and the socio-economic status of dwellers, in the coastal stretch.

The annual rainfall received by the district is more than 3,900 mm. In spite of a good amount of rainfall, acute shortage of fresh water is experienced during the non-monsoon months from December to May. The major problem encountered due to this imbalance is salinity ingress into aquifers adjacent to coast and along the river courses, due to tidal effect. The Central Ground Water Board (2012) has predicted that the water draft for domestic and industrial uses, is set to increase sharply in Dakshina Kannada and availability of required draft for irrigation will decrease drastically by the year 2025. The report points out that, the consumption of groundwater by the district's households

and industries will register a 42 per cent increase. In specific terms, an increase from 3,792 ha.m., in 2004 to 5,370 ha.m. by 2025. The groundwater available for irrigation will decrease by more than 8,600 ha.m. or about 31 per cent. The district consumed 27,623 ha m of groundwater for irrigation in 2004, By 2025, this figure is expected lower further to 18,997 ha. m.

The city of Mangalore, which is the district headquarter of Dakshina Kannada district, is rapidly growing and expanding its limit due to population growth and industrialisation. The city is located between the two rivers, Netravathi in the south and Gurupura in the north. Many industries have come up on the northern side of river Gurupura, namely Mangalore refinery and Petrochemicals (MRPL), BASF (Baden Aniline and Soda Factory) etc. The International Airport is also situated in the vicinity. The land mass between the boundaries of these industries, airport and the northern bank of river Gurupura, is very fertile and consists of agricultural fields and wetlands.

The developmental activities are undergoing in tremendous amount in this part. These developmental activities are leading to loss of wetland ecosystem. Due to extensive pumping for industrial and agricultural activities, many wetlands may not remain the same any more especially, during the pre-monsoon season. This loss in wetland may lead to imbalance in the ecosystem of the region. Also, overexploitation of the available water resources for industrial, agricultural and domestic needs of the water for the region may lead to salt water intrusion into the freshwater aquifers.

It is important to mention here that river Gurupura has backwater effect during high tides and the tidal water is traveling up to 15km inland. Therefore, alternative supply and optimal pumping is inevitable for the sustainability of the groundwater system. To predict the future consequences on the groundwater system consisting of wetlands, due to overexploitation of groundwater in this region, a numerical model have been developed to represent the field scenario.

This model can simulate the future ground water level of the study region and also address the quality issues. So, that scientific assessments and reliable management strategies can be evolved to prevent the loss of wetlands and also to regain back the lost wetlands. The problem of groundwater modelling consisting of wetland systems is not attempted yet through numerical simulation, in coastal Dakshina Kannada district. A three dimensional variable density model SEAWAT Version 4 (Langevin et al., 2008)

is made use in the study to resolve the spatial and temporal variation of groundwater level and contaminant transport in the basin.

1.6 RESEARCH OBJECTIVES

The present investigation is intended to simulate the groundwater flow and contaminant transport in the study area which consists of wetland stretches, for the existing and anticipated future developments in the region. The simulation is proposed to be carried out using three-dimensional model SEAWAT, to identify the spatial and temporal distribution of the groundwater flow and contaminant. With this consideration, the objectives of the study are framed as follows:

1. To develop a representative three dimensional numerical groundwater flow and solute transport model using SEAWAT.
2. To apply the calibrated model to predict the groundwater flow dynamics considering future scenarios.
3. To simulate groundwater solute transport of the region for the present and future stress scenarios.
4. Sensitivity analysis of the hydrological stresses and aquifer parameters on groundwater flow and transport model.

1.7 OVERVIEW OF THE GROUNDWATER MODELLING METHODOLOGY ADOPTED

The conceptual modelling approach is used in the present work for the simulation which simplifies the field problem and stacks the required field data for better understanding of the behaviour of the aquifer system of the study area. The conceptual model is introduced into SEAWAT. Initially, the MODFLOW is executed, and then the transport parameters are introduced to execute a MT3DMS model. These models are combined with additional input of density parameters to execute the SEAWAT model. Sensitivity analysis is performed to learn the parameter importance in the model calibration. Besides, the calibration is performed using the observed water level and water quality data. The aquifer parameters are revised within the appropriate range to obtain better calibration results. The model is then validated to assess the model performance evaluation. The methodology adopted in the present research is shown in figure 1.3.

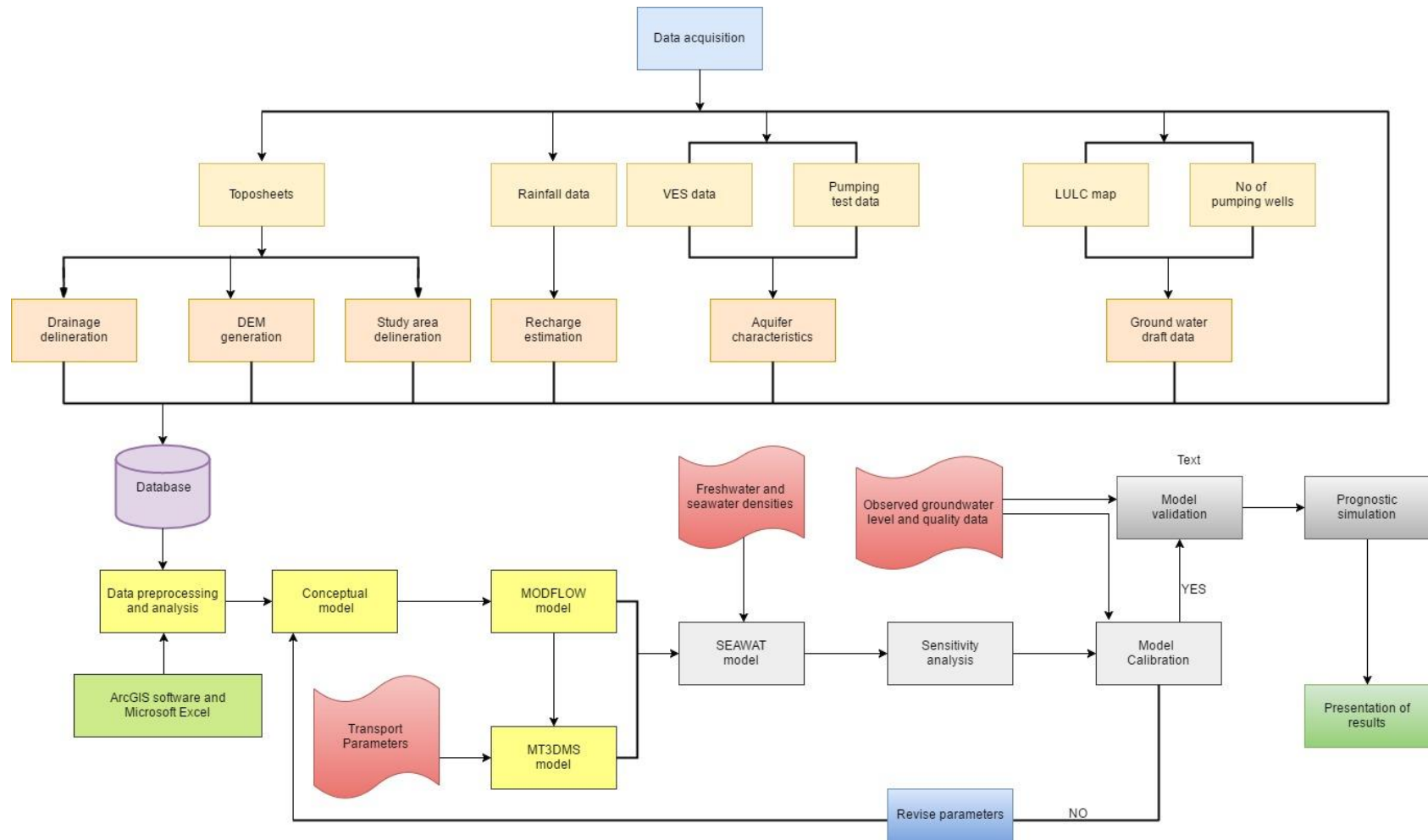


Figure 1.3 Flowchart of Methodology

1.8 ORGANIZATION OF THE THESIS

The thesis comprises of seven chapters, list of references and annexure. A brief description of the each chapter is presented here.

Chapter 1 provides an introduction to the problem and the objectives of the study, overview of the research methodology adopted and description of the study area.

Chapter 2 presents the literature review on the groundwater parameter estimation, groundwater flow and solute transport models.

Chapter 3 provides the detailed information of the study area and an insight on the various studies carried out to characterize the aquifer. The development of a groundwater flow model for the study area using MODLFOW, its applications and sensitivity analysis are detailed in **Chapter 4**.

Chapter 5 presents the investigations on solute transport model using SEAWAT, along with sensitivity analysis.

Chapter 6 illustrates the application of developed models for the region to simulate the impacts of future anticipated scenarios on groundwater development.

Finally, **Chapter 7** lists out the conclusions, limitations and scope for further research.

LITERATURE REVIEW

2.1 GENERAL

Groundwater flow models are very useful tools to assess the effect of human activities on groundwater dynamics (Xu et al., 2011) and to predict future scenarios. Over the years, many models have been developed to represent and study the problem of groundwater quantity and quality issues. They range from relatively simple analytical solutions to complex numerical models. Modelling of coastal groundwater systems is a challenging problem due to their highly dynamic boundary conditions and the coupling between the equations for groundwater flow and solute transport (Post, 2011). The characteristics of transition zones between freshwater and saltwater in coastal aquifers and the dynamics of their movements have been studied for several decades (Cooper et al., 1964 and Todd, 2005). The usefulness of digital computers have led to develop numerical algorithms and solution methods to solve the equations for variable-density groundwater flow and transport (Pinder and Cooper, 1970; Segol and Pinder, 1976).

2.2 CHARACTERIZATION OF AQUIFER

The capacity to hold water by an aquifer largely depends on the aquifer characteristics, namely transmissivity, hydraulic conductivity and storage co-efficient. In order to evaluate these parameters, pumping test is one of the methods used. Almost all the well hydraulics models are based on the assumption by Theis (1935) that the pumped well is a line source. This assumption proposed, may not be valid if the well bore storage effects are significant. The effects of well bore storage become important when the aquifer transmissivity and storage coefficient are small or the pumped well diameter is large. A semi-empirical, mathematical model capable of reproducing all three segments of the time drawdown curve in an unconfined aquifer was introduced by Boulton (1954, 1963). In this method, Boulton assumed that the amount of water released from storage

per unit horizontal area of the aquifer is the sum of volume of water instantaneously released and another volume of water, the release of which is delayed due to the aquifer characteristics. This method was later extended by Boulton (1970) and Boulton and Pontin (1971) to account for anisotropy and the effect of vertical flow components in the aquifer. The classical solutions developed by Boulton(1954), Dagan (1967) and Neuman (1972,1974) assume the pumped well to be infinitesimal in diameter. These solutions cannot be used to correctly interpret early time drawdown in pumped aquifer.

A solution that accounts for the finite diameter of the pumped well was developed by Kipp (1973). It was assumed that, the water to be incompressible and the porous matrix to be rigid. Boulton and Streltsova (1976) also have presented an analytical solution for flow to a partially penetrating large diameter well in an unconfined aquifer. The very complexity of the solution allows too many options to be selected for the curve matching process. There is no easily found unique solution. This method also requires relatively long pumping periods before a curve matching technique can be applied. Their solution allows for aquifer compressibility but, since the water table to be assumed as a constant head boundary, the effect of specific yield cannot be properly accounted.

The Neuman (1972, 1974) model when properly applied, can be used to estimate the most important water table aquifer parameters with reasonable accuracy (Moench,1995). But, accurate estimates of specific storage are often not possible with the Neuman (1974) model because they require use of early time drawdown data. Numerical models have been developed by several investigators to account for effects of a finite-diameter pumped well (Narasimhan and Zhu, 1993). Narasimhan and Zhu (1993) used the model developed, to demonstrate that, the effect of well storage in the pumped well can mask large parts of the early time and intermediate time responses as seen in Neuman's (1975) type curves. Singh (2006) proposed a simplified semi-analytical model for the drawdown due to pumping a large diameter and partially penetrated well which can take into account of pumping and recovery phases. The model yields transient drawdown in the well.

2.3 GROUNDWATER MODELLING

The recent challenge to water resource engineers is to maintain water quantity and quality of water in the aquifers against the effect of increasing demand, changing land use and weather, and long-term climate variability. The effects of these factors and water management decisions will be difficult to arrive at, because of the complex nature of a watershed hydrology. A computer model that is able to simulate possible scenarios and their effects on a watershed will be a useful management tool to investigate the watershed's sensitivity to change with respect to a variety of factors (Perkins and Sophocleous, 1999). Physically based numerical groundwater flow models are commonly used for refining hydro-geologic characterization and performing groundwater management decisions. The numerical flow models are powerful simulation tools because, they represent high spatial and temporal variability of aquifer properties and conditions inherent to natural systems (Coppola et al., 2005).

2.4 GROUNDWATER FLOW MODELLING AND WETLAND ENVIRONMENT

The groundwater flow modelling have become manageable by a number of commercial groundwater software with GIS (Geographical Information System) capabilities like Visual MODFLOW (Modular Flow model), GMS (Groundwater Modelling System), and Groundwater Vista etc. These models have been used to understand and manage various type of groundwater issues, such as groundwater resource management (Rejani et al., 2008; Kushwaha et al., 2009; Sudhir Kumar, 2011), simulation of the effect of subsurface barrier on groundwater flow (Senthilkumar and Elango, 2011), management of coastal aquifer system (Shammas et al., 2009), groundwater flow modeling (Ahmed and Umar, 2009), modeling flow and salt transport in a salinity threatened irrigated valley (Gates et al., 2002). Several investigators adopted different methods for groundwater flow and transport modelling in normal aquifers and in the aquifers of wetland region. Some of studies carried out are discussed here.

Bradley (1995) describes the application of a transient three-dimensional groundwater model to simulate water flux through a floodplain wetland, Narborough Bog, in Central England. A three-layer groundwater model for the wetland was developed using

MODFLOW considering some limitations. The accuracy of the model is then assessed by comparing daily model predictions of water-table response at specific monitoring points. A regional groundwater flow model (MODFLOW) was developed by Dufresne and Drake (1999) using existing hydro-geologic data from state and federal agencies in order to simulate the existing hydrologic conditions of a karst area, in Lake City Florida, USA and to predict withdrawal impacts. The model was calibrated by matching potentiometric surface maps and spring flows to within reasonable ranges. The drawdowns in the Floridian and surficial aquifers predicted by the model showed minimal impacts to existing legal users and only a 5% reduction in the flow at 21km away in the Ichetucknee Springs, Florida, USA.

Abdulla et al. (2000) applied three dimensional MODFLOW to simulate water level change in the complex multi-aquifer system (the Upper and Middle aquifers) of the Azraq basin, Jordan. To predict the aquifer system responses for the period of 1997-2005, 4 different pumping schemes (scenarios) have been investigated. If the pumping rate was increased to 1.5 times the present rate, an approximate 39m drop in the water level by 2050 was revealed. Three dimensional groundwater modelling experiments were carried out by Reeve et al. (2001) to test the hypothesis that regional groundwater flow is an important component of the water budget in the Glacial Lake Agassiz Peatlands of northern Minnesota, USA encompassing an area of 10,160 km².

A 3-D mathematical model to simulate ground water flow in the lower Palar river basin in southern India was formulated by Senthilkumar et al, (2004). The effectiveness of groundwater modelling as a powerful tool for multipurpose such as framework for organizing hydrologic data, quantifying properties and behaviour of the systems and allowing quantitative prediction of responses of those systems to externally applied stress. MODFLOW package has been used to develop the conceptual model and simulation of the salt water intrusion. The study indicates the role of groundwater extraction in amplifying the phenomenon of salt water intrusion.

Studies were conducted by Laura K. Lautz and Donald I. Siegel (2006), to identify the locations of maximum hyporheic interaction along the experimental reach in the creek's watershed, and to examine the geomorphic and hydrologic features driving the exchange at those sites, such as debris dams and meanders. Two numerical modelling

packages, MODFLOW and MT3D were used to quantify the degree of hyporheic interaction along an experimental reach of Red Canyon Creek, Wyoming. Debris dams are a key driver of rapid surface water groundwater exchange and their installation may be a viable strategy for influencing nutrient transformations along Red Canyon Creek.

A Wetland Change Model to identify the vulnerability of coastal wetlands at broad spatial and temporal scales (modelling period of 100 years) was developed by McFadden (2007). The transitions between different vegetated wetland types and open water under a range of scenarios of sea-level rise and changes in accommodation space from human intervention, were studied. The process of quantifying broad-scale vulnerabilities of coastal wetlands to forcing from sea-level rise were discussed.

Martinez-Santos et al. (2008) described an interdisciplinary exercise of scenario design and modeling through finite difference code for providing a methodology to couple hard science numerical modeling approaches with the involvement of key water sectors. Given the long-standing conflicts in the area, modeling work largely focused on carrying out a vulnerability assessment rather than on trying to find solutions. a three dimensional steady-state finite difference groundwater flow model was developed by Ayenew et al. (2008) and used to quantify the groundwater fluxes and analyse the subsurface hydrodynamics in the Akaki catchment, Central Ethiopia by giving particular emphasis to the well field that supplies water to the city of Addis Ababa. The calibrated model was used to forecast groundwater flow pattern, the interaction of groundwater and surface water, and the effect of pumping on the well field under different scenarios.

The conceptual groundwater modelling approach of MODFLOW along with GIS was used by Kushwaha et al (2009), to develop a groundwater model for the northern part of Mendha sub-basin in the semi-arid region of north-eastern Rajasthan. The observed water level data from 1998 to 2003 were used for calibration and data during year 2003 to 2005 were used for model verification. The model generated groundwater scenario from 2006 to 2020 considering the existing rate of groundwater draft and recharge.

MODFLOW and FEMWATER were used by Feng-Rong Yang et al (2009), to determine the impacts of tunnelling excavation on the hydrogeological environment in

a regional area around the tunnel and a local hot springs area, at the “Tseng-Wen Reservoir Transbasin Diversion Project”, in Taiwan. MODFLOW was applied to simulate groundwater flow pattern for the hydrogeological conceptual model in the tunnel area and FEMWATER for solving 3-D groundwater flow problems, in which hydrogeological characteristics are integrated into a geographic information system (GIS), is applied to evaluate the impacts of tunnel construction on adjacent hot spring.

Wetland processes in hydrological and water quality models for regional applications were described by Hattermann et al, (2010). Both approaches considered water and nutrient fluxes, but they had different levels of complexity depending on data availability and objectives of the study. The first approach illustrates how a very simple supply/demand approach can help to notably improve the modelling results in terms of seasonal river discharge and nutrient loads in catchments with a notable share of wetlands. The second, more advanced, approach is introduced at the level of hydrological response units (HRU) and takes into account fluctuations in groundwater table and flow distances.

The groundwater model of Nankou area was developed by Feng Sun et al (2011), using software OpenGeoSys (OGS). It was proved that, with the object-oriented structure of OGS, it is possible for users to develop their own model by integrating OGS directly into pre or post-data process tools such as geographic information system (GIS) and GMS. An independent nonlinear parameter estimation code PEST(parameter estimation system) was applied with OGS for parameter identification. The 3D hydrogeological solid model was created using GMS. Both GMS and PEST were integrated to OGS for creating the final model.

Kumar et al, (2011) investigated the groundwater scenario of Nadia district, West Bengal to evaluate the existing trend and availability of groundwater in time and space and its movement for proper planning in future. Using Visual MODFLOW software, groundwater flow model for the study area was formulated by providing input hydro geological data and appropriate boundary conditions. The groundwater flow pattern of the study area indicated the occurrence of base flow which feed the Rivers *Bhagirathi* and *Jalangi* throughout the year. The computed hydraulic heads were calibrated by comparing with observed groundwater level data for years 2004 to 2006 and were

verified with the data of 2007. The outcome of modelling showed that this model can be used for prediction purpose in the future by updating input boundary conditions and hydrologic stresses during the preceding year. The model optimized unit draft for deep tube well as 556.5 m³/day and the same for shallow tube well as 41 m³/day. Hypothesis was done keeping the existing tube well structures in running condition and maintaining the present and recent past trends of groundwater level.

A 3-D groundwater flow model was developed by Fethi Lachaal et al (2012), to characterize the groundwater flow system and the groundwater levels in the ZBH (Zéramdine–Béni Hassen Miocene aquifer system) east-central Tunisia area, using coupling of MODFLOW and Geographic Information System (GIS) tools. The model was calibrated and validated with datasets during the 1980–2007 period. Topographic and geological maps (1:50,000) were digitized and geo-referenced, and attributes of vectors and areas. The General Direction of Water Resources (DGRE), Tunisian Ministry of Agriculture provided the information about 73 water wells. Twenty- four seismic reflexion profiles were provided by the Tunisian Company of Petroleum Activities. The simulating period is divided in to two periods: 1980–2004 period is used to transient model calibration and the 2005–2007 period is used to model verification.

Panagopoulos (2012) used MODFLOW for simulating groundwater flow in the Trifilia Karst aquifer, Greece. The steady and transient state calibrations gave encouraging results for the equivalent porous media approach, which does not consider pipe flow or turbulence.

An integrated methodology was developed by Lachaal et al. (2012), to investigate hydrological processes in Zéramdine–Béni Hassen Miocene aquifer (east-central Tunisia) and to validate the groundwater properties deduced from the geological, geophysical, hydrodynamic and hydro-chemical studies using the coupling of groundwater flow model MODFLOW with Geographic Information System tools. It was concluded that, the model can be regarded as a useful tool for analyzing the hydrological processes for complex groundwater problems.

The Rajshahi city is the fourth largest metropolitan city in Bangladesh on the bank of the river Padma (Ganges). Here an upper semi-impervious layer overlies aquifer – the

source for large-scale groundwater development. The groundwater resource study adjoining the river Ganges using Visual MODFLOW (Haque et al., 2012) showed that, the total groundwater abstraction in 2004 (15000 million litres) was lower than total input to aquifer through river induced recharge. Groundwater resources assessment, modeling and management are hampered considerably by a lack of data in semi-arid and arid environments with a weak observation infrastructure especially in Dar-es-Salaam aquifer of Tanzania (Brunner et al., 2006). This issue was well addressed by Camp et al. (2013) later using MODFLOW by creating additional database through field tests. From the calibrated model, it was estimated that, the annual recharge in the area is in the range 80–100mm/year.

Louwyck et al. (2014) outlined a procedure to simulate axisymmetric groundwater flow in radially heterogeneous and layered aquifer systems using the unmodified version of MODFLOW. Several test cases were presented, which compare the calculated results with existing analytical solutions, the analytic element solver TTim, and the axisymmetric, finite-difference model MAXSym. It is concluded that the MODFLOW procedure is capable of simulating accurately axisymmetric flow in radially heterogeneous multi-aquifer systems. Yang et al. (2015) used MODFLOW as one of the three steps carried to prioritizing feasible locations for permeable pavement, taking into account environmental, economic, and social aspects in Mokgamcheon watershed, central Korea. Visual MODFLOW software is used to simulate groundwater levels with and without permeable pavement. The results showed that, by considering anthropogenic factors and hydrological effectiveness, the study effectively prioritizes feasible alternatives that can be implemented into comprehensive hydrological cycle rehabilitation plans.

The groundwater model (MODFLOW) was used by Kelbe et al. (2016), to simulate 10 year water table fluctuations on the Maputaland coastal plain in northern KwaZulu-Natal, South Africa from January 2000 to December 2010, to contrast the conditions between wet and dry years. Remote sensing imagery was used to map permanent and temporary wetlands in dry and wet years to evaluate the effectiveness of identifying the suitable conditions for their formation using numerical modelling techniques. The

results confirm that, topography plays an important role on a sub-regional and local level to support wetland formation.

The response of shallow, coastal unconfined aquifers to anticipated overdraft conditions and climate change effect was investigated by Lathashri and Mahesha (2016), using numerical simulation. The groundwater flow model MODFLOW and variable density groundwater model SEAWAT were used for this investigation. The study area was the coastal basins of Dakshina Kannada district. The study arrives at the conclusion that, regional sea level rise of 1 mm/year has no impact on the groundwater dynamics of the aquifer.

2.5 SOLUTE TRANSPORT MODEL

2.5.1 General

The studies on contaminant transport are carried out through various analogous models, physical models, and mathematical models. The analogous and physical models have certain limitations. Hence, the last few decades have witnessed developments in numerical groundwater models and their application for different aquifer systems, when it comes to contaminant transport. A number of numerical models capable of modelling three dimensional groundwater flow and solute transport are available, such as 3DFEMFAT, FEFLOW, AQUA3D, FEMWATER, HST3D, MOCDENS3D, and SEAWAT. These models play important role as a representation of field studies, leading to more reliable results. To simulate the groundwater problems in coastal regions, numerical tools prove to be the best compared with others because of their flexibility in handling complex boundary conditions. The SEAWAT program was developed to simulate variable-density, transient groundwater flow problems in coastal aquifers. A detailed review of SEAWAT 2000 model is presented by Simpson (2004). The major advantages of SEAWAT over other programs include formulation of flow equation based on conservation of mass and implicit coupling between the flow and solute transport equations. This leads to more accurate results and wide ranging applicability for hydrogeological problems. The performance of SEAWAT was verified with a number of bench mark problems and is capable of accurately simulating variable density groundwater flow (Langevin and Guo, 1999).

Both finite element and finite difference methods of numerical modelling techniques are being practiced to mitigate problems related to seawater intrusion in the coastal aquifers. The numerical models have been used for various management and planning activities, especially in the coastal aquifers during the past decade. Researchers have addressed the contaminant transport problem either by modelling a hypothetical boundary or case specific for a coastal aquifer.

2.5.2 The numerical transport models

Shamir et al (1971) presented the partial differential equation that describes the motion of the water interface and the free surface in a phreatic coastal aquifer. Also an implicit scheme has been presented to solve the set of partial differential equations. The scheme is based on linearization of the equations and employing a grid structure.

Nonlinear equations to build a sustainable model was formulated by Datta et al (1999), using optimization techniques, considering plausible scenarios for planned withdrawal and salinity control in coastal aquifers. The first multiple-objective management model was developed for spatial and temporal control of aquifer salinity through planned pumping (withdrawal) from locations closest to the ocean boundary. The second multiple-objective management model was used for maximizing sustainable water withdrawal from the aquifer for beneficial uses, while limiting the maximum salinity in the aquifer. The third multiple-objective management model was developed for maximizing sustainable water withdrawal from the aquifer for beneficial uses and minimizing the total pumping at locations adjacent to the ocean boundary to control the salinity in the aquifer. The constraint method of generating no inferior solutions was used to solve the multiple-objective management problems and the models were solved for a hypothetical unconfined coastal aquifer system. The solution results demonstrated feasibility of the developed optimization models and also the conflicting nature of the various objectives of coastal aquifer management.

Seawater intrusion mechanisms through various numerical simulations were presented by Sherif (1999), for the seawater intrusion in the vertical and aerial views of the Nile delta coast, Egypt. The study came out with recommendations for the mitigation of the seawater intrusion problem. Gates et al. (2002) applied a finite difference model

developed using the Groundwater Modeling System (GMS), to analyse and predict water table elevations, flow of water and salinity in the salinity threatened lower Arkansas River basin of Colorado, USA. The preliminary steady state modelling indicated that, only limited improvement can be expected from vertical drainage derived from increased pumping, or from decreased recharge brought about by reduced over irrigation.

Geophysical methods such as vertical electrical sounding methods, seismic methods were employed by Choudhary et al., (2000), to investigate the saline water intrusion in the belt of Digha in eastern India. Also integrated geophysical surveys employing vertical electrical sounding VES and shallow seismic refraction method ha delineated the various subsurface geological formations, the aquifer and the saline brackish ground water zones on the basis of their characteristic resistivity and velocity signatures. It was also revealed from geophysical interpretation that the thickness of the near surface saline zone decreases inland away from the shore.

The SEAWAT code was applied by Langevin (2003), to estimate the rates of submarine groundwater discharge to a coastal marine estuary in Florida, USA. The model demonstrated that, regional scale variable density models are potentially useful tools for estimating rates of submarine groundwater discharge. Lin and Medina (2003) incorporated the transient storage concept in modelling solute transport in the conjunctive stream-aquifer model. Three widely used USGS models were coupled to form the core of this conjunctive model: MODFLOW, DAFLOW and MOC3D. Rao et al. (2004) developed a density dependent groundwater flow and transport model using SEAWAT for simulating the dynamics of seawater intrusion and the simulated annealing algorithm for solving the optimization problem. SEAWAT was used by Bauer et al. (2006) for coupled flow/transport simulations for the Shashe river valley in Botswana. It was found that, the salinity distribution in and around the area as well as its temporal dynamics can be satisfactorily reproduced if the transpiration is modelled as a function of groundwater salinity. The spatial and temporal variations of hydraulic heads and solute concentrations of groundwater were simulated by Qahman and Larabi (2006), using SEAWAT for the Gaza aquifer in the Palestine. The predictive simulation

done for 17 years showed that, the seawater intrusion would worsen the state of aquifer if the current rates of groundwater pumping are continued.

It was concluded from the studies of Feseker (2007) that, rising sea level causes rapid progression of saltwater intrusion in coastal north-western Germany, whereas the drainage network compensates changes in groundwater recharge. The numerical model, MOCDENS3D was used by Giambastiani et al. (2007) to simulate the seawater intrusion in the unconfined coastal aquifer of Ravenna, Italy. The simulation results showed that, over the last century, artificial subsidence and heavy drainage started the salinization process in the study area and a relative sea level rise will accelerate the seawater water intrusion process. Moustadraf et al. (2008) developed a numerical transient model which related the intensive pumping during the periods of drought to the seawater intrusion in the aquifer of the Chaouia Coast of Morocco. The results indicated that, the severe degradation of the resource was primarily related to intensive pumping which was 7 meters during periods of drought.

The simulation of saltwater intrusion in the Gurupura and Pavanje river basin aquifers was done by Vyshali et. al., (2008), using Saturated Unsaturated Transport (SUTRA) model and comparison was done with the field observations. The model was also used to predict the impact of increasing stress on freshwater aquifers due to the developmental activities. It was observed from the studies that the aquifers along the river courses are getting contaminated during the summer months only and region in the proximity of the sea is affected throughout the year. The optimal pumping rates have also been worked out for the region with potential groundwater development to avoid the problem of saltwater intrusion.

A variable-density groundwater flow and miscible salt transport model (SEAWAT) was developed by Lin et al., (2009), to investigate the extent of seawater intrusion in the Gulf coast aquifers of Alabama, USA. Using the calibrated model and assuming all the hydrogeologic conditions remain the same as those in 1996, a predictive 40-year simulation run predicted that, further seawater intrusion into the coastal aquifers could occur in the study area. Vandenbohede et al. (2009) developed three dimensional model using MOCDENS3D (Essink 1998), for sustainable management of a phreatic aquifer in the Belgian plain that faces the problem of decline in groundwater head and seawater

intrusion because of overdraft of groundwater. The flow and transport model was developed by Kopsiaftisa et al., (2009), for an unconfined aquifer in Thira Island, Greece using FEFLOW. Two potential cases of aquifer replenishment, with natural and artificial recharge were simulated. The results showed that advancement of seawater intrusion depends on the initial and boundary conditions prevailing on the seaside boundary of the aquifer.

Three dimensional numerical model for flow and solute transport for the management of the Salalah aquifer, Oman was developed by Shamma and Thunvik (2009). The established simulation model was used to predict the distribution of the piezometric surface, salinity distribution and mass balance under various water management scenarios for the period 2006-2020. Gholami et al. (2010) presented a linear model and a non-linear model for estimating groundwater salinity on the Caspian southern coasts. The model efficiency was evaluated by applying them in the sites that their data were not used for presenting the models. The electrical conductivity of groundwater map was developed using the non-linear model and Geographic Information System in the Eastern part of Mazandaran province. Rozzel and Wong (2010) found in their study conducted for Shelter Island, New York that the effects of sea level rise on the fresh water volume would be relatively minor.

The Korba aquifer, Tunisia was numerically simulated by Kerrou and Tarhouni (2010) to understand the current aquifer situation. The model building process was difficult because of data required on groundwater discharge from thousands of unmonitored private wells. To circumvent that difficulty, indirect exhaustive information including remote sensing data and the physical parameters of the aquifer has been used in a multi-linear regression framework. The results showed that, the aquifer was over-exploited. Sedki and Ouazar (2011) constructed a transient simulation model characterizing groundwater flow in the coastal aquifer of Rhis-Nekor, Morocco using MODFLOW. The flow model was then used in conjunction with a genetic algorithm based optimization model to explore the optimal pumping schemes that meet current and future water demands while minimizing the risks for saltwater intrusion, excessive drawdown, as well as waterlogging and salinity problems.

A series of three-dimensional numerical simulations were performed by Sang, P and Jun Kim et al. (2012), using a multidimensional hydrodynamic dispersion numerical model to analyse various saltwater extraction schemes for mitigating seawater intrusion attributed to groundwater pumping in a coastal aquifer system. A steady state numerical simulation was performed first to obtain initial (pre- groundwater pumping) steady-state conditions before groundwater pumping, and then a transient-state numerical simulation was performed to obtain intermediate (post-groundwater pumping) steady-state conditions during groundwater pumping. In the subsequent series of transient-state numerical simulations as scenario and sensitivity analyses, four different saltwater extraction factors such as the amount of saltwater extraction, the number of extraction wells, the horizontal location of extraction wells, and the vertical interval of saltwater extraction were considered to determine an optimal saltwater extraction scheme for the coastal aquifer system threatened with seawater intrusion. The numerical simulation results show that seawater intrusion may be better mitigated when saltwater is extracted at 30% (up to 50%) of the groundwater pumping rate from a single extraction well, which is located horizontally midway between the pumping well and the coastline and is screened through the whole sand aquifer.

A three dimensional, finite element model of the coastal aquifer in California was constructed using FEFLOW (Diersch, 2006) by Loaiciga et al. (2012) to study the effect of groundwater extraction and sea level rise on the seawater intrusion. The simulation results showed that, groundwater extraction is the predominant driver of seawater intrusion in the study area. Sindhu et al. (2012) developed Visual MODFLOW and SEAWAT for Karikkakom to Pozhiyur region towards south of the coastal belt of Trivandrum, Kerala, India. The effect of 1% increase in pumping on intrusion was studied and it was predicted that, groundwater heads in most of the observation wells are decreasing. The author found that the lateral extent of saltwater intrusion was more at Karikkakom pumping well location when compared to all other well locations due to 1% increase in pumping.

SEAWAT was used by Cobaner et al., (2012), to develop a model to control seawater intrusion in the coastal aquifer of Goksu deltaic plain along the Mediterranean coast of Turkey. They evaluated the hydraulic and hydro-geologic parameters of the aquifer and

estimated the spatial variation of seawater intrusion in the aquifer for increase and decrease in groundwater extraction. Allow (2012) developed a three dimensional model using SEAWAT to study the groundwater volume and quality for the purpose of planning and management of water resources in the coastal aquifer in Syria. Sherif et al. (2012) used MODFLOW to simulate the groundwater flow and assess the seawater intrusion in the coastal aquifer of Wadi Ham, UAE. Due to the lack of natural replenishment from rainfall and the excessive pumping, groundwater levels had declined significantly causing an intrusion of seawater in the coastal aquifer.

A groundwater flow model was developed by Nowbuth et al., (2012) for the southern aquifer of Mauritius. The model has predicted the pathways for contaminants from source pollutants. If there is excessive abstraction of groundwater, then the radial flow towards the sea may decrease or even the flow pattern is reversed, thereafter causing seawater movement inland. Chaaban et al. (2012) coupled GIS and GMS, in order to find the possible scenarios which could lower the piezometric surface in south of Hardelot area, France. The model created in GMS was calibrated against the historical and observed water level data for 1995–2006. Then a hydro-dispersive model (MT3D code) was launched for evaluating seawater intrusion. Langevin and Zygnerski (2013) used SEAWAT to evaluate the relative importance of sea level rise compared to the other dominant hydrologic processes for a municipal well field in south-eastern Florida, USA. The model was used to predict the impact of future rises in sea level on seawater intrusion near the well field.

A stochastic study of long term forecasts of seawater intrusion was presented by Kerrou, (2013), with an application to the Korba aquifer, Tunisia using a geo-statistical model of the exploitation based on a multi-linear regression model combining incomplete direct data and exhaustive secondary information and the density dependent transient model. The forecasts of the impacts of two different management scenarios on seawater intrusion in the year 2048 were performed by means of Monte Carlo simulations, accounting for uncertainties in the input parameters as well as possible changes of the boundary conditions. The results of the stochastic long term forecasts showed that, most probably, the Korba aquifer will be subject to important losses in terms of regional groundwater resources.

SEAWAT was used by Zhou et al. (2014) to simulate tide-induced groundwater flow and the groundwater flow dynamics and the effect of beach slope on groundwater table in the unconfined aquifer of Donghai Island, China. The analysis indicated that, the water table fluctuation was especially sensitive to the hydraulic conductivity and specific yield, and the horizontal length of the model domain could affect the amplitude of the water table fluctuation. Moreover, it was found that, the variation of the amplitude is more evident when the beach slope angle changes in the range from 1.5 to 45°, especially in the range from 1.5 to 5°. Comte et al. (2014) concluded from their studies on coral island using SEAWAT model that long term changes in mean sea level and climatic conditions (rainfall and evapotranspiration) are responsible for an average increase in salinity. Green and MacQuarrie (2014), investigated the relative importance of sea level rise and climate change effects on recharge and groundwater extraction on seawater intrusion in the coastal aquifer of Atlantic Canada. The authors developed a three dimensional model of the aquifer using SEAWAT for the investigation and concluded that sea level rise has the least significant effect on the future seawater intrusion.

A salinization of groundwater by oilfield brine and seawater intrusion was detected in the plain of Wadi Al Ayn and Darouda in CapBon, northeast of Tunisia. The historical trends of saltwater distribution (Chekirbane et al., 2015) and the future dynamics were predicted. Based on the developed model with SEAWAT, it was concluded that, the oilfield brine plume needs at least 5 years to be naturally reduced to less than the half of its actual size, while the seawater–freshwater interface can reach inland to the extent of 1.3 km with a TDS of 10 g/L if, no counter measures will be taken until the next three decades. The tested remediation plan by model demonstrated that the artificial recharge with treated wastewater is the best solution to stop seawater intrusion just after 2 years of percolating 1 m/day with TDS of 1.5 g/L of recharge water.

Many coastal areas historically were inundated by seawater, but have since undergone land reclamation to enable settlements and farming. The coastal unconfined aquifer in the Po Plain near Ravenna, Italy, consists of freshwater present as isolated thin (1–5 m) lenses on top of brackish to saline water. Antonellini et al. (2015) used SEAWAT to simulate a 200 year freshening history, starting with a model domain that is saturated

with seawater, and applying recharge across the top model layer. The modelling results showed that, the current distribution of freshwater is largely controlled by the drainage network. Within and adjacent to the drains, the groundwater has high salinity due to up-coning of salt water. Between drains, the surface layers of the aquifer are fresh due to the flushing action of recharge.

2.6 LITERATURE GAP

Due to rapid urbanization, increasing population and industrial activities in the study area, the groundwater extracted in excess leading to decrease in water table, finally loss of wetlands. The decrease in water table is significant during the summer. Concerns in terms of resource planning should be more comprehensive as the annual rainfall of the region even though is normally more than 3000mm, it does not meet sufficiency for the needs in the region. This is due to the fact that, the rainfall in the region is not distributed evenly. Also, geomorphology and hydrogeology of the region does not facilitate adequate water storage for a dry season. Thus future prediction of the water table for the study area is necessary for proper planning and management, in order to conserve the wetlands in the region. Additionally, it is understood from the literature review that, intricate numerical modelling studies are not attempted in the study area, though a good number of geophysical and field studies have been performed.

The present study is taken up with a keen interest in understanding the response of an unconfined shallow coastal aquifer to future stress scenarios existing in tropical climatic conditions considering the spatial (zonal) variability of hydro-geologic parameters. The behaviour of groundwater variation around wetland region is not addressed in the earlier literatures as well. Testing the seasonal performance of the calibrated model is another important criterion to be fulfilled to get a better confidence on the model, which is lacking in the previous studies. This gap has been taken care in the present study by carrying out a monthly model evaluation of a coastal, shallow aquifer system. Future prediction of groundwater behaviour around wetland region is going to be very useful for groundwater management in the study area.

THE STUDY AREA AND AQUIFER CHARACTERIZATION

3.1 GENERAL

The Karnataka state is geographically located on the west coast of India. The state consists of three coastal districts, namely Dakshina Kannada, Udupi and Uttara Kannada. The Dakshina Kannada district is one of the developing districts of Karnataka. It is a maritime district situated on the south-western part of Karnataka, adjacent to the Arabian Sea. For administrative purpose, the district is divided into five talukas namely, Putturu, Sullia, Bantwala, Belthangady and Mangalore. The study area is located in Mangalore taluk and is spread between 74°48'24.16"E to 74°56'23.08"E and 12°56'0.18"N to 12°59'31.97"N as shown in Fig.3.1. The study area for the investigation is the coastal aquifer of Gurupura basin, with its southern boundary as Gurupura River, flowing from east to west. The areal extent of the region is about 57.73 km².

The mega industries like MRPL, MCF (Mangalore Chemicals and Fertilizers), BASF, MSEZ (Mangalore Special Economic Zone) and Mangalore International Airport is located in the region. In addition, other smaller units comprising of industrial estate, small scale industries are also existing in the region. The Oil and Natural Gas Corporation (ONGC) is exploring various options for diversification of its activities including setting up of special economic zones (SEZ) and storage of crude oil near Mangalore. The study area has a population of about more than 1,00,000, which is expected to grow with a decennial growth rate of about 12.1% as per 2011 population census of India. The main crops grown in the study area are, paddy, coconut and arecanut. Fishing is also a major source of income to a large community, residing in the region. The population is dependent on both surface water and groundwater resources for irrigation and domestic water requirements. The availability surface water is scarce

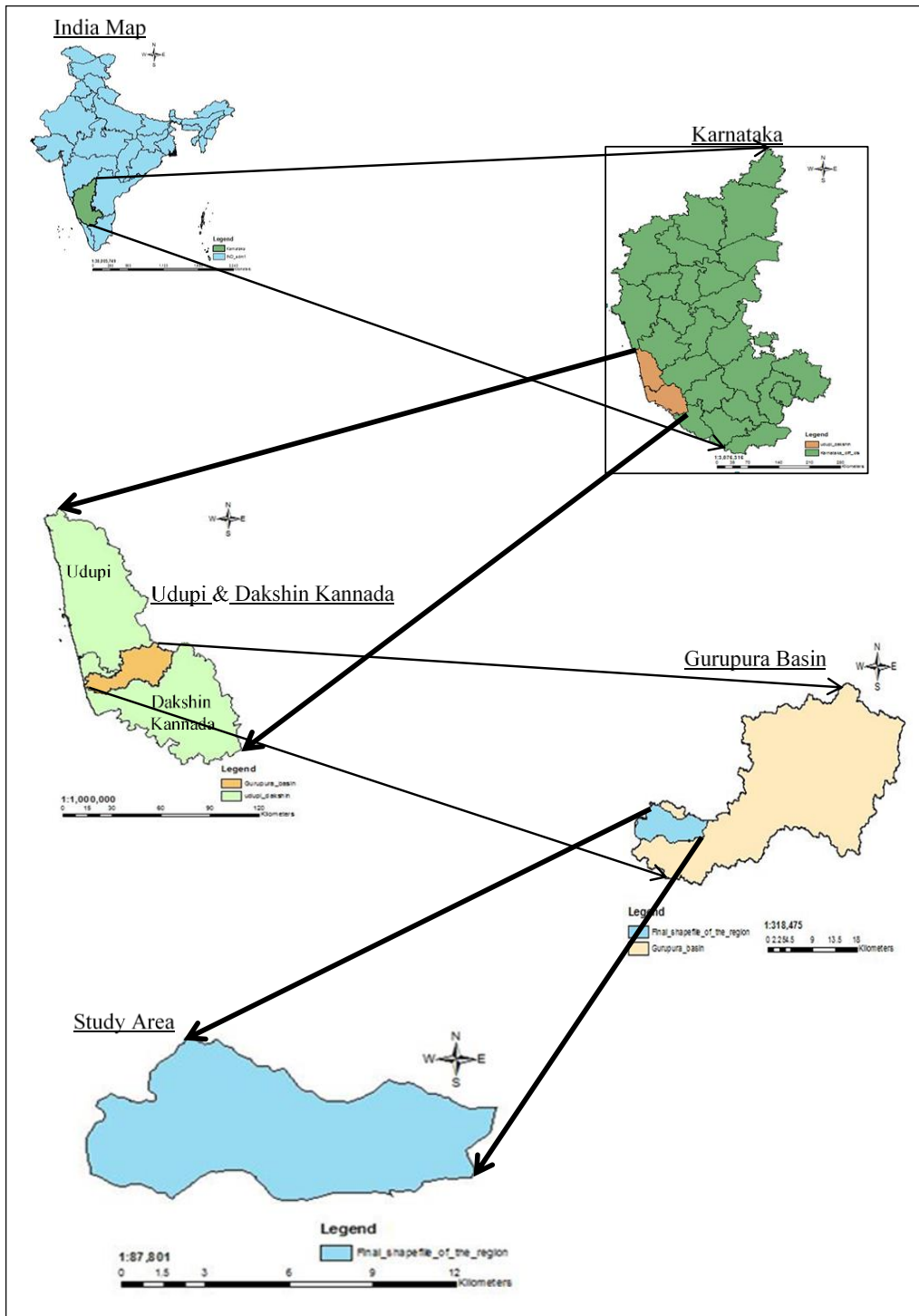


Figure 3.1 Location of the Study Area

during January to May. Hence, greater thrust is on the groundwater resources during these summer months.

The database generation is the first requirement for any model development. The topographic sheets, numbered 48L/13/NW, 48L/13/SW and 48L/13/SE with a scale 1:25,000 having a contour interval of 10m are procured from the Geological Survey of India. They are processed using ArcMap® (version 9.3) software to delineate the study area boundary. The Digital Elevation Model (DEM) was created and drainage network map was generated. The topographic sheets are geo-referenced and projected to UTM co-ordinate system.

The characterization of an aquifer requires two important attributes, hydrogeological investigation and pumping tests. The aquifer parameters are estimated based on the property of the aquifer material. The pumping tests are useful in determining aquifer parameters, such as specific yield and transmissivity. A particular method for the analysis of pumping test data is chosen based on the knowledge of the groundwater system under consideration and conformance of the site hydraulic conditions to the assumptions of the test method adopted. The purpose of the pumping test and the hydrogeological conditions present at the study site are the two important factors based on which the optimal well location, depth, pumping rate, test duration and analysis method are selected.

3.2 FEATURES OF THE STUDY AREA

3.2.1 Topography

The peninsular country, India is bounded by ocean on its three sides, west, east and south. The coastal land mass is situated between high mountain ranges called the Western Ghats towards the east and the Arabian Sea on the west. The west coastal landmass can be classified into upland Western Ghats hill slopes (high elevation), the mid-land region with undulating topography (medium elevation) and the coastal plains (low elevation). The study area is in coastal plains having gradual westerly sloping low-lying terrain with elevation ranging from 2 to 151 m above mean sea level (msl). The topography of the region is from plain to undulating with hilly regions and natural valleys, and is shown in figure 3.2.

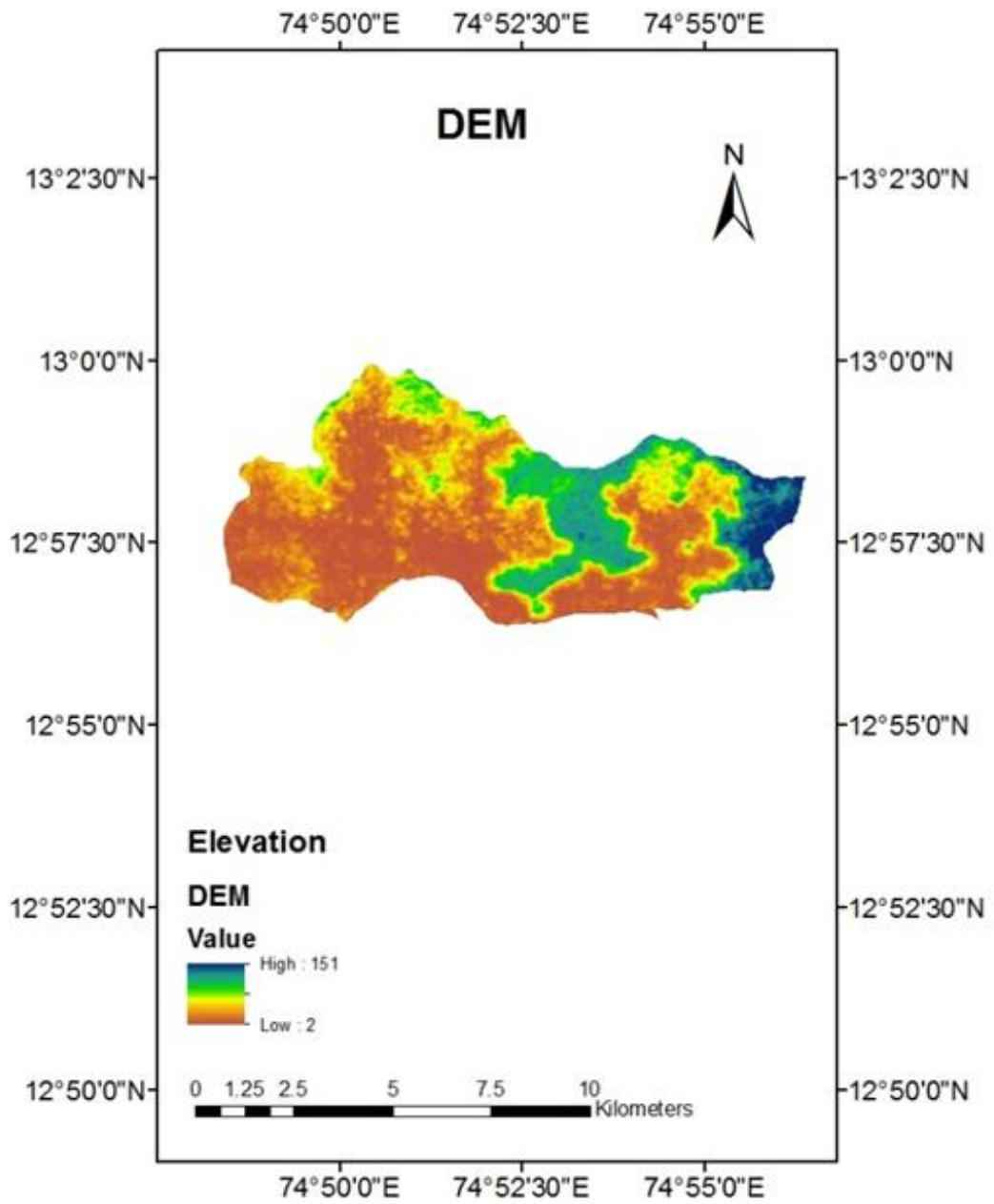


Figure 3.2 Topography of the Study Area

3.2.2 Climate

The India Meteorological Department (IMD) has classified a year into four seasons as the monsoon (June to September), post-monsoon (October to November), winter (December to January), and pre-monsoon or summer (February to May) seasons. The climate of the region is tropical humid type with moderate air temperatures of 36°C during May and 21°C during December. High levels of relative humidity ranging between 65% and 100% are observed in the region. The average annual rainfall of the region is about 3,500 mm. About 85% of the total annual precipitation occurs during the months of June through September on account of the southwest monsoon. This is evident in figure 3.3, where the monthly rainfall for a typical year is presented.

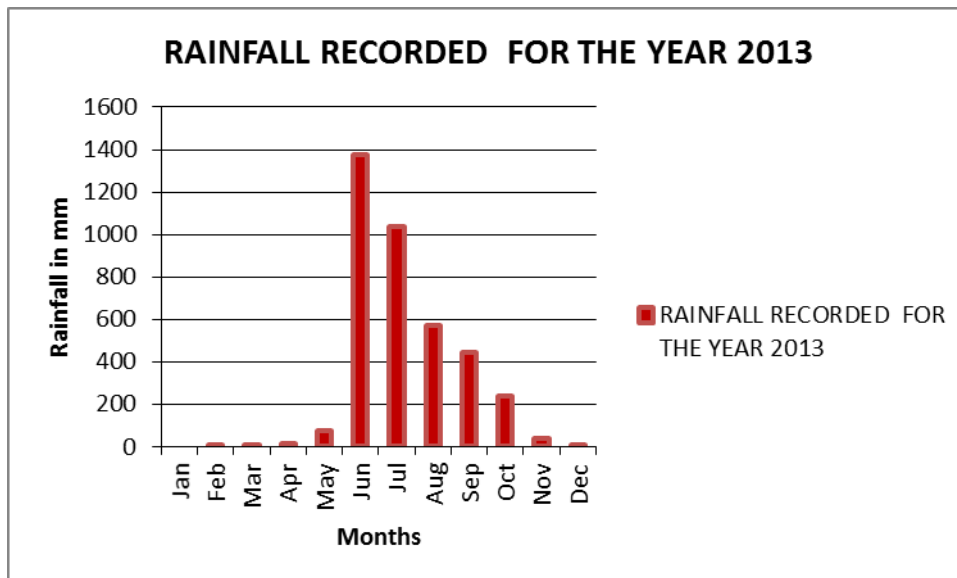


Figure 3.3 Monthly rainfall observed at Meteorological Office, Mangalore International Airport

3.2.3 Soil

The study area consists of laterite soils. The lateritic deposits belong to recent and sub-recent formations of the parent rock, granitic gneiss. The lateritic soil is generally fine grained and composed of hydrated aluminium and iron oxides.

The soil map prepared by the NBSS&LUP (1998) is extracted for the present study area using Arc GIS to get the spatial soil type distribution in the study region. Figure. 3.4 reveals the spatial distribution of these soil types sampled at depths varying from 8m to

18m and each soil class is described in table 3.1. Gravelly clay soils covers the about one third portion of the study area. The remaining parts are covered by sandy over loamy soils, gravelly clay soils with iron stone and gravelly clay soils with low AWC.

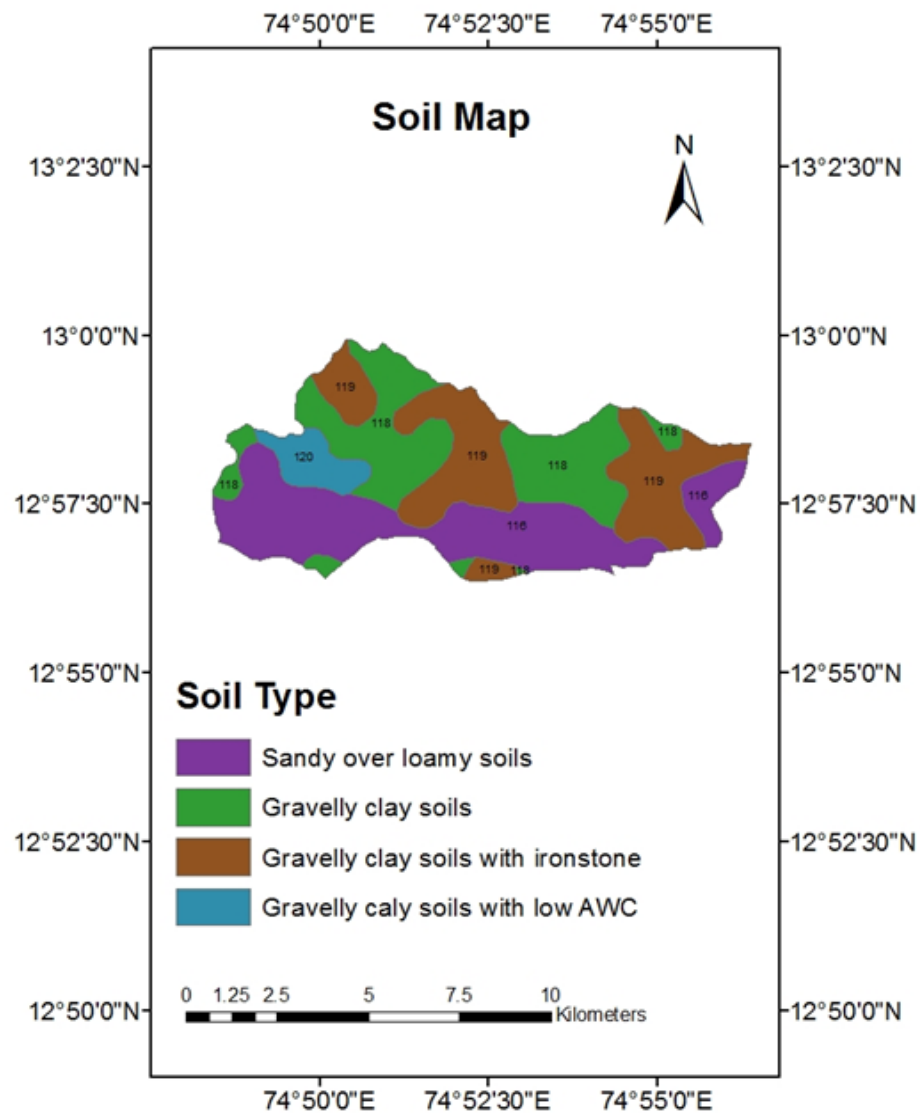


Figure 3.4 Soil map of the study area

Table 3.1 Soil type and Description

Soil Type	Description of the soil
Sandy over loamy soils	Deep, imperfectly drained, sandy over loamy soils of valleys, with shallow water table
Gravelly clay soils	Very deep, well drained, gravelly clay soils with surface crusting and compaction on undulating uplands, with moderate erosion.
Gravelly clay soils with iron stones	Moderately shallow, somewhat excessively drained, gravelly clay soils with hard ironstone on coastal plateau summits, with moderate erosion
Gravelly clay soils with low AWC	Moderately deep, well drained, gravelly clay soils with low AWC and surface crusting on undulating uplands, with moderate erosion

3.2.4 Land use and land cover of the Study Area

The land use/ land cover (LULC) distribution of the study area is presented in figure 3.5. The LULC data of scale 1:2,50,000 derived from Resourcesat-1 satellite's Linear Imaging Self scanning Sensor (LISS) -III data (2011-12) is downloaded from Bhuvan-Thematic Services website <http://bhuvannoeda.nrsc.gov.in/theme/thematic/theme.php>.

The data consists of 19 classes which are then merged to get 6 required classes for the study area, namely cropland, industrial, vegetation, barren land, water/wetland and roadway. According to the classification, 28 % of the total area is covered by cropland, 23% by industrial coverage, 38% by vegetation, 2% by barren land, 7% as waterbody and wetland and 2% as roadway.

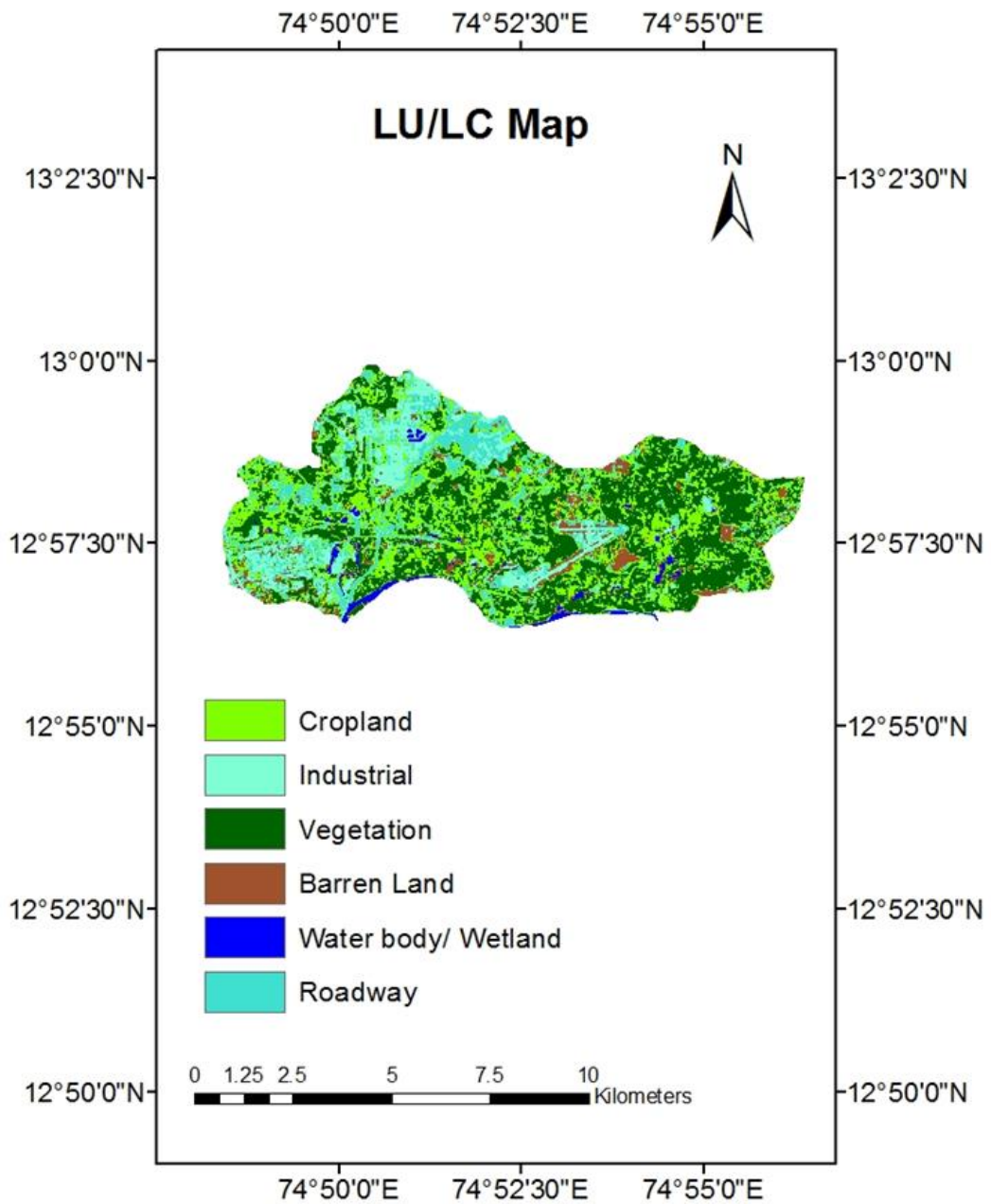


Figure 3.5 Land Use / Land Cover map of the study area

3.3 HYDROGEOLOGY OF THE STUDY AREA

3.3.1 Bore - log information

The coastal area is majorly occupied by lateritic formation. The lateritic formation in the study region is underlain by a thin bed of clay, granites, gneisses, and coastal alluvium. It is evident from the earlier investigations (Rao, 1974; Srikantiah, 1987; Lokesh, 1997 and Mahesha et al., 2012) that, the region is underlain predominantly by an unconfined aquifer with depth ranging from 12 to 30 m. The lithology of the bore log investigation carried out by the Central Ground Water Board (CGWB, 2008) in the Gurupura basin, is presented in figure 3.6. In the majority of Gurupura basin, laterite mainly covers the subsurface with depth of lateritic formation varying from 4 to 10 m.

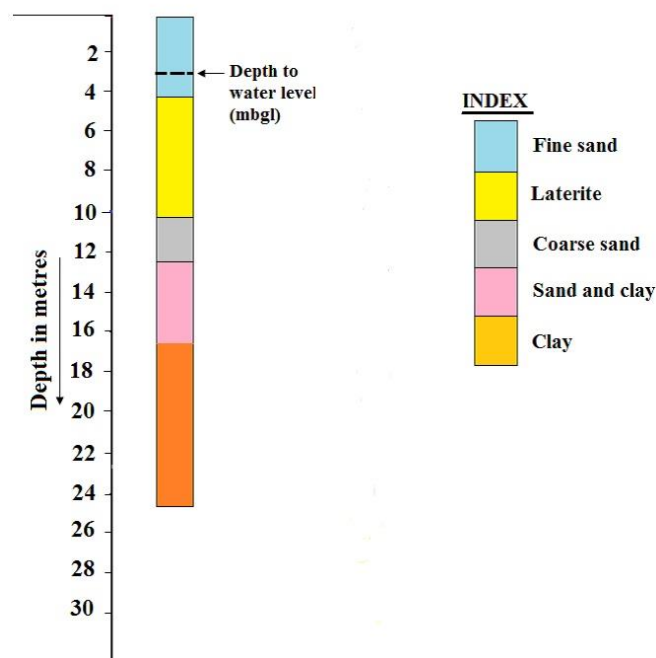
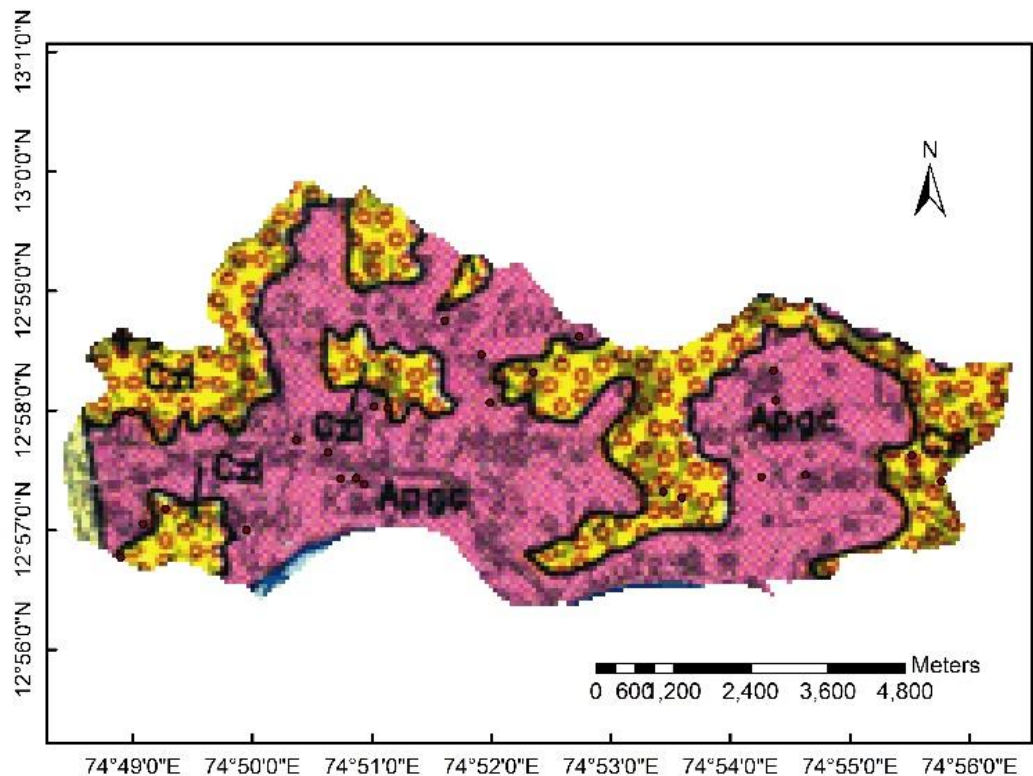


Figure 3.6 Bore log details

3.3.2 Lithology map

The lithological unit map (Ravindra and Ranganathan, 1994) for Karnataka State, is extracted for the study area and is presented in figure 3.7.



Legend

Q ₂ s	Alluvium, coastal sand
Q ₂ b	Red teri sand
C ₂	Laterite
NW	Crit. sandstone, clay with lignite intercalations
#Pgd	Dolerite
SPGg	Syenite; granite
Appc	Hornblende – biotite gneiss
Ak	Quartz – feldspar – garnet – sillimanite – graphite gneiss

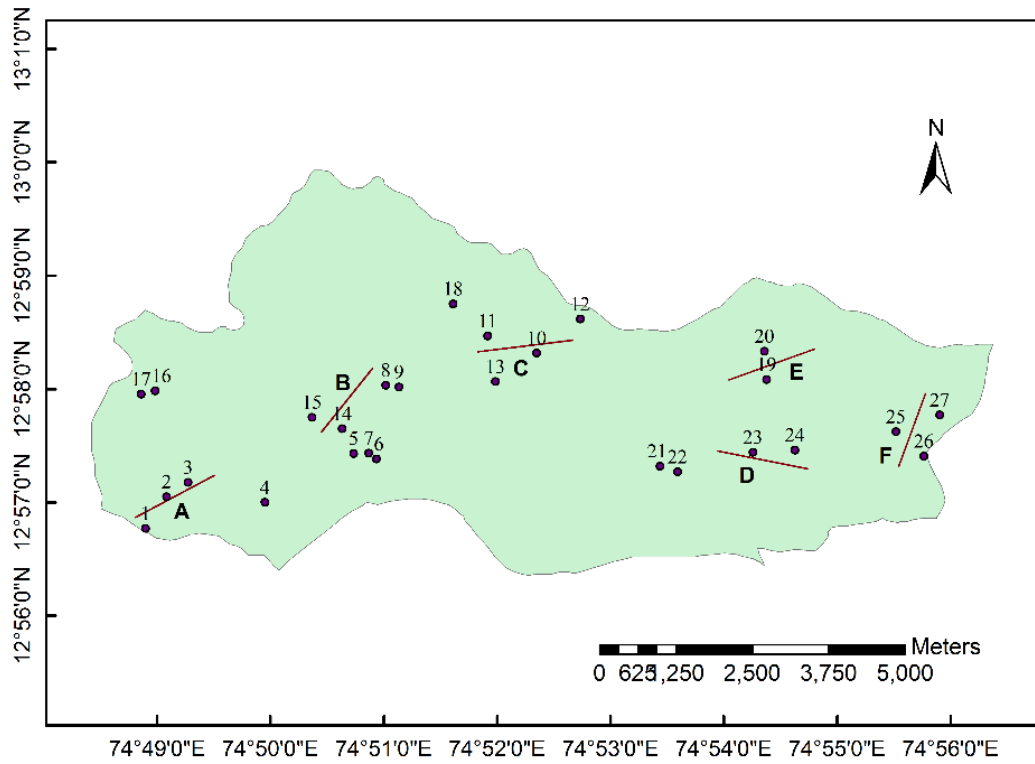
Figure 3.7 Lithology map of the study area

The coastal edge of the study area consists of alluvium. The study area is predominately depicted by laterite and hornblende-biotite gneiss. The laterite is seen occurring as capping on ridges and hillocks and as sheet like masses at elevated terrains. The thickness of the laterite cover is found to vary generally from 5 to 20m.

3.3.3 Vertical Electrical Sounding (VES)

The hydrogeology of the study area was assessed by conducting Vertical Electrical Sounding (VES) studies in six locations spread across the study region. The necessary data in this regard was obtained by the interpretation of test results for the study area. The locations where bore log and Vertical Electrical Sounding (VES) studies are carried out are shown in figure 3.8. The Surface electrical resistivity surveying is based on the principle that, the distribution of electrical potential in the ground around a current carrying electrode depends on the electrical resistivity and distribution of the surrounding soils and rocks. The Vertical Electrical Sounding (VES) is a geophysical method for investigation of a geological medium by Schlumberger method. The method is based on the estimation of the electrical conductivity or resistivity of the medium. The estimation is performed based on the measurement of voltage of electrical field induced by the distant grounded electrodes.

The Vertical Electrical Sounding survey is carried out at 6 locations in the study area. The snap shots of conduct of VES survey are shown in figure 3.9.



Legend

- Locations of observation wells
- VES locations

Figure 3.8 VES locations in the study area



Figure 3.9 Snap shots of conduct of VES survey in the study area

The lithological variation based on 6 locations situated across the study area is interpreted as shown in figure 3.10. This observation matches well with the bore log and lithology maps agreeing to the fact that, the region is underlain by shallow lateritic formation as a key aquifer material in the region. Laterites are generally coarse grained

and are composed of vermicular tube like structure. The thickness of the lateritic formation ranges from about 13m to 30m. The lateritic formation is topped by sand and top soil and beneath the laterite a huge mass of hard rock is detected up to a depth of about 90m. At the stretch where wetlands are present a thin layer of sand mixed with silt is found to be present in the study area. Also in the areas of agricultural land, similar soil strata is observed.

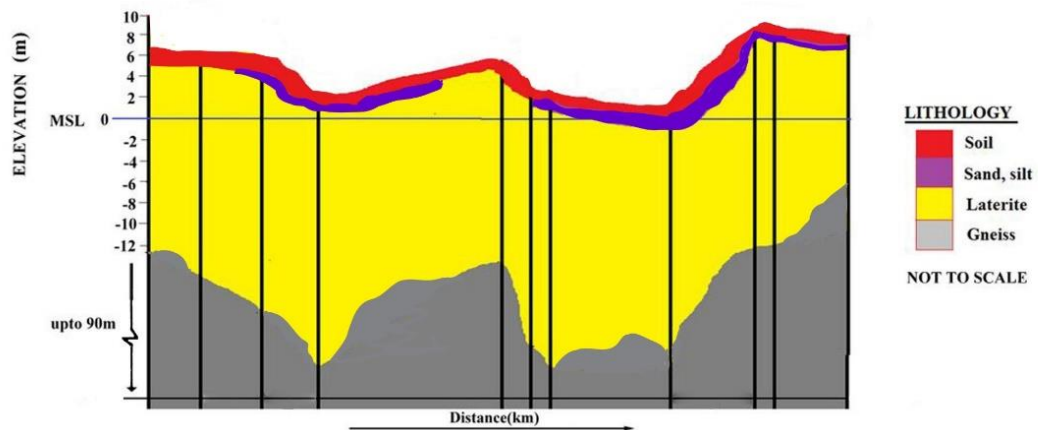


Figure 3.10 Aquifer profile as per VES

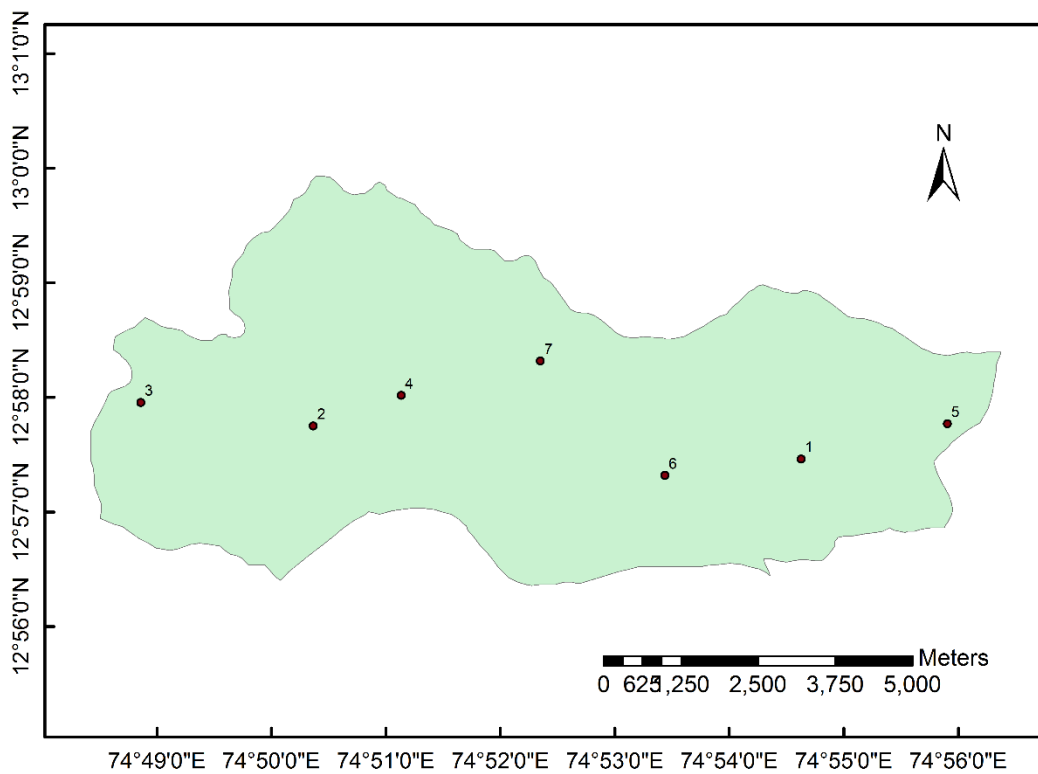
3.4 PUMPING TESTS

3.4.1 General

The aquifer hydraulic properties can be determined by the carrying out pumping tests. This involves pumping of water from a well at a controlled rate and observation of water level at the observation well with respect to time. The pumping tests will also provide information on the drawdown and yield of groundwater table (Karanth, 1987). Reliable results are obtained if pumping continues till the cone of depression has reached a stabilized position and does not seem to expand further as pumping continues. The cone of depression will continue to expand until the recharge of the aquifer equals the pumping rate (Rajagopalan, 1983). Prior knowledge of the lithological profile of the study area is of great help in planning the tests and interpreting the data.

3.4.2 Pumping Test methodology

In the study area, pumping tests are conducted in 7 open wells spread across the study region. These data are in addition to the data already available from aquifer characterization. Figure 3.11 shows the locations of pumping test wells in the study area. The photographs of the pumping wells 4, 5 and 6 are given in figures.3.12 to 3.14 respectively. The details of pumping wells are given in Table 3.2. The wells selected for the analysis are of shallow depth with depth of wells less than 10m.



Legend

- Pumping Test Wells

Figure 3.11 Locations of Pumping Test Wells



Figure 3.12 Photograph of pumping well no. 4



Figure 3.13 Photograph of pumping well no. 5



Figure 3.14 Photograph of pumping well no. 6

Table 3.2 Details of the pumping wells

Sl. No.	Location	Latitude (N)	Longitude (E)	Well Diameter (m)	Well depth (m)
1	Kulai	12° 57' 57"	74° 48' 52"	2.1	4.8
2	Baikampady	12° 57' 21"	74° 50' 16"	3.7	5.3
3	Kenjar	12° 58' 02"	74° 51' 02"	1.7	8.7
4	Jokkatte	12° 58' 21"	74° 52' 10"	2.5	7.8
5	Bajpe	12° 57' 17"	74° 53' 44"	1.5	5.1
6	Adyapady	12° 57' 32"	74° 54' 35"	3.7	4.8
7	Kandavara	12° 57' 22"	74° 54' 51"	3.5	6.3

Pumping rate

In the present study, two methods are adopted for measuring the discharge of wells, depending on the suitability. In the first method, suitable for small pumping rates, the time required to fill a collecting tank of known volume is noted using a stop watch and rate of discharge is calculated as follows:

$$\text{Discharge in } Q \text{ m}^3 / \text{sec} = \frac{\text{Collecting tank volume in m}^3}{\text{Time needed to fill the collecting tank in sec.}} \quad (3.1)$$

In the second method, the horizontal distance travelled by the trajectory of water out of the horizontal or inclined pipe for a vertical fall of 30cm is measured. The representative sketch for these two variations are shown in figures 3.15 (a) and 3.15 (b).

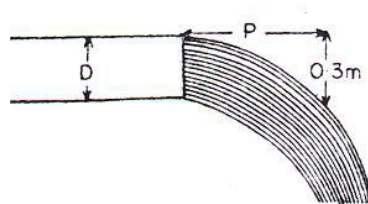


Figure 3.15 (a) Measurements for determining the discharge with horizontal pipe

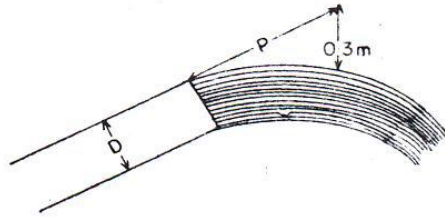


Figure 3.15 (b) Measurements for determining the discharge with inclined pipe

The discharge rate for trajectory method is calculated using the following relation:

$$Q = 0.017 CP \quad (3.2)$$

Where, Q = Discharge in m^3/sec

C = constant to be determined from the graph shown in figure 3.16 A

P = distance travelled by the stream, in m, measured parallel to the pipe for a 30 cm vertical drop

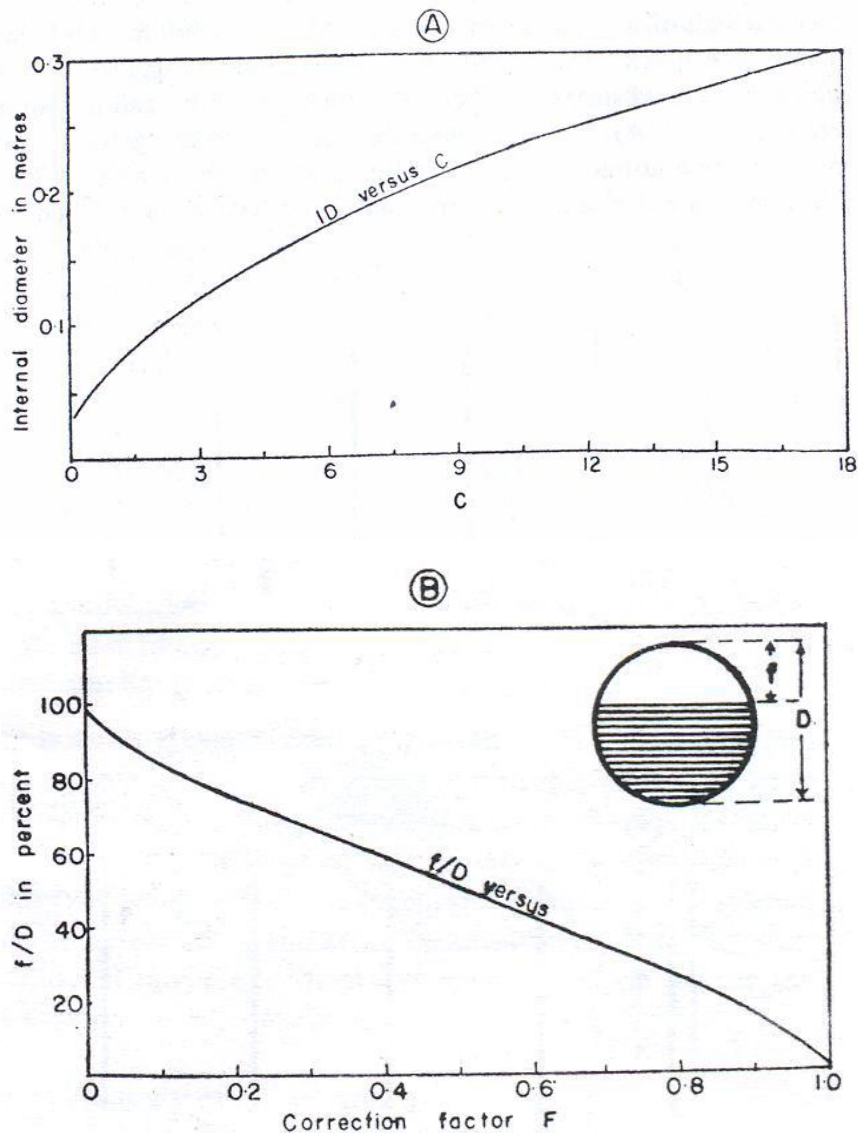


Figure 3.16 Curves for determining C and F for estimation of flow through inclined and horizontal pipes

When the pipes are only partially filled, the freeboard (f) and the internal diameter (D) are measured and the ratio f/D calculated as a percentage. The discharge is calculated as in the method for full pipes and a correction factor to be read from the curve in figure 3.16 B is applied to obtain the corresponding discharge values.

Hydraulic properties

Generally, for any groundwater related studies, the important hydraulic properties of aquifers are hydraulic conductivity, transmissivity, co-efficient of storage, specific yield and the specific capacity.

(i) Hydraulic conductivity (K)

The hydraulic conductivity, also known as the permeability is as measure of the ease with which fluid moves through a formation and is defined as the amount of flow per unit cross sectional area of aquifer under the influence of unit gradient (m/day). The hydraulic conductivity depends upon the properties of the fluid as well as the aquifer.

(ii) Transmissivity (T)

Transmissivity is a hydraulic characteristic of the aquifer which is defined as the rate of flow of water at the prevailing field temperature under a unit hydraulic gradient through a vertical strip of aquifer of unit width and extending through the entire saturated thickness of the aquifer. It is therefore the product of the average hydraulic conductivity (K) and the thickness (b) of the aquifer ($T = Kb$, m^2/day). The concept of transmissivity holds good in confined aquifer. In unconfined aquifer, as the saturated thickness of the aquifer changes with time, the T also change accordingly.

(iii) Coefficient of storage (S) and specific yield (S_y)

The aquifer has the capacity to store water which is expressed as a coefficient. The storage coefficient of an aquifer is defined as the volume of water it releases from or it takes into storage per unit surface area of the aquifer per unit change in the head. In the case of an unconfined aquifer, the concept of specific yield is analogous to that of storage coefficient.

In case of confined aquifer, the storage coefficient depends on the compressibility of the aquifer and the expansion of water. Since the unconfined aquifer is not bounded by confining layers, the specific yield or storage coefficient does not depend upon the compressibility of either the aquifer or the fluid. The specific yield for all practical purposes is same as effective porosity, because in the unconfined aquifer the effects of elasticity of the aquifer material or fluid are generally negligible in magnitude and the effect of gravity is predominant.

(iv) Specific capacity

It is a measure of both effectiveness of a well and of the aquifer characteristics. It is defined as the ratio of the pumping rate and the drawdown and is usually expressed in litres per minute per meter of drawdown for a specific period of pumping.

3.4.3 Analysis of pumping test data

The graphical type-curve analysis method is invariably used for estimating the hydraulic properties, in which dimensionless type curves derived from an assumed analytical model of ground water flow to a pumped well are used to analyse the time-drawdown measurements of hydraulic head in the observation wells. These analyses are carried out to estimate the hydraulic conductivity and specific yield of water table for unconfined aquifers. Three methods adopted for the present study are described in the following sections.

Theis (1935) method

Theis (1935) was the first to develop a formula for unsteady state flow that introduces the time factor and storativity. Theis noted that when a well penetrating an extensive confined aquifer is pumped at a constant rate, the influence of discharge extends outward with time. The rate of decline of head, multiplied by the storativity and summed over the area of influence, equals the discharge through the aquifer.

The Theis equation for unsteady state, which was derived from the analogy between the flow of groundwater and the conduction of heat, is written as follows;

$$s = \frac{Q}{4\pi T} \int_u^{\infty} \frac{e^{-u}}{u} du = \frac{Q}{4\pi T} W(u) \quad (3.3)$$

$$\text{Where, } u = r^2 S / 4Tt \text{ and consequently } S = 4Ttu/r^2 \quad (3.4)$$

s = drawdown, in metres

T = KD = transmissivity, in m²/day

Q = constant rate of discharge of well in m³/day

S = storage coefficient, dimensionless

t = time, in days, since pumping started

e = base of natural logarithm

r = radial distance from discharge well to the point of observation, in metres

In the above equation the exponential integral expression is symbolically expressed as W(u) for “well function of u”

$$W(u) = -0.5772 - \ln u + u - \frac{u^2}{2.2!} + \frac{u^3}{3.3!} + \frac{u^4}{4.4!} + \dots \quad (3.5)$$

Theis (1935) approximation for unconfined aquifers

The flow pattern around the well is nearly identical to that in a confined aquifer when a well screened in a thick unconfined aquifer without delayed yield is pumped, so that the Theis non-equilibrium formula is applicable under the same limiting conditions except the one regarding the confined condition of the aquifer. If the aquifer is thin, a correction has to be made to the drawdown to account for partial desaturation and consequent reduction during the course of pumping, in the transmissivity of the aquifer. In such a situation, the observed drawdown would be more than what it would have been had the transmissivity not decreased, appreciably, progressively, during pumping. Jacob (1963) showed that equations based on the assumption of negligible dewatering and radial flow can be used for aquifer test data analysis if the drawdown observed in thin unconfined aquifers is adjusted as shown below:

$$s_c = s - (s^2/2b) \quad (3.6)$$

where, s_c = drawdown that would have occurred in a confined aquifer

s = observed drawdown under water table conditions

b = initial saturated thickness of the aquifer

wherein the adjustment for dewatering of the aquifer is considered significant, $s - (s^2/2b)$ should be plotted against t and not s versus t. Such corrections are applicable if the flow is essentially radial and the corrections cannot be relied upon where vertical flow components are dominant, as in the case of partially penetrating wells. When the

drawdowns are adjusted, the non-equilibrium formula can be used with fair assurance even when the dewatering is as much as 25 percent of the initial saturated thickness.

The values of S can be determined by the equation (Jacob, 1963) as follows;

$$S = \left(\frac{b-s}{b}\right)S' \quad (3.7)$$

Where S = corrected storage coefficient

b = thickness of the aquifer

s = drawdown

S' = apparent coefficient of storage

Neuman (1974) method

When the pumping well and the observation well is perforated throughout the entire saturated thickness of the aquifer, the drawdown in the observation well is given by Neuman (1974) for unconfined aquifers is as shown below,

$$s(r, t) = \frac{Q}{4\pi T} \int_0^\infty 4yJ_0(y\beta^{1/2})[u_0(y) = \sum_{n=1}^\infty u_n(y)]dy \quad (3.8)$$

Where,

$$u_0(y) = \frac{\{1 - \exp[-t_s\beta(y^2 - \gamma_0^2)]\} \tanh(\gamma_0)}{\{y^2 + (1 + \sigma)\gamma_0^2 - [(y^2 - \gamma_0^2)^2/\sigma]\}\gamma_0} \quad (3.9)$$

$$u_n(y) = \frac{\{1 - \exp[-t_n\beta(y^2 + \gamma_n^2)]\} \tanh(\gamma_n)}{\{y^2 - (1 + \sigma)\gamma_n^2 - [(y^2 + \gamma_n^2)^2/\sigma]\}\gamma_n} \quad (3.10)$$

and the terms γ_0 and γ_n are the roots of the equations

$$\sigma\gamma_0 \sinh(\gamma_0) - (y^2 - \gamma_0^2) \cosh(\gamma_0) = 0$$

$$\gamma_0^2 < \gamma^2 \quad (3.11)$$

$$\sigma\gamma_n \sin(\gamma_n) + (y^2 + \gamma_n^2) \cos(\gamma_n) = 0$$

$$(2n - 1)(\pi/2) < \gamma_n < n\pi \quad n \geq 1 \quad (3.12)$$

The equation is based on the assumptions as stated below,

(1) The aquifer has a seemingly infinite areal extent. (2) The aquifer is homogeneous and of uniform thickness over the area influenced by the test. (3) Prior to pumping, the water-table is horizontal over the area that will be influenced by the test. (4) The aquifer is pumped at a constant discharge rate. (5) The well does not penetrate the entire thickness of the aquifer. (6) The aquifer is isotropic or anisotropic. (7) The flow to the well is in an unsteady state. (8) The influence of the unsaturated zone upon the drawdown in the aquifer is negligible. (9) An observation well screened over its entire length penetrates the full thickness of the aquifer. (10) The diameters of the pumped and observation wells are small, i.e. storage in them can be neglected.

The three independent dimensionless parameters σ , β , t_s or t_y , are related to each other by $t_y = \sigma t_s$. The curves lying to the left of the values of β in figure 3.17 are called type A curves and correspond to the top scale expressed in terms of t_s . The curves lying to the right of the values of β in the figure are called type B curves and correspond to the bottom scale expressed in terms of t_y . The Theis curves with respect to both dimensionless time parameters t_s and t_y have been included in the figure for reference purposes. Type A curves are intended for use with early drawdown data and type B curves with late drawdown data.

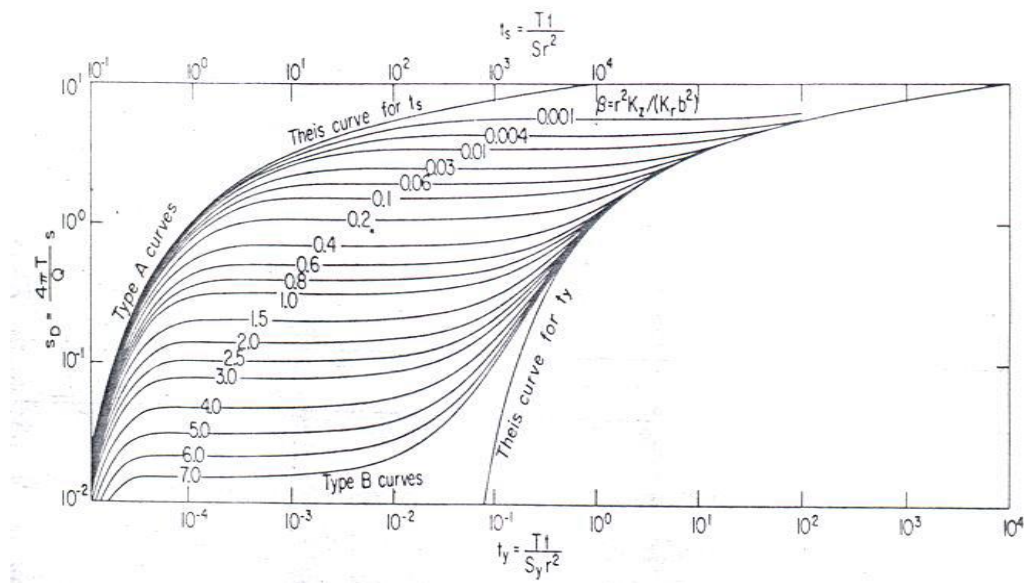


Figure 3.17 Type curves for fully penetrating wells (Neuman, 1975)

The field data, plotted on a logarithmic paper (drawdown, s versus time, t) is superimposed on the type B curves, keeping the vertical and the horizontal axes of both graphs parallel to each other and matching as much of the latest time-drawdown data to a particular type curve. The value of β corresponding to this type curve is noted and a match point is chosen anywhere on the overlapping portion of the two sheets of paper. The coordinates of this match point are s^* and s_d^* along the vertical axis and t^* and t_y^* along the horizontal axis. Hence, transmissivity

$$T = c_1(Qs_d^*/s^*) \quad (3.13)$$

and the specific yield

$$S_y = c_2(Tt^* / r^2t_y^*) \quad (3.14)$$

where c_1 and c_2 are constants and are equal to $1/4\pi$ and 1.0 in CGS units respectively. The transmissivity value is again calculated by superimposing the field data on the type A curve and its value should be approximately equal to that calculated from the late drawdown data.

Tartakovsky Neuman (2007) method

Tartakovsky and Neuman (2007) developed an analytical solution for flow to a partially penetrating well pumping at a constant rate from a compressible unconfined aquifer considering an unsaturated zone of infinite thickness. In their solution three dimensional, axially symmetric unsaturated flow was described by a linearized version of Richards' equation in which both relative hydraulic conductivity and water content vary exponentially with incremental capillary pressure head relative to its air entry value, the latter defining the interface between the saturated and unsaturated zones. Both exponential functions were characterized by a common exponent " k " having the dimension of inverse length, or equivalently a dimensionless exponent " $k_d = k_b$ ", where b is initial saturated thickness. A solution admitting two separate values of k , one characterizing relative hydraulic conductivity and the other water content, was developed by Mathias and Butler (2006). Whereas their solution allowed the

unsaturated zone to have finite thickness, it considered flow in the unsaturated zone to be strictly vertical and the pumping well to be a fully penetrating one.

3.4.4 Results and discussion

The analysis of aquifer test data by graphical type-curve method is frequently used, where dimensionless type curves derived from an assumed analytical model of groundwater flow to a pumped well are used. The pumping test analysis of unconfined aquifer should consider saturated thickness, reduction and vertical flow, since the pumping from an unconfined aquifer leads to dewatering of the aquifer. In the present study, Theis (1935) method, Nueman (1974) method and Tartakovsky Nueman (2007) methods are used for the analysis which are applicable for unconfined aquifer system. The time-drawdown and recovery data for the test conducted in pumping well number 4, 5 and 6 are listed in APPENDIX I, as sample data.

The plots of drawdown and recovery versus time are presented in figure 3.18 for pumping well no. 6, as sample.

Pumping well no., 5 was having faster drawdown compared to other wells. The recovery was faster in well nos. 4 and 5 with about 95% recovery in 200 minutes. The well numbers 2, 3 and 7 are having very slow recovery. The drawdown and recovery characteristics of well no., 1 is similar to well numbers 4, 5 and 6.

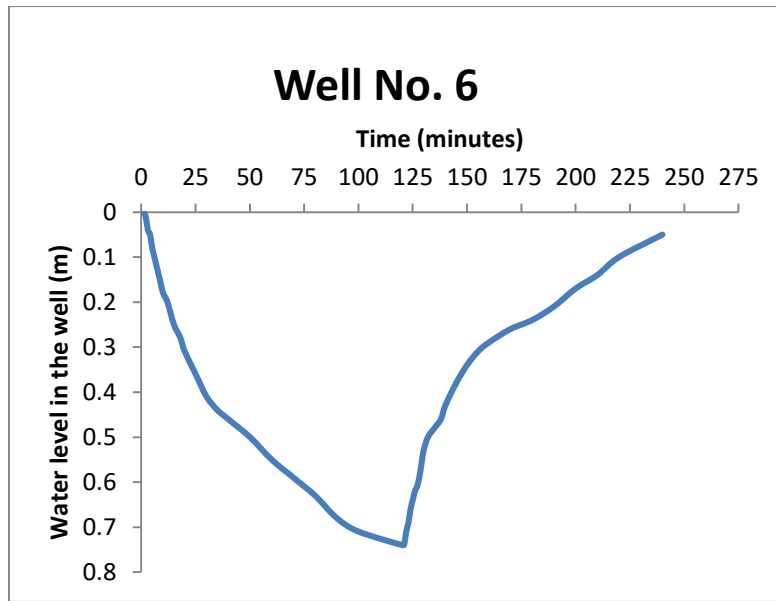


Figure 3.18 Graph of drawdown, recovery versus time for pumping well no. 6

The pumping test data is analysed using AQTESOLV ver.4.5 (Duffield, 2007) software developed for windows. This software is a package for the analysis of aquifer tests with analytical solutions, curve matching tools and report graphics. AQTESOLV applies the principle of superposition in time to simulate variable rate test including recovery by various methods. The data is entered for the pumping or recovery tests using the data set wizard and the results are obtained by choosing an appropriate method for confined, unconfined or leaky aquifer. The aquifer properties are obtained using visual or automatic curve matching. The final output is available in graphical or report formats.

The results obtained by all the three methods closely agree with each other. The parameters obtained by Neuman (1974) method are adopted as an addition to the database in the modelling study in the following chapters. This is because, the assumptions made in this method are much similar to the type of aquifer under study and the circumstances under which the test is carried out. The graphical solutions including displacement versus time curves from the analysis are presented for Neuman (1974) method for well numbers 6 in figure 3.19, as an example. The results of parameters for the Neuman (1974) for all 7 wells are presented in Table 3.2.

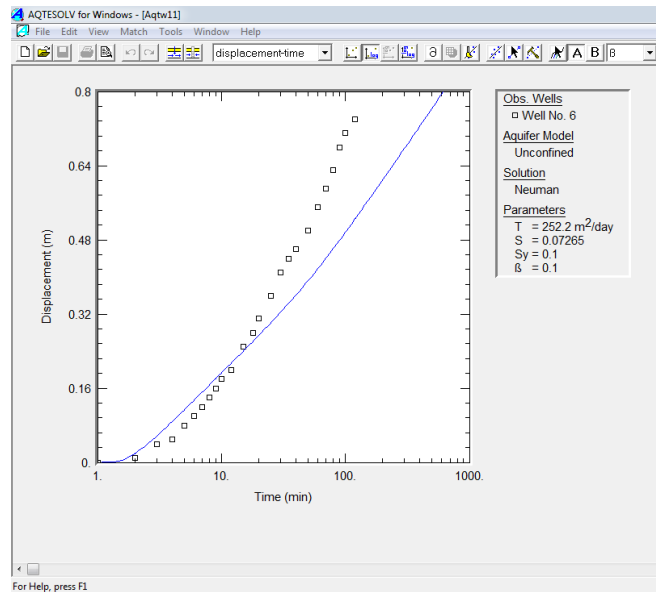


Figure 3.19 Time–drawdown graph of well no. 6 by Neuman(1974) method

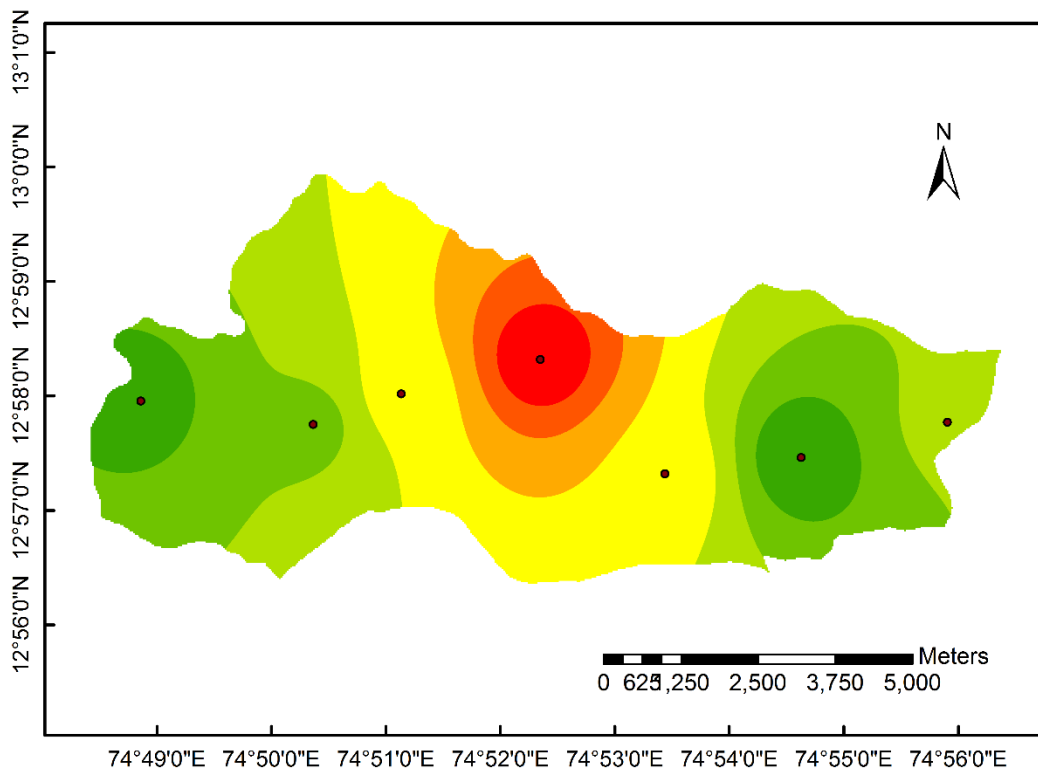
3.4.5 Evaluation of aquifer parameters

The pumping tests and laboratory tests been carried out extensively in the basin adjacent to the study area, by various investigators investigators (Harshendra, 1991; Vyshali, 2008 and Udaykumar, 2008) to explore the hydraulic parameters of the aquifer. Seven pumping tests are carried out in the study as a part of aquifer to add to the earlier studies.

Based on the data obtained for the study area, transmissivity is spatially mapped throughout all the study area using krigging interpolation technique available in ArcGIS 9.3, resulting into seven aquifer hydraulic parameter zones for the study area. Zones 1 represents lowest transmissivity zone and Zone 7 represent high transmissivity zone. The corresponding hydraulic conductivity values are obtained by dividing the transmissivity values by an approximate saturated aquifer thickness for each aquifer zone as initial guess during the calibration of the model. The aquifer property zones mapped for the study area is shown in figure 3.20. The range of initial values of transmissivity and specific yield that is assigned for the study area is presented in Table 3.3. The table shows that, transmissivity ranges between 61 m²/day and 655 m²/day in the entire study area.

Table. 3.3 Range of initial aquifer parameters

Zone	Transmissivity (m ² /day)	Specific Yield, S _y
1	61-146	0.01-0.04
2	147-231	0.009-0.027
3	232-316	0.01-0.023
4	317-401	0.014-0.033
5	402-486	0.023-0.039
6	487-571	0.061-0.082
7	572-655	0.08-0.1



Legend

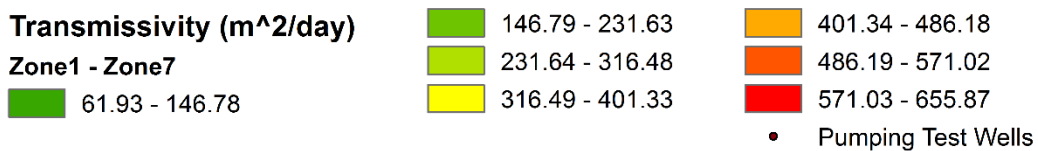


Figure 3.20 Aquifer property zonation map

3.5 CLOSURE

Aquifer characterization is an important part of any groundwater study. In the present study, bore-log data, Vertical Electrical Sounding information and lithology maps obtained are used. In addition to these, pumping tests are also carried out. As per the study, it is found that, the basin is predominantly an unconfined aquifer with depth ranging from 13m to 30m. The lateritic formation is topped by sand followed by the top soil. Beneath the laterite, a huge mass of gneiss is detected up to a depth of about 90m. At the regions where wetlands are situated, sand mixed with silty soil is present. All the seven wells considered for pumping test are shallow with depth less than 10 m. For the analysis of well data, methods most suitable for shallow unconfined aquifer are used. The Theis (1935), Neuman (1974) and Tartakovsky Neuman (2007) methods are adopted for the analysis of pumping test data to find the transmissivity and storage parameters. The results obtained by all three methods closely agree with each other. The parameters obtained by Neuman (1974) method are adopted in the modelling study in the following chapters. The assumptions made in this method are much similar to the type of aquifer under study and the circumstances under which the test is carried out. Based on the available data, aquifer zones each with transmissivity ranging from 61 m²/day to 655 m²/day.

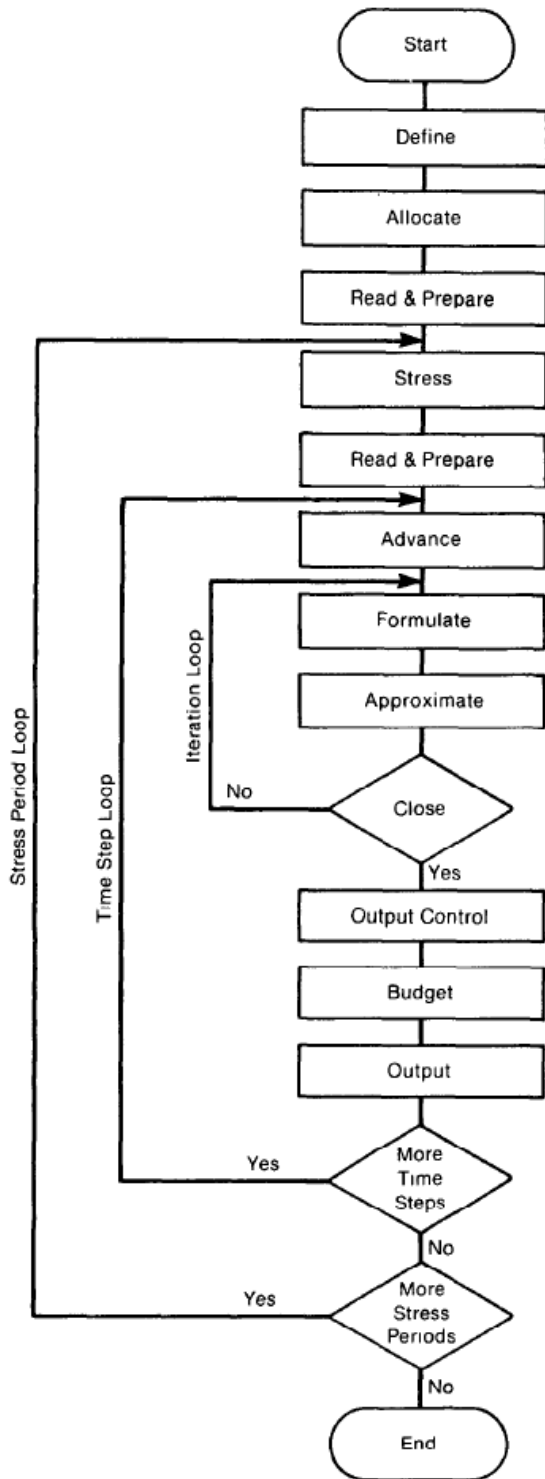
GROUNDWATER FLOW MODELLING**4.1 GENERAL**

Developing a groundwater model is a process where hydrogeological conditions of a specific aquifer region are simulated using mathematical equations, which are solved using computer programming. The conceptual model for the study area is developed using the available geological and hydro-geological data, including the spatial and temporal distribution of groundwater draft and recharge. A modular three dimensional finite difference ground water flow model MODFLOW 2000 (Harbaugh et al., 2000) is used to simulate the groundwater flow, in this study. This model as implemented in the GMS (Groundwater Modelling System) package, version 10.0.1, which is used in this study. The GMS has comprehensive graphical user environment for performing groundwater simulations and have been used by several hydrologists earlier (Feng Sun et al., 2011, Kushwaha et al., 2009; Ahmed and Umar, 2009 and Gates, 2002) to understand and manage various types of groundwater problems. The Aquaveo, LLC in Provo, Utah has developed the GMS interface. The output from the flow model is the hydraulic heads and the water budget. MODFLOW is a 3-D, cell-centered, finite difference, saturated flow model developed by the United States Geological Survey (McDonald & Harbaugh, 1988).

In the present study, the groundwater flow simulation of the aquifer system is carried out in two stages. Initially, a steady state water level for the month of September 2010 is adopted for the steady state calibration of the hydraulic conductivity, as well as for getting an estimate the water balance of the aquifer. In the subsequent step, transient conditions are used (2011-2013) to calibrate the specific yield, hydraulic conductivity and other parameters of the aquifer. The simulation period of two years, is divided into 24 monthly stress periods with daily time step. A stress period represents a period of time during which all model stresses remain constant, e.g. recharge, groundwater abstraction etc. In order to verify the effect of input parameters on simulated heads, the sensitivity analysis is also carried out.

4.2 PROGRAM STRUCTURE

There MODFLOW-2000 computer program modular structure consists of four modularization entities, namely procedures, packages, modules and process. These are illustrated with the help of a flow chart in figure 4.1. Each rectangle is termed a procedure. Prior to entering the stress loop, the program executes three procedures which pertain to the simulation as a whole. The “define” procedure is used to specify the size of the model, the type of simulation (transient or steady state), the number of stress periods, the hydrologic options, and the solution scheme. The “allocate” procedure is used to assign memory space required by the program. The “read and prepare” procedure reads the data that are not functions of time. The work within the procedures is performed by individual subroutines, or modules, called by the main program. The modular structure of the computer program consists of a main program and a series of highly independent subroutines called "modules". The modules are grouped into packages, which deals with a specific feature of the hydrologic system which is to be simulated. Table.4.1 lists the MODLFLOW packages used for the flow simulation in the present study, with a brief description of the package operation. A process is a part of the code that solves a fundamental equation by a specified numerical method. The finite difference equation (4.1) is solved to yield the head at each node. The iterative solution procedure is used to solve for the heads for each time step. Thus, within a simulation, there are three nested loops namely, a stress period loop, within which there is a time step loop, which in turn contains an iteration loop.



DEFINE-Read data specifying number of rows, columns, layers, stress periods, and major program options.

ALLOCATE-Allocate space in the computer to store data.

READ AND PREPARE-Read data which is constant throughout the simulation. Prepare the data by performing whatever calculations can be made at this stage.

STRESS - Determine the length of a stress period and calculate terms to divide stress periods into time steps.

READ AND PREPARE - Read data which changes from one stress period to the next. Prepare the data by performing whatever calculations can be made at this stage

ADVANCE - Calculate length of time step and set heads at beginning of a new time step equal to heads calculated for the end of the previous time step.

FORMULATE - Calculate the coefficients of the finite difference equations for each cell.

APROXIMATE - Make one cut at approximating a solution to the system of finite difference equations.

OUTPUT CONTROL - Determine whether results should be written or saved on disk for this time step. Send signals to the BUDGET and OUTPUT procedures to indicate exactly what information should be put out.

BUDGET - Calculate terms for the overall volumetric budget and calculate and save cell-by-cell flow

terms for each component of flow.

OUTPUT - Print and save heads, drawdown and overall volumetric budgets in

accordance with signals from OUTPUT CONTROL procedure.

Figure 4.1 Flow chart for the program structure of MODFLOW (McDonald and Harbaugh, 1988)

Table. 4.1 The MODFLOW packages used for simulation of groundwater flow

Package name	Description	Reference
Basic (BAS)	The tasks that are part of the model as a whole, such as; specification of boundaries, determination of time-step length, establishment of initial conditions, and printing of results are carried out.	McDonald and Harbaugh(1988)
Layer-Property Flow (LPF)	Performs the cell by cell flow calculations. The input to this package includes layer types and cell attributes such as specific yield and hydraulic conductivity	Harbaugh et al., (2000)
Well (WEL)	The well recharge rate (negative sign indicates discharge) can be defined using parameters. It is a head independent package. Adds terms representing flow to wells to the finite difference equations.	McDonald and Harbaugh(1988)
Recharge (RCH)	The Recharge flux can be defined using parameters. It is a head independent package. Adds terms representing areally distributed recharge to the finite difference equations.	McDonald and Harbaugh(1988)
River (RIV)	The riverbed conductance can be defined using parameters. It is a head dependent package. Adds terms representing flow to rivers to the finite difference equations.	McDonald and Harbaugh(1988)
Drain (DRN)	The drain conductance can be defined using parameters. Adds terms representing flow to drains to the finite difference equations.	McDonald and Harbaugh(1988)

Time-Variant Specified-Head (CHD)	It allows parameters to define the specified head.	Leake and Prudic (1991)
Preconditioned Conjugate Gradient (PCG2)	Method for solving the simultaneous equations resulting from the finite-difference method. It is a solver package.	Hill(1990)

4.3 GOVERNING EQUATION

The Three dimensional movement of constant density groundwater through a porous media is described by the following parabolic partial differential equation, called groundwater flow equation (McDonald and Harbaugh,1988)

$$\frac{\partial}{\partial x} \left\{ K_{xx} \frac{\partial h}{\partial x} \right\} + \frac{\partial}{\partial y} \left\{ K_{yy} \frac{\partial h}{\partial y} \right\} + \frac{\partial}{\partial z} \left\{ K_{zz} \frac{\partial h}{\partial z} \right\} - W = S_s \left\{ \frac{\partial h}{\partial t} \right\} \quad (4.1)$$

where, x, y, z = the cartesian coordinates aligned along the major axes of hydraulic conductivities K_{xx} , K_{yy} , and K_{zz}

h = potentiometric head (L)

S_s =specific storage of the porous material (L^{-1})

t =time (T)

W =volumetric flux per unit volume and represents sources and sinks of water (T^{-1}).

The right hand side of the equation (4.1) is zero for steady state condition. The equation when combined with boundary and initial conditions, describes transient three dimensional groundwater flow in a heterogeneous and anisotropic medium. The groundwater flow process solves the above equation using the finite difference method in which, the groundwater flow system is divided into a grid of cells as represented in Fig. 4.2. There is a single point for each celol, called a node, at which head is calculated. The finite difference equation for each cell is defined as (McDonald and Harbaugh, 1988):

$$CR_{ij-\frac{1}{2},k} (h_{ij-1,k}^m - h_{i,j,k}^m) + CR_{ij+\frac{1}{2},k} (h_{ij+1,k}^m - h_{i,j,k}^m)$$

$$\begin{aligned}
& +CC_{i-\frac{1}{2},j,k}(h_{i-1,j,k}^m - h_{i,j,k}^m) + CC_{i+\frac{1}{2},j,k}(h_{i+1,j,k}^m - h_{i,j,k}^m) \\
& +CV_{i,j,k-\frac{1}{2}}(h_{i,j,k-1}^m - h_{i,j,k}^m) + CV_{i,j,k+\frac{1}{2}}(h_{i,j,k+1}^m - h_{i,j,k}^m) \\
& +P_{i,j,k}h_{i,j,k}^m + Q_{i,j,k} = SS_{i,j,k}(DELR_j \times DELC_i \times THICK_{i,j,k}) \frac{h_{i,j,k}^m - h_{i,j,k}^{m-1}}{t^m - t^{m-1}} \quad (4.2)
\end{aligned}$$

Where,

$h_{i,j,k}^m$ = head at cell i, j, k at time step m (L);

CV, CR and CC = hydraulic conductance values, between node i, j, k and a neighbouring node (L^2/T)

$P_{i,,}$ = sum of coefficients of head from source and sink terms

$Q_{i,,}$ = sum of constants from source and sinks terms, with $Q_{i,j,k} < 0.0$ for flow out of the groundwater system and $Q_{i,j,k} > 0.0$ for flow in (L^3/T)

$SS_{i,,}$ = specific storage (L^{-1})

$DELR_j$ = cell width of column j in all rows (L)

$DELC_i$ = cell width of row i in all columns (L)

$THICK_{i,,}$ = vertical thickness of cell i,j,k (L)

t_m = time at time step m (T).

To designate hydraulic conductance between nodes, as opposed to hydraulic conductance within a cell, the subscript notation “1/2” is used. For example $CR_{i,+1/2},k$ represents the conductance between nodes i, j, k and i, j+1, k. For steady state stress periods, the storage term and therefore the right hand side of equation (4.2) is set to zero.

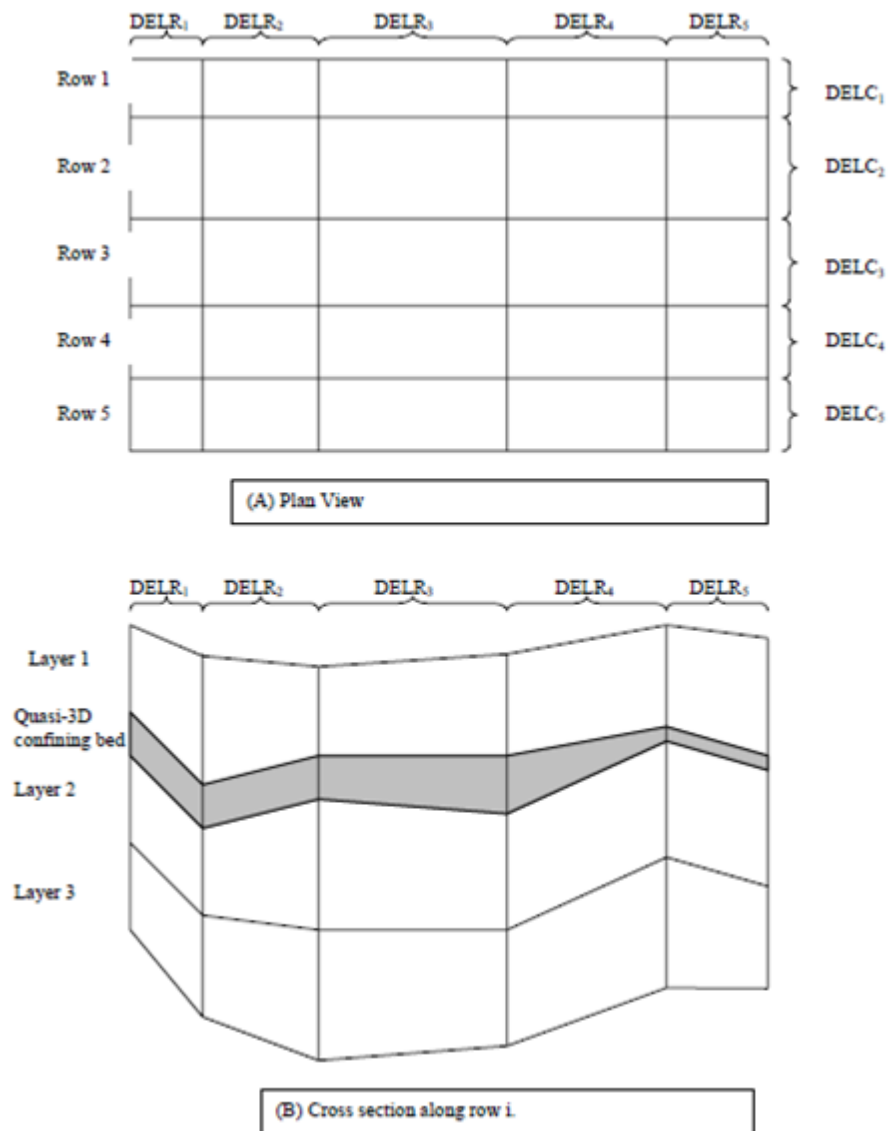


Figure 4.2 Finite difference grid (Harbaugh et al., 2000)

4.4 MODELLING APPROACH

The essential step in model design is conceptual modelling. It helps in understanding the formation of the problem which would assist in determining the approach for modelling. This approach simplifies the field problem and stacks the required field data in a well organised manner for easy analysis of the aquifer system. Further, a conceptual model is very useful tool for identifying data gaps those must be filled before a quantitative model is constructed. The specific steps involved in groundwater flow and solute transport modelling as applied in this study is illustrated in figure 1.1. However, discretization of model domain, sources and sinks, initial and boundary conditions assigned to the model in addition various input parameter in contemplation to groundwater flow model are discussed here.

4.4.1 Data

The details of data collected related to groundwater table and TDS in the study area are mentioned in Table 4.2.

Table 4.2 Availability of water level and TDS data in the study area

Data Period	Data Duration	Source
2011-2015	Fortnightly	Field Visits

The data used in the present study are displayed in APPENDIX II, for typical years.

4.4.2 Discretization of the basin

The boundary of the basin is represented by river on its south and representative ridge line along rest of the part. The aquifer is unconfined, with the ranging between -30m to 151m.

Spatial discretization

The model of the basin has two dimensional grids in the horizontal plane with an approximate cell dimension of 100×100m. The vertical section is represented by a single grid of varying dimension. The digital elevation model as represented in figure 3.2, is interpolated to the top elevation of the model grid. The base of the model layer is set at -30m with respect to mean sea level, which corresponds to the base of the

shallow unconfined aquifer. Table 4.3 shows the details of spatial discretization of basin model.

. Table 4.3 Spatial discretization of basin model.

Origin (UTM WGS 1984, zone 43)		Number of cells		Number of active cells	Surface elevation (m)
x-direction	y-direction	x-direction	y-direction		
520961 E	1436252 N	112	61	5781	2-151

Temporal discretization

The time steps plays an important role in analysing groundwater system. The size of time step depends on the dynamic character of the hydrologic process to be modelled. The aquifer system in the present study is modelled for transient state with daily time step. The steady state simulation is performed prior to transient run, in order to set up initial groundwater head for the transient simulation. The monthly data for the hydrologic stresses (Pumping rate and recharge rate) are assigned to the model as inputs.

4.4.3 Hydrologic sources and sinks

The concept involved in the development of the groundwater flow equation is the continuity equation, which states that, the sum of all flows into and out of the cell must be equal to the rate of change in storage within the cell. The equation stated in earlier section involves all inflows and outflows into a representative finite model domain of the aquifer, with well-known external and internal hydrologic sources as recharge and sinks as groundwater draft. The sinks are analysed as negative sources. In the present model, sources include recharge, mainly from rainfall and sinks are groundwater extractions from agricultural pumping wells.

Groundwater recharge

The groundwater recharge varies spatially, based on factors like rainfall, land use, topography, and soil type. The concept of “recharge coefficient” is used in the present numerical simulation. The recharge coefficient is defined as the ratio of the recharge to

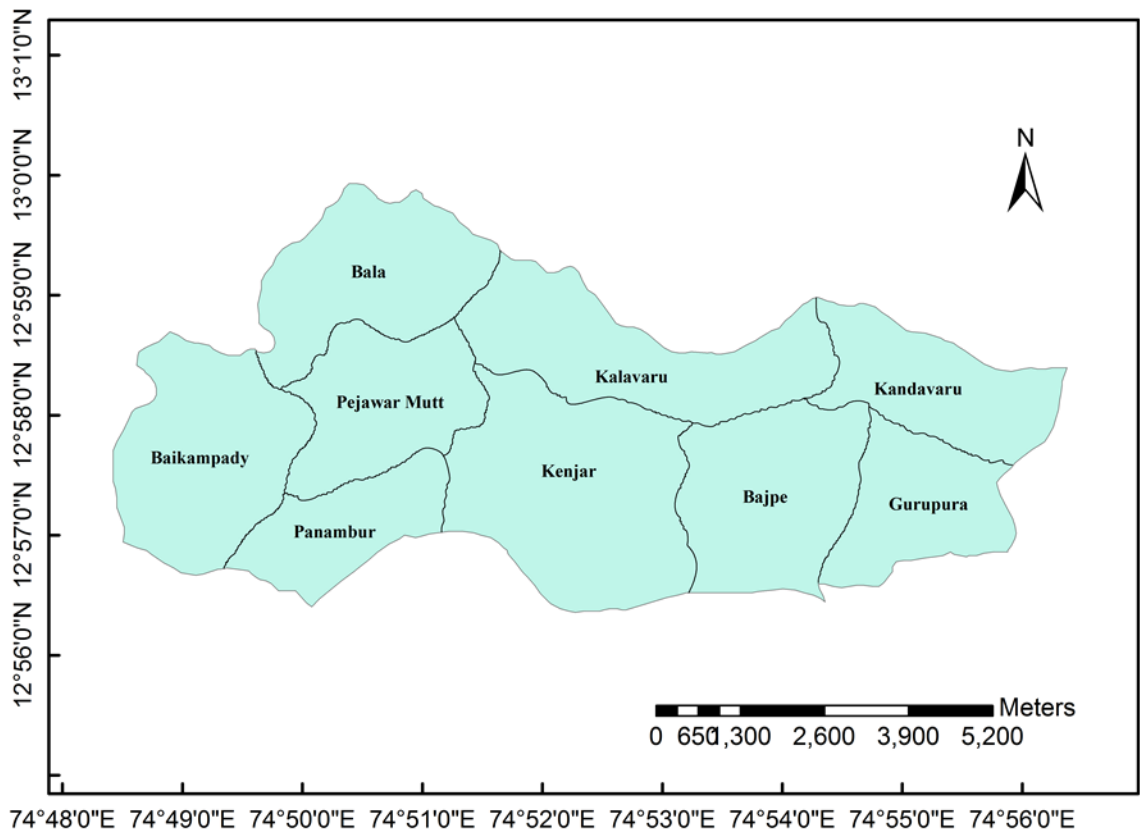
the precipitation. The recharge package (RCH), is used in MODFLOW to simulate the areally distributed recharge to the groundwater system. The natural recharge from rainfall replenishes the aquifer to the saturation level, through infiltration and percolation to the sub-surface soil layers every year due to the copious monsoon rains (June to September) to the extent of about 3000mm. The Groundwater Estimation Committee (GEC, 1997) recommends the recharge coefficient value of 7% for lateritic formations. Further, according to earlier investigation (Udaykumar, 2008) for the area adjacent to the study area, the recharge coefficient was estimated to be 8% to 26.5%. The recharge estimation for the present study is assumed as percentage of the rainfall observed at the nearby meteorological station at Mangalore Airport. The recharge is assigned on the uppermost active wet layer of the model for each vertical column of grid cell and is modified and refined within the specified range during the calibration stage.

Abstractions from agricultural wells

The WEL package in MODFLOW, is used to simulate the wells which withdraw water from the aquifer at a specified rate during a given stress period. The well discharge is handled in the WEL package by specifying the rate Q, at which, each individual well extracts water from the aquifer during each stress period. In order to indicate well discharge, negative values of Q are used. Groundwater in the study area is extensively used for irrigation, industrial and domestic purposes during the summer. In the absence of actual well draft data, the draft per well is assigned based on the water requirement of crops, that is evapotranspiration of 7mm/day, 6mm/day and 5mm/day during the pre-monsoon months (February to May), monsoon months (June to September) and post-monsoon months (October to January) periods respectively as estimated by Kumar (2010), among the region adjacent to the study area. . The village map of Dakshina Kannada district procured from the KRSAC (Karnataka State Remote Sensing Applications Centre) is used to develop a village map for the present study area (figure 4.3). The village-wise data of freshwater draft considered are presented in Table.4.4 Also, the major drafts by the MRPL (1900 m³/day) and the Mangalore Airport (330 m³/day) are considered during the simulation.

Table 4.4. Village-wise details of pumping rates

Village	Area (km ²)	No. of wells	Well draft (m ³ /day)		
			Post-Monsoon	Monsoon	Pre-monsoon
Panamburu	8.21	127	144.54	194.67	245.98
Baikampady	4.42	56	25.65	35.62	24.34
Kenjar	8.98	182	95.54	7.02	8.02
Bajpe	8.77	156	178.21	215.05	257.76
Kalavaru	5.13	57	423.47	429.33	562.23
Pejavara	3.19	43	37.43	44.92	52.41
Kandavara	4.31	52	7.14	8.57	11.23
Gurupura	5.88	71	15.40	18.48	21.56
Bala	4.32	66	63.22	69.07	79.75



Legend

— Village Boundaries

Figure 4.3 Village map of study area

4.4.4 Boundary conditions

The boundary conditions are mathematically classified into Dirichlet (constant head or concentration), Neumann (specific flux), and Cauchy (head-dependent flux or mixed boundary) conditions. Among these, Dirichlet and Neumann boundary conditions are applied to the study area. Apart from these, the pumping or injection wells and physical processes such as evapotranspiration and recharge that impose boundary conditions on the groundwater regime are implemented to equation (4.1) through source/ sink terms.

Dirichlet boundary

The Dirichlet boundary is also called as Type I boundary. The head or concentration value may vary from point to point or as a function of time and is treated as a known quantity in the solution of the equation. A Dirichlet boundary condition of constant head equal to 2 m above mean sea level (AMSL) is assigned to the southern boundary for the model, which corresponds to the Gurupura River, flowing from east to west. The time variant specified head (CHD) package of MODFLOW is used to simulate the Dirichlet boundary condition. The starting and the end node of the arc representing the southern boundary is assigned a value equal to 2. This level is confirmed during low tide along the southern boundary by conducting fly levels. The effect of tidal fluctuation is neglected because of very high computational requirements. However, since the effect of tidal fluctuations (saline water) on groundwater levels is limited to areas very close to the river boundary (less than 500m or so), it's effect on adjoining well field can be neglected when compared to groundwater pumping effects (Narayan et al., 2007). The Dirichlet boundary extends for a distance of 7km along the southern boundary. The figure 4.4 shows the Dirichlet boundary condition applied to the study area.

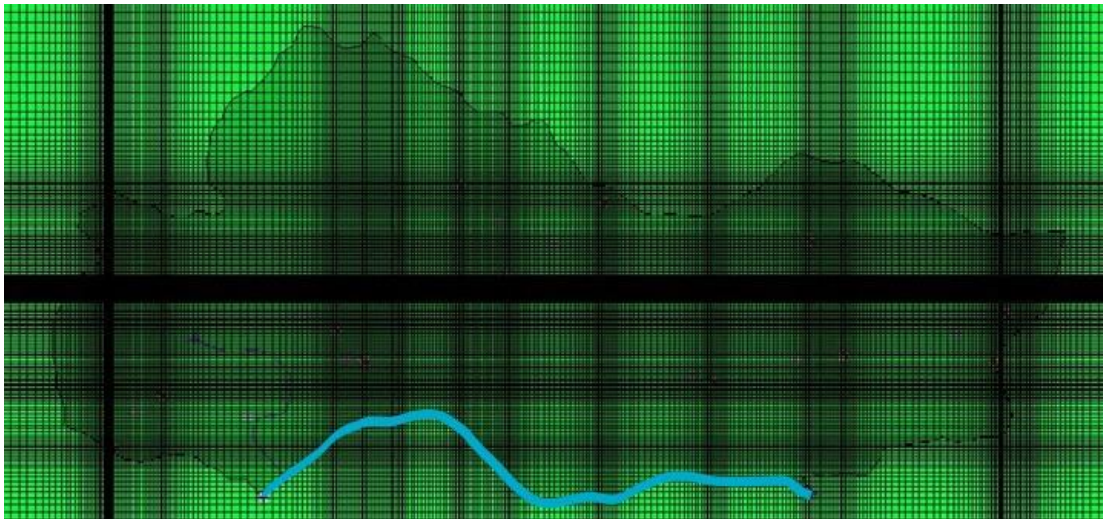


Figure 4.4 Dirichlet boundary condition applied to study area

4.5 MODEL CALIBRATION

The process in which the hydraulic parameters are varied until the simulated values of groundwater heads match the observed groundwater heads, thus improving the accuracy of the model is referred to as the model calibration. The model parameters can either be varied manually or automatically, during calibration process. In the present approach, Parameter Estimation (PEST) version 12.2 (Doherty, 2004) is adopted to calibrate the model. PEST works by making use of a template file containing parameters to be estimated. Before carrying out calibration by PEST, parameters are varied by trial and error method and the model is run several times to obtain the approximate range of parameter values, which is then be used as input for PEST. A comprehensive review of various model evaluation techniques (statistical and graphical) is provided by Moriasi et al. (2007). This would facilitate model evaluation in terms of the accuracy of simulated data compared to measured data. Each method has its own advantages and disadvantages, hence it is desirable to use a combination of different evaluation methods for better estimation of model results. In the present analysis, the model simulated and measured groundwater head are compared using the following four methods, for observing the accuracy of calibration process.

- Slope and y-intercept: The scatter plot of observed and model simulated values are plotted with x and y axes having the same intervals and a 1:1 trend line (or 45° line) is fitted diagonally at point (0,0) across the plot area. This line has a slope of 1 and y intercept of 0 indicating that the model perfectly reproduces the magnitudes of measured data (Willmott, 1981). Hence, the alignment of the scatter plot with the 45° line reveals the reliability of the model results.
- Coefficient of determination (R^2): Describes the degree of co-linearity between simulated and measured data and the proportion of the variance in measured data explained by the model. R^2 ranges from 0 to 1, with higher values indicating less error variance, and typically values greater than 0.5 are considered acceptable (Santhi et al., 2001 and Van Liew et al., 2003).
- Root mean square error (RMSE): RMSE indicate the error between simulated and measured data. RMSE values of 0 indicate a perfect fit. It is calculated as,

$$RMSE = \sqrt{\frac{1}{n} \sum (Y_{obs} - Y_{sim})^2} \quad (4.5)$$

Where, Y_{obs} are observed values and Y_{sim} are simulated values.

- Nash-Sutcliffe Efficiency (NSE): A method recommended for model evaluation by the ASCE (1993) is most commonly used in hydrological applications. This determines the relative magnitude of the residual variance compared to the measured data variance and is calculated as,

$$NSE = 1 - \left(\frac{\sum (Y_{obs} - Y_{sim})^2}{\sum (Y_{obs} - Y_{mean})^2} \right) \quad (4.6)$$

Where, Y_{obs} are observed values, Y_{sim} are simulated values and Y_{mean} are mean of the observed values.

NSE values between 0 and 1 are generally considered as acceptable for model performance and values less than or equal to zero, indicate unacceptable performance.

4.5.1 Groundwater levels using observation wells

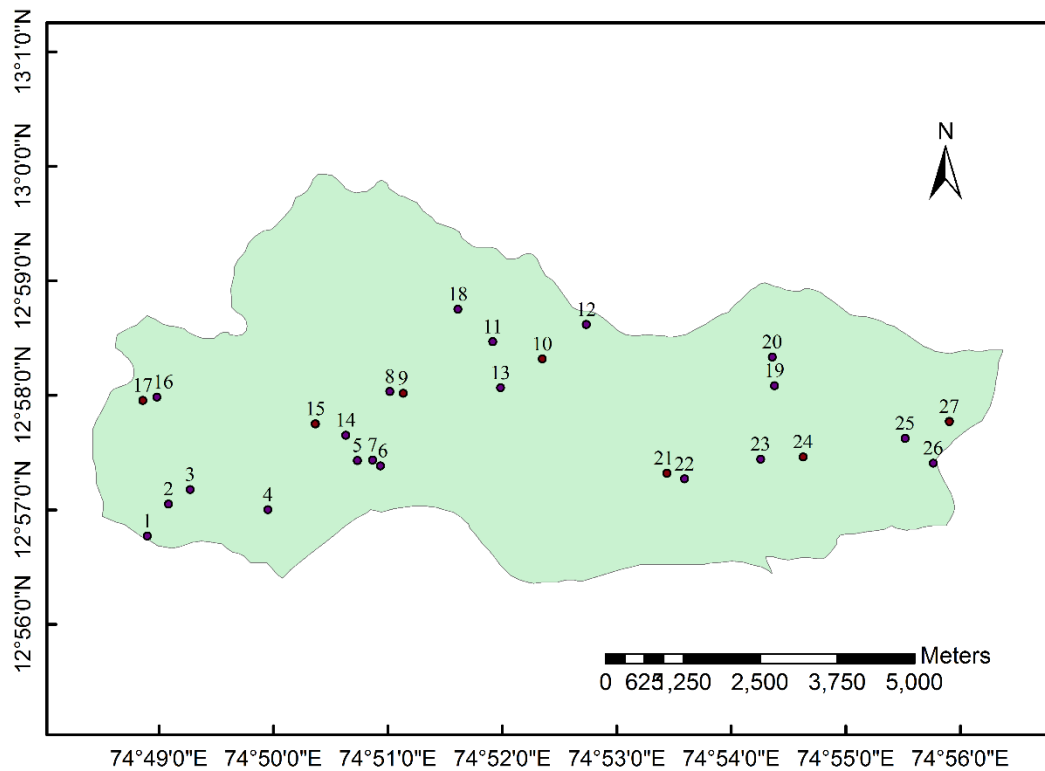
The observed groundwater heads used for transient calibration of the model are obtained from the water levels measured at 31 observation wells on fortnightly basis for a period of 4 years (2011-15). Out of the 31 wells, 4 wells are falling just out of the ridge line. However, Google Earth imagery is used to establish the elevation of well location, in the study. An average error of +1.4m was estimated and was corrected accordingly. To further minimize the errors involved, DGPS (Differential Geographic Positioning System) survey was conducted in order to recalculate hydraulic head from measured groundwater depths.

Differential Geographic Positioning System

The technique of Differential Geographic Positioning System was developed in the early 1980s and is a method of improving the accuracy of the receiver by adding a local reference station to augment the information available from the satellites. An accuracy of up to a centimetre resolution is generally possible with this technique, whereas the non-DGPS can only achieve a resolution of a few meters. In the present study, Trimble® Juno® 3 series handheld instruments along with tripod stand is used for this

purpose. Differential GPS survey is conducted with the utilization of two receivers, one that is stationary and set up at a precisely known location (base or reference receiver) and another will be roving around making position measurements. The stationary receiver compares its calculated GPS location with the actual location based on satellite signals and computes the error associated with the unknown rover position. As the base station is fixed, the difference between the measurement of the base and the rover receivers is used to create an error correction vector. The precise location of the rover can then be calculated by applying the error correction over all the satellite data. The data that is captured is post-processed on a computer using special processing software. In the present work, Trimble® Business Center Software ver.1.10 is used. The details of the observation wells in the study area are given in Table 4.5. Figure 4.6 shows the location of wells in the study area. Figures 4.7.a, 4.7.b, 4.7.c and 4.7.d show the photographs of the wells.

The steps involved in groundwater flow model building is explained in APPENDIX III.



Legend

- Locations of observation wells

Figure 4.6 The study area with well numberings



Well No. 2



Well No. 3



Well No. 4



Well No. 5



Well No. 6



Well No. 7



Well No. 8

Figure 4.7.a Photographs of well no. 1 to well no. 8



Well No. 9



Well No. 10



Well No. 11



Well No. 12



Well No. 13



Well No. 14



Well No. 15



Well No. 16

Figure 4.7.b Photographs of well no. 9 to well no. 16



Well No. 17



Well No. 18



Well No. 19



Well No. 20



Well No. 21



Well No. 22



Well No. 23



Well No. 24

Figure 4.7.c Photographs of well no. 10 to well no. 24



Well No. 25



Well No. 26



Well No. 27



Well No. 28



Well No. 29



Well No. 30



Well No. 31

Figure 4.7.d Photographs of well no. 25 to well no. 31

Table 4.5 Details of observation wells in the study area

SL. No.	Location	Latitude (N)	Longitude (E)	Well Diameter(m)
1	Near NMPT Baikampady	12° 56' 46"	74° 48' 54"	0.8
2	Malabar Oxygen Company Industrial Area, Baikampady	12° 57' 3"	74° 49' 5"	4.5
3	Achal Industries Baikampady	12° 57' 11"	74° 49' 16"	3.7
4	Ruchi Gold, Baikampady	12° 57' 0"	74° 49' 57"	2.33
5	Shri T. Shekhar, Kenjar	12° 57' 26"	74° 50' 44"	4.3
6	Shri Ganapathy Bhatt Pejavar Matt Kenjar	12° 57' 23"	74° 50' 56"	3.75
7	Lalitha Shetty, Jokatte Kenjar	12° 57' 26"	74° 50' 52"	1.65
8	Shobha Kenjar Kana Jokkate	12° 58' 2"	74° 51' 1"	1.36
9	Prabhakar Ganesh Keripa Kenjar Kana Jokkate	12° 58' 1"	74° 51' 8"	2.47
10	Shariabba Tharikamble Bajpe	12° 58' 19"	74° 52' 21"	2.85
11	Opp MRPL Site 3rd Plant Bajpe Road	12° 58' 28"	74° 51' 55"	2.14
12	Nawaz, Bajpe	12° 58' 37"	74° 52' 44"	1.5
13	Chandrahara Bajpe Balikamani Deyavara	12° 58' 4"	74° 51' 59"	4.5

14	Nazir, Kenjar	12° 57' 39"	74° 50' 38"	1.57
15	Railway Colony, Jokatte	12° 57' 45"	74° 50' 22"	0.6
16	Jagnath Shetty, Kulai	12° 57' 59"	74° 48' 59"	2.25
17	Mahabala T Salian House Kulai	12° 57' 57"	74° 48' 52"	1.2
18	Shanthi Gudda Kalavar Govt well	12° 58' 45"	74° 51' 37"	3.38
19	Umavathi Kolambe	12° 58' 5"	74° 54' 23"	2.10
20	Sanju Kulai, Kolambe	12° 58' 20"	74° 54' 22"	2.17
21	Near Govt School Adyapady	12° 57' 19"	74° 53' 26"	2.81
22	Near Panchayet (Govt Well) Adyapady	12° 57' 16"	74° 53' 35"	3.66
23	Bhaskar Mestry Kandavara	12° 57' 27"	74° 54' 15"	2.40
24	Chandra Shetty Kandavara	12° 57' 28"	74° 54' 38"	3.50
25	Pompei church Road Kadavara	12° 57' 37"	74° 55' 31"	3.0
26	V.C.Shekhar Pompei Church Road Kandavara	12° 57' 24"	74° 55' 49"	2.4
27	Alvin paris Kaikamba Road	12° 57' 46"	74° 55' 54"	2.55

4.5.2 Steady state calibration

The groundwater level in the aquifer is said to attain steady state when the flow tend to get balanced and the water levels do not change with time. Such condition may quite

possibly arise more than once in the region. Normally, unless the aquifer system is analysed much beyond in time for past data, it is hard to get the actual steady state condition for a specific period. The limitation of data availability in the study area restricts conducting such precedent investigation. Hence, based on preliminary investigation, the aquifer system was found to be close to steady state condition during September 2010. Therefore, the model was run and calibrated under steady state for this period and the calibrated hydraulic conductivity distribution and overall porosity values are obtained. The head obtained during the steady state calibration is assigned as the starting head for the transient simulation. Altogether, a total of 27 available observation well records are used in the steady state calibration process. The values of statistical parameters obtained as an indication of model performance are: co-efficient of correlation (r) = 0.97, co-efficient of determination (R^2) = 0.96, and root mean square error (RMSE) = 0.98m. A scatter plot of the simulated versus the observed heads is shown in figure 4.8. The plot reveals that, the model fits the observed groundwater heads rather well.

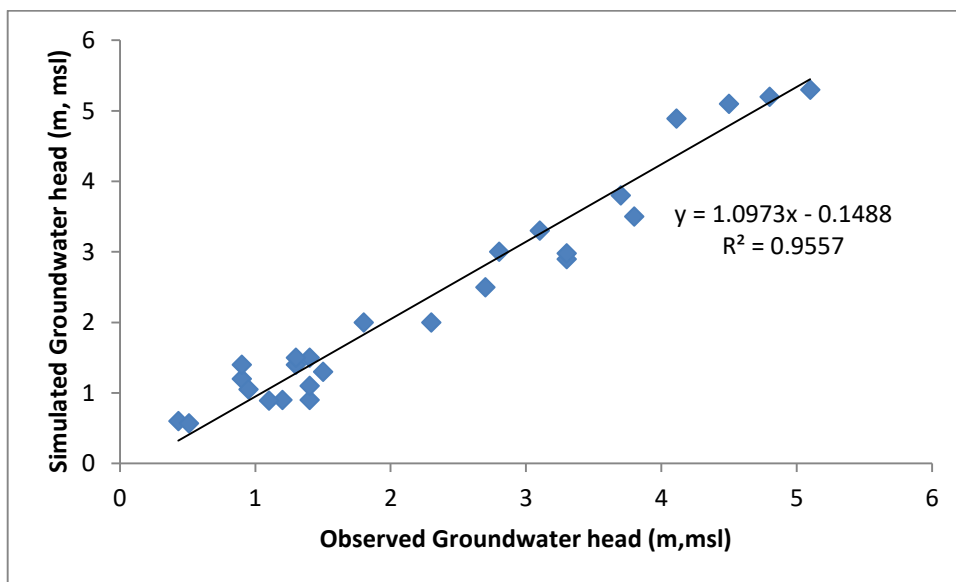


Figure 4.8 Scatter plot for steady state calibration

4.5.3 Transient calibration

The period elapsing September 2011 to August 2013 is adopted for transient calibration. The simulation period of two years was divided into 24 stress periods. Daily time step was considered for the transient simulation applying all the hydro-geologic conditions existing during the same period. The spatial variability of the aquifer parameters and the seasonal performance of the model, were accounted for while carrying out calibration. Other than the aquifer parameters already calibrated in the steady state model namely, the hydraulic conductivity and porosity, the transient calibration requires the specific yield (Sy). After successful calibration, the values of horizontal hydraulic conductivity obtained for the unconfined aquifer was estimated to be in the range 2.54 m/day to 19.16 m/day and specific yield was estimated to be 0.007 to 0.089 respectively. Optimal parameter values obtained after seasonal calibration are given in Table 4.6. The calibrated aquifer parameters obtained for different zones are given in Table 4.7.

Table. 4.6 Optimal parameter values obtained after seasonal calibration

<i>Description of Parameter</i>	<i>Parameter Value</i>
Porosity	30
Recharge coefficient	20%
Horizontal anisotropy	1

Table. 4.7 The calibrated aquifer parameters obtained for different zones

<i>Zone No.</i>	<i>Hydraulic conductivity (m/day)</i>	<i>Specific Yield</i>
1	2.54	0.007
2	3.89	0.013
3	5.72	0.015
4	7.11	0.017
5	10.96	0.031
6	12.37	0.067
7	19.16	0.089

Table 4.8 gives values of R^2 , RMSE and NSE for all months of the calibration period. It is observed that, the model performance is satisfactory as the parameters are well within the acceptable ranges. However, the model performance during the monsoon (June to Sept) is not convincing. All the three evaluation indicators showing deviation

from the acceptable levels. The reason for the deviation could be greater inter mixing of river water with aquifer, additional later inflow/ outflow during monsoon months. This phenomenon is not well addressed by the model. These results may be treated as satisfactory for the model developed with the scarce input data.

Table 4.8 Monthly model efficiency values for flow model during 2011-13

Month	R ²	RMSE (m)	NSE
January	0.91	1.08	0.49
February	0.92	0.92	0.55
March	0.90	0.99	0.47
April	0.92	0.74	0.58
May	0.80	0.71	0.48
June	0.56	2.42	0.36
July	0.52	2.55	0.44
August	0.55	2.36	0.63
September	0.59	2.21	0.57
October	0.61	1.82	0.87
November	0.89	0.97	0.72
December	0.90	1.06	0.69

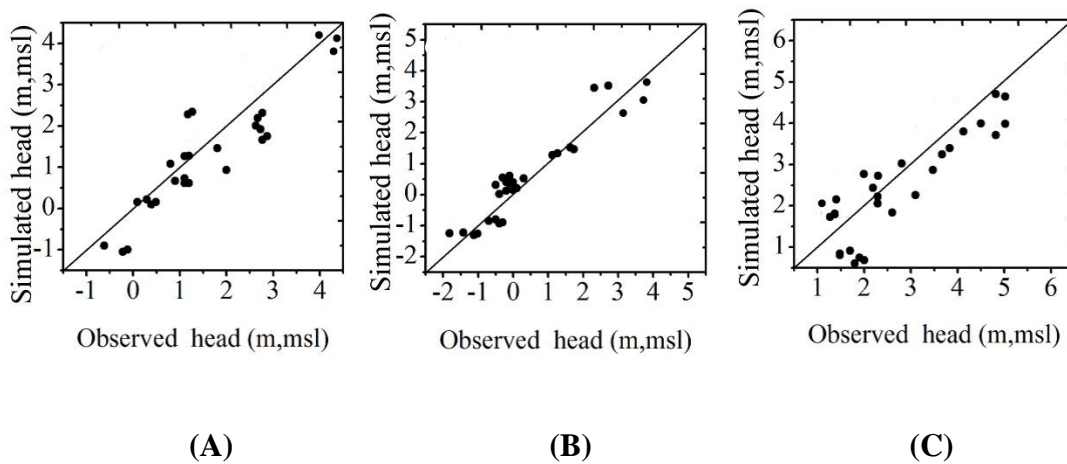


Figure 4.9 Scatter plots of Simulated and observed groundwater heads (2011-13) for seasons (A) Post-monsoon (B) Pre-monsoon and (C) Monsoon

The model performance is presented through scatter plot of selected months in post-monsoon, monsoon and pre-monsoon and are presented in figure 4.9. It is observed that, the graphs show good agreement with the observed and simulated groundwater heads. It is also seen from the graphs that, for the monsoon season, the model tends to under estimate the groundwater head, as few point appear below the 1:1 line. The reason

for this is again could be greater inter mixing of river water with aquifer, additional later inflow/ outflow during monsoon months.

The well hydrographs for the observed and simulated water levels for few selected wells are presented in figure 4.10 a, and 4.10 b which confirms a reasonably good match.

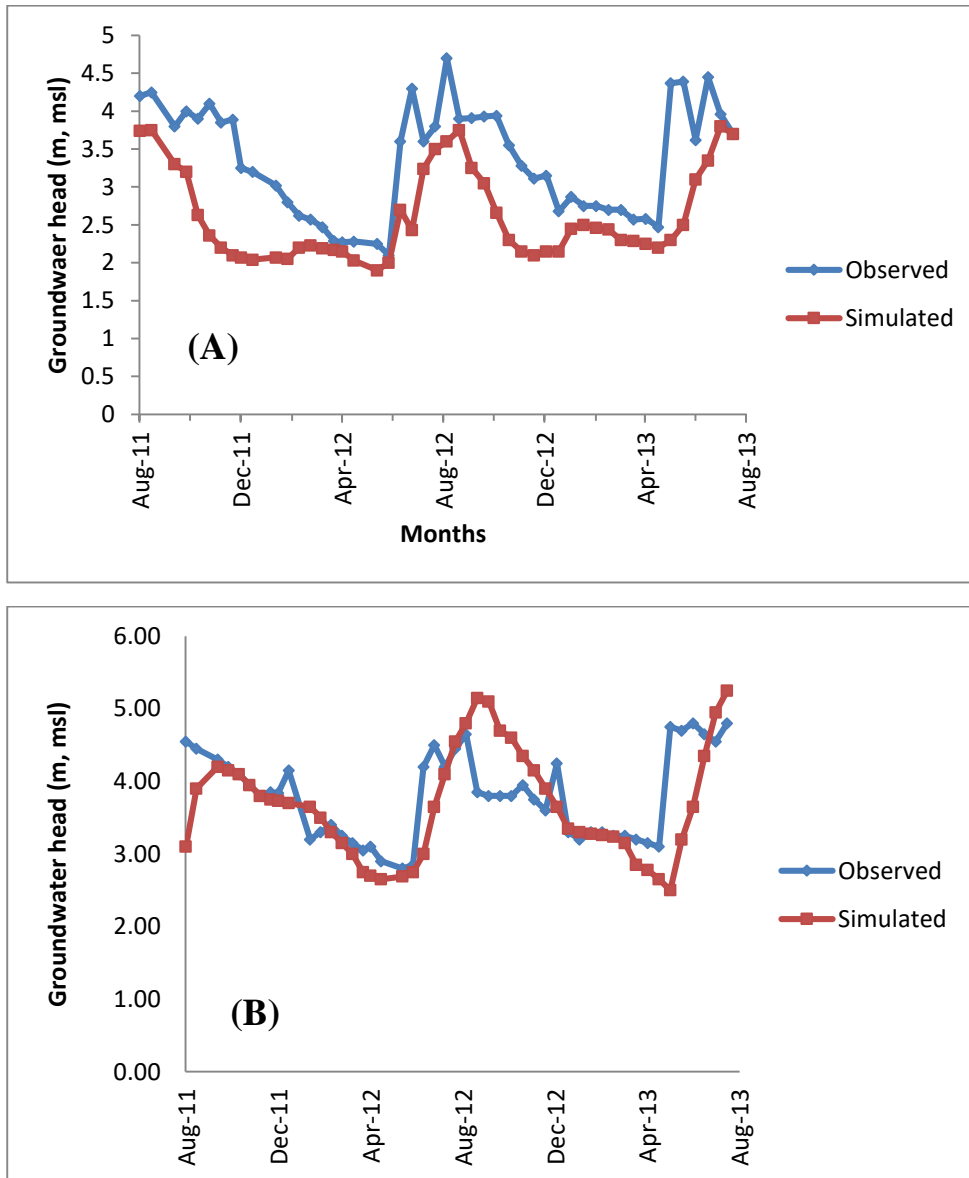


Figure 4.10 a Simulated and observed groundwater heads during the calibration period (2011 – 2013) for (A) well no.3 (B) well no.4

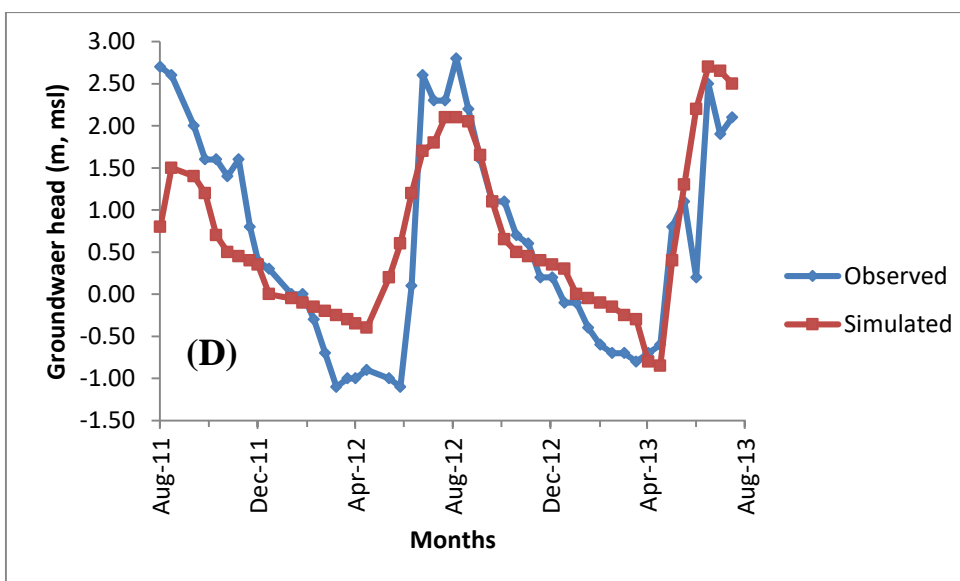
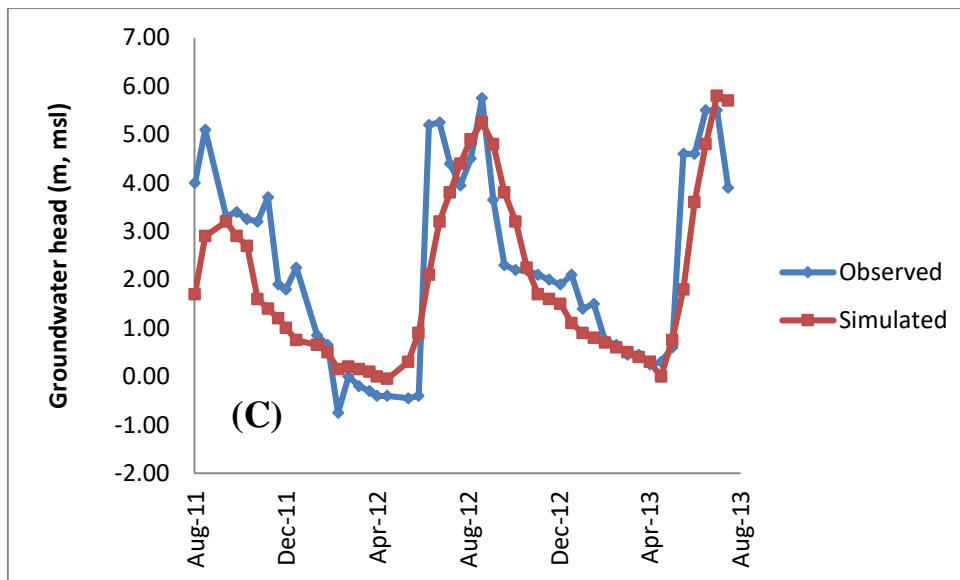
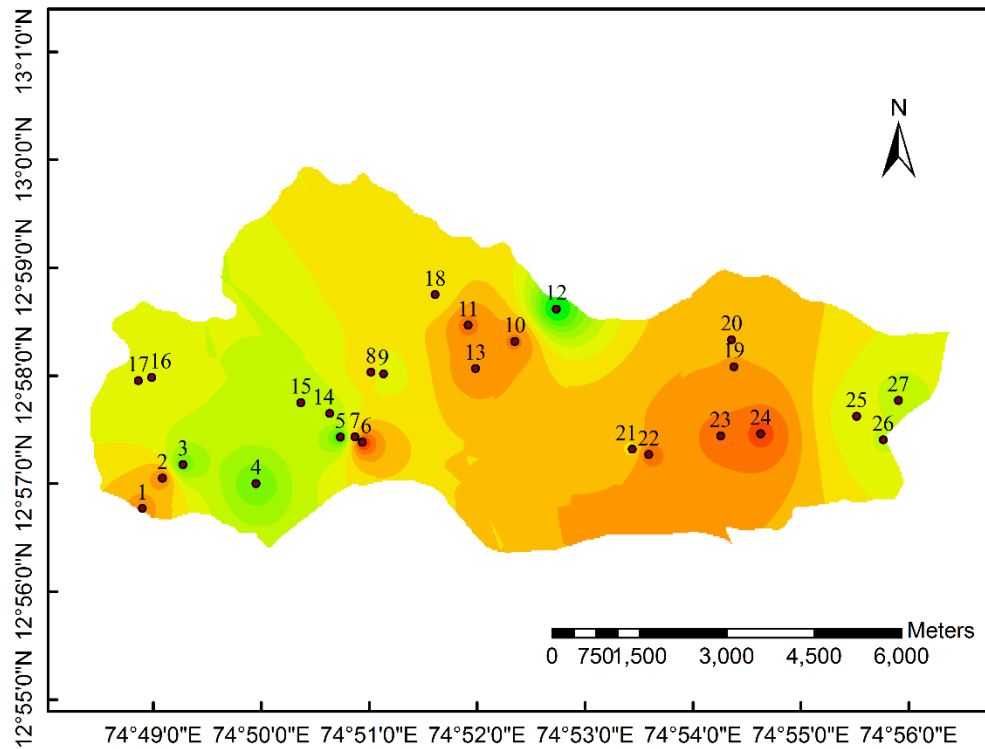


Figure 4.10 b Simulated and observed groundwater heads during the calibration period (2011 – 2013) (C) well no.5 (D) well no.10

The wells 3, 4 and 5 are located around the region where wetland exists. The simulated results for these wells represent presence of groundwater at reasonably higher level even during peak summer. This confirms that, the wetland region is governed by presence of water during summer months, even though there are no other source of water that can feed the wetland system in the study area.

The calibrated groundwater flow pattern for the months of November 2012 to May 2013 are presented in figures 4.11 to 4.17. The flow patterns for the months June, July,

August September and October are not simulated convincingly. This fact is well correlated to the performance statistics evaluation presented in Table 4.8. These water table maps can be compared with that of aquifer zonation map. It can be observed that, the high water table potential zones coincide with that of low hydraulic conductivity zones and similarly, the low water table potential zones coincide with the zones of high hydraulic conductivity. Overall, the simulation results of the basin show a similar trend with the groundwater table gradually increasing from the river boundary at south, towards the landward side. The water table rises to maximum elevation of about 6 m above mean sea level. It is clearly evident from the figures that, the month of May is drier when compared to rest of the months in the year. An important observation is that water table is at higher elevation even during the month of May where wetlands are present in the study area.



Legend

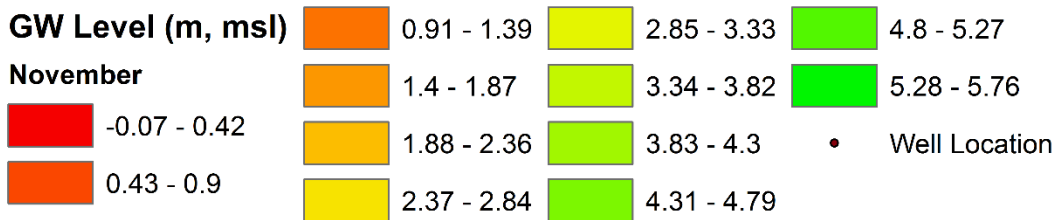
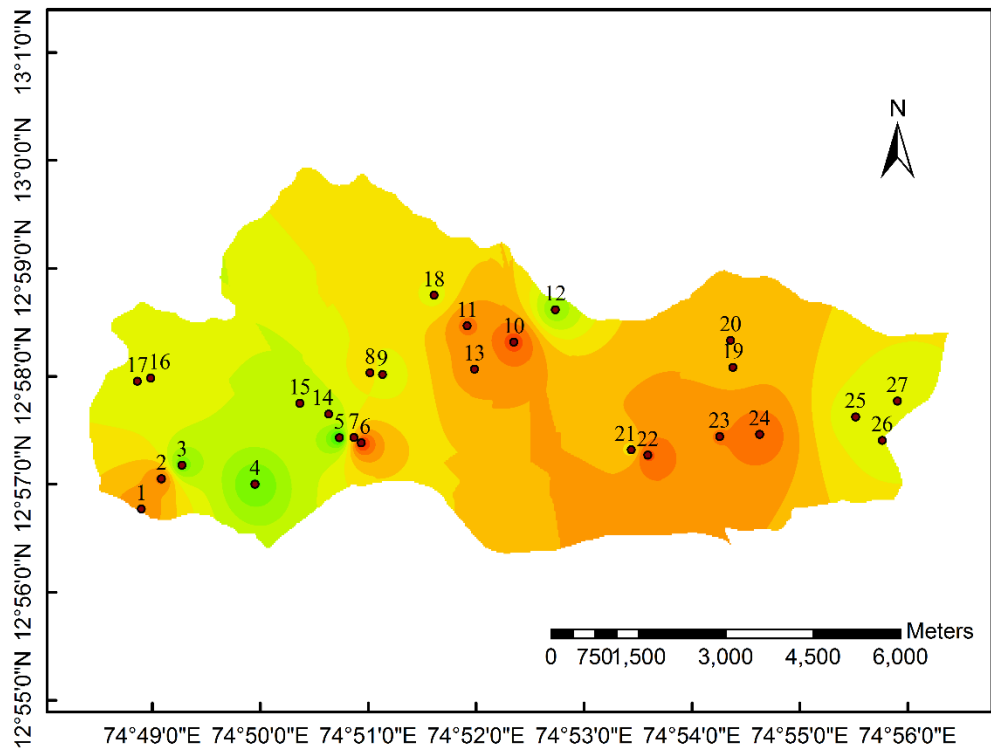


Figure 4.11 Groundwater flow contours for November 2012



Legend

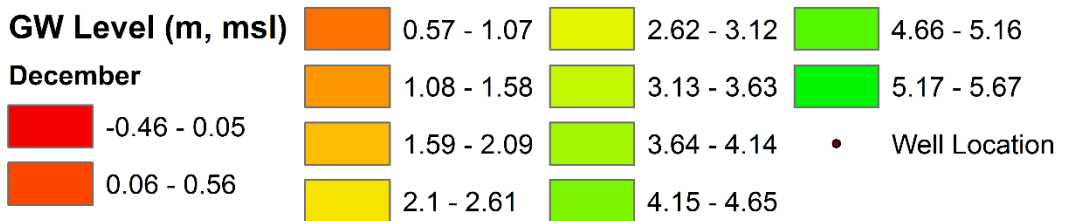
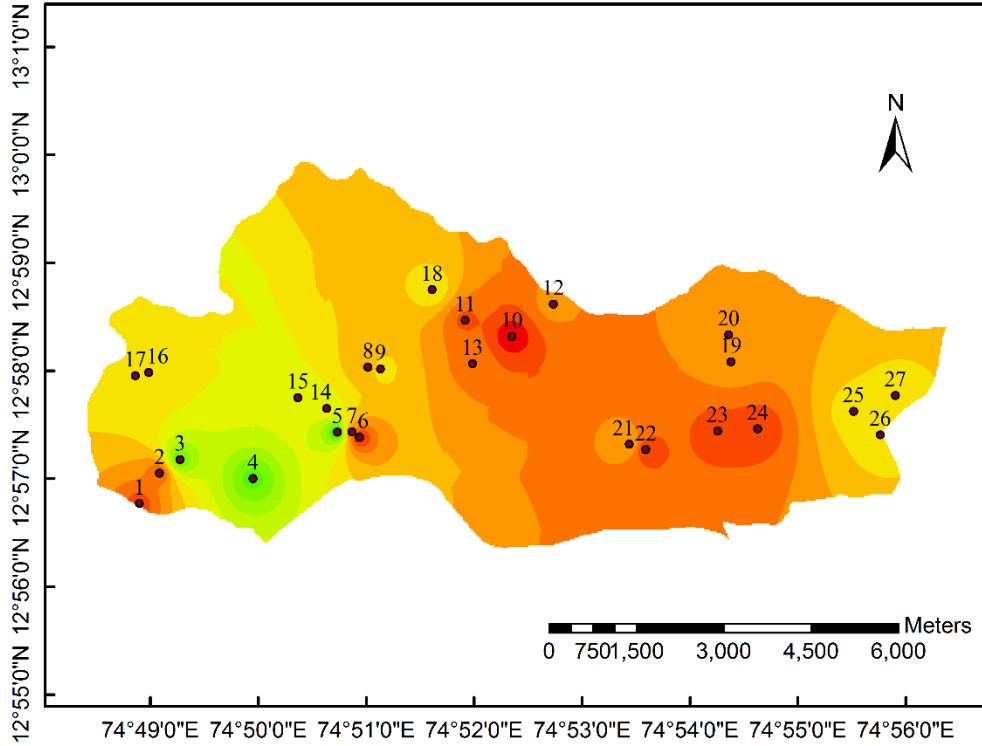


Figure 4.12 Groundwater flow contours for December 2012

Ground Water Table Level - January



Legend

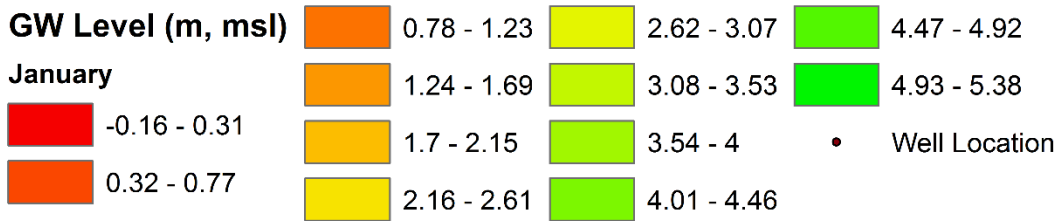
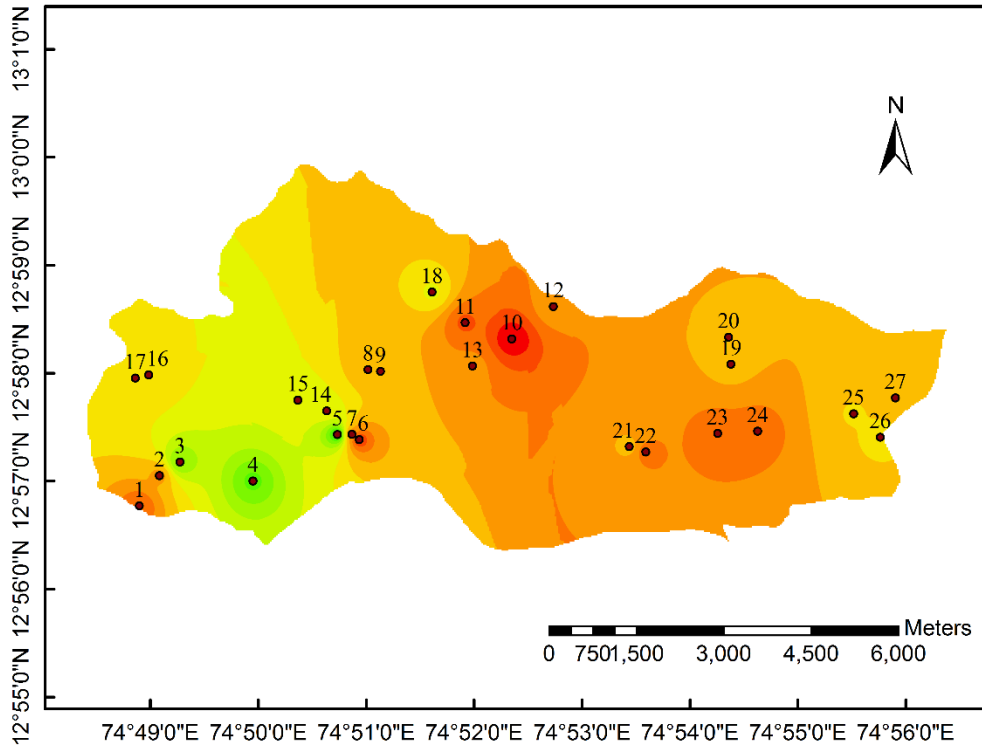


Figure 4.13 Groundwater flow contours for January 2013

Ground Water Table Level - February



Legend

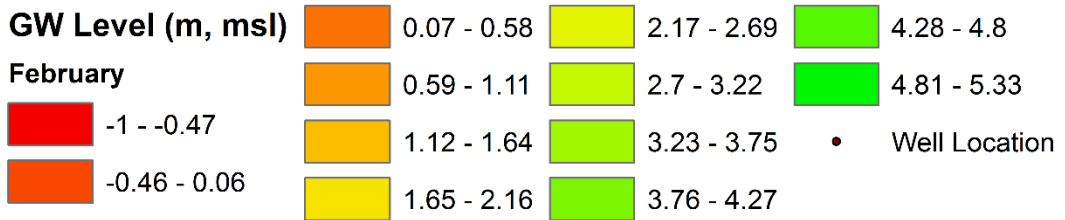
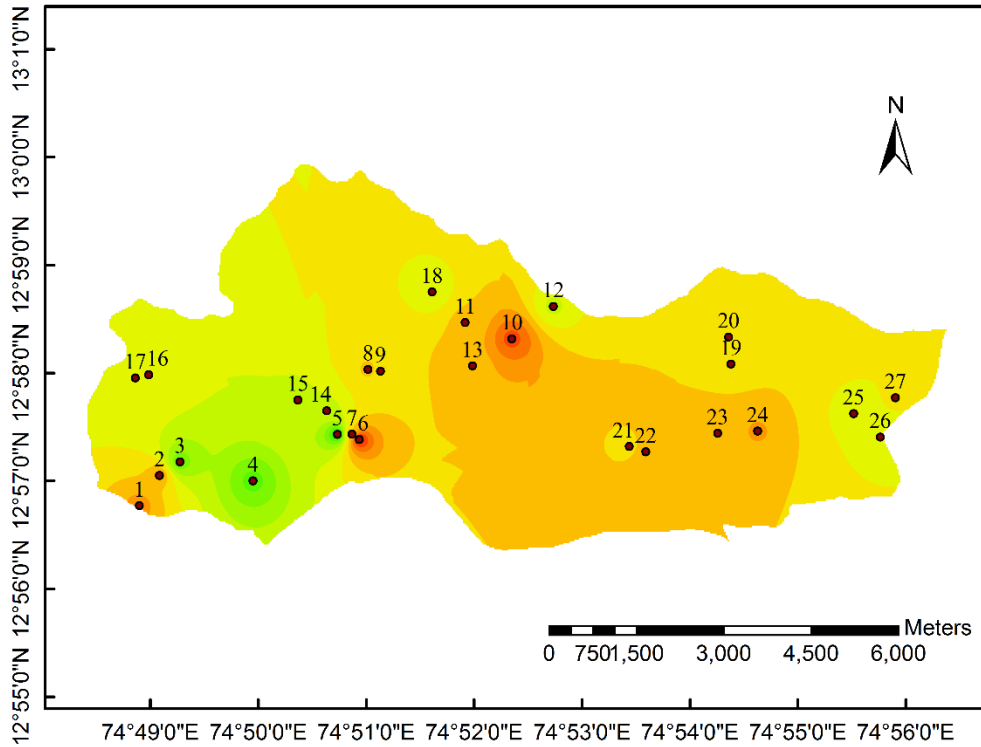


Figure 4.14 Groundwater flow contours for February 2013

Ground Water Table Level - March



Legend

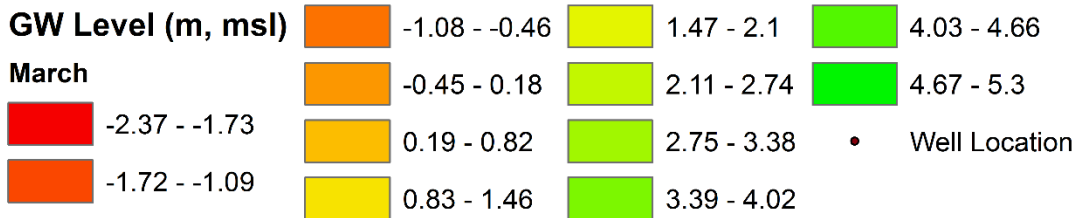
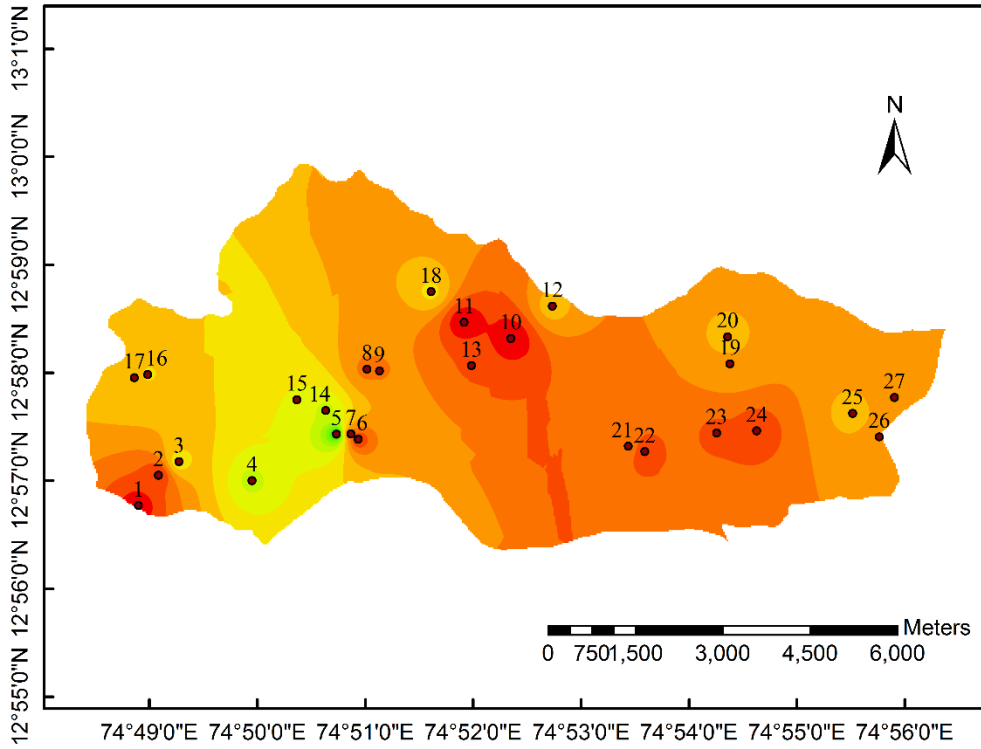


Figure 4.15 Groundwater flow contours for March 2013

Ground Water Table Level - April



Legend








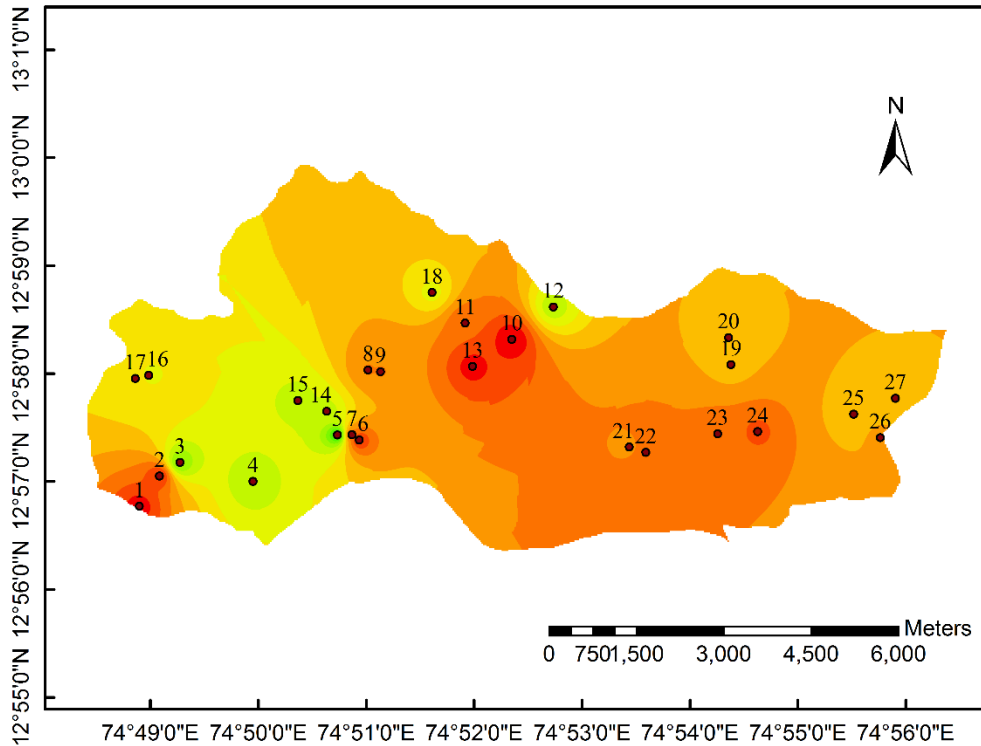
GW Level (m, msl)	0.33 - 0.78	2.14 - 2.58	3.95 - 4.39
April	0.79 - 1.23	2.59 - 3.03	4.4 - 4.84
 -0.58 - -0.13	 1.24 - 1.68	 3.04 - 3.48	 Well Location
 -0.12 - 0.32	 1.69 - 2.13	 3.49 - 3.94	

Figure 4.16 Groundwater flow contours for April 2013

Ground Water Table Level - May



Legend

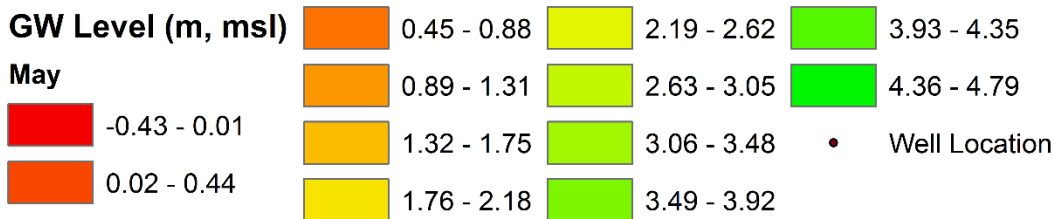


Figure 4.17 Groundwater flow contours for May 2013

4.6 VALIDATION OF FLOW MODEL

The process of validation is essential for checking the authenticity of the model before applying it for prognostic simulation. The validation is carried out for a period of two years during 2013-15 subsequent to the calibration run. The data of 27 wells monitored in the study area are used for validation purpose. The water level is converted to groundwater head in meters above mean sea level, using the grid elevation at the well location.

The R^2 , RMSE and NSE values obtained after analysing the observed and calibrated groundwater head at various observation points are provided in Table 4.9. The results are found to be consistent with that of the calibration results and therefore, the model can be considered reliable for future predictions. To perceive the agreement between the observed and simulated groundwater head data during the validation period, combined scatter plot for two years is presented in figure 4.18. The trend observed from the scatter plot is convincing.

Table.4.9 Groundwater flow model performance during the period 2013-15

Season	R^2	RMSE (m)	NSE
Pre-Monsoon	0.90	0.85	0.51
Monsoon	0.57	2.38	0.52
Post-Monsoon	0.84	1.21	0.68

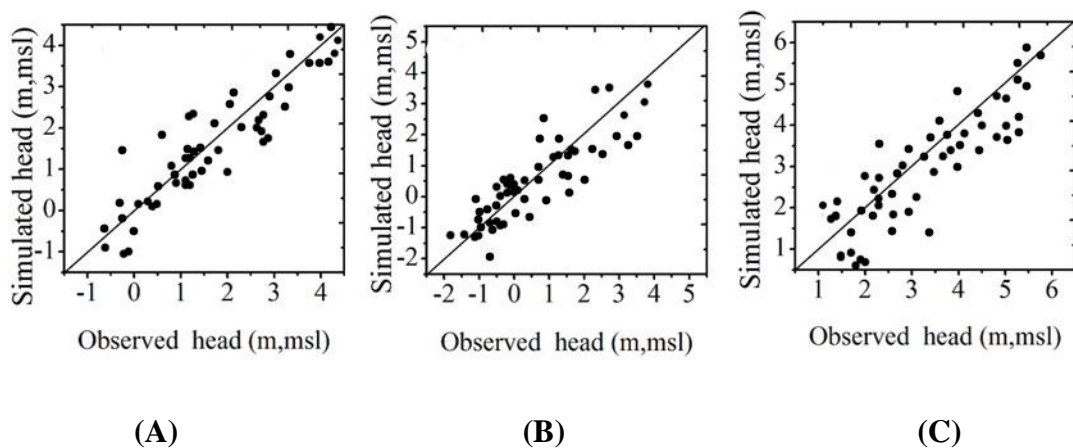


Figure 4.18 Scatter plots of simulated and observed groundwater heads (2013-15) for seasons (A) Post-monsoon (B) Pre-monsoon and (C) Monsoon

4.7 APPLICATION OF FLOW MODEL

4.7.1 The water balance

The results from the MODFLOW are used for running the groundwater mass balance simulation package, “ZONEBUDGET”, which estimates the budget of volumetric flow rate of water in the whole aquifer system under consideration. It uses cell-by-cell flow data in order to calculate the net inflows and outflows for a cell. The water budget of

the model is presented schematically in figure 4.19. The rainfall recharge, contribution from the river, and storage due to aquifer properties form the inflow into the aquifer. The aquifer loses water due to pumping, discharge to the wetland system, river and drains. Table 4.10 presents the volumetric water budget during the monsoon (August) and summer (May). In both cases, the water movement into and out of the aquifer system can be considered dynamically stable, with the percentage discrepancy between the two being almost negligible.

The figures in the Table 4.10 confirm that more than 50% of available water is being discharged to the river during the wet season and during the dry season 82% of water is discharged through the southern boundary. During the dry periods, the volume of water flowing out of the aquifer is lesser than the flow into the aquifer indicating higher probability of contamination ingress from the river carrying salinity during high tides. Since the river is tidal in nature, the contribution of river saline water is considerable to the aquifer system during the non-monsoon months. It is also observed that, major input into the aquifer is through rainfall recharge, contributing to 74% of input.

During the period of maximum potential position (August), the component of groundwater contributing to wetland is 4.5% of total outflow. During dry season with minimum potential head, the groundwater contribution to wetland is 1.4% of total outflow. Rest of the outflow contributes to river discharge and pumping of wells. Hence, the presence of water in the wetland during the non-monsoon months is established by the contribution of only groundwater, in the study area.

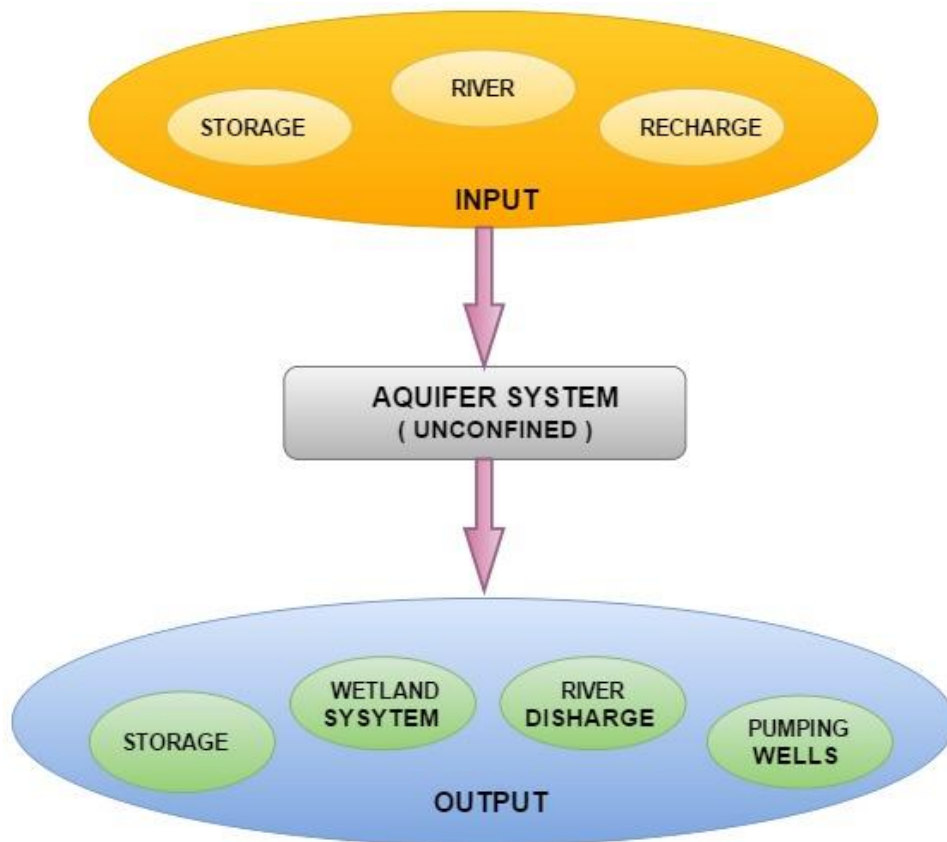


Figure 4.19 Schematic representation of water budget of the aquifer in the study area

Table 4.10 Aquifer volumetric groundwater budget

Water balance component (m ³ /day)	Maximum potential position (August)		Minimum potential position (May)	
	In	Out	In	Out
Storage	0	153008.13	62173.10	0
Pumping wells	0	24493.21	0	28409.18
Wetland	0	17560.39	0	2489.53
River discharge	102270.19	195481.01	117192.85	148415.28
Recharge	288241.33	0	0	0
Total	390511.52	390542.74	179365.95	179313.99
In ~ Out	31.22		51.96	
% Discrepancy	0.008		0.028	

4.8 SENSITIVITY ANALYSIS

4.8.1 General

The sensitivity analysis is an essential part of groundwater modelling (Ting et al., 1998). The sensitivity analysis quantifies the uncertainty in estimating aquifer parameters, stresses and boundary conditions in a calibrated model (Senthil Kumar and Elango, 2004). The groundwater modelling is an approach which involves data intensive operations. Hence, testing the sensitivity of the model to variations among the parameters' values becomes an essential component of groundwater modelling. In the present study, the prime groundwater parameters are systematically varied within appropriate ranges and adopted in the model in order to learn their influence on the model results. The sensitivity of the water table to a particular parameter in the calibrated solution is assessed in the model output. This provides a better understanding of model performance.

4.8.2 Methodology of Sensitivity Analysis

The sensitivity analysis for the present study is carried out by using Sensitivity Index (SI) method. In this method, each of the specific yield, recharge rate and hydraulic conductivity values in the calibrated model were given increments in terms of percentages of values ranging 25%, 50% and 75% and decrements of same ranges of percentages. The sensitivity is expressed by a dimensionless index namely Sensitivity Index (SI), which is the ratio of the relative (absolute) change of model output $|\Delta y|/y_0$ and the relative change of an input parameter $\Delta x/x_0$, i.e. $SI = (|\Delta y|/y_0) / (\Delta x/x_0)$ (Lenhart et al., 2002; Arlai et al., 2006). The calculated sensitivity indices are ranked into four classes, as shown in Table 4.11.

Table 4.11 Sensitivity Index (SI) and Nature of Class (Lenhart et al., 2002)

SI	Nature	Class
$0 \leq II \leq 0.05$	Small to Negligible	I
$0.05 \leq II \leq 0.20$	Medium	II
$0.20 \leq II \leq 1$	High	III
$ II \geq 1$	Very High	IV

4.8.3 Results and discussion

The sensitivity analysis is performed for 27 wells existing in the study area. The sensitivity analysis is conducted for the validation period 2013 - 2015. The hydraulic conductivity, recharge rate and specific yield are the parameters considered to be of prime importance in the study area. The parameter values are picked from the zonal values of parameters, those are obtained after simulations, towards the end of simulation period. The simulated values of parameters are picked from the look-out table. Since these values are zonal values of parameters, the same need to be assigned for specific well locations and the model is run for simulations again, for the entire validation period in order to obtain the unique parameter value to be adopted for sensitivity analysis. This procedure is repeated for all the incremented parameter values and for all the wells in the study area. The values obtained after simulations are considered for the calculations of Sensitivity Index (SI).

Sensitivity Characteristics

The Sensitivity Index as a function of percentage change in Specific Yield, Hydraulic Conductivity and Recharge Rate are plotted and analysed for their characteristics. The sensitivity plots are shown in APPENDIX IV.

Specific Yield (Sy)

Table 4.12 provides location of wells based on sensitivity classification in the study area.

Table 4.12 Sensitivity classification of wells for specific yield

The Sensitivity Classification						
I	II	III	IV	Low for	Low for	Mixed
Small	Medium	High	V. High	Higher Sy	Low Sy	
				High for	High for	
				Low Sy	High Sy	
Well Numbers						
15, 16, 17, 24	1, 2, 3, 4, 8, 18, 19, 20, 21, 23	5, 7 , 22, 25	9, 13	6, 10, 11, 12, 26, 27	NIL	14

The well numbers which are falling under “small” and “medium” sensitivity range happens to fall under Zone 2 of specific yield range as observed in Table 4.7. This zone is represented by second lower region of specific yield values (0.007 and 0.013). The wetland is located in the same region of the study area. The observation from the sensitivity analysis is that, the aquifer feeding to the wetland is having lower sensitivity to specific yield.

The wells 5, 7, 22 and 25 fall under sensitivity classification “High”. This region falls under Zone III of specific yield distribution in the study area, as per Table 4.7 (0.015). The wells 9 and 13 happens to be having “Very High” sensitivity towards specific yield in the study area. While the well 13 is located in a region having highest specific yield value (0.089) among the zones, that is Zone V.

Hydraulic Conductivity (k)

The hydraulic conductivity is considered to be the important parameter when it comes to the sensitivity of the aquifer in the study area. It is observed that, a small percentage of change in hydraulic conductivity causes a considerable change in the hydraulic head all through the study area. Table 4.13 represents classification of wells based on Sensitivity Index.

Table 4.13 Sensitivity classification of wells for hydraulic conductivity

The Sensitivity Classification						
I Small	II Medium	III High	IV V. High	Low for Higher h High for Low h	Low for Low h High for High h	Mixed
Well Numbers						
NIL	18, 19, 20, 24,	1, 2, 3, 5, 8, 9, 16, 17, 21, 22, 23,	10, 11, 12, 26, 27	4, 6, 24	NIL	7, 13, 14, 15

The well numbers 1,2,3,5,16 and 17 are falling in Zone 2 of hydraulic conductivity range as per Table 4.7, with a lower hydraulic conductivity value (3.89 m/day). These wells are marked with SI as “High”. The wetland is located in this region of lower hydraulic conductivity, which is a conducive environment for existence of wetlands. This region is also in the near vicinity of coast and river boundary at south. The variation of levels in the sea as well as river has a greater influence on the groundwater table in this region. This observation is supported by higher sensitivity index.

The wells 18, 19 and 20 are having medium sensitivity index. These are the wells located towards northern boundary of the study area. The wells 10, 11, 12, 26 and 27 are the wells with “Very High” sensitivity index. These wells are located very close to the no flow boundary.

Response to Hydrological Stress through Aquifer Sensitivity: Recharge rate (r)

The aquifer sensitivity to the applied hydrological stresses, namely areal recharge rate is tested by conducting a similar process with increment and decrement of values with respect to the calibrated parameter values. The areal recharge due to precipitation considered in the present study was found to be the most sensitive parameter. The recharge rate has a considerable effect on the system in areas with a shallow water table.

Table 4.14 gives the distribution of sensitivity index amongst all the wells in the study area.

Table 4.14 Sensitivity classification of wells for recharge rate

The Sensitivity Classification						
I	II	III	IV	Low for Higher r High for Low r	Low for Low r High for High r	Mixed
Small	Medium	High	V. High			
Well Numbers						
NIL	24,	5, 6, 7, 8, 14, 15, 16, 17, 18, 19, 20, 23,	1, 2, 3, 4, 9, 10, 11, 12, 13, 21, 22, 25, 26, 27	NIL	NIL	NIL

The stretch of the aquifer in the study area consisting of wells 1,2,3,4,5,6,7,14 and 15 exhibit high to very high sensitivity trend to recharge rate. This region is marked as shallow water region of the aquifer. The wetland is also existing in this region. Due to the lateral inflow in this zone, the effect of rainfall recharge gets reduced. The aquifer gets recharged sooner due to high sensitivity of aquifer towards recharge rate and shallow water conditions in the region. This region is geographically located closer to coast on western side and river on southern side. The difference in hydraulic gradient between aquifer water table and phreatic surface of river as well as sea will have the contribution in keeping the recharge rate to have higher sensitivity to recharge rate. The sensitivity class of the model due to recharge rate can be categorised into III and IV, with sensitivity index increasing beyond 0.20 and 1.00 over the entire aquifer. Also, the model is extremely sensitive to the higher values of recharge rate as compared to lower values.

4.9 CLOSURE

The numerical groundwater simulation is carried out using MODFLOW for effective assessment of groundwater resources in a tropical, coastal aquifer comprising of wetland. The study is focused on a shallow, lateritic, unconfined aquifer, with good groundwater potential. This kind of study gives insight into the river–aquifer interaction, with quantitative estimates, especially to understand the contribution of groundwater to a wetland present in the study area.

The results of calibration are analysed using graphical as well as analytical methods. The analysis confirms that, there exists a reasonably good correlation between the simulated and observed water levels, with R^2 ranging from 0.61 to 0.92, except for the monsoon months. The RMSE and NSE (≥ 0.5) values also exhibit similar satisfactory trend. However, the summer months give good results, which are more critical for the investigation on contamination ingress. After successful transient calibration, recharge co-efficient of 20% of rainfall and porosity of 30% are obtained as suitable parameters. The calibrated values of various hydraulic properties of the aquifer are appropriately within the range established by the earlier studies. Also, the values of horizontal hydraulic conductivity and specific yield of the unconfined aquifer is estimated to be in the range 2.54m/day to 19.16 m/day and 0.007 to 0.089 respectively.

The model is validated with reasonable accuracy having $R^2 > 0.80$, for future applications. The water budget analysis reveals the water movement process and the volume of water exchanged internally and across the aquifer boundaries. The water budget study provides an indication for the possible saltwater intrusion into the low lying areas during the dry periods, through the tidal river flowing at the southern boundary of the river. The river-aquifer interaction study carried out in the present work indicates that, a good amount of river water is being lost into the river throughout the year. The groundwater budget confirms that, the wetland present in the study are is having a considerable contribution from the groundwater, especially during dry periods. The results of sensitivity analysis clearly shows that, the overall aquifer system is sensitive to hydraulic conductivity and recharge rate. The model is sensitive to lower values of hydraulic conductivity and higher values of recharge rate. The results also show that, specific yield is a sensitive parameter.

SOLUTE TRANSPORT MODELLING

5.1 GENERAL

The Modular 3-D Multi-Species Transport Model, referred to as MT3DMS, is unique in that it includes the three major classes of transport solution techniques in a single code, i.e., the standard finite difference method; the particle-tracking-based Eulerian-Lagrangian methods; and the higher-order finite-volume TVD (Total Variation Diminishing) method. The combination of these solution techniques, each having its own strengths and limitations, is believed to offer the best approach for solving the most wide-ranging transport problems with desired efficiency and accuracy.

MT3DMS can be used to simulate changes in concentrations of miscible contaminants in groundwater considering advection, dispersion, diffusion and some basic chemical reactions, with various types of boundary conditions and external sources or sinks. The basic chemical reactions included in the model are equilibrium-controlled or rate-limited linear or non-linear sorption, and first-order irreversible or reversible kinetic reactions. More sophisticated, multispecies chemical reactions can be simulated by add-on reaction packages. MT3DMS can accommodate very general spatial discretization schemes and transport boundary conditions, including: 1) confined, unconfined or variably confined/unconfined aquifer layers; 2) inclined model layers and variable cell thickness within the same layer; 3) specified concentration or mass flux boundaries; and 4) the solute transport effects of external hydraulic sources and sinks such as wells, drains, rivers, areal recharge and evapotranspiration. MT3DMS is designed for use with any block-centered finite-difference flow model, such as the U.S. Geological Survey modular finite-difference groundwater flow model, MODFLOW, under the assumption of constant fluid density and full saturation. However, MT3DMS can also be coupled with a variably saturated or density-dependent flow model for simulation of transport under such conditions.

The solutions to these complex governing equations were sought using numerical techniques, in the recent past [(SUTRA code (Voss, 1984), HST3D code (Kipp, 1986), SEAWAT (Guo and Bennett, 1998) and MOCDENS3D (Essink, 1998)], which enables thorough three dimensional modeling of freshwater-seawater interactions. For site specific and hypothetical cases, SEAWAT model was extensively used by researchers all over the world (Chang and Clement, 2013; Praveena et al., 2011; Vandenbohede et al., 2014; Cobaner et al., 2012; Lin et al., 2009; Gates et al., 2002; El-Kadi et al., 2014; Qahman and Larabi, 2006; Bauer et al., 2006) wherein the objective has been to assess the sustainable use of groundwater resources in the coastal aquifers and predict the freshwater–saltwater interface. For the current work for modelling solute transport, SEAWAT package is used.

5.2 BASIC PRINCIPLES AND CONCEPTS OF SEAWAT

5.2.1 Description of the Model

The simulation of three dimensional, variable-density ground-water flow and multi-species transport is achieved by SEAWAT, wherein MODFLOW (Harbaugh et al., 2000) and MT3DMS (Zheng and Wang, 1999; Zheng, 2006) are coupled together. The effects of density differences due to mixing of high salt concentrations in seawater with freshwater is observed to be predominant in the coastal groundwater system. Hence, the coupling of MODFLOW and SEAWAT becomes inevitable. The SEAWAT is one of the widely used codes to simulate saltwater intrusion (Werner et al., 2013).

The Variable-Density Flow (VDF) process in SEAWAT is based on the constant-density Ground-Water Flow (GWF) process of MODFLOW-2000. The VDF process uses the familiar and well established MODFLOW methodology to solve the variable-density ground-water flow equation (Langevin et al., 2003).

The MT3DMS (Modular Three Dimensional Multispecies Transport Model) which is a part of SEAWAT, referred to as the Integrated MT3DMS Transport (IMT) Process, solves the solute transport equation. Both the flow and transport equations are solved during one SEAWAT time step. However, the MODFLOW is modified in the SEAWAT version, in a way that fluid mass is conserved instead of fluid volume and the Darcy's equation is solved to obtain the variable density flow in terms of an

equivalent freshwater head. The Darcy's law which describes the fluid flow in the porous medium and the equations of continuity that relates the fluid mass conservation and solute advection–diffusion are solved simultaneously in the process.

In MT3DMS, MT3D stands for the Modular 3-Dimensional Transport model, and MS denotes the Multi-species structure for accommodating add-on reaction packages. It is based on the assumption that changes in the concentration field will not affect the flow field significantly (Zheng and Wang, 1999). MT3DMS computer program uses a modular structure similar to MODFLOW (McDonald and Harbaugh, 1988) and consists of a main program and a large number of highly independent subroutines, called modules, which are grouped into a series of packages. The MT3DMS packages deals with a single aspect of the transport simulation. The solution scheme of third order TVD (ULTIMATE) is used in advection package and modified incomplete Cholesky pre-conditioner is used in GCG (Generalized Conjugate Gradient) solver in the current transport simulation. The transport packages used in the present study are listed in table 5.1 with a brief description of operations involved.

Table. 5.1 The MT3DMS packages used for solute transport modelling

Package name	Description	Reference
Basic transport (BTN)	Handles basic tasks that are required by the entire transport model. Among these tasks are definition of the problem, specification of the boundary and initial conditions, determination of the step size, preparation of mass balance information, and printout of the simulation results.	Zheng and Wang (1999)
Flow Model Interface (FMI)	FMI Interfaces with a flow model. The FMI package prepares heads and flow terms in the form needed by the transport model.	Zheng and Wang (1999)
Generalized Conjugate Gradient Solver (GCG)	If the GCG solver is selected, dispersion, sink/source, and reaction terms are solved implicitly without any stability constraints.	Zheng and Wang (1999)

Advection (ADV)	Solves the concentration change due to advection with an explicit scheme or formulates the coefficient matrix of the advection term for the matrix solver.	Zheng and Wang (1999)
Dispersion (DSP)	Solves the concentration change due to dispersion with the explicit finite difference method.	Zheng and Wang (1999)
Source/Sink Mixing (SSM)	Solves the concentration change due to sink/source mixing explicitly or formulates the coefficient matrix of all sink/source terms for the matrix solver.	Zheng and Wang (1999)
Utility (UTL)	Contains utility modules that are called upon by primary modules to perform such general-purpose tasks as input/output of data arrays.	Zheng and Wang (1999)

5.2.2 The SEAWAT Program Structure

In the coastal aquifers, it is observed that, there exists a complex process due to the non-uniform distribution of high concentration solute. Large density variation arise in the saline groundwater, due to the increase in concentration of solute which in turn affects the flow of groundwater in coastal aquifers. Therefore, in the variable-density flow and transport, the groundwater flow equation and the solute transport equation are coupled with each other by an equation of state for the density as a function of the solute concentration. As the flow is unaffected by the consequent concentration solution of the transport equation, the simulation is less complicated in the constant-density groundwater flow and solute transport modelling.

In the present study, the coupling between flow and transport is performed through a synchronous time stepping approach that cycles between MODFLOW solutions of the flow equation and MT3DMS solutions of the transport equation using an iterative computational process. The flow chart of the SEAWAT program is shown in figure 5.1.

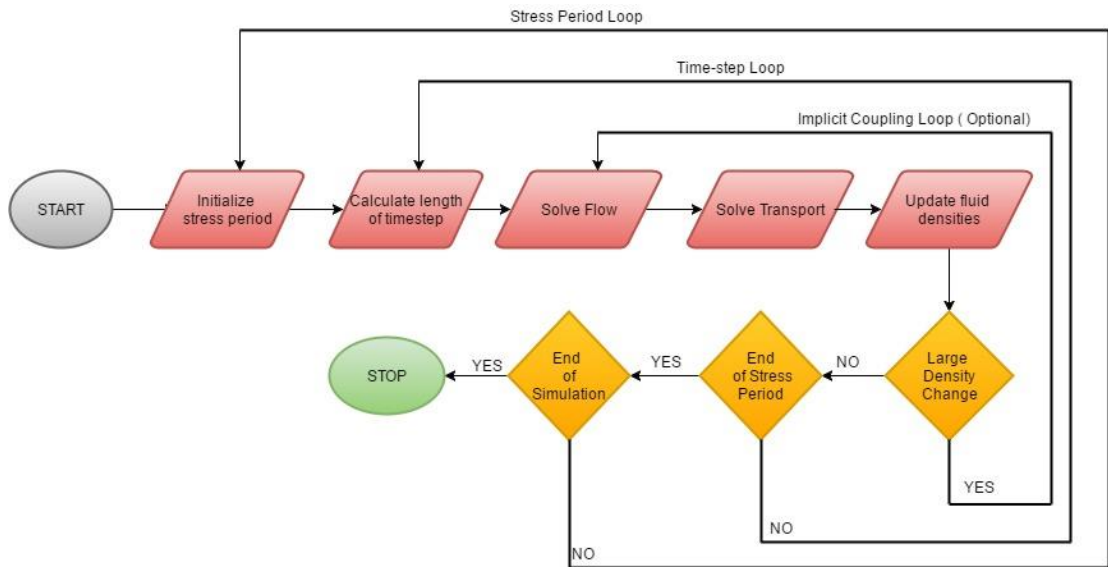


Figure 5.1 Flow chart of SEAWAT module (Guo and Langevin, 2002)

5.2.3 Equivalent fresh water head concept

The concept of equivalent fresh water head is used to develop SEAWAT model. The saltwater-freshwater interface is the region where non-uniform fluid densities exist because of different saltwater concentrations. Therefore, all the equations are written in terms of equivalent fresh water head “ h_f ”, whose effective value depends on the local variable density. This concept is better explained with a simple experimental setup (Guo and Langevin, 2002), figure 5.2.

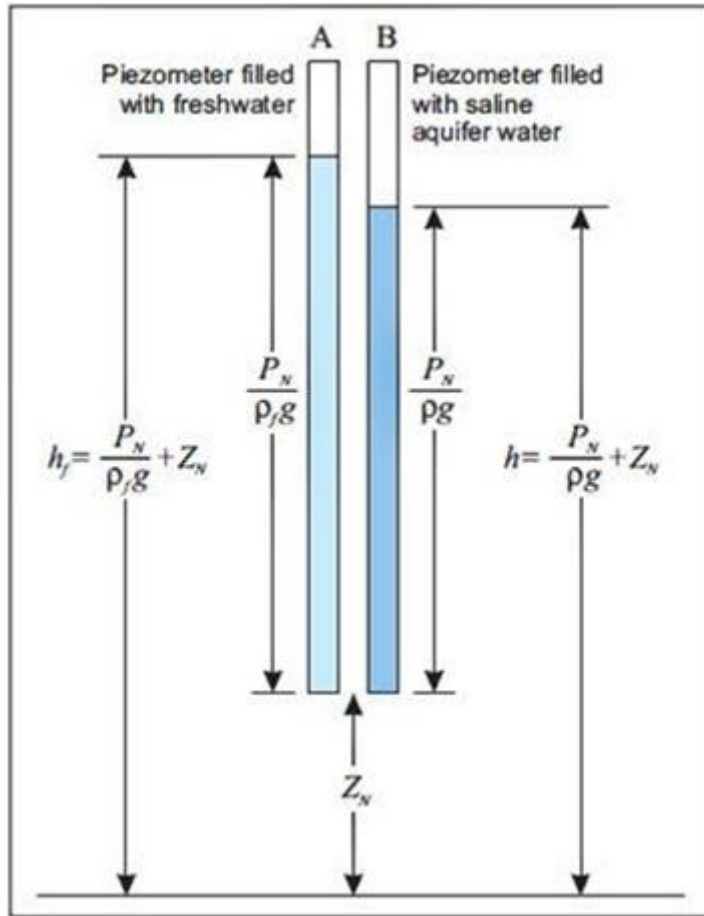


Figure 5.2 Concept of equivalent freshwater head (Guo and Langevin, 2002)

The setup displayed in figure 5.2 consists of two piezometers pertaining to a given point N in an aquifer, containing saline water. The piezometer A contains freshwater and is equipped with a mechanism that prevents saline water in the aquifer from mixing with freshwater. The piezometer B contains water identical to that present in the saline aquifer at point N. The elevation of the water level in piezometer A above the datum is the freshwater head at point N, given by

$$h_f = \frac{P_N}{\rho_f g} + Z_n \quad (5.1)$$

Where

h_f = the equivalent freshwater head [L], P_N = the pressure at point N [$ML^{-1}T^{-2}$],

ρ_f = the density freshwater [ML^{-3}], g = the acceleration due to gravity [LT^{-2}] and

$$h_f = \frac{P_N}{\rho_f g} + Z_n \quad (5.2)$$

Where

h = head [L], ρ = the density of saline groundwater at point N [ML^{-3}].

Equations (5.1) and (5.2) can be expressed in terms of pressure at point N (P_N) and replacing Z_n with a more general datum Z as;

$$P_N = \rho_f g(h_f - Z) \quad (5.3)$$

$$P_N = \rho g(h_f - Z) \quad (5.4)$$

Equating equations (5.3) and (5.4), relation between the total head and equivalent freshwater head and vice versa can be obtained.

$$h_f = \frac{\rho}{\rho_f} h - \frac{\rho - \rho_f}{\rho_f} Z \quad (5.5)$$

$$h = \frac{\rho_f}{\rho} h_f - \frac{\rho - \rho_f}{\rho} Z \quad (5.6)$$

The SEAWAT model, considers equation 5.6, wherein the total head h appearing in the Darcy equation and the pressure P in the groundwater balance equation are written in terms of the equivalent freshwater head h_f . The basic structure of the fundamental equations remains intact facilitating the use of the MODFLOW software. This allows relatively little modifications in SEAWAT model.

5.2.4 The governing equation

The governing equation for the variable density flow in terms of freshwater head as per the concept of equivalent freshwater head discussed in section 5.2.3 is expressed as follows (Guo and Langevin, 2002);

$$\begin{aligned} & \frac{\partial}{\partial \alpha} \left\{ \rho K_{f\alpha} \left[\frac{\partial h_f}{\partial \alpha} + \frac{\rho - \rho_f}{\rho_f} \frac{\partial Z}{\partial \alpha} \right] \right\} + \frac{\partial}{\partial \beta} \left\{ \rho K_{f\beta} \left[\frac{\partial h_f}{\partial \beta} + \frac{\rho - \rho_f}{\rho_f} \frac{\partial Z}{\partial \beta} \right] \right\} + \frac{\partial}{\partial \gamma} \left\{ \rho K_{f\gamma} \left[\frac{\partial h_f}{\partial \gamma} + \frac{\rho - \rho_f}{\rho_f} \frac{\partial Z}{\partial \gamma} \right] \right\} \\ & = \rho S_f \frac{\partial h_f}{\partial t} + \theta \frac{\partial \rho}{\partial t} \frac{\partial C}{\partial t} - \bar{\rho} q_s \end{aligned} \quad (5.7)$$

where α, β, γ = orthogonal coordinate axes, aligned with the principal directions of permeability; $K_{f\alpha}, K_{f\beta}, K_{f\gamma}$ = equivalent freshwater hydraulic conductivities in the three coordinate directions, respectively [LT^{-1}]; ρ = fluid density [ML^{-3}]; ρ_f = density of freshwater [ML^{-3}]; h_f = equivalent freshwater head [L]; Z = elevation above datum of the centre of the model cell [L]; S_f = equivalent freshwater specific storage [L^{-1}]; θ = effective porosity [dimensionless]; C = solute concentration [ML^{-3}]; ρ = density of water entering from a source or leaving through a sink [ML^{-3}]; q_s = volumetric flow rate of sources or sinks per unit volume of aquifer [T^{-1}] and t = time [T]. The pre-conditioned conjugate-gradient (PCG2) package is used to solve the flow equation.

The solute mass is transported in porous media by the flow of groundwater (advection), molecular diffusion, and mechanical dispersion. MT3DMS is used to solve the solute transport in groundwater by the SEAWAT code with the following partial differential equation (Zheng and Bennett, 2002),

$$\frac{\partial C}{\partial t} = \nabla \cdot (D \cdot \nabla C) - \nabla \cdot (\bar{v} C) - \frac{q_s}{\theta} C_s + \sum_{k=1}^N R_k \quad (5.8)$$

where, D = hydrodynamic dispersion coefficient [L^2T^{-1}]; \bar{v} = fluid viscosity [LT^{-1}]; C_s = solute concentration of water entering from sources or leaving through sinks [ML^{-3}] and $R_k (k=1, 2, \dots, N)$ = rate of solute production or decay in reaction k of N different reactions [$\text{ML}^{-3}\text{T}^{-1}$].

For a coupled variable density flow and solute transport simulation, fluid density is assumed to be a function only of solute concentration and the effects of pressure and temperature on fluid density are ignored (Langevin et al., 2003). A linear equation of state is used by the SEAWAT to convert solute concentration to fluid density as follows,

$$\rho = \rho_f + \frac{\partial \rho}{\partial C} C \quad (5.9)$$

In this equation, $\partial\rho/\partial C$ = Slope of the equation, whose value is entered by the user and depends on the units used for the simulation. In the present simulation, the concentration and density of seawater are defined as 35 kg/m^3 and 1025 kg/m^3 respectively. The freshwater is considered as the reference fluid with zero concentration and density equal of 1000 kg/m^3 . Therefore, the value of $\partial\rho/\partial C$ is set to 0.714. This is approximately the change in fluid density divided by the change in solute concentration for freshwater and seawater.

The limitations of the model applicability are stated in the SEAWAT-2000 documentation (Langevin et al., 2003). In the advection package, the solution scheme of third order TVD (ULTIMATE) is used.

5.3 APPLICATION TO THE STUDY AREA

5.3.1 General

The MODFLOW model is encompassed by the SEAWAT model, within its basic conceptual model structure. The SEAWAT model is developed by incorporating the density parameters to the originally developed groundwater flow model and transport parameters, through the MT3DMS model. Hence, the structure of both these models are learnt to be identical. Therefore, the SEAWAT model setup for the study area as executed in GMS software is directly relying on groundwater flow model (MODFLOW) set-up. The details are provided in Chapter 4. Hence, the comprehensive description of SEAWAT model development is not considered in this chapter. It is also important to mention that, the domain discretization, hydrologic sources and sinks and boundary conditions as adopted for the constant density model as described in section 4.4 of Chapter 4, under the subhead “Modelling Approach”, are incorporated in the SEAWAT model during the transient simulation of the saltwater-freshwater interface in the study region.

5.3.2 The Boundary Conditions

The SEAWAT requires the concentration of Total Dissolved Solids (TDS) which determines the density of the saline fluid, rather than the chloride concentrations. Therefore, Total Dissolved Solid (TDS) is used as an indicator of salinity, in the solute

transport model (Langevin and Zygnerski, 2013; Qahman and Larabi, 2006 and Cobaner et al., 2012). For the resolution of the solute transport equation in the model domain, the Neumann boundary condition is adopted in the present model.

As it is observed during the field visits, due to the high tide in the sea, the seawater will have a backwater effect up to more than 15 km into the river. This phenomenon encourages to apply the Neumann boundary condition to the stretch of river existing as a southern boundary of the study area. The Neumann boundary condition is assigned to the river with a TDS values of 35kg/m^3 during non-monsoon (October to May) months. The TDS value of 17.5 kg/m^3 is considered during monsoon (June to September) considering the quantum of mixing of freshwater and seawater as per the guidelines given by Lin et al. (2009). This value is assigned to account for the salinity carried by the backwater flow from the sea. Also, the field studies conducted by Harshendra (1991) have shown that, the chloride concentration of river water is enormously high starting from October as compared with the period from June to September. The salinity introduced due to the infiltration of contaminant water from the rainfall recharge is neglected, due to its very little effect compared to the seawater intrusion.

5.3.3 The Initial Conditions

The TDS is one of the indicators of salinity in solute transport model. The measured TDS in the observation wells during 2011-2013 is introduced to the sub-basin and using ArcGIS 9.3 the spatial distribution of TDS concentration is obtained. This is assigned to each cell as initial concentration for the transport model.

5.3.4 Density and Transport Parameters

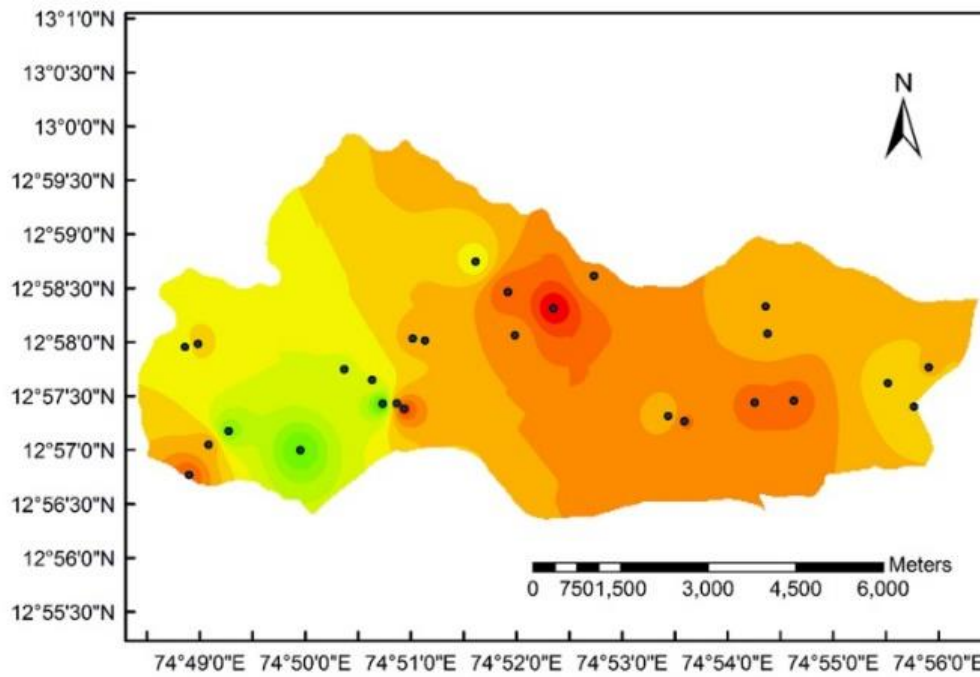
For solving Solute Transport Equation 5.7, the solute transport parameter, namely the hydrodynamic dispersivity is essential. The values of hydrodynamic dispersivity are initially assigned as per available data which are adjusted by trial and error method during calibration of the model. The longitudinal dispersion is much larger than the transversal dispersion for transport simulations (Fetter (2000)). Also, the horizontal transverse dispersivity of 1/10th of the longitudinal dispersivity is suggested by Cobaner et al., (2012). The longitudinal dispersivity values ranging between 15 to 150m is arrived at by Bhosale and Kumar (2001) under similar aquifer conditions, which is

used as a range for calibration process. The diffusion coefficient used is $8.64 \times 10^{-5} \text{m}^2/\text{day}$. The molecular diffusion is an insensitive parameter and it can be ignored in the salinity calibration, as suggested by Langevin et al., (2008).

5.4 MODEL CALIBRATION

5.4.1 Calibration of flow parameters

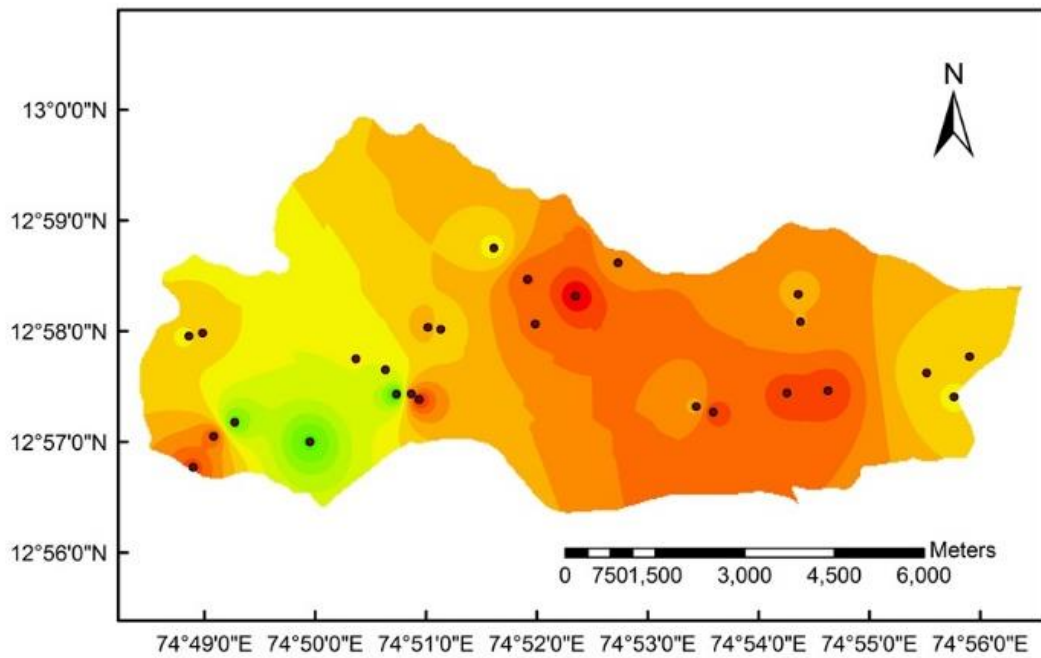
The calibrated aquifer parameters obtained from the MODFLOW model are adopted directly in the SEAWAT. Hence, it is essential to validate the SEAWAT model through calibration, once again. This step is inevitable to gain acceptance in the variable-density flow and transport model results. This is achieved by comparing the groundwater head values obtained by the constant density model with that of the variable density model. It was found that the SEAWAT simulates the aquifer system with nearly the same accuracy as that of the MODFLOW. The results of both MODFLOW and SEAWAT transient simulation (2011-13) presented in figure 5.3 and figure 5.4. The groundwater head contours of the both the simulations have an almost identical pattern with very slight variation. Hence, no further refinement is carried to validate the SEAWAT model.



Legend

GW Levels		
0.46 - 0.94	2.40 - 2.89	4.35 - 4.84
-0.99 - -0.51	0.94 - 1.43	2.89 - 3.38
-0.51 - -0.02	1.43 - 1.92	3.38 - 3.86
-0.02 - 0.46	1.92 - 2.40	3.86 - 4.35

Figure 5.3 MODFLOW Simulated groundwater heads at the end of transient calibration.



Legend

GW Levels	
1.12 - 1.54	2.82 - 3.25
1.54 - 1.97	3.25 - 3.67
0.27 - 0.69	1.97 - 2.39
0.69 - 1.12	2.39 - 2.82
-0.15 - 0.27	3.67 - 4.10
	4.10 - 4.52
	4.52 - 4.95
	4.95 - 5.37

Figure 5.4 SEAWAT Simulated groundwater heads at the end of transient calibration.

5.4.2 Calibration of Transport Parameters

The calibration of transport parameters is performed similar to that of the flow parameters as elaborated in section 4.5. The observation well data of 27 wells are measured for TDS values, on fortnightly basis during 2011-2013, are used to calibrate the model. The calibration in steady state is not carried out in the present study due to non-availability of quality data. The accuracy of the seasonal performance of the solute transport model is tested using the four model evaluation techniques used for evaluation of the flow model. Apart from the aquifer parameters calibrated in the MODFLOW, the dispersivity parameter is calibrated in the SEAWAT model by varying the values within the range specified in section 5.3.4 by trial and error method.

5.4.3 Transient Calibration

The transient calibration was done successfully and the solute transport parameters are obtained. These parameters are listed in Table 5.2. The monthly RMSE, R^2 and NSE values obtained are listed in Table 5.3.

Table 5.2 Calibrated Solute Transport Parameters

Solute Transport Parameters	Value
Recharge Coefficient (%)	10
Effective Porosity (%)	20
Longitudinal Dispersivity (m)	30
Transverse Dispersivity (m)	3
Molecular Diffusion Coefficient (m^2/day)	8.64×10^{-5}

Table 5.3 Monthly SEAWAT Efficiency Values during 2013-2015

Month	RMSE	R²	NSE
January	0.05	0.78	0.75
February	0.10	0.70	0.70
March	0.06	0.78	0.78
April	0.05	0.66	0.54
May	0.06	0.79	0.78
June	0.08	0.77	0.68
July	0.05	0.76	0.13
August	0.05	0.72	0.21
September	0.06	0.72	0.46
October	0.05	0.72	0.51
November	0.05	0.65	0.54
December	0.05	0.78	0.77

As observed in Table 3.2, the model performance is satisfactory, as the values are well within the acceptable ranges. The model performance during the monsoon (June to Sept) is not very convincing when compared to rest of the months. Also, the observed TDS data of wells that are very close to the river, do not match well with the simulated results. This could be because of the complex river-aquifer interaction which is not well addressed by the model. The scarcity of the data may be the reason behind this mismatch.

The simulated TDS distribution across the study area, for years 2013 and 2014 are shown in figures 5.6 – 5.9.

The results obtained by the graphical method for selected months of monsoon, post-monsoon, winter and summer months are shown in figure 5.5. The graphs show a convincingly good agreement with the observed and simulated groundwater heads, except that during the monsoon season. A considerable deviation in TDS value is seen in the plot for the monsoon season. It could be possibly due to the mixing of flood water

of the river, during monsoon season, with the groundwater of the aquifer in the study area.

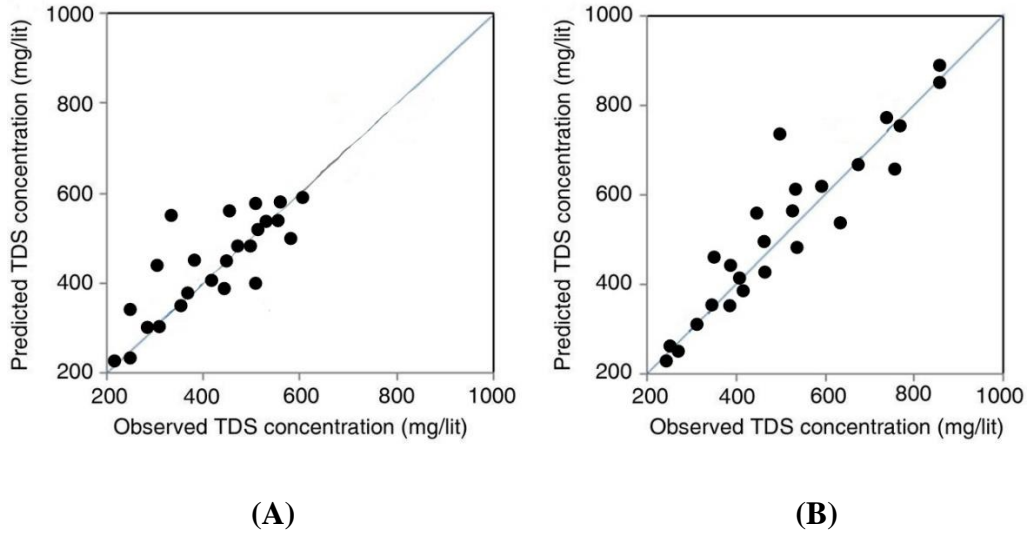


Figure 5.5 Simulated and observed TDS values (2011-13) during (A) monsoon and (B) post-monsoon respectively.

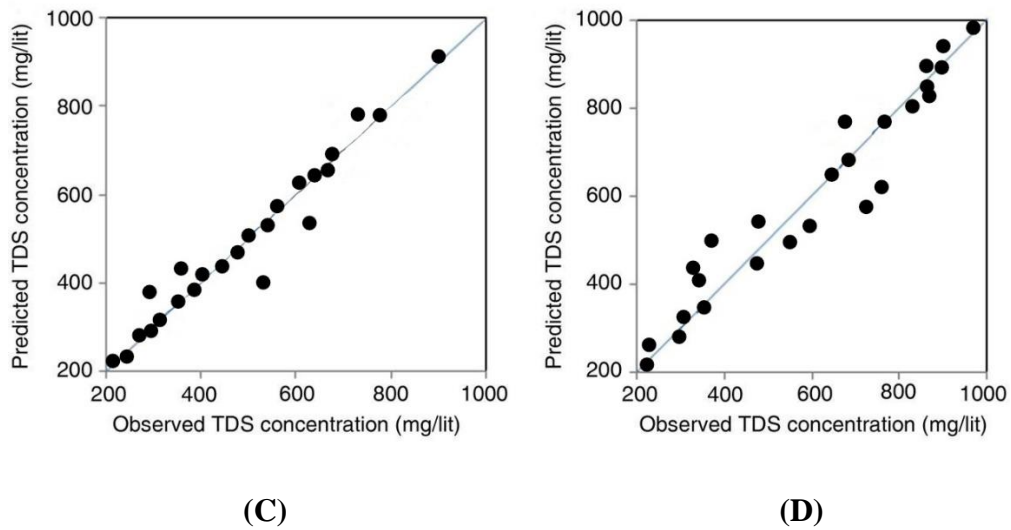
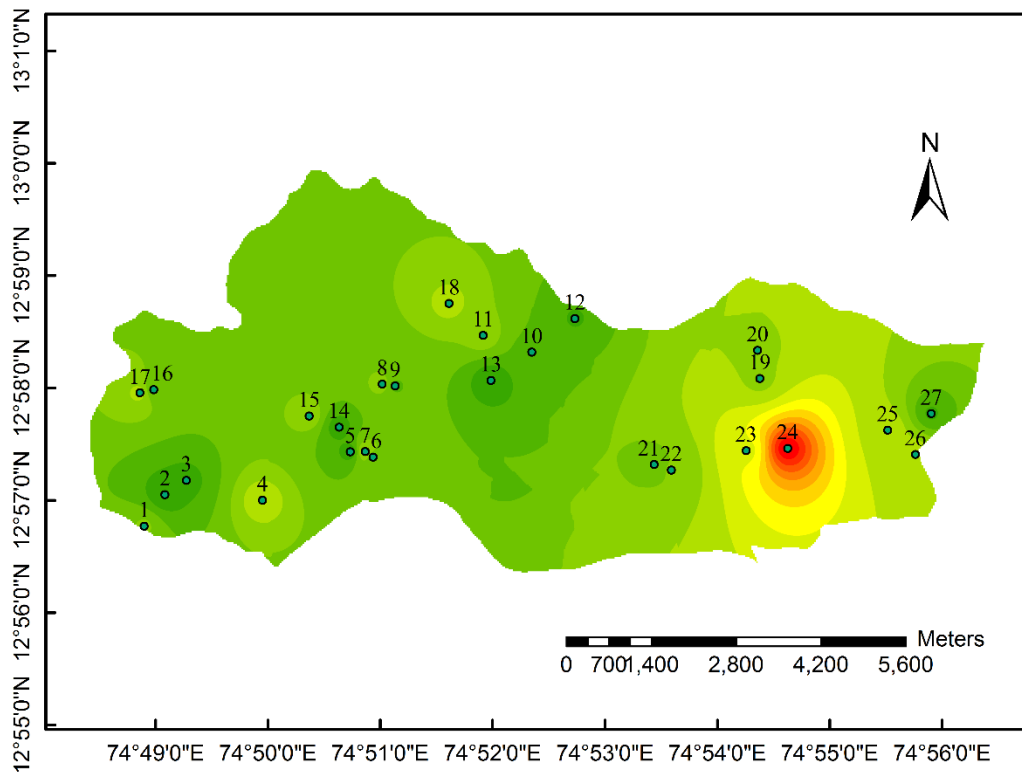


Figure 5.5 Simulated and observed TDS values (2011-13) during (C) winter and (D) summer respectively.

Total Dissolved Solids Monsoon - 2012

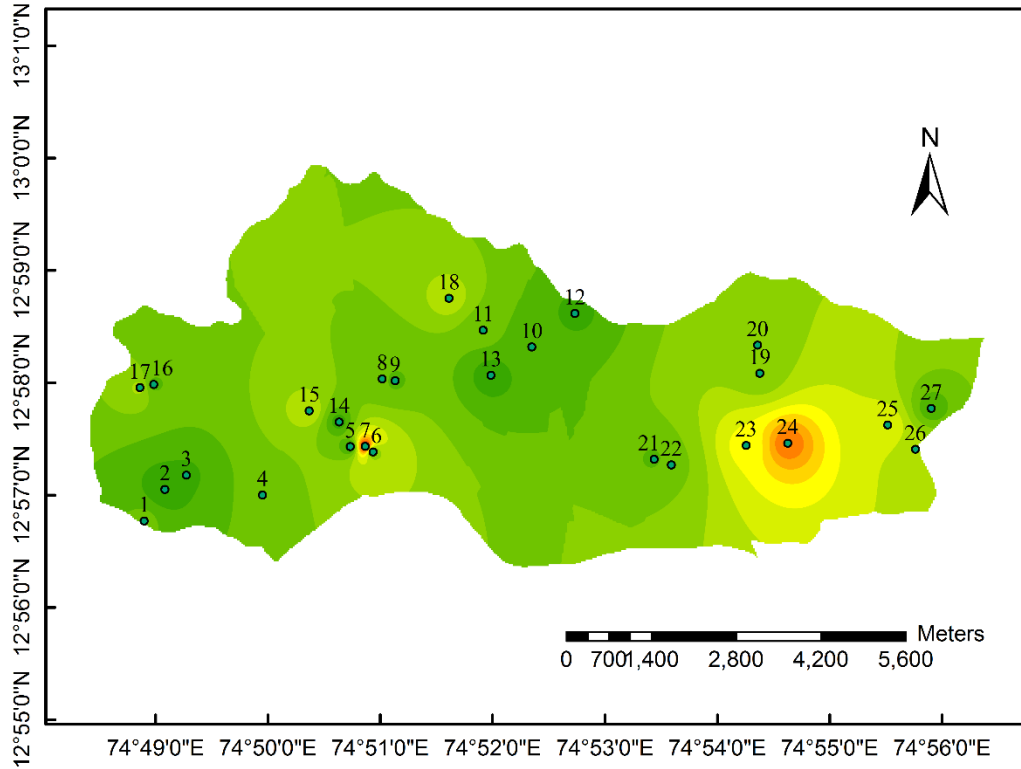


Legend

TDS (mg/lts)		Monsoon_2012	
128.84 - 172.22	302.33 - 345.71	475.83 - 519.20	Well Location
172.22 - 215.59	345.71 - 389.08	519.20 - 562.57	
42.10 - 85.47	215.59 - 258.96	389.08 - 432.45	
85.47 - 128.84	258.96 - 302.33	432.45 - 475.83	

Figure 5.6 Simulated TDS distribution for Year 2012 (July – September)

Total Dissolved Solids Post Monsoon - 2012

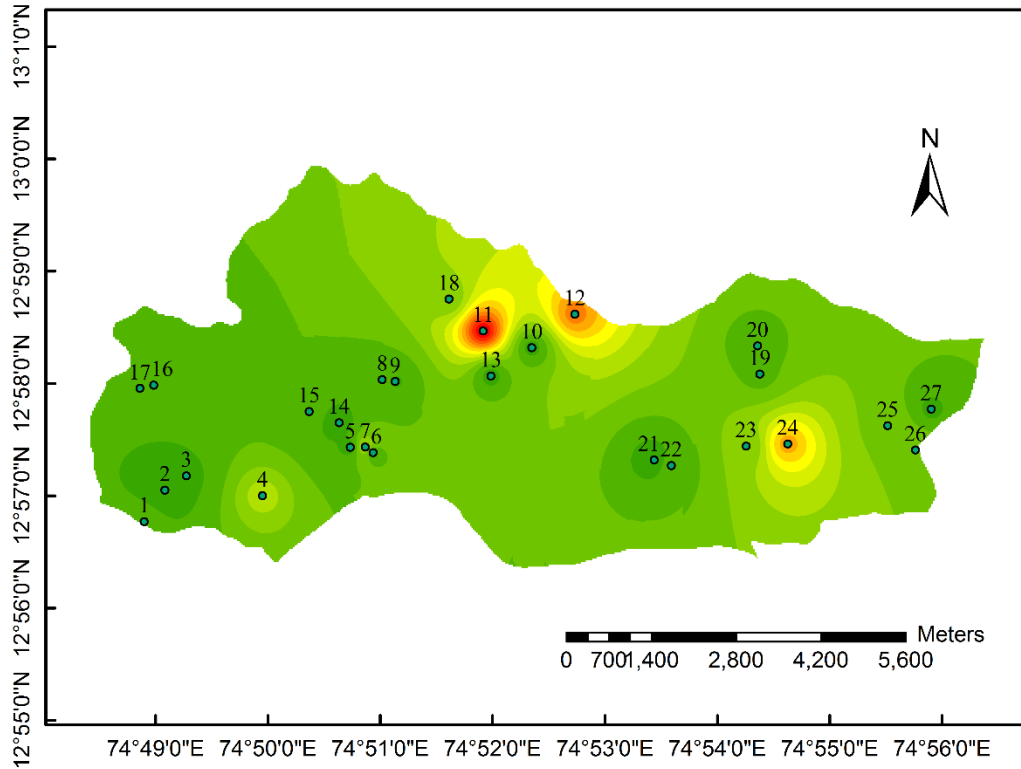


Legend

TDS (mg/lts)	171.99 - 238.48	437.93 - 504.42	703.87 - 770.36
Post_Monsoon_2012	238.48 - 304.96	504.42 - 570.90	770.36 - 836.85
	304.96 - 371.45	570.90 - 637.39	836.85 - 903.33
	105.51 - 171.99	371.45 - 437.9389	637.39 - 703.87
			• Well Location

Figure 5.7 Simulated TDS distribution for Year 2012 (October – November)

Total Dissolved Solids Summer - 2013



Legend

TDS (mg/lts)	 246.42 - 364.62	 719.21 - 837.41	 1,192.00 - 1,310.20
Summer_2013	 364.62 - 482.82	 837.41 - 955.61	 1,310.20 - 1,428.40
	 10.03 - 128.22	 955.61 - 1,073.80	 1,428.40 - 1,546.59
	 128.22 - 246.42	 601.01 - 719.21	 1,073.80 - 1,192.00
			 Well Location

Figure 5.9 Simulated TDS distribution for Year 2013 (April – June)

During the months from July to September, the TDS values in the study area range from 42 mg/lit to 302 mg/lit, among majority of the region except around well number 24, where the values are between 302 mg/lit to 600 mg/lit. The region around well number 24 is marked with widespread agriculture fields and coconut plantations, spreading till the banks of the river Gurupura on southern boundary. The aquifer holds close interaction with the river water in the region. The wells around the wetland (well

numbers 3, 4, 5, 6, 7, 14 and 15) are found to have lower TDS values (42 mg/lit to 205 mg/lit).

The post-monsoon season (October – November) is depicted with TDS values touching 900 mg/lit around well number 24. The intensive agricultural activities may be the reason for the rise in TDS levels in the region. The wells around wetlands show slightly higher TDS levels during post – monsoon season compared to monsoon season (170 mg/lit to 700 mg/lit).

During the months of December to March, the TDS values are observed to remain stable with almost same range of values, among the wells around wetland. The highest value of TDS (689 mg/lit), in the study area during December to March lies around well number 24. In the rest of the region in the study area, TDS values are maintained in lower range (25 mg/lit to 290 mg/lit).

The TDS trend during summer months from April to June is found to be around 400 mg/lit to 719 mg/lit, for wells nearby wetland. Around well number 24, the summer TDS values are highest observed among all seasons, that is 1192 mg/lit. Apart from these, well numbers 12 and 11 shows highest TDS values in the range of 1200 mg/lit to 1500 mg/lit.

The total dissolved solids (TDS) combine the sum of all ion particles that are smaller than 2 microns (0.0002 cm). This includes all of the disassociated electrolytes that make up salinity concentrations, as well as other compounds such as dissolved organic matter. In “clean” water, TDS is approximately equal to salinity. In wastewater or polluted areas, TDS can include organic solutes (such as hydrocarbons and urea) in addition to the salt ions. While TDS measurements are derived from conductivity, some states, regions and agencies often set a TDS maximum instead of a conductivity limit for water quality. At most, freshwater can have 2000 mg/lit of total dissolved solids (IS 10500: 2012). The EPA (Environmental Protection Agency), USPHS (United State Public Health Service) and AWWA (American Water Works Association) recommend an upper limit of 500 mg/L TDS. The limits of TDS for various water classes are shown in figure 5.10.

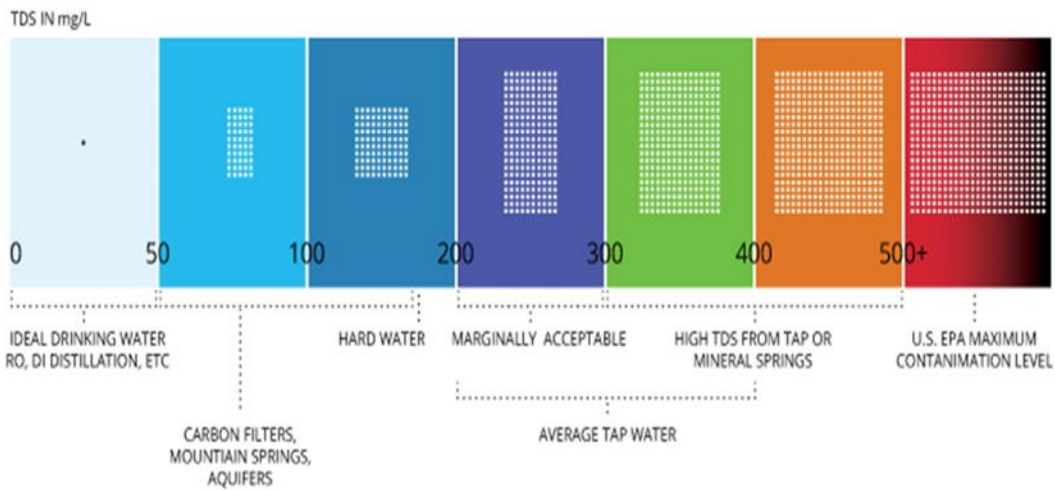


Figure 5.10 The EPA, USPHS and AWWA recommended TDS limits for classes of water (Lagasse et. al., 2012)

Hence, the groundwater around the region, though are of higher in terms of TDS concentration, is suitable for agricultural purpose.

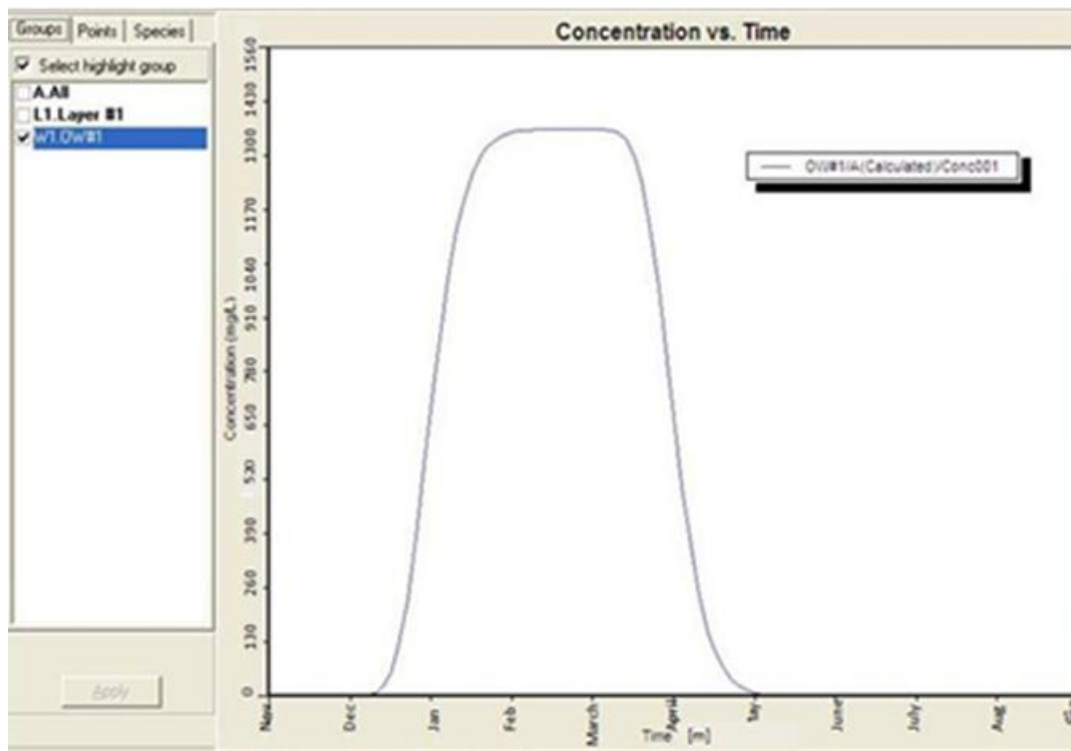


Figure 5.11 Specific Predictive Trend Analyser for TDS by SEAWAT

The specific predictive trend analyser has shown (figure 5.11) exceptional high concentration of TDS to be touching 1500 mg/lit, during the summer months. However, the quality of groundwater could be considered as reasonably fresh, even during these months.

5.5 VALIDATION OF SEAWAT MODEL

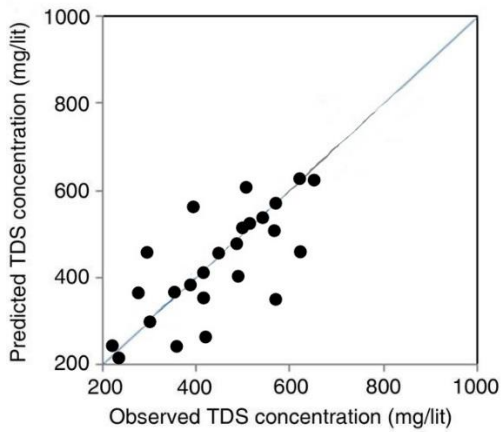
For the purpose of application of the calibrated solute transport model for future contamination scenario, validation of the model is carried out for a period during 2013-15. Monthly stress periods are provided for obtaining the results of validation in terms of TDS values. The results of validation are as shown in figures 5.13 to 5.16.

The observed values of TDS during calibration period are in tune with the trends followed during the simulation period (2011-2013), except for summer 2015, wherein the model results are slightly under estimated.

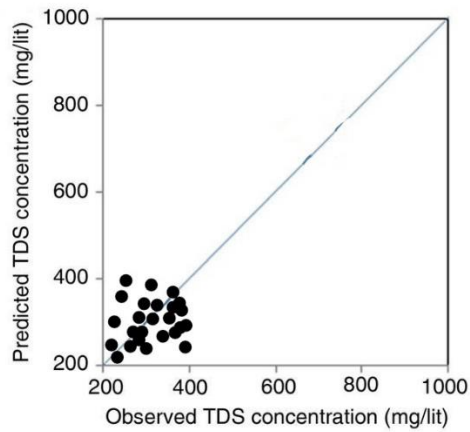
The R^2 , RMSE and NSE values obtained after analysing the observed and validated TDS values at various observation points are provided in Table 5.4. The results are found to be consistent with that of the calibration results and therefore, the model can be considered reliable for future predictions. To perceive the agreement between the observed and simulated groundwater head data during the validation period, combined scatter plot for two years is presented in figure 5.12. The trend observed from the scatter plot is convincing.

Table 5.4 Groundwater solute transport model performance during the period 2013-15

Season	R^2	RMSE (m)	NSE
Monsoon	0.71	0.39	0.54
Post-Monsoon	0.66	0.63	0.42
Winter	0.74	0.21	0.68
Summer	0.63	0.54	0.53

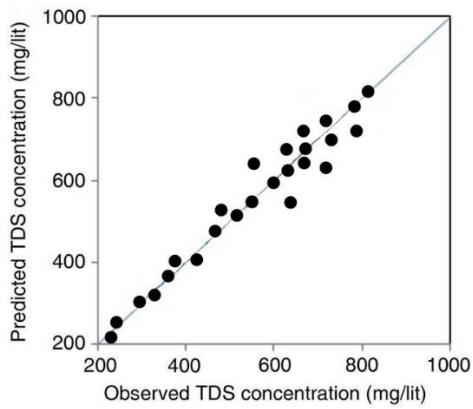


(A)

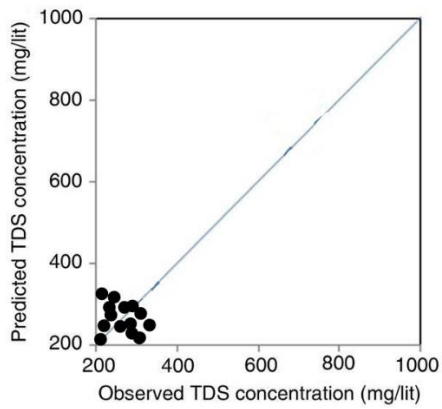


(B)

Figure 5.12 Scatter plots of simulated and observed TDS values (2013-15) for seasons (A) monsoon (B) post-monsoon respectively



(C)

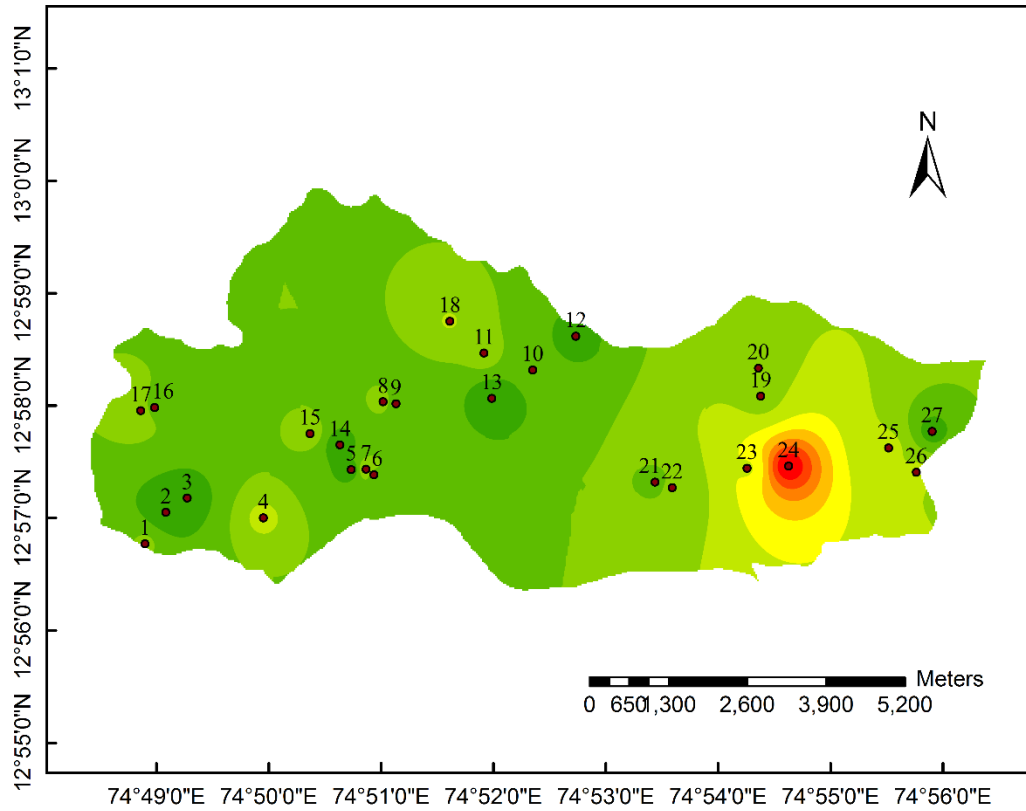


(D)

Figure 5.12 Scatter plots of simulated and observed TDS values (2013-15) for seasons (C) winter (D) summer respectively

The scatter plots indicate that the model is under predicting during post-monsoon and summer seasons. This is reflected in the statistics of Table 5.3. The model predicts fairly well for monsoon and winter seasons.

Total Dissolved Solids in Monsoon - 2014

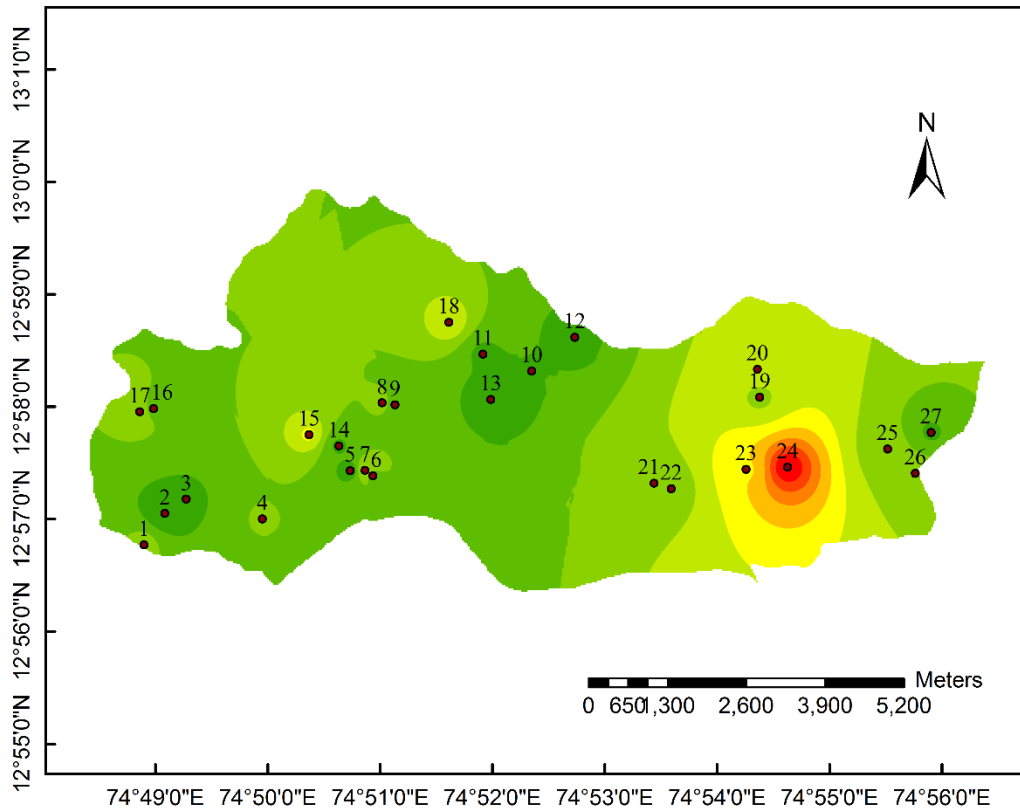


Legend

TDS (mg/lts)	 167.40 - 230.05	 418.00 - 480.65
Monsoon_2014	 230.05 - 292.70	 480.65 - 543.30
 42.10 - 104.75	 292.70 - 355.35	 543.30 - 605.94
 104.75 - 167.40	 355.35 - 418.00	 Well Location

Figure 5.13 Validated TDS distribution for Year 2014 (July – September)

Total Dissolved Solids in Post-Monsoon - 2014

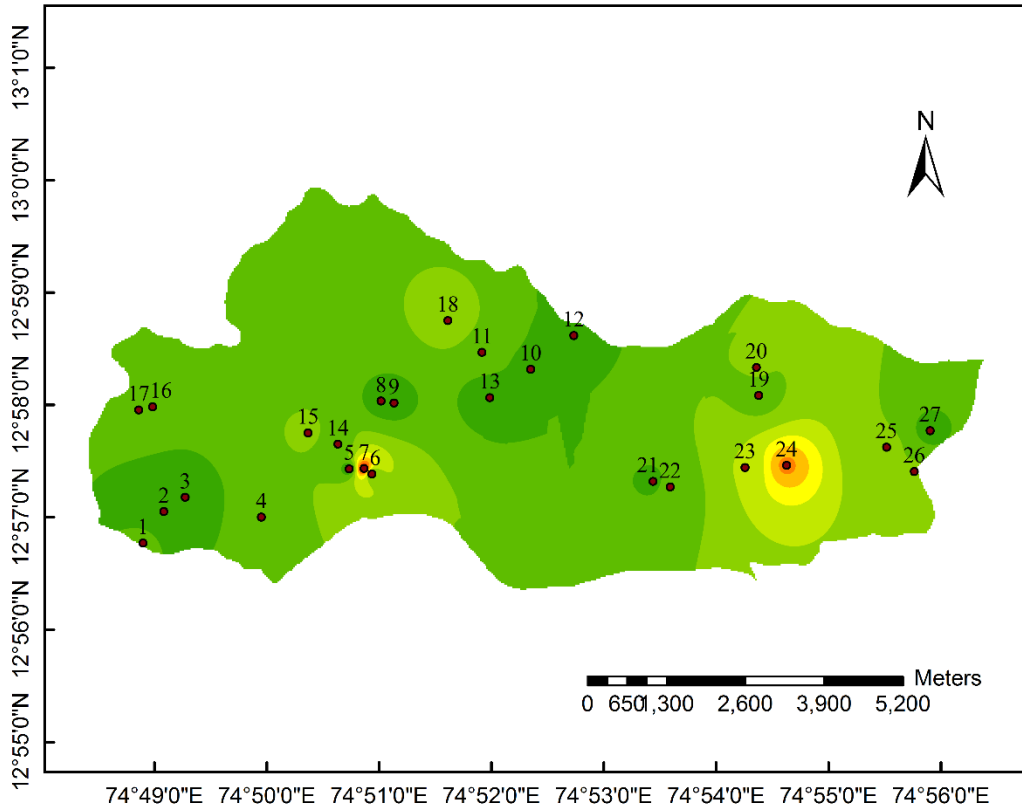


Legend

TDS (mg/lts)		
		105.33 - 147.00
		147.00 - 188.66
		188.66 - 230.32
		230.32 - 271.98
		271.98 - 313.64
		313.64 - 355.30
		355.30 - 396.96
		Well Location

Figure 5.14 Validated TDS distribution for Year 2014 (October – November)

Total Dissolved Solids in Winter - 2014-2015

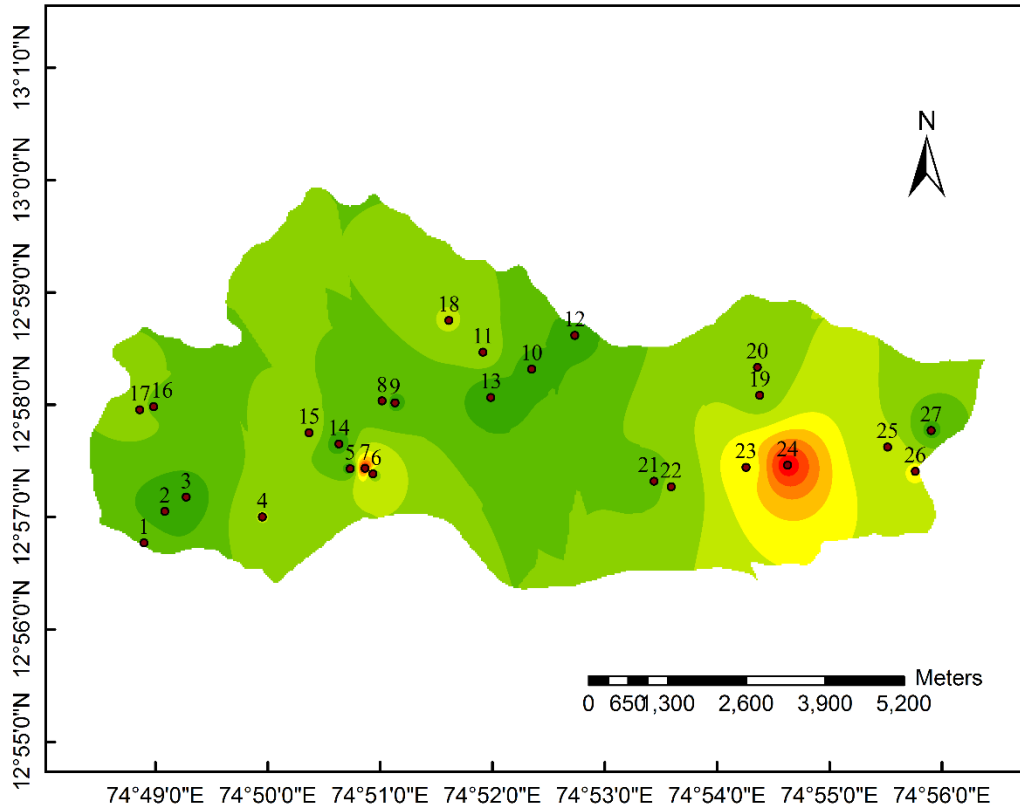


Legend

TDS (mg/lts)		Winter_2014-2015	
	208.58 - 297.73		297.73 - 386.87
	30.29 - 119.43		386.87 - 476.02
	119.43 - 208.58		476.02 - 565.17
			565.17 - 654.31
			654.31 - 743.46
			743.46 - 832.60
			Well Location

Figure 5.15 Validated TDS distribution for December 2014 – March 2105

Total Dissolved Solids in Summer - 2015



Legend











TDS (mg/lts)	 81.53 - 112.77	 206.48 - 237.72
Summer_2015	 112.77 - 144.00	 237.72 - 268.96
 19.05 - 50.29	 144.00 - 175.24	 268.96 - 300.20
 50.29 - 81.53	 175.24 - 206.48	 Well Location

Figure 5.16 Validated TDS distribution for Year 2015 (April – June)

5.6 SENSITIVITY ANALYSIS OF SOLUTE TRANSPORT MODEL

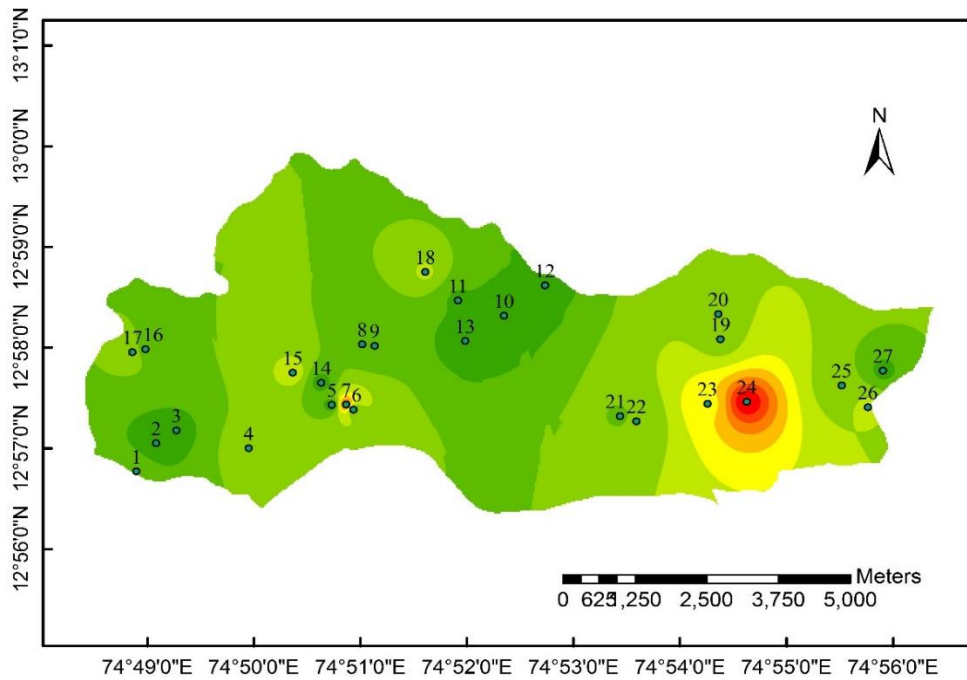
The sensitivity analysis of solute transport model is carried out to assess the effects of the hydrodynamic dispersion coefficient D on the performance of the density-dependent solute transport. In most of the cases, the dispersivity value is not known in an aquifer. Hence, this study is essential to be conducted. The sensitivity analysis of the hydrodynamic dispersion is carried out by performing simulations with 25%, 50% and 75% increase in longitudinal dispersivity values. The horizontal transverse dispersivity

of 1/10th of the longitudinal dispersivity is assigned as discussed in section 5.3.4., while conducting the simulations.

The salinity distribution simulated by the SEAWAT at the end of transient simulation period (year 2013) with 25%, 50% and 75% increased values of longitudinal dispersivity are displayed in figures 5.17 (A), (B) and (C). It could be observed from the figures that, the simulated lower TDS values shows lesser sensitivity to the dispersivity value. The lowest levels of TDS values observed are 38.05 mg/l, 50.02 mg/l and 62.19 mg/l respectively for 25%, 50% and 75% of increase in longitudinal dispersivity. The incremental variation is in the order of 31%, between 25% increase and 50 % increase and 24% between 50% and 75% increase in longitudinal dispersivity.

Higher TDS values are observed to be sensitive to increase in the values of longitudinal dispersivity. It can be observed that the highest values of TDS observed in study area are 750.93 mg/l, 662.95 mg/l and 873.92 mg/l respectively for 25%, 50% and 75% of increase in longitudinal dispersivity. There is a decrease of 11.7% in values of TDS, between 25 % to 50% increase in the values of longitudinal dispersivity. But, an increase of 31.82% in the values of TDS is observed between an increases of 50% to 75% increase in the values of longitudinal dispersivity. Marginal sensitivity is observed as a response to increase in longitudinal dispersivity values among higher values of TDS values.

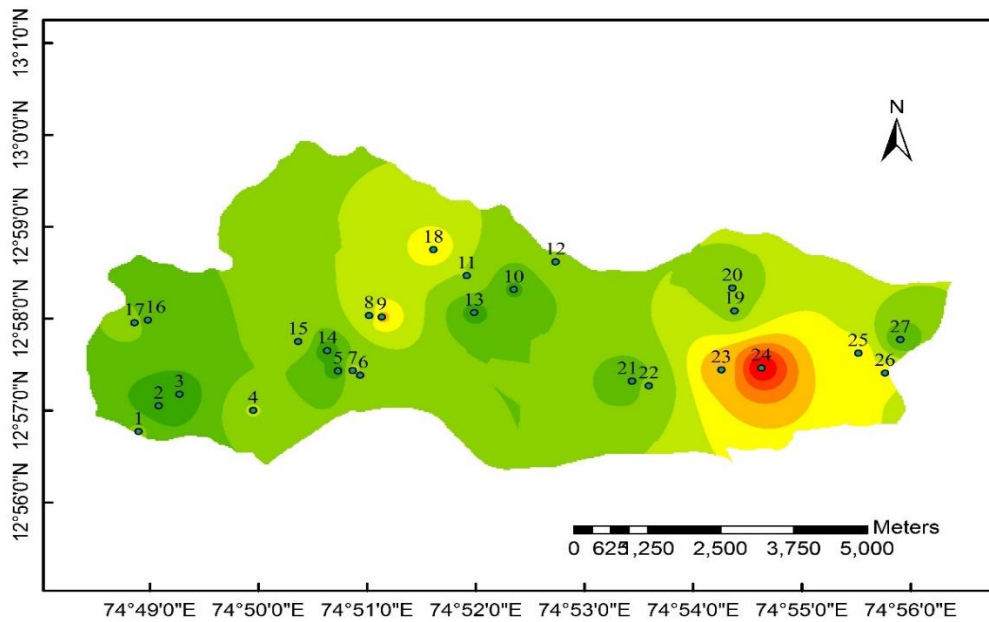
Better consistency is observed among lower TDS values. Also, major area in the region is shown with acceptable range (38 mg/l to 330 mg/l) of TDS values.



Legend

TDS (mg/lts)	 196.47 - 275.68	 513.31 - 592.51
 275.68 - 354.89	 354.89 - 434.10	 592.51 - 671.72
 38.05 - 117.26	 434.10 - 513.31	 671.72 - 750.93
 117.26 - 196.47	 Well Location	

Figure 5.17 (A) Spatial distribution of TDS concentration as simulated by SEAWAT during the year 2013 for increase of the longitudinal dispersivity by 25%



Legend

TDS (mg/lts)

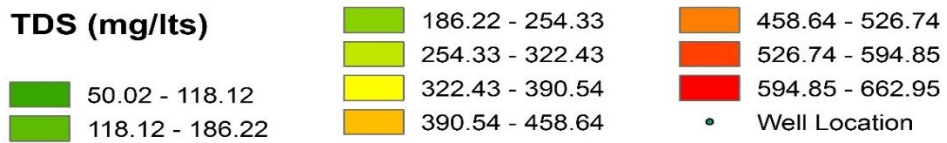
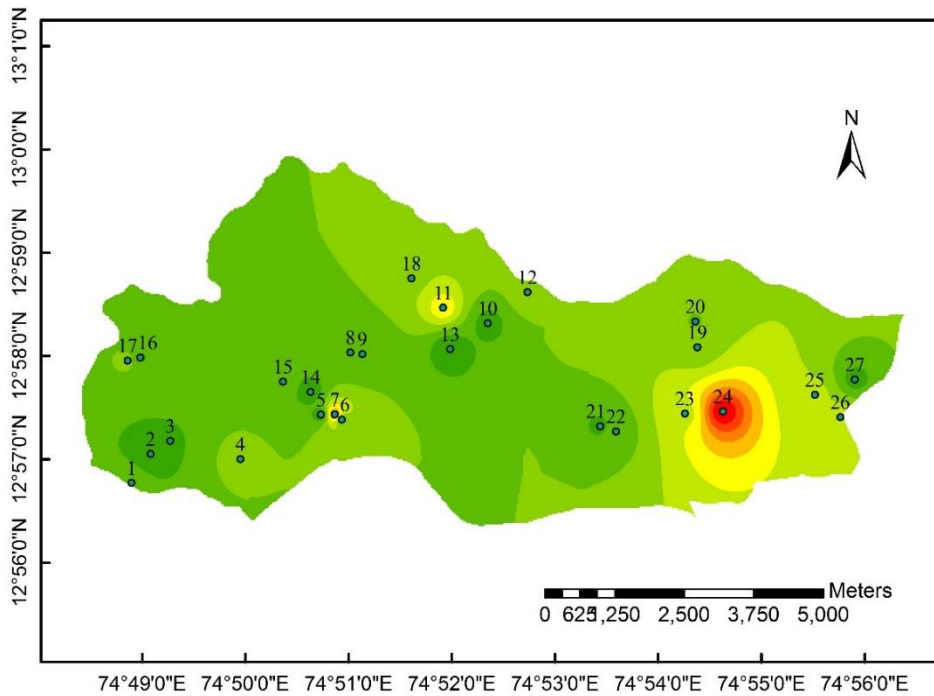


Figure 5.17 (B) Spatial distribution of TDS concentration as simulated by SEAWAT during the year 2013 for increase of the longitudinal dispersivity by 50%



Legend

TDS (mg/lts)	 242.58 - 332.77	 603.34 - 693.54
	 332.77 - 422.96	 693.54 - 783.73
	 62.19 - 152.39	 783.73 - 873.92
	 152.39 - 242.58	 Well Location
	 422.96 - 513.15	
	 513.15 - 603.34	

Figure 5.17 (C) Spatial distribution of TDS concentration as simulated by SEAWAT during the year 2013 for increase of the longitudinal dispersivity by 75%

5.7 CLOSURE

In order to simulate the contaminant transport in the form of TDS, the variable density groundwater flow model, SEAWAT is applied to the study area. The model domain remains almost same, as the SEAWAT model involves similar model structure as that of MODFLOW, with minor changes. The flow and density parameters are introduced in the SEAWAT model, in order to bring in the concept of equivalent fresh water head.

The calibration and validation of the SEAWAT model are carried out with reasonable accuracy, by having NSE ≥ 0.5 . It is admitted that, the model performance is not encouraging during the monsoon period. The reasons for this are discussed in the

context of the constant density flow model performance. The flow parameters and transport parameters are standardised for the study area through the process of calibration.

The model results show that, the river that is flowing along the southern boundary, contribute significantly to contamination in the study area. The river is tidal in nature and carries saline water with its flow after the month of October till May. However, under the current scenario, the aquifer system of the study area remains safe with TDS < 1000 mg/lit throughout the study area, except a few locations. The validation of the SEAWAT confirmed that, the TDS values observed are in consistency with those observed during calibration period. The sensitivity analysis resulted in trends of better agreement as far as lower values of TDS are concerned. Whereas, higher values of TDS are showing marginal sensitivity for longitudinal dispersivity.

PROGNOSTIC SIMULATIONS

6.1 GENERAL

The study area considered has an equal impetus to both agricultural and industrial activities. The population growth and the industrial development in the area are taking place at alarming rate. Due to these considerations, the demand for groundwater would certainly increase in future. The study area also comprises of wetlands, which are maintaining the hydrological balance naturally. Human intervention by means of disturbing the natural habitat and filling the wetlands for industrial purpose, would hamper the system to an irreparable extent. Unplanned and uncontrolled withdrawal of groundwater resources may lead to drastic lowering of groundwater table. The lowered water table could attract quality issues in a long run. This would result in harmful effects on utilisation of groundwater in the domain of domestic use, vegetation, industries, and other activities. According to the rainfall trend analysis carried out for the region (Shetkar and Mahesha, 2011), it was found that over a 100-year period, the annual and seasonal rainfall trends of 14 weather stations are decreasing at a rate of 6–18% of average annual rainfall of 3,900 mm.

An attempt is made in the present study to explore the feasibility of the effects of various stress scenarios on the aquifer for the period 2015-35, using the numerical simulation. The study investigates the response of the aquifer for increased pumping rates, and decreased recharge rates in terms of the potential of groundwater. The density dependent flow and transport model SEAWAT is used for this purpose. Specifically, the calibrated SEAWAT model is employed to simulate the effects of various near-future scenarios on the groundwater quantity and quality of the aquifer in the study area.

6.2 DESCRIPTION OF DIFFERENT SCENARIOS

In the earlier chapters, the MODFLOW and SEAWAT models are calibrated and are used to investigate the seasonal variability of groundwater, salinity distribution, and water balance under transient conditions during the calibration period 2011-13. In the present chapter, the SEAWAT is applied to simulate the groundwater flow and solute transport for future anticipated groundwater development in the study area. The following are the scenarios considered for investigation:

Scenario 1: The simulation considers current abstraction rate and calibrated recharge rate. The existing status of groundwater utilization is listed in Table 4.4. The calibrated recharge rate for the region is 20% of rainfall. The present conditions are assumed to prevail for another two decades, up to the year 2035. This scenario is considered to be conservative in estimating the groundwater utilization based on the crop evaporation data in view of lack of temporal and quantitative groundwater draft data from each well.

Scenario 2: The simulation considers recharge rate of 10%, in view of anticipated decrease in rainfall resulting from climate change and lowered infiltration capabilities of the soil in the region due to human intervention. According to the studies conducted in the adjacent region, the recharge co-efficient can be as low as 8% (Udaykumar, 2008), which gives a justification for the case. In this scenario, the model is run for a period of 20 years with 10% recharge rate.

Scenario 3: The simulation in this scenario will address increase in the rate of groundwater utilization. It is important to know the behaviour of the aquifer system to increased rate of pumping. In this simulation, it is assumed that, the aquifer is getting recharged due to rainfall with a recharge co-efficient of 0.20. Three separate cases with 50%, 100% and 150% increase in pumping rate for the wells listed in table 4.4 are considered for simulations. These simulations are indicated as case 1, case 2 and case 3 respectively and analysed separately.

Scenario 4: In this simulation, combination of increase in abstraction rate with decrease in recharge rate is considered. This scenario can be considered as extreme stress condition for the aquifer, with increased draft and decreased recharge. The groundwater draft is increased by 50%, 100% and 150% respectively along with 10% of recharge

rate. These simulations are indicated as case 1, case 2 and case 3 respectively and analysed separately.

6.3 RESULTS AND DISCUSSION

The calibrated model (2011-2013) is used to predict the spatial and temporal impacts of all the 4 scenarios on the vulnerability of the aquifer, for 20 years period. The WHO recommends permissible TDS limit of 500 mg/ltr and excessive limit of 1,500 mg/ltr for drinking purpose. Therefore, the solute transport effect is studied with respect to the lateral movement of the 1500 mg/ltr iso-line from the river boundary at south.

6.3.1 Spatial effect on the aquifer

Effect on water table

The groundwater table elevation and groundwater TDS distribution at the observation wells simulated for all the scenarios by November 2035, are listed in Table 6.1 and Table 6.2 respectively.

The groundwater table falls by an average of 0.26m over the entire region, due to the decrease in recharge rate corresponding to Scenario 2 compared to Scenario 1 (extension of present scenario). There is a fall of groundwater table of approximately 0.17 m observed around the region of wetlands by the end of simulation period (2035), compared to present status (wells 3, 4, 5,14, 15, 16 and 17). The intense agricultural region in the study area finds a slump of approximately 0.45m, in groundwater table level by 2035 (Scenario 2).

The Scenario 3, Case 3 depicts an average fall of 0.36m of groundwater table over the entire study area when compared to Scenario 1, by the end of year 2035. The wetland region would experience a fall in groundwater table, of approximately 0.29m according to Scenario 3 Case 3. The intense agriculture around wells 21, 22, 23 and 24 will have 0.43m fall in water table. All the cases of scenario 3 show a decline of approximately 0.1m by the end of simulation period.

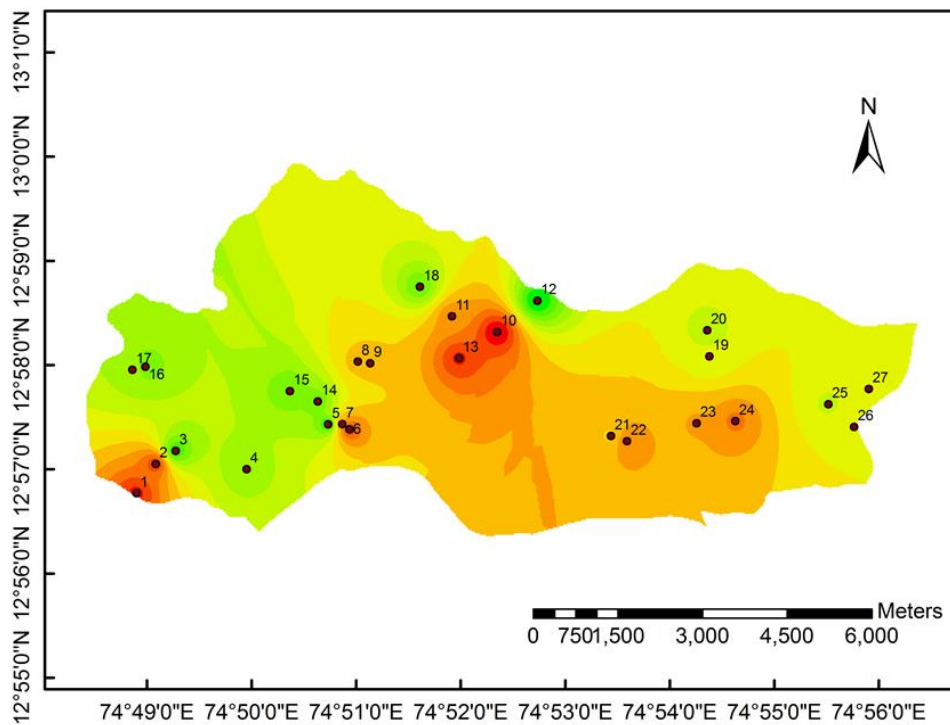
The worst case scenario is represented in Case 3 of Scenario 4. The average fall in groundwater table is 0.92m across the entire aquifer. The wetland region is finding a fall of 0.66m. The intense agricultural region of the study area will have a fall of groundwater table of approximately 0.99m by the end of simulation period, 2035. All the cases of scenario 4 show a decline of approximately 0.2 m by the end of the simulation period.

**Table 6.1 Groundwater table elevation (with respect to mean sea level) during
end of simulation year (2035)**

Description	Well no.	Scenario 1	Scenario 2	Scenario 3			Scenario 4		
				Case 1	Case 2	Case 3	Case 1	Case 2	Case 3
Groundwater Elevation (m, msl)	1	-0.23	-0.67	-1.07	-1.12	-1.16	-1.53	-1.59	-1.69
	2	-0.07	-0.51	-0.92	-0.97	-1.01	-1.38	-1.44	-1.54
	3	2.62	2.45	2.53	2.43	2.31	2.49	2.12	1.89
	4	2.05	1.90	1.96	1.89	1.74	1.99	1.55	1.38
	5	2.79	2.56	2.78	2.66	2.52	2.56	2.33	2.09
	6	-0.19	-0.63	-1.03	-1.08	-1.12	-1.49	-1.55	-1.65
	7	0.63	0.48	0.60	0.56	0.33	0.45	0.29	0.02
	8	0.84	0.40	0.81	0.77	0.71	0.34	0.28	0.18
	9	0.85	0.39	0.83	0.73	0.69	0.31	0.26	0.15
	10	-0.43	-0.87	-1.28	-1.32	-1.36	-1.73	-1.79	-1.89
	11	0.48	0.04	0.41	0.37	0.33	-0.04	-0.10	-0.20
	12	2.91	1.17	2.42	2.92	2.40	0.98	0.57	0.56
	13	-0.21	-0.59	-1.00	-1.04	-1.08	-0.61	-0.67	-0.75
	14	2.35	2.18	2.26	2.19	2.07	2.13	1.86	1.76
	15	2.36	2.19	2.28	2.19	2.08	2.12	1.96	1.72
	16	2.31	2.17	2.29	2.22	2.01	0.37	-0.20	-0.76
	17	1.77	1.62	1.65	1.55	1.47	1.38	1.22	1.17
	18	2.34	1.90	2.30	1.82	1.30	0.93	0.87	0.78
	19	1.50	1.05	1.46	1.41	1.41	1.37	1.31	1.20
	20	1.66	1.23	1.64	1.61	1.58	1.21	1.15	1.01
	21	1.01	0.55	0.97	0.93	0.49	0.52	0.46	-0.59
	22	0.43	-0.01	0.42	0.38	0.1	-0.02	-0.08	-0.33
	23	0.66	0.21	0.62	0.57	0.11	0.15	0.09	-0.22
	24	0.33	-0.10	0.31	0.28	0.01	-0.15	-0.21	-0.42
	25	1.57	1.16	1.56	1.53	1.48	1.11	1.04	0.95
	26	1.25	0.81	1.22	1.17	1.14	0.77	0.72	0.65
	27	1.45	1.00	1.43	1.40	1.35	0.98	0.92	0.79

To substantiate the results, the spatial distribution map of water table contour for Scenario 1, Scenario 2, Scenario 3 (Case 3) and Scenario 4 (Case 3) are presented in Fig.6.1. The simulated heads show significant spatial variability over the period due to the application of various scenarios.

The decline in water table elevations for Scenario 3 and Scenario 4 are remarkably evident compared to Scenario 1 and Scenario 2. The region around wetland maintains comparatively higher groundwater table levels even at the end of simulation period, year 2035.



Legend





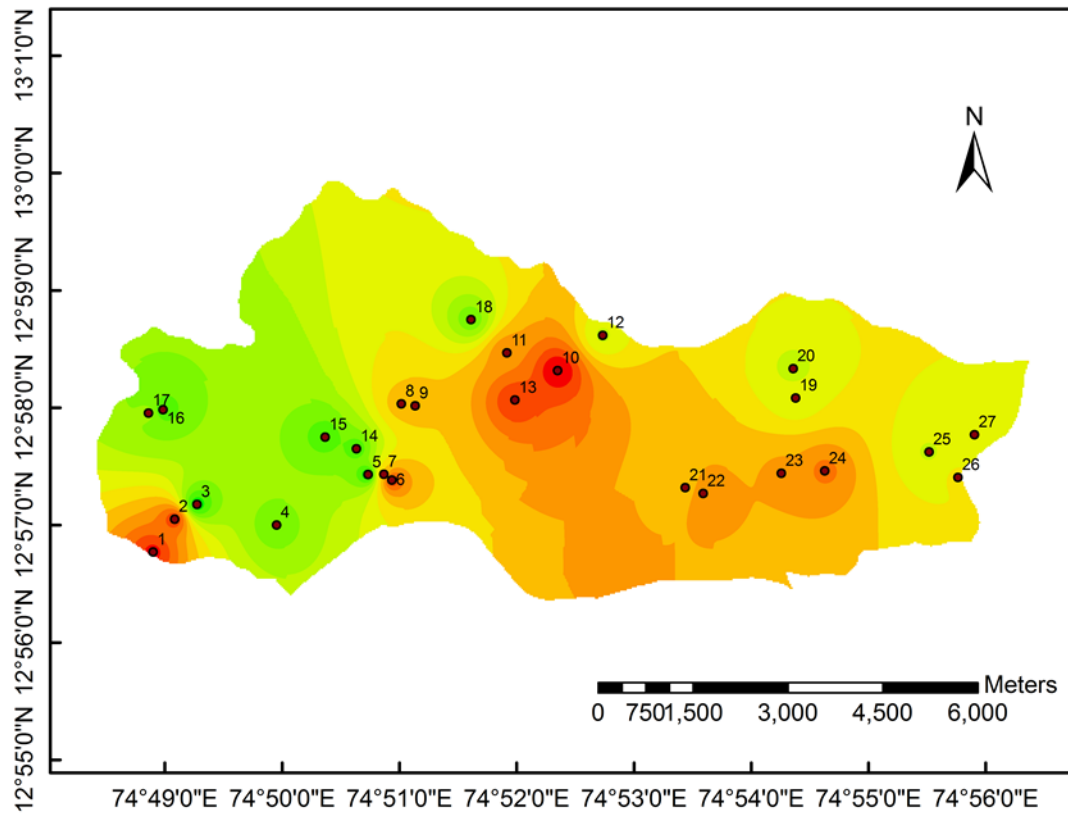
Scenario 1 (m, msl)	 0.42 - 0.68	 1.25 - 1.52	 2.08 - 2.35
 -0.43 - -0.15	 0.69 - 0.96	 1.53 - 1.8	 2.36 - 2.63
 -0.14 - 0.13	 0.97 - 1.24	 1.81 - 2.07	 2.64 - 2.91
 0.14 - 0.41			

Figure 6.1 Spatial distribution of groundwater table for (A) Scenario 1



Legend

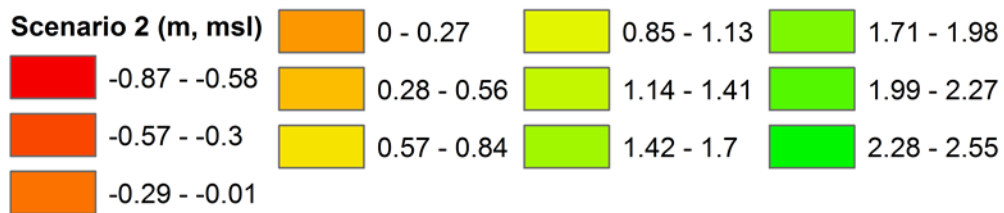
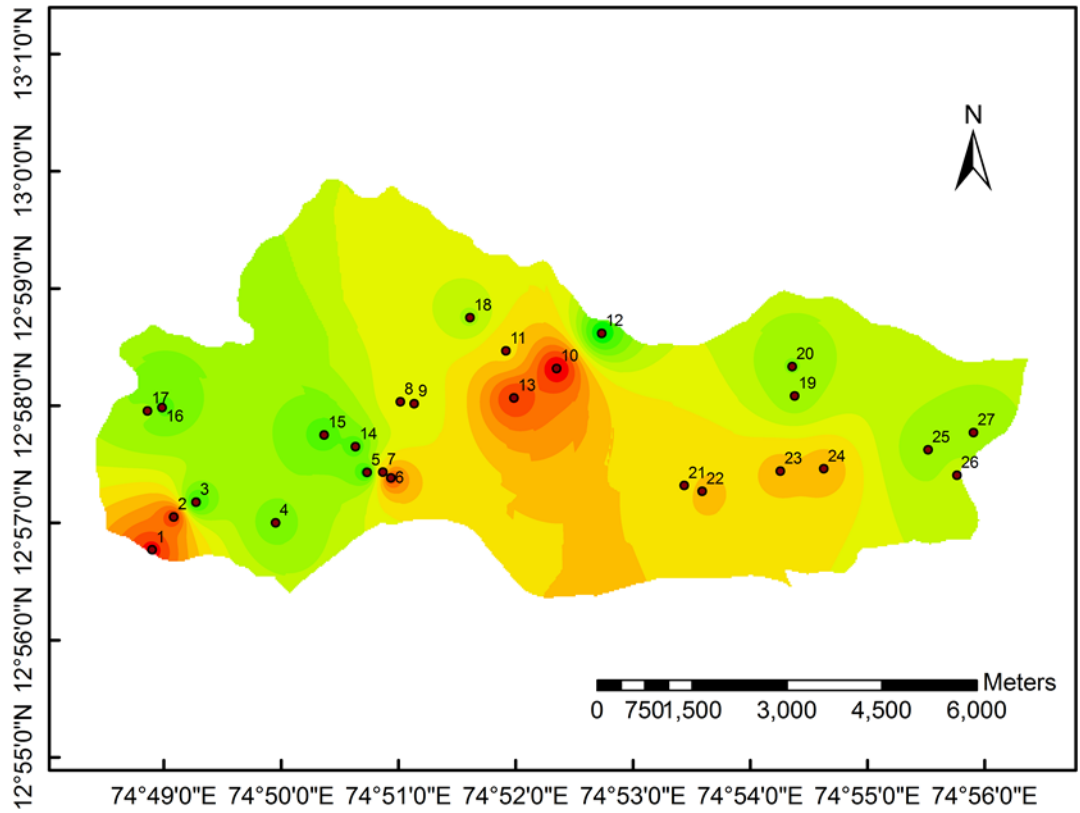


Figure 6.1 Spatial distribution of groundwater table for (B) Scenario 2 by the end of 20 year simulation (Year 2035)



Legend

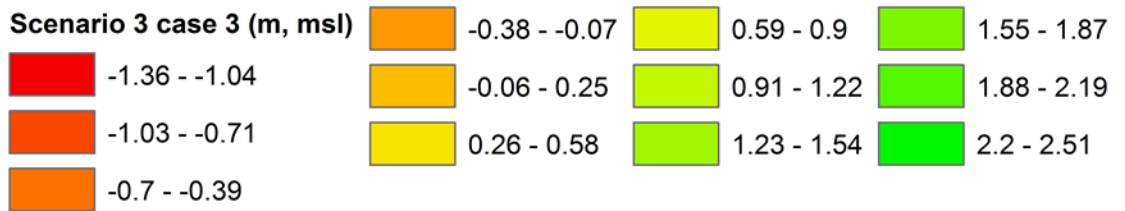
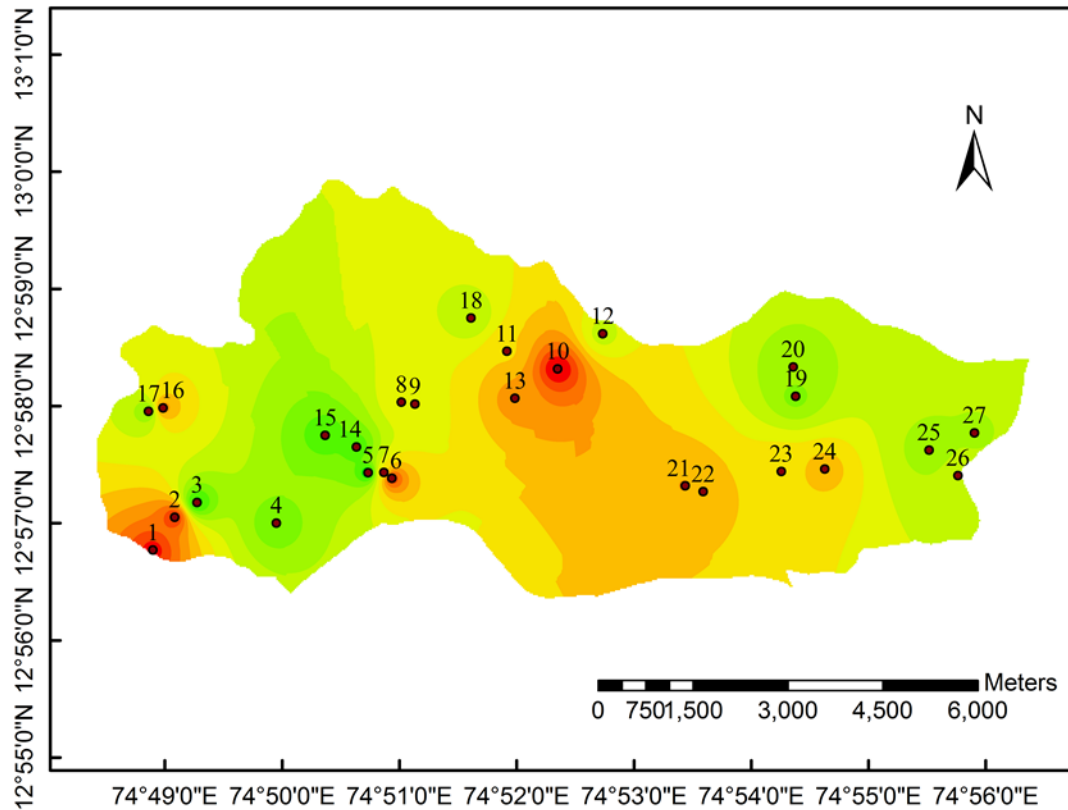


Figure 6.1 Spatial distribution of groundwater table for (C) Scenario 3 (Case 3) by the end of 20 year simulation (Year 2035)



Legend

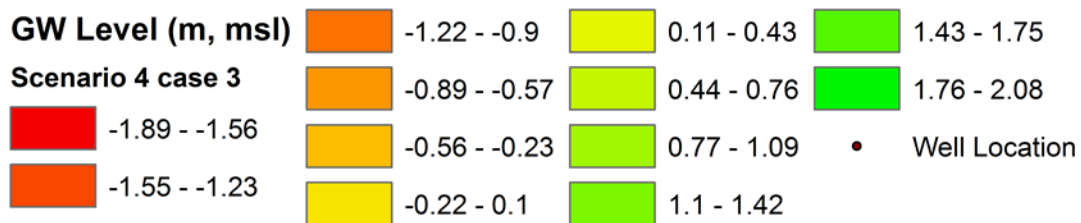


Figure 6.1 Spatial distribution of groundwater table for (D) Scenario 4 (Case 3) by the end of 20 year simulation (Year 2035)

Effect on TDS distribution

In general, from the TDS values listed in Table 6.2 as well as from the figure 6.2, it can be seen that, the area in the near vicinity of river (< 500m) is prone to higher level of TDS when the model is simulated for the extension of present condition of Scenario 1 (wells 1, 4, 7, 6, 22, 23, 24, 25, and 26). The aquifer region nearer to sea is also experiencing higher TDS value, towards west of the study area (well 17).

Table 6.2 TDS distribution (mg/ltr) for end of simulation year (2035)

Description	Well no.	Scenario 1	Scenario 2	Scenario 3			Scenario 4		
				Case 1	Case 2	Case 3	Case 1	Case 2	Case 3
Groundwater TDS (mg/ltr)	1	225	531	241	462	676	702	1023	1478
	2	65	82	76	93	195	243	321	865
	3	146	423	152	289	409	522	967	1062
	4	292	962	352	720	921	1028	1236	1459
	5	69	91	82	106	221	269	351	897
	6	222	526	239	459	669	695	1029	1456
	7	700	992	729	962	1069	1147	1369	1475
	8	154	476	179	301	452	632	1027	1165
	9	153	468	177	295	448	624	1019	1159
	10	110	392	116	234	362	445	621	761
	11	496	825	499	582	793	901	1236	1472
	12	307	628	331	452	609	823	968	1395
	13	62	77	73	89	186	226	309	811
	14	66	87	83	89	193	235	309	796
	15	222	522	265	522	686	692	991	1298
	16	140	403	139	259	573	478	693	832
	17	280	603	277	456	586	794	882	1283
	18	118	238	129	169	211	236	276	302
	19	271	596	267	246	563	786	869	1266
	20	237	537	271	501	693	709	1011	1329
	21	130	391	122	233	559	469	677	813
	22	210	501	241	483	656	673	963	1335
	23	389	723	421	523	924	1023	1203	1562
	24	874	1569	883	902	1029	1115	1532	1554
	25	359	693	396	463	782	932	1011	1332
	26	375	719	411	412	911	998	1195	1533
	27	117	399	127	249	371	457	639	788

The wetland region will have an increase in TDS value to approximately 441 mg/ltr for Scenario 2, from the status of Scenario 1 wherein the TDS value is 173 mg/ltr.

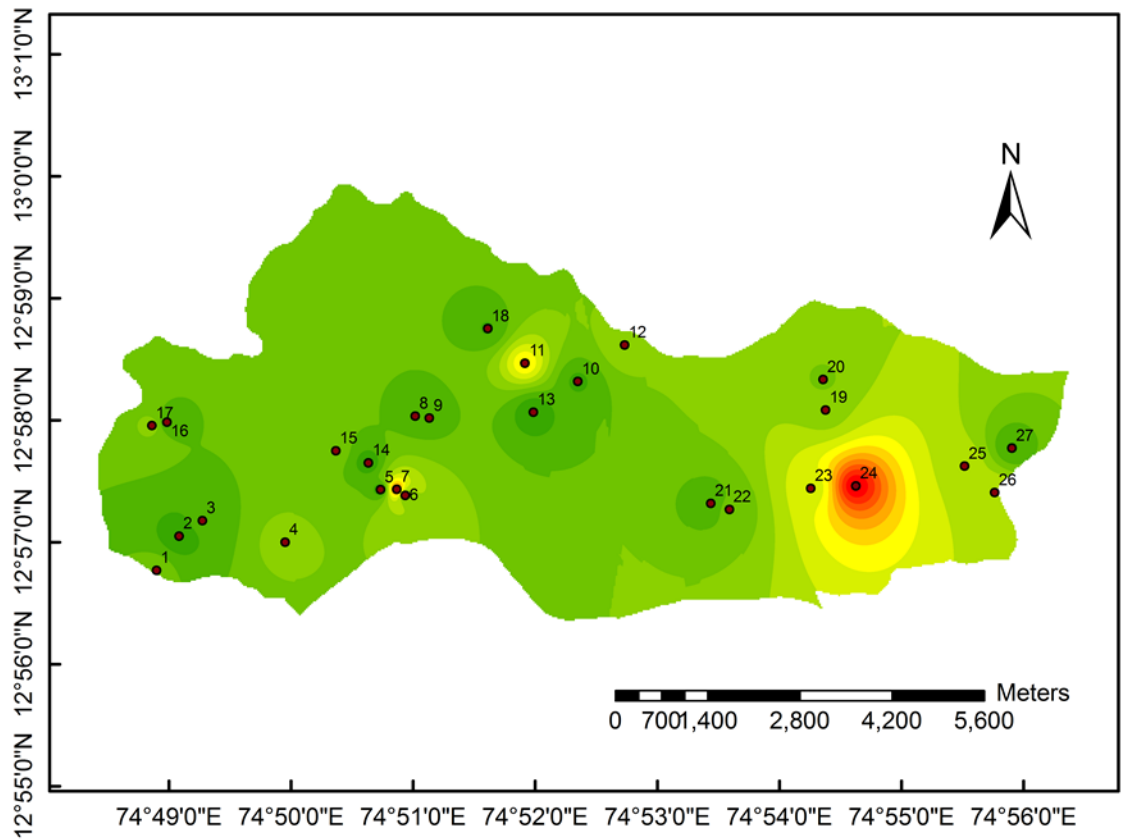
The ingress of TDS is predominant in the areas of intense agriculture for Scenario 2, because of the direct proximity of the river reaches (well no. 21, 22, 23 and 24).

The rise in average TDS value from the present situation to Scenario 2 is 251 mg/ltr to 535 mg/ltr, by the end of simulation period of 20 years.

Only marginal increase in average TDS value of 535 mg/ltr is observed for Case 3 of Scenario 3, throughout the study area. The wetland region is having an increase of 339 mg/ltr during Scenario 3 (Case 3), wherein the Scenario 1 predicted 173 mg/ltr of TDS. The groundwater status is safe as far as quality is concerned for Case 3 of Scenario 3.

There is noticeable increase in values of TDS estimated for Case 3 of Scenario 4. The average value of TDS across the study area is in the order of 1165 mg/ltr. The increase is almost 4.5 times than that of the Scenario 1 (extension of current condition). The region in the wetland area shows ever highest values of TDS among wells 3, 4, and 15 with 1062 mg/ltr, 1459 mg/ltr and 1298 mg/ltr respectively. However these values are within the maximum limit of 1500 mg/ltr specified by WHO.

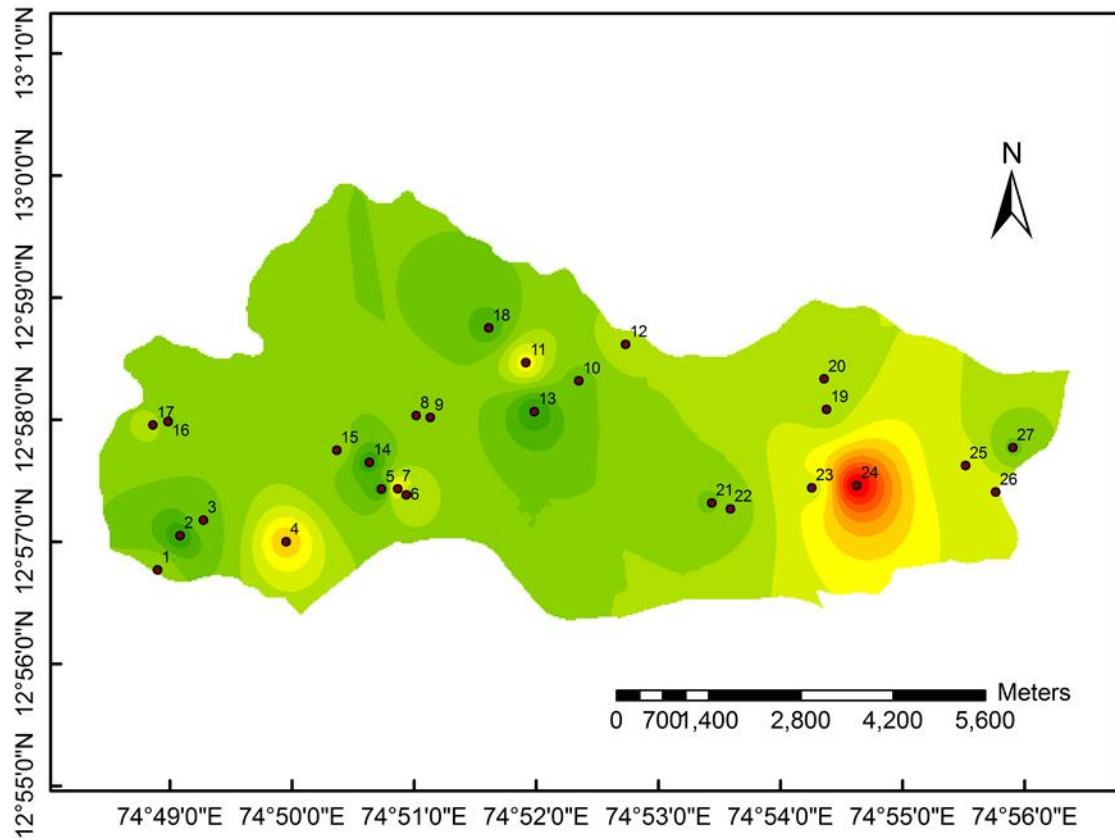
Similar trend is found among wells 22, 23, 24, 25 and 26, which lie in the region of active agriculture. The TDS values in these wells show drastic increase for Case 3 of Scenario 4. The wells 23, 24, 26 are having 1562 mg/ltr, 1554 mg/ltr and 1533 mg/ltr of TDS values respectively. These wells are crossing the limiting value of TDS with well no., 22 is having 1335 mg/ltr of TDS. This region of study area will be subjected to TDS contamination beyond acceptable limits, by the end of year 2035, as predicted in Scenario 4, Case 3.



Legend

Scenario 1 (mg/ltr)			
249.34 - 311.76	499.05 - 561.46	748.75 - 811.16	
62.06 - 124.48	311.77 - 374.19	561.47 - 623.89	811.17 - 873.59
124.49 - 186.91	374.2 - 436.61	623.9 - 686.31	
186.92 - 249.33	436.62 - 499.04	686.32 - 748.74	

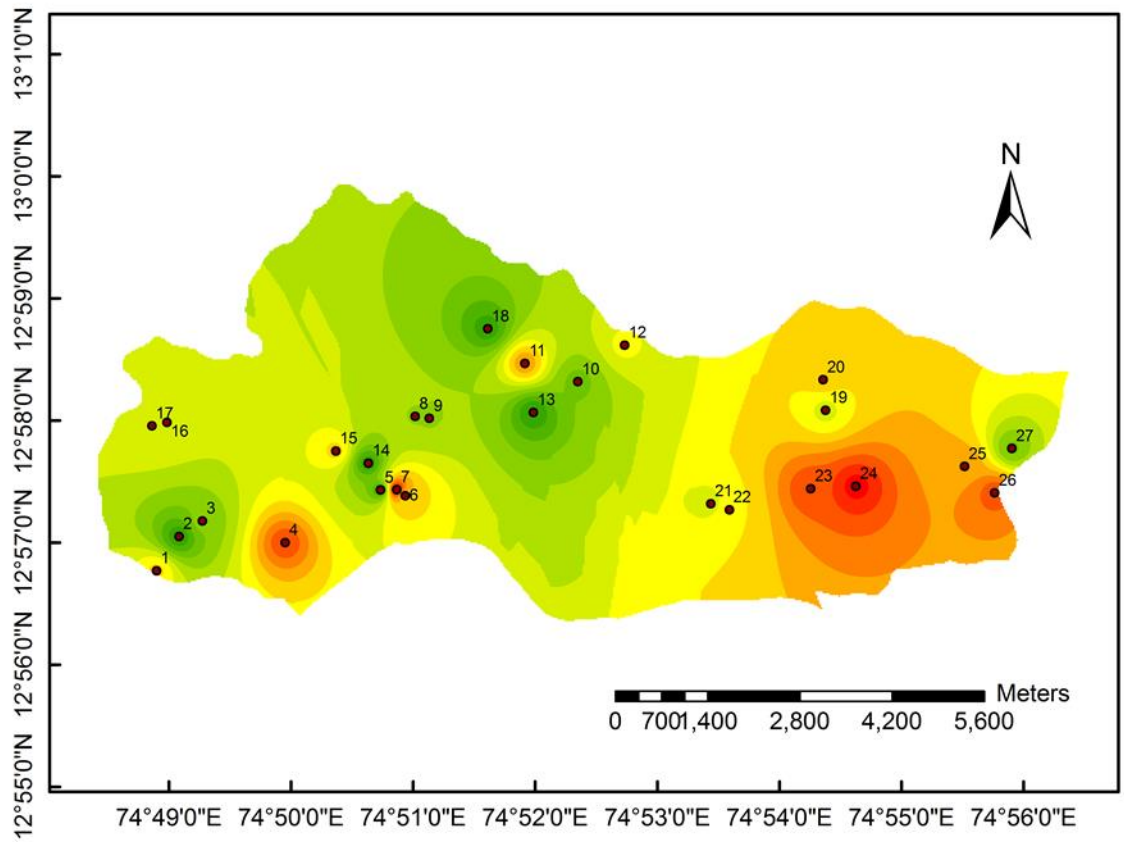
Figure 6.2 Spatial distribution of TDS for (A) Scenario 1



Legend

Scenario 2 (mg/ltr)			
	421.26 - 535.96		880.09 - 994.78
	77.13 - 191.84		994.79 - 1,109.49
	191.85 - 306.54		1,109.5 - 1,224.19
	306.55 - 421.25		1,224.2 - 1,338.9
			1,338.91 - 1,453.61
			1,453.62 - 1,568.31

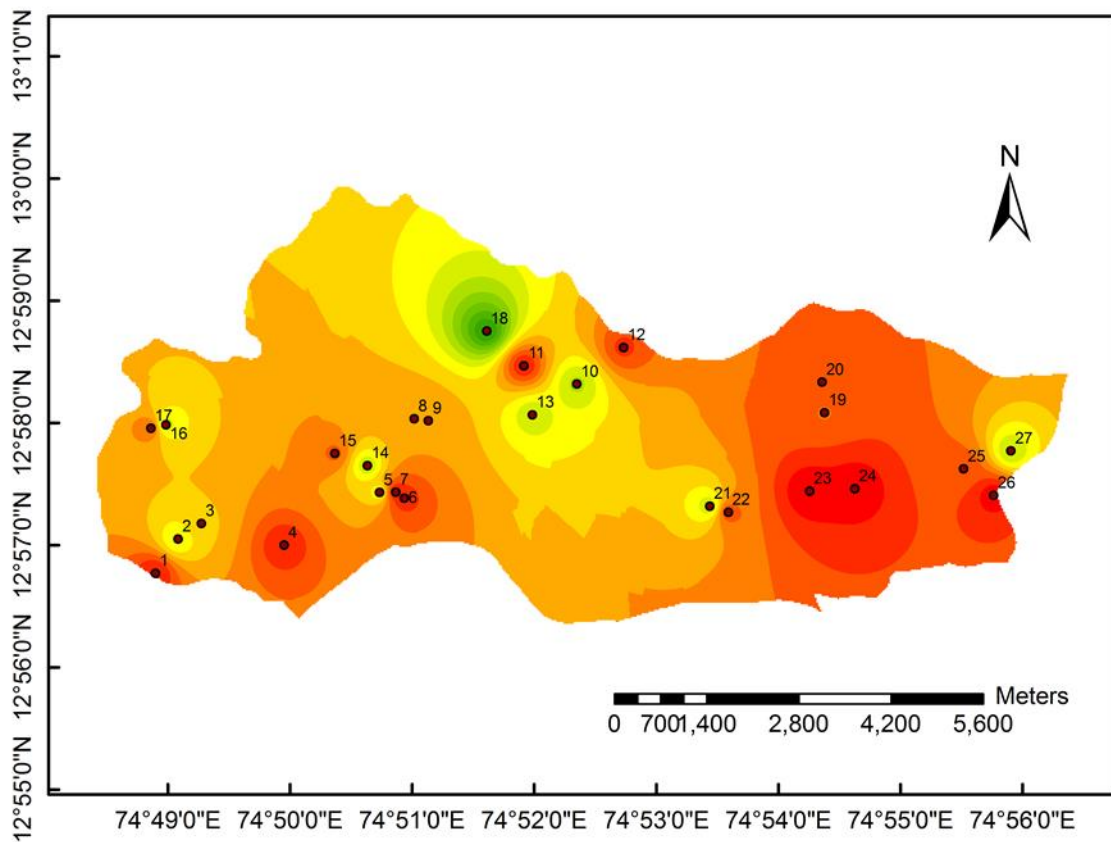
Figure 6.2 Spatial distribution of TDS for (B) Scenario 2



Legend

Scenario 3 case 3 (mg/ltr)			
■ 186.1 - 253.51	■ 388.35 - 455.76	■ 658.01 - 725.41	■ 927.66 - 995.07
■ 253.52 - 320.93	■ 455.77 - 523.17	■ 725.42 - 792.83	■ 995.08 - 1,062.48
■ 320.94 - 388.34	■ 523.18 - 590.58	■ 792.84 - 860.24	■ 860.25 - 927.65
	■ 590.59 - 658	■ 860.25 - 927.65	

Figure 6.2 Spatial distribution of TDS for Scenario 3 (Case 3)



Legend

Scenario 4 case 3 (mg/ltr)		
593.13 - 689.99	980.61 - 1,077.47	1,368.09 - 1,464.95
302.51 - 399.38	690 - 786.86	1,077.48 - 1,174.34
399.39 - 496.25	786.87 - 883.73	1,174.35 - 1,271.21
496.26 - 593.12	883.74 - 980.6	1,271.22 - 1,368.08
		1,464.96 - 1,561.82

Figure 6.2 Spatial distribution of TDS for (D) Scenario 4 (Case 3)

6.3.2 The temporal effects of scenario on the aquifer

The aquifer responds more or less alike to the various scenario of simulations mentioned above. The response of the aquifer system during the 20 years of simulation period is illustrated by presenting comparative graphs for water table elevation and groundwater TDS loading, at earmarked location in the study region.

Effect on water table

The variation of groundwater table through 20 year simulation period for the 4 scenarios considered are depicted for a location (x = 483053 E and y = 1433008 N), which is at a distance of 1900m from the river boundary and is located in the region where wetlands are present in the study area (figure 6.3). The temporal variation of water table is presented for the summer month of May in Fig.6.3 and the monsoon month of September in Fig.6.4 at this location for various scenarios assumed during the prognostic simulations.

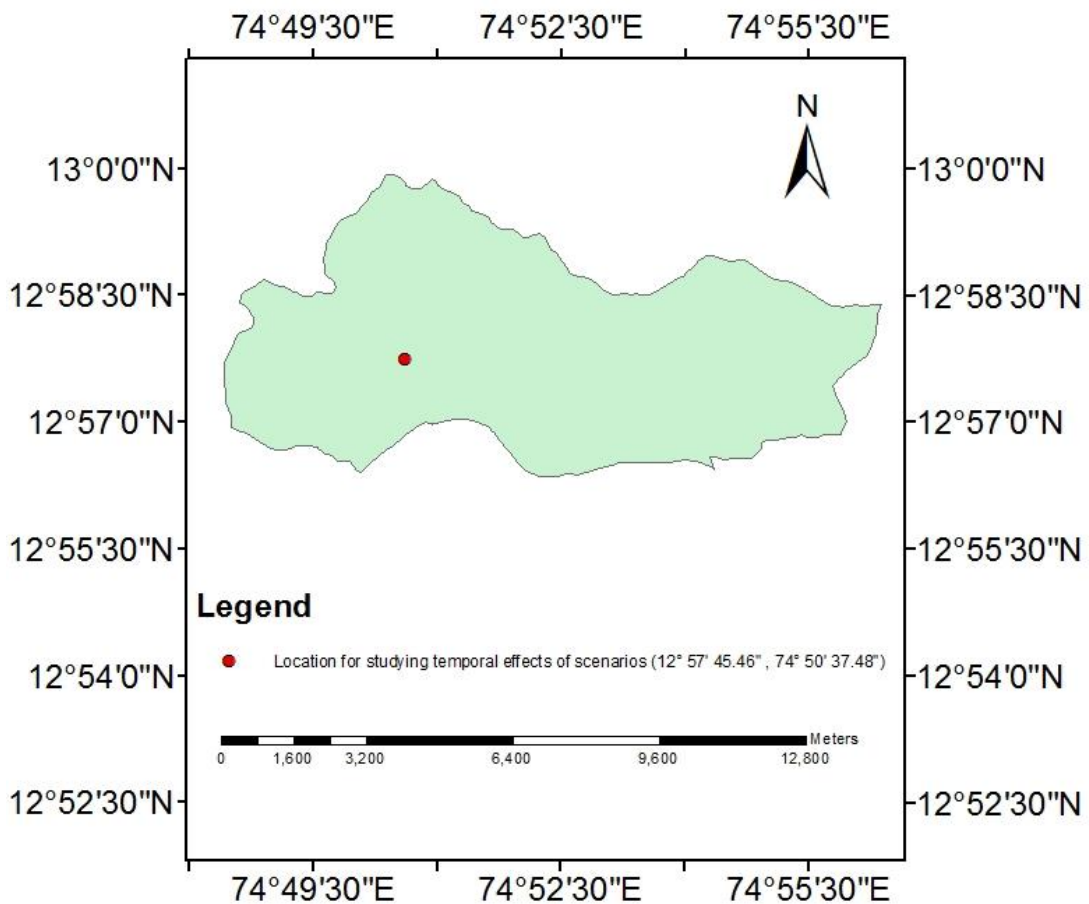


Figure 6.3 Location for studying temporal effects of various scenarios

While all the 4 scenarios of simulations are compared in figure 6.4 A, the water table around the wetland region is estimated to have a fall of approximately 0.3m for case 3 of scenario 3 and 0.6 m for case 3 of Scenario 4 compared to Scenario 1.

The groundwater table in the wetland region is predicted to have a slump of approximately 0.2m by the end of 20 years period in case of Scenario 2 simulation when compared to that of Scenario 1. The plot for the month of May for the case 3 of Scenario 3, as seen in figure 6.4 B shows a noticeable fall in the water table by the middle of the simulation period. All the cases of Scenario 4 show a decline of 0.1 m by the end of the simulation period as shown in figure 6.4 C.

The wetland will experience maximum decrease in groundwater table level for 10% recharge rate and 150% increase in pumping rate. This decrease in groundwater level will be around 0.6m from Scenario 1, in the month of May during the year 2035 (figure 6.4 A).

During the month of September, the decrease in groundwater level around wetland will be about 1m for case 3 of Scenario 4, when compared to Scenario 1 (figure 6.5 A), by the year 2035. However, the groundwater table will be at a higher elevation when compared the levels during the month of May 2035.

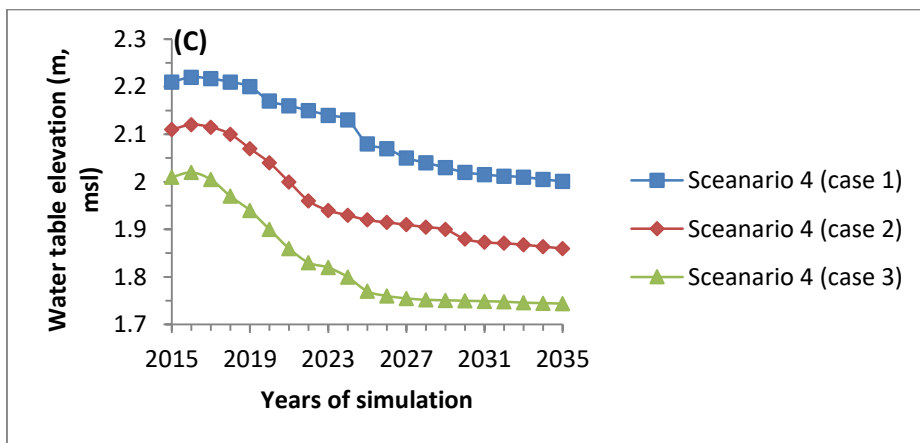
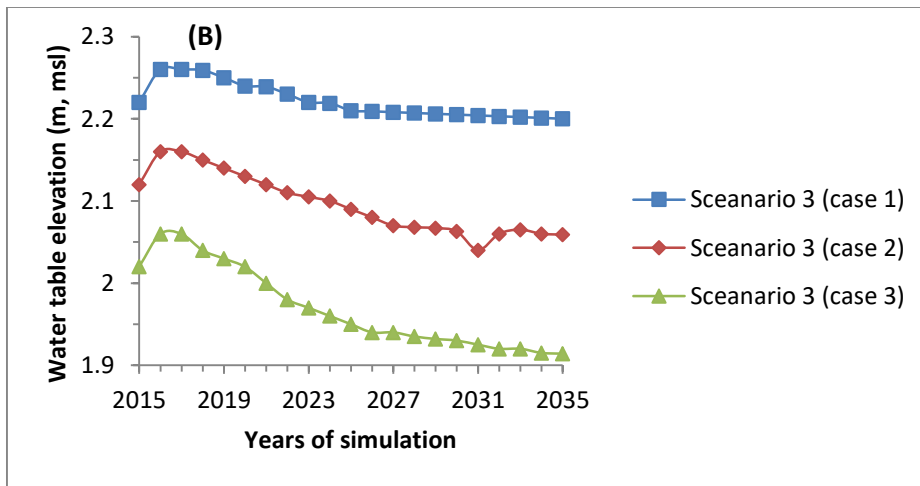
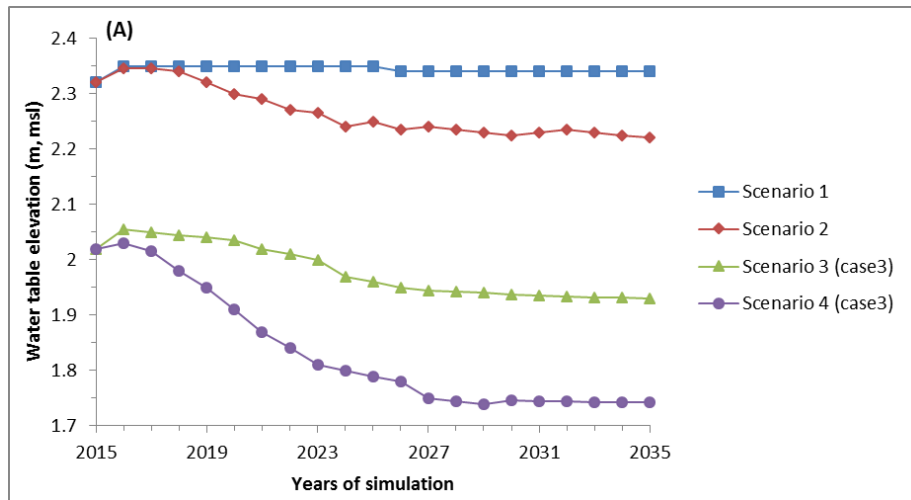


Figure 6.4 Status of Groundwater table over 20 year period during the month of May.

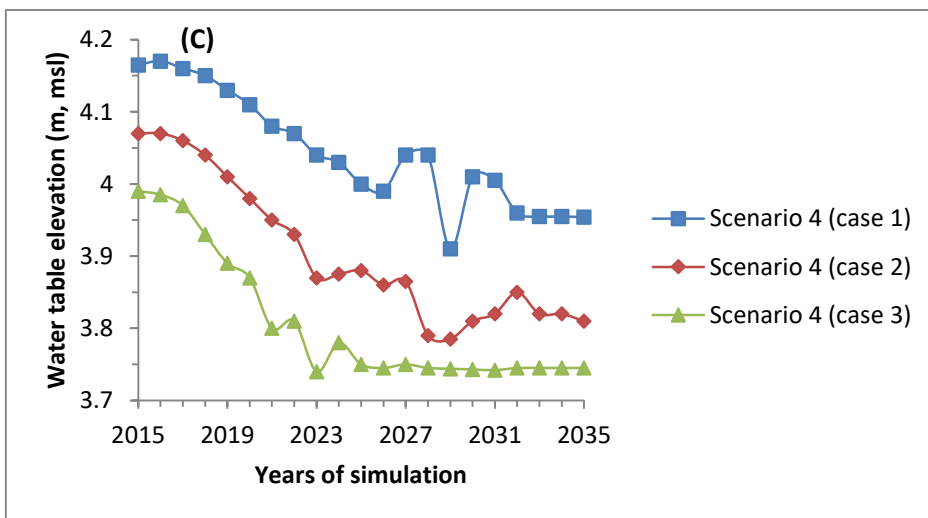
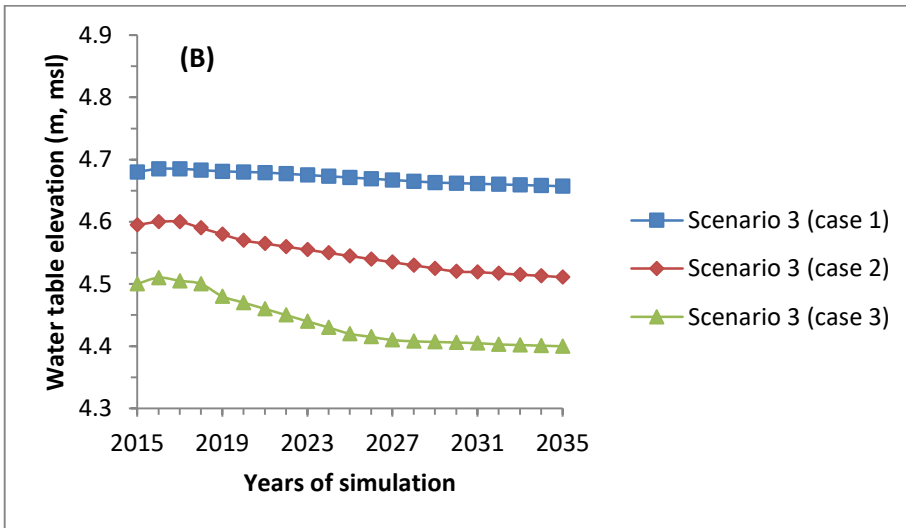
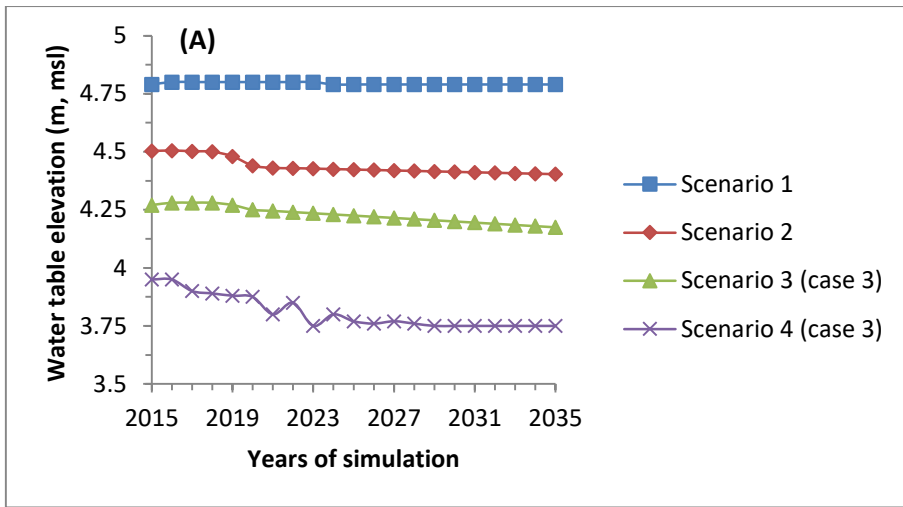


Figure 6.5 Status of Groundwater table over 20 year period during the month of September.

Trend of TDS variation

The variation of TDS with time over a simulated period of 20 years at the same location is presented in figure 6.6 (A) for scenarios 1 to 4. This graph shows that, the decrease in recharge rate (Scenario 2) alone can raise the TDS to 600mg/ltr in the first 8 years of simulation and thereafter increases to 900mg/ltr by the end of 20 years of simulation. However, with the present rate of groundwater utilization and recharge rate, the aquifer can be considered safe for the next 16 years with TDS<1500 mg/ltr, which reaches a TDS of 1450 mg/ltr by the end of 20 years.

The quality of groundwater remains safe for drinking purpose (TDS < 1500 mg/ltr) till 20 years, except for case 3 of Scenario 4. The TDS levels tends to reach a level of 1450 mg/ltr by the end of 20 years. The groundwater quality is deprived for cultivation (TDS >1000 mg/ltr) over the next 14 years under Scenario 4, case 2.

As per figure 6.6 B, every 50% increase in groundwater utilization causes the salinity to increase considerably every year till the end of 20 year period. The decrease in recharge rate with increase in withdrawal rate is suspected to have a serious impact on the aquifer system. As only 50% increase in groundwater utilization rate combined with reduction in recharge rate (figure 6.6 C) causes the salinity to rise in TDS level up to 1000 mg/ltr in 20 years.

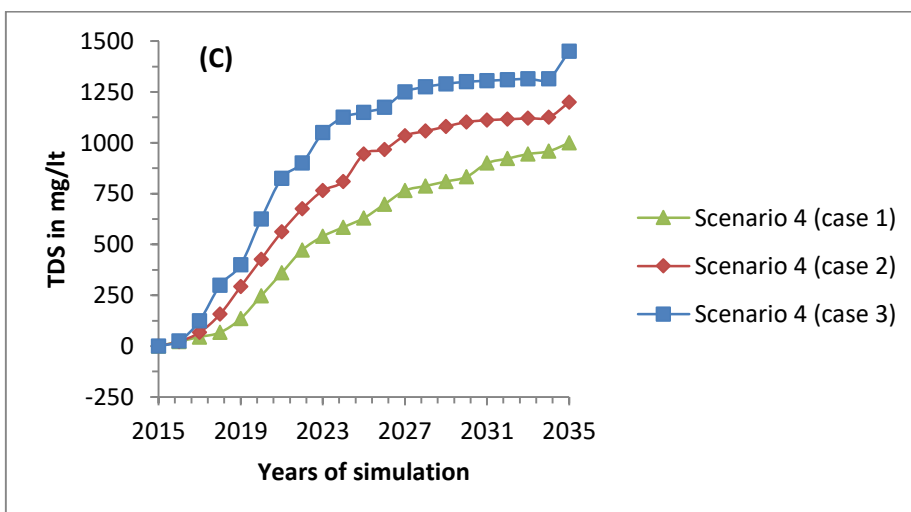
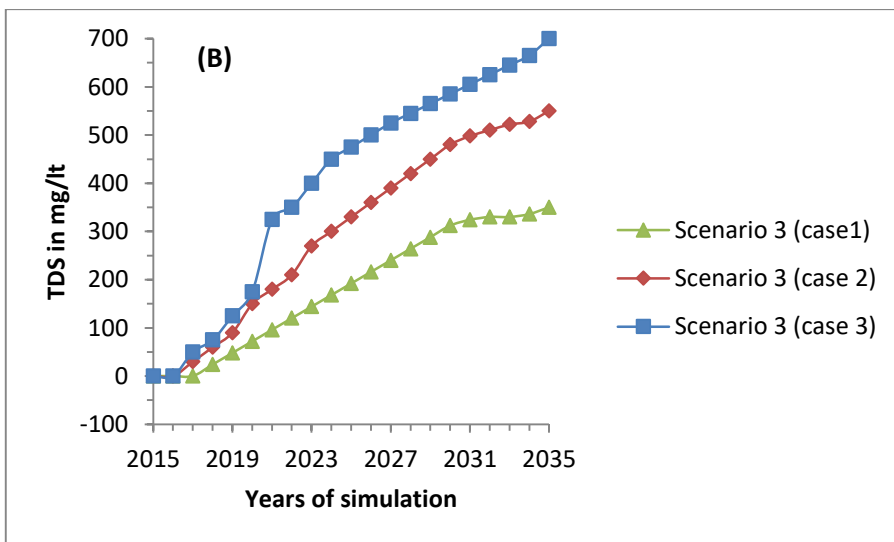
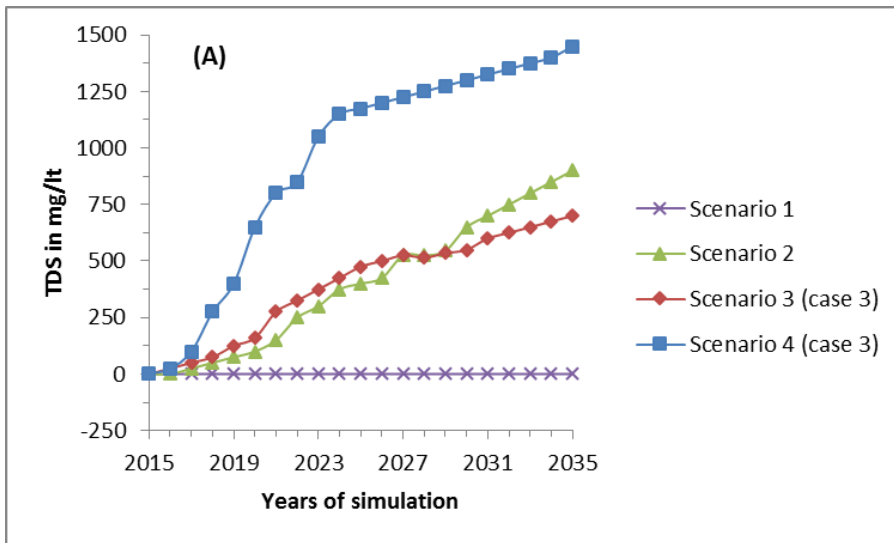


Figure 6.6 Status of TDS over 20 year period.

6.5 CLOSURE

The SEAWAT model after validation is applied to evaluate the regional impact on the aquifer for four likely scenarios. The simulation is executed for a reasonably longer period of 20 years elapsing from 2015 to 2035. The scenarios are planned keeping in view the possible hydrological stresses those could be exerted on the aquifer due to probable changes in growth status in terms of groundwater usage. The study is formulated in such a way that, the combinations of different recharge and pumping rates can be analysed with respect to the aquifer response in the future. Such a study would be of use in view of utilizing groundwater in a planned and optimal manner, thereby maintaining a sustainable development of groundwater resources in the study area.

The effect of scenarios of simulations on the aquifer is analysed in different aspects, considering the temporal and spatial variation.

The study reveals that the worst case combination of reduced recharge rate with increased pumping rates has a serious impact on the aquifer system with fall in water table. The TDS values also approaches the limiting values for the worst combinations of scenario simulations, by the end of simulation period.

However, the water table in the region of wetland and intense agriculture area will remain stable at higher level, though in the rest of the area water table finds slump of around 0.9m for the extreme simulation scenario. Similarly, the TDS levels remain well within the acceptable limits, in the wetland region, for all the cases of simulation scenarios. The intense agriculture region will have TDS values reaching limiting values for extreme scenario case. Otherwise, the groundwater in the study area is safe from drinking and agriculture perspective.

SUMMARY AND CONCLUSIONS

Water resources in the coastal areas and wetlands take up a special significance since any developmental activity will largely depend upon availability of fresh water to meet domestic, industrial and agricultural requirements. However, fresh water resources in these aquifers are likely to experience disastrous and irreversible impacts in the coming times due to overexploitation of groundwater resources and sea level rise. Groundwater withdrawals in excess of safe yields and reduced recharges to groundwater due to rapidly changing land use pattern along the coasts are likely to have the incidences of aggressive seawater intrusions into the coastal aquifers.

Hence, groundwater resources in coastal aquifers have to be managed in a sustainable manner to overcome the challenges. The present study is focused on the above issue by taking up the simulation of the shallow, coastal aquifer involving wetland patches, for the present and future anticipated groundwater variations in terms of quantity and quality. The numerical simulation was carried out using SEAWAT. In addition, aquifer characterization was also being done through the field tests. The results obtained from the investigation may be useful for scientific assessment of freshwater resources under similar conditions elsewhere. The conclusions drawn from the study are presented here.

AQUIFER CHARACTERIZATION

The pumping tests, Vertical Electrical Sounding and bore log details were used to evaluate the aquifer parameters, in the study area.

1. The data from various bore log and VES investigations in the study area confirms that, the basin is predominantly an unconfined aquifer with depth ranging from 13m to 30m. Also, the lateritic formation is topped by sand followed by the top soil. Beneath the laterite, a huge mass of hard rock material (gneiss) is detected upto a depth of about 90m. The region where wetlands are present, sand mixed with silty soil were found to be present.

2. The transmissivity and specific yield evaluated from the pumping tests using Neuman's method range from 61 to 655 m²/day and 0.009 to 0.1 respectively. Compared to other methods, the Neuman's method was found to be more appropriate for the study area.

GROUNDWATER FLOW MODEL

The development of groundwater flow model was carried out using MODFLOW. The model of study area is built with finite difference grid size of 100m×100m in the horizontal plane. In the vertical plane, the model follows the top elevation interpolated with the DEM generated for the region. Based on the field tests, the bottom of the model is set at - 30m (with respect to mean sea level). Apart from evaluating the seasonal performance of the model with respect to the calibrated parameters, an effort was made to evaluate the spatial distribution of water table and water budget estimation.

1. The values of RMSE during the calibration period (2011-13) are usually less than or equal to 1 m, except that for the monsoon season. This is reasonable for the kind of model developed with the execution of scarcely available input data. The NSE greater than or equal to 0.5, except during the monsoon months, confirms the ability of the model to simulate the monthly groundwater table with reasonable accuracy both during the calibration and validation phases.

2. The values of horizontal hydraulic conductivity and specific yield of the unconfined aquifer is estimated during calibration are in the range 2.54m/day to 19.16 m/day and 0.007 to 0.089 respectively which agree with the range established earlier. Also, recharge co-efficient of 20% of rainfall, porosity of 30% are obtained as appropriate parameters during the calibration phase.

3. From the water budget study performed it is found that, during the period of maximum potential position (August), the component of groundwater contributing to wetland is 4.5% of total outflow. During dry season with minimum potential head, the groundwater contribution to wetland is 1.4% of total outflow. Hence, the presence of water in the wetland during the non-monsoon months is established by the major contribution of groundwater, in the study area.

4. It is also confirmed from water budget analysis that more than 50% of available water is being discharged to the river during the wet season and during the dry season 82% of water is discharged through the southern boundary. During the dry season, the volume of water flowing out of the aquifer is lesser than the flow into the aquifer indicating higher probability of sea water ingress from the river carrying salinity during high tides. Since the river is tidal in nature, the contribution of river saline water is considerable to the aquifer system during the non-monsoon months. It is also observed that, the major input into the aquifer is through rainfall recharge, contributing to 74% of input.

SOLUTE TRANSPORT MODEL

The solute transport model simulation for the study area is carried out using MODFLOW incorporated into MT3DMS with SEAWAT model. The study leads to following conclusions:

1. The model is performing better during the non-monsoon season than during the monsoon season. The calibration results show that, the ability of the model to simulate contaminant transport is reasonably good with $NSE \geq 0.5$.
2. Longitudinal dispersivity of 30m, transverse dispersivity of 3m and molecular diffusion co-efficient of $8.64 \times 10^{-5} \text{m}^2/\text{day}$ are achieved during calibration of transport model.
3. The calibration results indicate that, the study area remains safe against contaminant transport ($\text{TDS} < 1500 \text{ ppm}$) for the present scenario of groundwater draft.
4. During the months from July to September (monsoon), the TDS values in the study area range from 42 mg/l to 302 mg/l, among majority of the region which is very much within the desirable limit.
5. The wetland region is found to have lower TDS values (42 mg/l to 205 mg/l) during monsoon months. The wells around wetlands show slightly higher TDS levels during post – monsoon season compared to monsoon season (170 mg/l to 700 mg/l). The TDS trend during summer months from is found to be around 400 mg/l to 719 mg/l, for wells nearby the wetland.

6. The specific predictive trend analyser has shown exceptional high concentration of TDS to be touching 1500 mg/lit, during the summer months, in some of the areas. However, the quality of groundwater could be considered as reasonably fresh, even during these months, throughout the study area.

SENSITIVITY ANALYSIS

The response of the aquifer in the study area to various flow parameters namely recharge rate, horizontal hydraulic conductivity, specific yield and transport parameter (longitudinal dispersivity) are investigated. The conclusions drawn based on this study are:

1. The aquifer region feeding to the wetland is having lower sensitivity to specific yield.
2. The wetland region is located at a zone with a lower hydraulic conductivity value (3.89 m/day). These wells around are marked with “High” sensitivity index. The wetland is located in this region of lower hydraulic conductivity, which is a conducive environment for existence of wetlands. This region is also in the near vicinity of sea coast and river boundary at south. The variation of levels in the sea as well as river have a greater influence on the groundwater table in this region. This observation is supported by higher sensitivity index.
3. The region around the wetland is marked as shallow water region of the aquifer, showing high sensitivity to recharge rate. Due to the lateral inflow in this zone, the effect of recharge due to rainfall gets reduced. The aquifer gets recharged quickly after the rains due to high sensitivity of aquifer towards recharge rate and shallow water conditions in the region.

PROGNOSTIC SIMULATIONS

The SEAWAT is made use of to simulate the future realistic scenarios of various stress combinations. The conclusions drawn based on 20 years of simulation are given below.

1. The groundwater table falls by an average of 0.4m over the entire aquifer region, due to the decrease in recharge rate (10%).

2. There is a fall of groundwater table of approximately 0.17 m observed around the region of wetlands by the end of simulation, for the extreme scenario case (Scenario 4, case 3).
3. The intense agricultural region in the study area may lead to a slump of approximately 0.45m, in groundwater table level by the end of year 2035.
4. The wetland region would experience a fall in groundwater table, of approximately 0.29m according to Scenario 3 case 3.
5. The average fall in groundwater table is 0.90m across the entire aquifer for Scenario 4 Case 3. In the case of wetland region, it is limited to 0.66m.
6. The wetland region will have an increase in TDS value to approximately 441 mg/ltr for Scenario 2, from the Scenario 1 wherein the TDS value is 173 mg/ltr.
7. Only marginal increase in average TDS value of 535 mg/ltr is observed for Case 3 of Scenario 3, throughout the study area. The wetland region is having a rise of 339 mg/ltr during Scenario 3 (Case 3), wherein the Scenario 1 predicted 173 mg/ltr of TDS as present status. The groundwater status is safe as far as quality is concerned for case 3 of Scenario 3.
8. There is noticeable increase in values of TDS observed for case 3 of Scenario 4. The average value of TDS across the study area is in the order of 1165 mg/ltr. The increase is almost 4.5 times than that of the Scenario 1 (current condition). The region in the wetland area shows ever highest values of TDS among wells 3, 4, and 15 with 1062 mg/ltr, 1459 mg/ltr and 1298 mg/ltr respectively. However, these values are within the maximum limit of 1500 mg/ltr specified by WHO.
9. The water table around the wetland region is found to have a fall of approximately 0.3m for case 3 of scenario 3 and 0.6 m for Case 3 of Scenario 4 from that of Scenario 1 which is the extension of current state of the aquifer around the wetlands.
10. The wetland will experience maximum decrease in groundwater table level for 10% recharge rate and 150% increase in pumping rate. This decrease in groundwater level will be around 0.6m from the current situation, in the month of May during the year 2035.

LIMITATIONS OF THE STUDY

1. The vertical non-homogeneity is not considered in the present study.
2. The model performance during the monsoon months from June to September is not encouraging. All the three evaluation techniques are showing deviation from the acceptable levels. There could be greater interaction or increased inflow between river water and seawater for these months and during high tides. This issue is not well addressed by the model.

SCOPE FOR FUTURE STUDIES

1. The modelling may be carried out incorporating complete details of sub-strata.
2. Wetland's surface water and groundwater interaction studies can be taken up for better understanding of the wetland behaviour.

REFERENCES

- Abdulla, F. and Al-Assad, T. (2006). "Modelling of groundwater flow for Mujib aquifer", Jordan." *J. Earth Sys. Sci.*, 115(3), 289-297.
- Abdulla, F. A., Al-Khatib, M. A. and Al-Ghazzawi, Z. D. (2000). "Development of groundwater modeling for the Azraq Basin, Jordan." *Environ. Geol.*, 40, 1-2.
- Abdalla, O.A.E. (2009). "Groundwater modeling in semiarid Central Sudan: adequacy and long-term abstraction." *Arab J. Geosci.*, 2, 321–335.
- Adrian, D., Werner, J.D., Ward, L. K., Morgan, C. T., Simmons, N. I., Robinson, M. D. and Teubner, M. D. (2012). "Vulnerability indicators of seawater Intrusion". *Ground Water*, 50 (1), 48-58.
- Aggarwal, R., Sondhi, S. K., Jain, A. K. and Kaushal, M. P. (2005). "Groundwater simulation model for South-West Punjab." *IE(I) Journal –AG*, 86(2),18-23.
- Ahmed, I. and Umar, R. (2009). "Groundwater flow modelling of Yamuna–Krishni inter stream, a part of central Ganga Plain Uttar Pradesh." *J. Earth Sys. Sci.*, 118 (5), 507–523.
- Allow, K. A. (2012). "The use of injection wells and a subsurface barrier in the prevention of seawater intrusion: A modelling approach." *Arab J. Geosci.*, 5, 1151-1161.

- Al-Salamah, I. S., Ghazaw, Y. M. and Ghumman, A. R. (2011). "Groundwater modeling of Saq Aquifer Buraydah Al Qassim for better water management strategies." *Environ. Monit. Assess.*, 173(1-4), 851-860.
- Amer, A. M. (1995). "Saltwater intrusion in coastal aquifers." Proc., Int. Conf. on Water Resources Management in Arid Countries, Muscat, 521–529.
- Anderson, M. and Woessner, W. (1992). "Applied groundwater modeling simulation of flow and advective transport." Academic Press, San Diego, CA, 381.
- Antonellini, M., Allen, D. M., Mollema, P. N., Capo, D. and Greggio, N. (2015). "Groundwater freshening following coastal progradation and land reclamation of the Po Plain, Italy." *Hydrogeol J.*, 23(5), 1009-1026.
- Arlai, P., Koch, M. and Koontanakulvong, S. (2006). "Statistical and stochastic approaches to assess reasonable calibrated parameters in a complex multi-aquifer system", *In: Proc. of CMWR XVI - Computational Methods in Water Resources*, Copenhagen, Denmark.
- Asghar, M. N., Prathapar, S. A. and Shafique, M. S. (2002). "Extracting relatively fresh groundwater from aquifers underlain by salty groundwater." *Agr. Water Manag.*, 52,119–137.
- Ataie-Ashtiani, B., Volker, R. E. and Lockington, D. A. (1999). "Tidal effects of seawater intrusion in unconfined aquifers." *J. Hydrol.*, 216, 17-31.

Ayeneu, T., Demlie, M. and Wohnlich, S. (2008). "Application of Numerical Modeling for Groundwater Flow System Analysis in the Akaki Catchment, Central Ethiopia." *International Association for Mathematical Geology*, 40, 887–906.

ASCE, 1993. "Criteria for evaluation of watershed models." *J. Irrigation Drainage Eng.*, 119(3), 429-442.

Bauer, P., Held, R. J., Zimmermann, S., Linn, F. and Kinzelbach, W. (2006). "Coupled flow and salinity transport modelling in semi-arid environments: The Shashe river valley, Botswana." *J. Hydrol.*, 316, 163-183.

Bear, J., Cheng, A .H.D., Sorek. S., Ouazar, D. and Herrera, I. (1999). "Seawater intrusion in coastal aquifers: concepts, methods and practices." *Theory and Applications of Transport in Porous Media*, 14. Kluwer, Dordrecht, Netherlands.

Bhosale, D.D. and Kumar, C.P. (2001). "Simulation of seawater intrusion in Ernakulam coast ." (<http://www.angelfire.com/nh/cpkumar/publication/ernac.pdf>), Dec. 8, 2013.

Bradley C. (1995), "Transient modelling of water-table variation in a floodplain wetland, Narborough Bog, Leicestershire". *Journal of Hydrology*, 185 (1996), 87-114.

- Bobba, A. G. (2002). "Numerical modelling of salt-water intrusion due to human activities and sea-level change in the Godavari Delta, India." *Hydrolog. Sci. J.*, 47, 67-80.
- Boulton, N. S. (1954). "Unsteady radial flow to a pumped well allowing for delayed yield from storage." *Intern. Assoc. Sci. Hydrol. Rome. Publ.* 37, 472-477.
- Boulton, N. S. (1963). "Analysis of data from non-equilibrium pumping tests allowing for delayed yield from storage." *Proc., Inst. Civ. Eng., USA*, 26, 469-482.
- Boulton, N. S. (1970). "Analysis of data from pumping tests in unconfined anisotropic aquifers." *J. Hydrol.*, 10, 369–378.
- Boulton, N. S. and Pontin, J. M. A. (1971), "An extended theory of delayed yield from storage applied to pumping tests in unconfined anisotropic aquifers." *J. Hydrol.*, 14, 53–65.
- Boulton, N. S. and Streltsova, T. D. (1975). "The drawdown near an abstraction well of large diameter under non-steady conditions in an unconfined aquifer." *J. Hydrol.*, Vol. 30, 29-46.
- Brunner, P., Hendricks, F. H. J., Kgotlhang, L., Bauer-Gottwein, P. and Kinzelbach, W. (2006). "How can remote sensing contribute in groundwater modeling?." *Hydrogeol J.*, 15(1), pp. 5–18.

- Camp, V. M., Mjemah, I. C., Al Farrah, N. and Walraevens, K. (2013). "Modeling approaches and strategies for data-scarce aquifers: example of the Dar es Salaam aquifer in Tanzania." *Hydrogeol J.*, 21(2), 341-356.
- Carrera, J., Hidalgo, J. J., Slooten, L. J. and Vázquez-Suñé, E. (2010). "Computational and conceptual issues in the calibration of seawater intrusion models." *Hydrogeol J.*, 18(1), 131-145.
- Chaaban, F., Darwishe, H., Louche, B., Battiau-Queney, Y., Eric Masson., El Khattabi, J. and Carlier, E. (2012). "Geographical information system approach for environmental management in coastal area (Hardelot-Plage, France)." *Environ. Earth Sci.*, 65,183–193.
- Chang, S. W. and Clement, T. P. (2013). "Laboratory and numerical investigation of transport processes occurring above and within a saltwater wedge." *J. Contam. Hydrol.*, 147, 14-24.
- Chekirbane, A., Tsujimura, M., Kawachi, A., Isoda, H., Tarhouni, J. and Benalaya, A. (2015). "3D simulation of a multi-stressed coastal aquifer, northeast of Tunisia: salt transport processes and remediation scenarios." *Environ. Earth Sci.*, 73(4), 1427-1442.
- Cobaner, M., Yurtal, R., Dogan, A., and Motz, L. H. (2012). "Three dimensional simulation of seawater intrusion in coastal aquifers: A case study in the Goksu deltaic plain." *J. Hydrol.*, 262-280.

- Comte, J. C., Join, J. L., Banton, O. and Nicolini, E. (2014). "Modelling the response of fresh groundwater to climate and vegetation changes in coral islands." *Hydrogeol. J*, 22(8), 1905-1920.
- Cooper, H. H. Jr., Kohout, F. A., Henry, H. R. and Glover, R. E. (1964). "Sea water in coastal aquifers." *US Geol Surv Water Supply*, 1613-1626.
- Coppola, E. A., Anthony. J. R., Mary M. P., Ferenc, S. and Vincent, W. U. (2005). "A neural network model for predicting aquifer water level elevations." *Ground Water*, 43(2), 231-241.
- Crowe Allan S., Shikaze Steven G., Ptacek Carol J. (2004), "Numerical Modelling of groundwater flow and contaminant transport to point Pelee marsh, Ontario, Canada, *Hydrological Processes*, Vol. 18. 293-314.
- Custodio, E. and Galofre, A. (1992). "Study and modeling of saltwater intrusion into aquifers." *Proc. of the saltwater intrusion meeting*, Barcelona, Spain. CIMNE Publisher.
- CGWB (2008). Central Groundwater Board. "Groundwater resources and development potential of Dakshina Kannada district, Karnataka." (AAP 2004-2005), *Govt. of India, Ministry of Water Resources*, South western region, Bangalore.
- CGWB (2012), Central Ground Water Board. "Groundwater information booklet, Dakshina Kannada district, Karnataka." *Govt. of India, Ministry of Water Resources*, South western region, Bangalore, 18.

Dagan, G. (1967). "A method of determining the permeability and effective porosity of unconfined anisotropic aquifers." *Water Resour. Res.*, 3(4), 1059-1071.

De Louw, P. G., Eeman, S., Siemon, B., Voortman, B. R., Gunnink, J., Van Baaren, E. S. and Essink, O.G. (2011). "Shallow rainwater lenses in deltaic areas with saline seepage." *Hydrol. Earth Syst. Sci.*, 15, 3659-3678.

Diersch, H.J.G (2006). "FEFLOW 5.3: Finite element subsurface flow and transport simulation system user manual version 5.3." Berlin Germany: WASY GmbH Institute for Water Resources Planning and Systems Research. In: Loaiciga, H. A., Pingel, T. J. and Garcia, E. S. (2012). "Seawater intrusion by sea-level rise: Scenarios for the 21st century." *Ground Water*, 50 (1), 37-47.

Doherty, J. (2004). "PEST- Model Independent Parameter Estimation, User manual." *Watermark Numerical Computing*.

Duffield, G. M. (2007). "AQTESOLV for Windows Version 4.5 User's Guide." Hydro SOLVE, Reston, VA.

Dufresne, D. P. and Drake, C.W. (1999). "Regional groundwater flow model construction and wellfield site selection in a karst area, Lake City, Florida." *Eng.Geol.*, 52, 129–139.

El-Bihery, M. A (2009). "Groundwater flow modeling of Quaternary aquifer Ras Sudr, Egypt." *Environ. Geol.*, 58, 1095–1105.

El-Kadi, A. I., Tillery, S., Whittier, R. B., Hagedorn, B., Mair, A., Ha, K. and Koh, G.

- W. (2014). "Assessing sustainability of groundwater resources on Jeju Island, South Korea, under climate change, drought, and increased usage." *Hydrogeol. J.*, 22(3), 625-642.
- Essink, G.H.P. (1998). "MOC3D adapted to simulate 3D density-dependent groundwater flow." In: Proc. of the MODFLOW'98 Conference Golden, CO, USA, 291-303.
- Essink, G. O. (2001). "Improving fresh groundwater supply: problems and solutions." *Ocean Coast. Manage.*, 44, 429–449.
- Feng-Rong Yang, Cheng-Haw Lee, Wen-Jui Kung, and Hsin-Fu Yeh, (2009), "The impact of tunneling construction on the hydrogeological environment of Tseng-Wen Reservoir Transbasin Diversion Project in Taiwan", *Engineering Geology*, 103, 39-58
- Feng Sun, Haibing Shao, Thomas Kalbacher, Wenqing Wang, Zhongshan Yang, Zhenfang Huang and Olaf Kolditz (2011), "Groundwater drawdown at Nankou site of Beijing Plain: model development and calibration", *Environ Earth Sci* (2011) 64:pp. 1323–1333.
- Feseker, T. (2007). "Numerical studies on saltwater intrusion in a coastal aquifer in northwestern Germany." *Hydrogeol. J.*, 15, pp. 267-279.
- Fethi Lachaal , Ammar Mlayah, Mourad Be´dir, Jamila Tarhouni and Christian Leduc (2012) "Implementation of a 3-D groundwater flow model in a semi-arid region using MODFLOW and GIS tools: The Ze´ramdine–Be´ni Hassen Miocene aquifer system (east-central Tunisia)", *Computers & Geosciences*, 48 (2012) pp. 187–198.

Freeze, R. A and Cherry, J. A. (1979). "Groundwater", Prentice-Hall Inc., Eaglewood N.J.

Fried, J. J. and Combamous, M. A. (1971). "Dispersion in porous media. *Adv. Hydrosci.*, 7, 420-435.

Gates, T. K., Burkhalter, J., John, W. L., James, C. V. and Broner, I. (2002). "Monitoring and Modeling Flow and Salt Transport in a Salinity-Threatened Irrigated Valley." *J. Irrig. Drain. Eng.*, 128(2), 87-99.

Geyh, M. A. and Soefner, B. (1996). "Groundwater mining study by simplified collection in the Jakarta Basin aquifer, Indonesia." *Isotopes in Water Resources Management*. IAEA, The International Atomic Energy Agency, Vienna, 174–176.

Gholami, V., Zabihollah, Y and Hosseinali, Z, R. (2010). "Modeling of Ground Water Salinity on the Caspian Southern Coasts." *Water Resour. Manag.*, 24, 1415–1424.

Giambastiani, M. B., Antonellini, M., Essink, G. H. and Stuurman, R. J. (2007). "Saltwater intrusion in the unconfined coastal aquifer of Ravenna (Italy): A numerical model." *J. Hydrol.*, 340, 91-104.

- Green, N.R. and MacQuarrie, K. T. B (2014). "An evaluation of the relative importance of the effects of climate change and groundwater extraction on seawater intrusion in coastal aquifers in Atlantic Canada." *Hydrogeol. J.*, 22, 609-623.
- Guo, W. and Bennett, G. D. (1998). "SEAWAT version 1.1, A computer program for simulations of ground water flow of variable density." A report prepared by Missimer International Inc.
- Guo, W and Langevin, C.D (2002). "User's Guide to SEAWAT: A Computer Program for Simulation of Three-Dimensional Variable-Density Ground-Water Flow." U.S. Geological Survey Techniques of Water Resources Investigations of the USGS, Book 6, Chapter A7, 87.
- GEC (1997). "Groundwater Resource Estimation Methodology." Report of the Groundwater Resource Estimation Committee, Ministry of Water Resources, Government of India, New Delhi.
- Harbaugh, A. W., Banta, E. R., Hill, M. C. and McDonald, M. G. (2000). "MODFLOW-2000, the U.S. Geological Survey Modular Ground-Water Model: User guide to modularization concepts and the ground-water flow process." *U.S. Geological Survey*, Open-File Report 00-92.
- Harshendra, K. (1991). "Studies on water quality and soil fertility in relation to crop yield in selected river basins of D.K. District of Karnataka State." Ph.D. Thesis, Mangalore University, Karnataka, India.

Hattermann Fred F., Valentina Krysanova and Cornelia Hesse (2010), “Modelling wetland processes in regional applications.”, *Hydrological Sciences Journal*, 53:5, pp. 1001-1012,

Haque , Al Mamunul, M., Jahan, C.S., Mazumder, Q.H., Nawaz, S.M.S., Mirdha, G.C., Mamud, P and Adham, M.I. (2012). “Hydrogeological Condition and Assessment of Groundwater Resource Using Visual Modflow Modeling, Rajshahi City Aquifer, Bangladesh.”, *J. Geol. Soc. India*, 79, pp. 77-84.

Hill, M. C. (1990). “Preconditioned conjugate-gradient 2 (PCG2), a computer program for solving ground-water flow equations”. Department of the Interior, US Geological Survey, 90-4048.

INCCA (2010). “Indian Network for Climate Change Assessment 2010 Climate change and India: A 4X4 Assessment sectoral and regional analysis for 2030s”. Ministry of Environment & Forests Government of India. (<http://www.moef.nic.in/downloads/public-information/fin-rpt-incca.pdf>) (April 17, 2015).

IPCC (2008). “Intergovernmental Panel on Climate Change.” Technical Paper VI- Climate Change and Water, Bates B.C, Kundzewicz S. Wu and J.P Palutik of, Eds, 210 pp. (<http://www.ipcc.ch/pdf/technical-papers/climate-changewater-en.pdf>) (August 4, 2014).

Jacob, C. E. (1963). “Correction of drawdowns caused by a pumped well tapping less than the full thickness of an aquifer.” Methods of determining permeability, transmissivity and drawdown. US Geol. Survey, Water-Supply paper, 272-282.

- Jaimini Sarkar (2011). "Ramsar Convention and India." *Current Science*, vol. 101, no. 10, 25 November 2011, 1266-1268.
- Jayappa, K. J. (1991). "A textural and mineralogical study of the beach sands between Talapady and Surathkal." *J. Geotech. Soc. India*, 37, 151-163.
- Juckem, P.F, Hunt, R.J. and Anderson, M. P. (2006). "Scale effects of hydrostratigraphy and recharge zonation on base flow." *Ground Water*, 44 (3), 362- 370.
- Karant, K. R. (1987). "Ground water assessment: development and management." Tata McGraw-Hill Education.
- Kelbe, B. E., Grundling, A. T. and Price, J. S. (2016). "Modelling water-table depth in a primary aquifer to identify potential wetland hydrogeomorphic settings on the northern Maputaland Coastal Plain, KwaZulu-Natal, South Africa." *Hydrogeol. J.*, 1-17.
- Kerrou, J., Renard, P., Cornaton, F. and Perrochet, P. (2013). "Stochastic forecasts of seawater intrusion towards sustainable groundwater management: application to the Korba aquifer (Tunisia)." *Hydrogeol. J.*, 21(2), 425-440.
- Kerrou, J., Renard, P. and Tarhouni, J. (2010). "Status of the Korba groundwater resources (Tunisia): observations and three-dimensional modelling of seawater intrusion." *Hydrogeol. J.*, 18(5), 1173-1190.

- Kipp, K. L. Jr. (1973). "Unsteady flow to partially penetrating, finite radius well in an unconfined aquifer." *Water Resour. Res.*, 9(2), 448-462.
- Kipp, K. L. (1986). "HST3D—A computer code for simulation of heat and solute transport in 3D ground water flow systems." *US Geological Survey, Water resources Investigations. Report 86-4095.*
- Kopsiaftisa, G., Mantogloua, A. and Giannouloupolos, P. (2009). "Variable density coastal aquifer models with application to an aquifer on Thira Island." *J. Desal.*, 237, 65-80.
- Kruseman, G.P. and Ridder, N. A. (1994). "Analysis and Evaluation of Pumping Test Data (2nd ed.)", Publication 47, Intern. Inst. for Land Reclamation and Improvement, Wageningen, The Netherlands, 370p.
- Kumar, R.B.C. (2010). "Modelling regional actual evapotranspiration over Netravathi basin using satellite data". M.Tech. Thesis, National Institute of Technology Karnataka, Surathkal, Mangalore, India.
- Kumar, A., Jayappa, K.S. and Deepika, B. (2011). "Application of remote sensing and geographic information system in change detection of the Netravati and Gurpur river channels, Karnataka, India." *Geocarto Int.*, 25 (5), 397–425.
- Kushwaha, R. K., Pandit, M.K. and Rohit, G. (2009). "MODFLOW Based Groundwater Resource Evaluation and Prediction in Mendha Sub-Basin, NE Rajasthan." *J. Geol. Soc. India*, 74, 449-458.

- Lachaal, F., Mlayah, A., Be´dir, M., Tarhouni, J. and Christian, L. (2012).
 “Implementation of a 3-D groundwater flow model in a semi-arid region using MODFLOW and GIS tools:The Ze´ramdine–Be´ni Hassen Miocene aquifer system (east–central Tunisia).” *Comput. Geosci.*, 48, 187-198.
- Lagasse, P. F., Zevenbergen, L. W., Spitz, W. J., & Arneson, L. A. (2012). Hydraulic Engineering Circular No. 20: *Stream Stability at Highway Structures* (Fourth Ed.). US Department of Transportation, Federal Highway Administration.
- Langevin, C. D. (2003). "Simulation of submarine groundwater discharge to a marine estuary: Biscayne Bay, Florida." *Ground Water*, 41 (6), 758-771.
- Langevin, C .D. Shoemaker, WB. and Guo, W. (2003). “MODFLOW-2000, the U.S. Geological Survey Modular Ground-Water Model”, *Documentation of the SEAWAT-2000 version with the variable density flow process (VDF) and the integrated MT3DMS Transport Process (IMT)*. USGS Open-File Report 03-426.
- Langevin, C., Thorne, D., Dausman, A., Sukop, M. and Guo, W. (2008). “SEAWAT Version 4: A Computer Program for Simulation of Multi-Species Solute and Heat Transport.” *U.S. Geological Survey Techniques and Methods*, Book 6, Chapter A22.
- Langevin, C.D. and Guo, W. (1999). "Improvements to SEAWAT, a variable density modelling code.” *Eos Trans*, 80(46), F-373.
- Langevin, C. D. and Guo, W. (2006). “MODFLOW/MT3DMS–Based Simulation of Variable-Density Ground Water Flow and Transport.” *Ground Water*, 44(3),

339-351.

Langevin, C. D. and Zygnerski, M. (2013). "Effect of sea-level rise on saltwater intrusion near a coastal well field in South - eastern Florida." *Ground Water*, 51 (5), 781-803.

Lathashri.U.A and A. Mahesha (2015), "Simulation of Saltwater Intrusion in a Coastal Aquifer in Karnataka, India.", International Conference On Water Resources, Coastal And Ocean Engineering – ICWRCOE'2015, National Institute of Technology Karnataka, Surathkal. *Aquatic Procedia (Elsevier)*,4, 700-705

Leake, S. A. and Prudic, D. E. (1991). "Documentation of a computer program to simulate aquifer-system compaction using the modular finite-difference ground-water flow model." US Department of the Interior, US Geological Survey.

Lenhart, T., Eckhardt, K., Fohrer, N. and Frede, H. G. (2002). "Comparison of two different approaches of sensitivity analysis." *Phys.Chem. Earth*, 27(9-10), 645-654.

Li, W., Liu, Z., Guo, H., Li, N. and Kang, W. (2011). "Simulation of a groundwater fall caused by geological discontinuities." *Hydrogeol. J.*, 19, 1121–1133.

Lin, J.J., Snodsmith, B. and Zeng, C. (2009). "A modeling study of seawater intrusion in Alabama Gulf coast, USA." *Environ. Geol.*, 57, 119-130.

Lin, Y.C. and Medina, Jr. M. A. (2003). "Incorporating transient storage in

conjunctive stream–aquifer modelling.” *Adv. Water Resour.*, 26, 1001–1019.

Liu, C. W., Yen-Lu, C., Shien-Tsung, L., Gin-Jie, Lin. and Cheng-Shin, J. (2010).
“Management of High Groundwater Level Aquifer in the Taipei Basin.”
Water Resour. Manag., 24, 3513–3525.

Loaiciga, H. A., Pingel, T. J. and Garcia, E. S. (2012). "Seawater intrusion by sea- level rise: Scenarios for the 21st century." *Ground Water*, 50 (1), 37-47.

Lokesh, K. N. (1997). “Some principles and methods for mineral exploration: An overview.” National Seminar on Emerging Technology in Surface Mining and Environmental Challenges, Dept. of Mining Engineering, Karnataka Regional Engineering College, Surathkal, India, 63–66.

Louwyck, A., Vandenbohede, A., Bakker, M. and Lebbe, L. (2014). “MODFLOW procedure to simulate axisymmetric flow in radially heterogeneous and layered aquifer systems.” *Hydrogeol. J.*, 22(5), 1217-1226.

Mahesha, A and Lakshmikanth, P. (2014). “Saltwater intrusion in coastal aquifers subjected to freshwater pumping.” *J.Hydrol.Engg.*, ASCE,17 , 448-456.

Mahesha, A., Vyshali, Lathashri, U. A. and Ramesh, H. (2012). "Parameter estimation and vulnerability assessment of coastal unconfined aquifer to saltwater intrusion." *J.Hydrol.Engg.*, ASCE,17 (8), 933-943.

Manghi, F., Dennis, W., Jack, S. and Moshrik, R. H. (2012). “Groundwater Flow Modeling of the Arlington Basin to Evaluate Management Strategies for

- Expansion of the Arlington Desalter Water Production.” *Water Resour. Manag.*, 26, 21–41.
- Mao, X.S., Jia, J.S., Liu, C.M. and Hou, Z.M. (2005). “A simulation and prediction of agricultural irrigation on groundwater in well irrigation area of the piedmont of Mt. Taihang, North China.” *Hydrol. Process*, 19(10), 2071–2084.
- Martinez-Santos, P., Ramon, M. L. and Pedro, E. M. (2008). “Vulnerability assessment of groundwater resources: A modelling-based approach to the Mancha Occidental aquifer, Spain.” *Environ. Model. Softw.*, 23, 1145-1162.
- Mathias, S. A. and Butler, A. P. (2006). “Linearized Richards' equation approach to pumping test analysis in compressible aquifers.” *Water Resour. Res.*, 42(6).
- McDonald, M. G. and Harbaugh, A.W. (1988). “A modular three dimensional finite-difference groundwater flow model.” USGS Open File Report, 83-875.USGS, Washington, D.C.
- McFadden L. (2007), “Broad-scale modelling of coastal wetlands: what is required?” *Hydrobiologia*, 577(1):pp. 5-15
- Moench, A. F. (1995). “Combining the Neuman and Boulton models for flow to a well in an unconfined aquifer.” *Ground Water*, 33(3), 378-384.
- Mollema, P. N., & Antonellini, M. (2013). Seasonal variation in natural recharge of coastal aquifers. *Hydrogeol. J*, 21(4), 787-797.

- Moriasi, D. N., Arnold, J. G., Van Liew, M. W., Bingner, R. L., Harmel, R. D. and Veith, T. L. (2007). "Model evaluation guidelines for systematic quantification of accuracy in watershed simulations." *Trans. Asabe*, 50(3), 885-900.
- Moustadraf, J., Razack, M. and Sinan, M. (2008). "Evaluation of the impacts of climate changes on the coastal Chaouia aquifer, Morocco, using numerical modelling." *Hydrogeol. J.*, 16, 1411–1426
- Narasimhan, T. N. and Zhu, M. (1993). "Transient flow of water to a well in an unconfined aquifer-applicability of some conceptual models." *Water Resour. Res.*, 29 (1), 179–191.
- Narayan, K. A., Schleeberger, C. and Bristow, K. L. (2007). "Modelling seawater intrusion in the Burdekin Delta irrigation area, North Queensland, Australia." *Agric. Water Manage.*, 89, 217-228.
- Neuman, S.P. (1972). "Theory of flow in unconfined aquifers considering delayed response of the water table." *Water Resour. Res.*, 8(4), 1034-1044.
- Neuman, S.P. (1974). "Effects of partial penetration on flow in unconfined aquifers considering delayed aquifer response." *Water Resour. Res.*, 10(2), 303-312.
- Neuman, S.P. (1975). "Analysis of pumping test data from anisotropic unconfined aquifers considering delayed gravity response." *Water Resour. Res.*, 10(2), 303-312

Nowbuth, M. D., Rambhojun, P and Bhavana, U. (2012). "Numerical groundwater flow and contaminant transport modeling of the southern aquifer, Mauritius." *Earth Sci. India*, 5(3), 79-91.

NBSS&LUP. (1998). "National Bureau of soil survey and land use planning (Indian council of agricultural research). Soils of Karnataka for optimising land use." *State soil survey, department of agriculture*, Bangalore, Karnataka. NBSS Publ.47.

Palma, H.C. and Bentley, L.R. (2007). "A regional-scale groundwater flow model for the Leon-Chinandega aquifer, Nicaragua." *Hydrogeol. J.*, 15, 1457–1472.

Panagopoulos, G. (2012). "Application of MODFLOW for simulating groundwater flow in the Trifilia karst aquifer, Greece." *Environ. Earth Sci.*, 6, 425-438.

Park, S. U., Kim, J. M., Yum, B. W. and Yen, G. T. (2012). "Three-dimensional numerical simulation of saltwater extraction schemes to mitigate seawater intrusion due to groundwater pumping in a coastal aquifer system." *J. Hydrol. Engg.*, ASCE, 17, 10-22.

Perkins, S. P. and Marios, S. (1999). "Development of a comprehensive watershed model applied to study stream yield under drought conditions." *Ground Water*, 37(3), 418-426.

Pinder, G. F., Cooper, H. H. Jr. (1970). "A numerical technique for calculating the transient position of the saltwater front." *Water Resour Res*, 9, 1657–1669.

- Pisinaras.V., Petalas. C., Tsihrintzis.V.A. and Zagana. E. (2007). "A groundwater flow model for water resources management in the Ismarida plain, North Greece." *Environ. Model. Assess.*, 12, 75-89.
- Post, V.E.A. (2011). "A new package for simulating periodic boundary conditions in MODFLOW and SEAWAT." *Comput Geosci.*, 37, 1843–1849.
- Praveena, S. M., Abdulla, M. H., Aris, A. Z., Yik, L. C. and Bidin. (2011). "Numerical modeling of seawater intrusion in Manukan Island Aquifer." *Resear. World Appl .Sci. J*, ISSN 1818-4952.
- Qahman, K. and Larabi, A. (2006). "Evaluation and numerical modeling of seawater intrusion in the Gaza aquifer (Palestine)." *Hydrogeol. J.*, 14, 713-728.
- Radheshyam, B.(2009). "Study of coastal processes and solution to erosion problems in the vicinity of Netravathi-Gurupur river estuary - A modelling approach." Ph.D. thesis, National Institute of Technology, Karnataka, Surathkal, India.
- Rahnama, M.B. and Zamzam, A. (2011). "Quantitative and qualitative simulation of groundwater by mathematical models in Rafsanjan aquifer using MODFLOW and MT3DMS." *Arab. J. Geosci*, DOI 10.1007/s12517-011-0364-x.
- Ranganna, G., Gurappa, K, M., Gajendragad, M, R. and Chandrakantha, G. (1986). "Hazardous effects of groundwater pollution and mitigative measures thereof." Report submitted by Department of Applied Mechanics and Hydraulics, NITK, Surathkal to the Department of Environment, Government of India,128.

- Rao, B. N. (1974). "Geotechnical investigations of the marine deposits in the Mangalore harbor project." *Indian Geotech. J*, 4 (1), 78-92.
- Rao. S.V.N , Murty, B. S., Thandaveswara, B.S. and Sreenivasulu .V. (2005). "Planning Groundwater Development in Coastal Deltas with Paleo Channels." *Water Resour. Manag.*, 19, 625–639.
- Rajgopalan, S. P., Prabhashankar, P. N. and Balakrishnan, V. (1983). "Pumping test and analysis data of open wells in the coastal tract of Kozikode district", GW/R-56/83. Centre for Water Resour. Develop. Mgmt. Kozikode, Kerala, 43.
- Rao, S. V. N., Sreenivasulu, V., Bhallamudi, S. M., Thandaveswara, B. S. and Sudheer, K. P. (2004). "Planning groundwater development in coastal aquifers/Planification du développement de la ressource en eau souterraine des aquifères côtiers." *Hydrolog. Sci. J.*, 49(1), 155-170.
- Reeve, A.S., Warzocha. J., Glaser, P.H. and Siegel.D.I. (2001). "Regional groundwater flow modeling of the Glacial Lake Agassiz Peatlands, Minnesota." *J. Hydrol.*, 243, 91–100.
- Rejani. R, Madan K. Jha , Panda.S.N and Mull. R (2008). "Simulation modelling for efficient groundwater management in Balasore Coastal Basin, India." *Water Resour. Manag.*, 22, 23–50.
- Rojas, R. and Dassargues, A. (2007). "Groundwater flow modelling of the regional aquifer of the Pampa del Tamarugal, northern Chile." *J. Hydrol*, 15, 537–551.

- Rozell, D. J. and Wong, T. F. (2010). "Effects of climate change on groundwater resources at Shelter Island, New York State, USA." *Hydrogeol J* , 18(7), 1657-1665.
- Rushton, K. (2007). "Representation in regional models of saturated river–aquifer interaction for gaining/losing rivers." *J. Hydrol*, 334(1), 262-281.
- Sakiyan, J. and Yazicigil, H. (2004). "Sustainable development and management of an aquifer system in western Turkey." *Hydrogeol J*, 12, 66–80.
- Sanford, W. E. and Konikow, L. F. (1985). "A two-constituent solute-transport model for ground water having variable density." *US Geol Surv Water Resour Invest Rep*. 85-4279.
- Santhi, C. J. G., Arnold, J. R., Williams, W. A., Dugas, R., Srinivasan. and Hauck, L.M. (2001). "Validation of the SWAT model on a large river basin with point and nonpoint sources." *J. Am. Water Resour. Assoc.*,37(5), 1169-1188.
- Santhosh, K.C. (2011). "Groundwater flow and transport modeling of Pavanje basin using GMS." M.Tech, Thesis, Department of Applied Mechanics & Hydraulics, National Institute of Technology Karnataka, Surathkal, Mangalore.
- Sanz, D., Santiago, C., Eduardo, C., Andres, S., Juan, J. G. A., Salvador, P. and Alfonso, C. (2011). "Modeling aquifer–river interactions under the influence of groundwater abstraction in the Mancha Oriental System (SE Spain)." *Hydrogeol. J*, 19, 475–487.

- Sedki, A. and Ouazar, D. (2011). "Simulation-Optimization Modeling for Sustainable Groundwater Development: A Moroccan Coastal Aquifer Case Study." *Water Resour. Manag.*, 25, 2855–2875.
- Segol, G. and Pinder, G. F. (1976). "Transient simulation of saltwater intrusion in southeastern Florida." *Water Resour. Res.*, 12, 65–70.
- Senthilkumar, M. and Elango, L. (2004). "Three-dimensional mathematical model to simulate groundwater flow in the lower Palar River basin, southern India." *Hydrogeol. J.*, 12(2), 197-208.
- Senthilkumar, M. and Elango, L. (2011). "Modelling the impact of a subsurface barrier on groundwater flow in the lower Palar River basin, southern India." *Hydrogeol. J.*, 19, 917–928.
- Shammas, M.I. and Thunvik, R. (2009). "Predictive simulation of flow and solute transport for managing the Salalah coastal aquifer, Oman." *Water Resour. Manag.*, 23(3), 2941-2963.
- Sherif, M. (1999). "Seawater intrusion in the Nile delta aquifer-An overview." 296-308. <http://aquas.igme.es/igme/publica/tiac-02/EGIPTO-Ipdf>>(June5,2006)
- Sherif, M., Kacimov, A., Javadi, A. and Ebraheem, A. A. (2012). "Modeling groundwater flow and seawater intrusion in the coastal aquifer of Wadi Ham, UAE." *Water Resour. Manag.*, 26, 751-774.

- Shetkar, R. V. (2008). “Studies on the efficacy of vented dams as water harvesting structures across the river Netravathi of D.K. district, Karnataka.” Ph.D. Thesis, National Institute of Technology, Karnataka, Surathkal, India.
- Shetkar, R.V. and Mahesha, A. (2011). "Tropical, seasonal river basin development: Hydrogeological analysis." *J. Hydrol. Engg., ASCE*, 16(3), 280-291.
- Shivakumar J. Nyamathi and A. Vittal Hegde (2005), “Wetland Hydrology – Monitoring and Modelling.” Proceedings of Workshop on Wetland Monitoring and Management, February 2, 2005, Department of Applied Mechanics and Hydraulics, NITK Surathkal, pp. 51-69.
- Shivanagouda. H. S. (2015). “Studies on aquifer characterization and seawater intrusion vulnerability assessment of coastal Dakshina Kannada district, Karnataka.” Ph.D. Thesis, National Institute of Technology Karnataka, Surathkal India,184.
- Simpson, M. J. (2004). “SEAWAT-200: Variable –density flow processes and integrated MT3DMS transport processes.” *Ground Water*, 42(5), 642-645.
- Sindhu, G., Ashitha, M., Jairaj, P.G. and Rajesh, R. (2012). “Modelling of Coastal Aquifers of Trivandruml.” *Proc. Engineering*, 38, 3434 – 3448.
- Singh, S. K. (2006). “Semi-analytical model for drawdown due to pumping a partially penetrating large diameter well.” *J. Irrig. Drain., ASCE*, 133(2), 155-161.

- Srikantiah, H. R. (1987). "Laterite and lateritic soils of west coast of India." In B. T. Proc. 9th South-east Asian Geotechnical Conference. Asian Institute of Technology: Bangkok, Thailand,159-169.
- Sudhir, K., Subrata, H. and Singhal, D. C. (2011). ""Groundwater Resources Management through Flow Modeling in Lower Part of Bhagirathi - Jalangi Interfluve, Nadia, West Bengal." *J. Geol Soc India.*, 78, 587-598.
- Suresh, B. D. S., Atul, K. S., Mauricio, A. N. and Eduardo, M. (2008). "Hydraulic response of a tidally forced coastal aquifer, Pontal do Parana, Brazil." *Hydrogeol. J*, 16, 1427–1439.
- Surinaidu, L., Gurunadha, V.V.S. and Ramesh, G. (2011). "Assessment of groundwater inflows into Kuteshwar Limestone Mines through flow modeling study, Madhya Pradesh, India." *Arab. J Geosci.* DOI 10.1007/s12517-011-0421-5
- Sylus, K. J. and Rahesh, H. (2015). "The Study of Sea Water Intrusion in Coastal Aquifer by Electrical Conductivity and Total Dissolved Solid Method in Gurpur and Netravathi River Basin." *Aquatic Proc. (Elsevier)*, 4, 57-64 DOI:10.1016/j.aqpro.2015.02.009
- Takounjou, F.A., Gurunadha,V.V.S, Ndam, N. J., Sigha, N .L. and Ekodeck, G.E. (2009). "Groundwater flow modelling in the upper Anga'a river watershed, Yaounde, Cameroon." *Afr. J Environ. Sci. Technol.*, 3 (10), 341-352.

- Tartakovsky, G. D. and Neuman, S. P. (2007). "Three-dimensional saturated-unsaturated flow with axial symmetry to a partially penetrating well in a compressible unconfined aquifer." *Water Resour. Res.*, 43(1).
- Theis, C.V (1935). "The Relation between lowering the piezometric surface and the rate and duration of discharge of a well using ground water storage." *Trans Am. Geophys.Union.*, 2, 519-524.
- Ting, C. S., Kerh, T. and Liao, C. J. (1998). "Estimation of groundwater recharge using the chloride mass-balance method, Pingtung Plain, Taiwan." *Hydrogeol. J.*, 6(2), 282-292.
- Todd, D. K. (1959). "Ground water hydrology." Wiley, New York
- Todd, D.K. and Mays, L. W. (2005). "Groundwater hydrology." 3rd edition, John Wiley and Sons, New York, 93.
- Udayakumar, G. (2008). "Subsurface barrier for water conservation in lateritic formations", Ph.D. thesis, Department of Applied Mechanics & Hydraulics, National Institute of Technology, Karnataka, Surathkal, India, 88-92.
- Unnikrishnan, A. S. and Shankar, D. (2007). "Are sea-level-rise trends along the coasts of the north Indian Ocean consistent with global estimates?." *Global and Planet. Change*, 57(3), 301-307.
- Van Liew, M. W., Arnold, J.G and Garbrecht, J.D. (2003). "Hydrologicsimulation on agricultural watersheds: Choosing betweentwo models." *Trans. ASAE* 46(6),

1539-1551.

Vandenbohede, A., Houtte, E.V. and Lebbe, L. (2009). "Sustainable groundwater extraction in coastal areas: a Belgian example." *J. Environ. Geol.*, 57, 735–747.

Vandenbohede, A., Mollema, P. N., Greggio, N. and Antonellini, M. (2014). "Seasonal dynamic of a shallow freshwater lens due to irrigation in the coastal plain of Ravenna, Italy." *Hydrogeol. J.*, 22(4), 893-909.

Varni, M.R and Usunoff, E. J (1999). "Simulation of regional-scale groundwater flow in the Azul River basin, Buenos Aires Province, Argentina." *Hydrogeol. J.*, 7, 180–187.

Volker, A. (1983). "Rivers of SE Asia: their regime, utilisation and regulation." *Hydrology of humid tropical regions*, 140, 127–138.

Voss, C. (1984). "SUTRA: A finite-element simulation model for saturated-unsaturated fluid-density-dependent groundwater flow with energy transport or chemically-reactive single-species solute transport." *U.S.Geol.Surv. Water Resour. Invest.Rep.*84-4369, USA.

Vyshali. (2008). Studies on saltwater intrusion in the coastal D.K district, Karnataka.Ph.D. Thesis, Department of Applied Mechanics & Hydraulics, National Institute of Technology Karnataka, Surathkal, Mangalore, India. 52-72

- Wang, S., Jingli, S., Xianfang, S., Yongbo, Z., Zhibin, H. and Xiaoyuan, Z. (2008).
 “Application of MODFLOW and geographic information system to groundwater flow simulation in North China Plain, China.” *Environ. Geol.*, 55, 1449–1462.
- Webb, M. D. and Howard, K. W. F. (2011). "Modelling the transient response of saline intrusion to rising sea-levels." *Ground Water*, 49 (4), 560-569.
- Weiss, M. and Gvirtzman, H. (2007). —Estimating ground water recharge using flow models of perched karstic aquifers. *Ground Water*, 45(6), 761-773.
- Werner, A. D., Bakker, M., Post, V. E., Vandenbohede, A., Lu, C., Ataie-Ashtiani, B. and Barry, D. A. (2013). “Seawater intrusion processes, investigation and management: recent advances and future challenges.” *Adv. Water Resour.*, 51, 3-26.
- Willmott, C. J. (1981). “On the validation of models.” *Physical Geography* 2, 184-194.
- Xi, H., Qi, F., Wei, L., Jian, H. S., Zongqiang, C. and Yonghong, Su. (2010). “The research of groundwater flow model in Ejina Basin, Northwestern China.” *Environ. Earth Sci.*, 60, 953–963.
- Xu, G. H., Zhongyi, Q. and Luis, S. P. (2011). “Using MODFLOW and GIS to Assess Changes in Groundwater Dynamics in Response to Water Saving Measures in Irrigation Districts of the Upper Yellow River Basin.” *Water Resour. Manag.*, 25, 2035–2059.

- Yang, J. S., Son, M. W., Chung, E. S. and Kim, I. H. (2015). "Prioritizing Feasible Locations for Permeable Pavement Using MODFLOW and Multi-criteria Decision Making Methods." *Water Resour. Manag.*, 29(12), 4539-4555.
- Yang, Q., Wenxi, L. and Yanna, F. (2011). "Numerical Modeling of Three Dimension Groundwater Flow in Tongliao (China)." *Proc. Engineering*, 24, 638 – 642.
- Yeh, G., Cheng, J. and Cheng, H. (1994). "3DFEMFAT: A 3-dimensional finite element model of density-dependent flow and transport through saturated-unsaturated media, version 2.0." *Technical Report, Dept. of Civil and Environ. Eng.*, Pennsylvania State Univ., University Park, PA.
- Zheng, C. (2006). "MT3DMS v5.2 supplemental user's guide." *Department of Geological Sciences, University of Alabama, Technical Report*, U.S. Army Engineer Research and Development Center.
- Zheng, C. and Bennett, G. D. (1995). "Applied contaminant transport modeling, theory and practice." Van Nostrand Reinhold.
- Zheng, C. and Bennett, G. D. (2002). "Applied contaminant transport modeling.", Vol. 2, New York, Wiley-Interscience.
- Zheng, C. and Wang, K. (1999). "A modular three dimensional multispecies transport model for simulation of advection, dispersion and chemical reactions of contaminants in groundwater systems." *Contract Report SERD99-1*, U.S. Army Corps of Engineers, United States.

Zhou, P., Li, G., Lu, Y. and Li, M. (2014). “Numerical modeling of the effects of beach slope on water-table fluctuation in the unconfined aquifer of Donghai Island, China.” *Hydrogeol. J.*, 22(2), 383-396.

Zume, J. and Tarhule, A. (2008). “Simulating the impacts of groundwater pumping on stream–aquifer dynamics in semiarid northwestern Oklahoma, USA.” *Hydrogeol. J.*, 16, 797–810.

APPENDIX I

Time-drawdown and recovery data for well no. 4

Time (min)	During Pumping		After Pumping	
	Depth To Water Level(m)	Drawdown(m)	Depth To Water Level(m)	Recovery(m)
1	0.84	0.01	1.24	0
2	0.85	0.02	1.22	0.02
3	0.88	0.05	1.19	0.05
4	0.9	0.07	1.17	0.07
5	0.91	0.08	1.15	0.09
6	0.93	0.1	1.13	0.11
7	0.94	0.11	1.11	0.13
8	0.95	0.12	1.09	0.15
9	0.98	0.15	1.06	0.18
10	0.99	0.16	1.03	0.21
12	1.03	0.2	1.02	0.22
15	1.05	0.22	1	0.24
18	1.06	0.23	0.98	0.26
20	1.07	0.24	0.97	0.27
25	1.1	0.27	0.95	0.29
30	1.12	0.29	0.93	0.31
35	1.13	0.3	0.92	0.32
40	1.15	0.32	0.91	0.33
50	1.19	0.36	0.88	0.36
60	1.2	0.37	0.85	0.39
70	1.21	0.38	0.84	0.4
80	1.23	0.4	0.84	0.4
110	1.25	0.42	0.84	0.4
120	1.26	0.43	0.84	0.4

Time-drawdown and recovery data for well no. 5

Time (min)	During Pumping		After Pumping	
	Depth To Water Level(m)	Drawdown(m)	Depth To Water Level(m)	Recovery(m)
1	1.54	0.03	2.23	0
2	1.57	0.06	2.2	0.03
3	1.59	0.08	2.18	0.05
4	1.62	0.11	2.17	0.06
5	1.65	0.14	2.15	0.08
6	1.66	0.15	2.13	0.1
7	1.69	0.18	2.12	0.11
8	1.71	0.2	2.11	0.12
9	1.73	0.22	2.1	0.12
10	1.75	0.24	2.09	0.14
12	1.79	0.28	2.06	0.17
15	1.85	0.34	2.03	0.21
18	1.88	0.37	2	0.24
20	1.91	0.4	1.97	0.27
25	1.96	0.45	1.92	0.31
30	2.02	0.51	1.89	0.35
35	2.06	0.55	1.86	0.37
40	2.1	0.59	1.82	0.41
50	2.16	0.65	1.77	0.47
60	2.19	0.68	1.73	0.5
70	2.22	0.71	1.7	0.53
80	2.24	0.73	1.68	0.55
90	2.25	0.74	1.66	0.57
120			1.51	0.72

Time-drawdown and recovery data for well no. 6

Time (min)	During Pumping		After Pumping	
	Depth To Water Level(m)	Drawdown(m)	Depth To Water Level(m)	Recovery(m)
1	5.51	0	6.21	0
2	5.52	0.01	6.18	0.03
3	5.54	0.04	6.16	0.05
4	5.56	0.05	6.13	0.08
5	5.58	0.08	6.11	0.1
6	5.6	0.1	6.09	0.12
7	5.62	0.12	6.08	0.13
8	5.64	0.14	6.06	0.15
9	5.66	0.16	6.03	0.18
10	5.68	0.18	6	0.21
12	5.7	0.2	5.97	0.24
15	5.75	0.25	5.95	0.26
18	5.78	0.28	5.93	0.28
20	5.81	0.31	5.9	0.31
25	5.86	0.36	5.85	0.36
30	5.91	0.41	5.81	0.4
35	5.94	0.44	5.78	0.43
40	5.96	0.46	5.76	0.45
50	6	0.5	5.74	0.48
60	6.05	0.55	5.71	0.5
70	6.09	0.59	5.68	0.53
80	6.13	0.63	5.65	0.57
90	6.18	0.68	5.61	0.6
100	6.21	0.71	5.58	0.64
120	6.24	0.74	5.52	0.69

APPENDIX II

TDS values (mg/ltr) of the water sample for the year 2012-2013

Well no.	Winter (Dec, Jan, Feb, March 2013)	Summer (Apr, May, June 2013)	Monsoon (July, Aug, Sept)	post monsoon (Oct, Nov)
1	223	200	179	194
2	26	10	46	39
3	105	105	69	94
4	157	557	251	179
5	24	44	46	49
6	197	154	143	193
7	895	590	245	909
8	120	209	196	178
9	122	108	118	159
10	51	81	113	127
11	284	1547	205	200
12	180	1139	82	88
13	46	75	42	57
14	31	10	50	62
15	239	209	209	378
16	153	141	128	148
17	258	144	234	328
18	370	371	235	356
19	225	201	201	235
20	219	179	204	271
21	82	33	155	157
22	219	200	174	224
23	449	374	287	468
24	573	1020	606	711
25	361	331	247	428
26	322	363	240	358
27	111	100	78	127

Well water levels in m (msl), for year 2012-2013

Well No	Water table elevation above the sea level [m]										
	Nov	Nov	Dec	Jan	Jan	Feb	Mar	April	April	May	May
1	1.74	1.54	1.14	0.64	0.43	0.07	-0.09	-0.51	-0.35	-0.15	-0.31
2	1.69	1.27	0.91	0.78	0.72	0.9	0.31	-0.12	-0.17	0	-0.132
3	4.87	4.54	4.47	4.41	4.39	3.89	3.8	3.31	3.54	3.88	3.36
4	4.79	4.79	4.7	4.7	4.6	4.43	4.23	3.27	3.14	3.13	2.96
5	5.59	5.58	5.68	5.42	5.36	5.34	5.31	4.84	4.87	4.91	4.68
6	-0.8	0.63	-0.48	-0.13	-0.2	-0.62	-2.4	-0.98	-0.36	-0.13	-0.51
7	2.59	2.42	2.14	1.43	1.29	0.82	0.89	0.61	0.59	0.67	0.58
8	2.36	2.21	2.1	1.63	1.51	1.2	0.74	0.46	0.8	0.94	0.73
9	3.68	3.19	3.26	2.57	2.33	1.4	0.91	0.87	0.58	0.72	0.98
10	1.52	1.04	0.36	-0.05	-0.09	-1	-1.34	-1.85	-0.73	0.03	-0.88
11	1.24	1.19	0.94	0.75	0.54	-0.07	-0.65	-1.01	-0.15	0.54	0.42
12	5.82	5.7	3.96	1.2	1.62	0.94	2.23	1.72	1.17	3.09	2.73
13	1.47	1.35	1.33	0.96	1.11	0.76	0.43	0.1	0.48	-0.93	0.52
14	3.59	3.5	3.34	2.91	2.74	2.4	2.32	2.84	2.62	3.09	2.6
15	3.81	3.74	3.49	2.9	2.72	2.46	2.25	1.87	2.41	3	2.72
16	3.06	2.9	2.59	2.18	2.06	1.82	1.66	1.34	2.08	2.63	1.98
17	3.49	3.19	2.9	2.56	2.37	2.01	1.79	1.44	1.63	1.79	1.74
18	2.78	2.93	2.78	2.63	2.53	2.29	2.05	1.63	1.96	2.3	2.38
19	1.86	1.79	1.75	1.59	1.53	1.35	1.17	1.07	1.33	1.58	1.42
20	2.27	1.78	1.83	1.69	1.56	1.37	1.3	1.31	1.49	1.7	1.61
21	2.44	2.57	2.29	1.84	1.6	1.31	1.08	0.75	0.06	1.14	0.87
22	1.13	1.09	0.94	0.47	0.33	0.35	0.24	0.13	0.32	0.43	0.43
23	1.16	1.24	1.06	0.41	0.6	0.27	0.35	0.25	-0.25	0.68	0.64
24	0.73	0.64	0.58	0.38	0.25	0.2	0.11	-0.06	0.06	0.24	0.41
25	3.11	3.14	2.94	2.41	2.37	1.68	1.68	1.23	1.66	1.57	1.57
26	3.45	3.33	2.82	2.61	2.35	2.02	1.79	0.93	1.17	1.45	1.04
27	3.6	3.62	3.09	2.49	2.09	1.68	1.41	0.88	0.95	1.54	1.35

APPENDIX III

Steps in building groundwater flow model

There are two methods to build model in MODFLOW. They are:-

- MODFLOW grid approach
- MODFLOW Conceptual Model Approach

Grid approach involves working directly with the 3D grid, where sources/sinks and other model parameters are applied on a cell-by-cell basis. To develop a conceptual model of the site, the conceptual model approach involves using the GIS tools in the Map module. The data of the conceptual model are later copied to the grid. Most of the input can be in terms of physical objects, such as wells, lakes, recharge zones etc. in conceptual model, which can then be converted to a grid based mathematical model with the help of pre-processor. Since MODFLOW conceptual model represent more accurately the in real world conditions, so it has been used in the present study. The steps for conceptual model are discussed below.

1. Import background image (topo sheet or image) or shapefile.
2. Define the units. **Edit-→Units.**

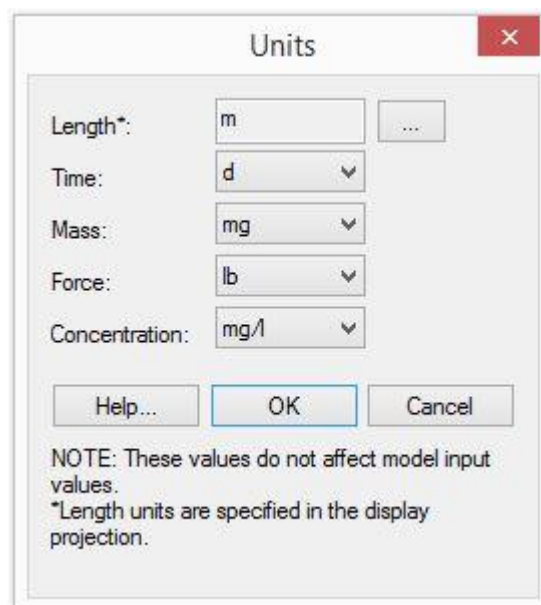
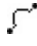


Fig.1. Set units

3. Create Coverage's

Right-click on the empty space in the Project Explorer then, from the pop-up menu select New → Conceptual Model command. Right-click on the New conceptual model created and select the New Coverage. Five coverage were created for the model.

3.1. Boundary Coverage:- Change the Coverage name to **Boundary**. Select the Create Arc tool  and define the boundary.

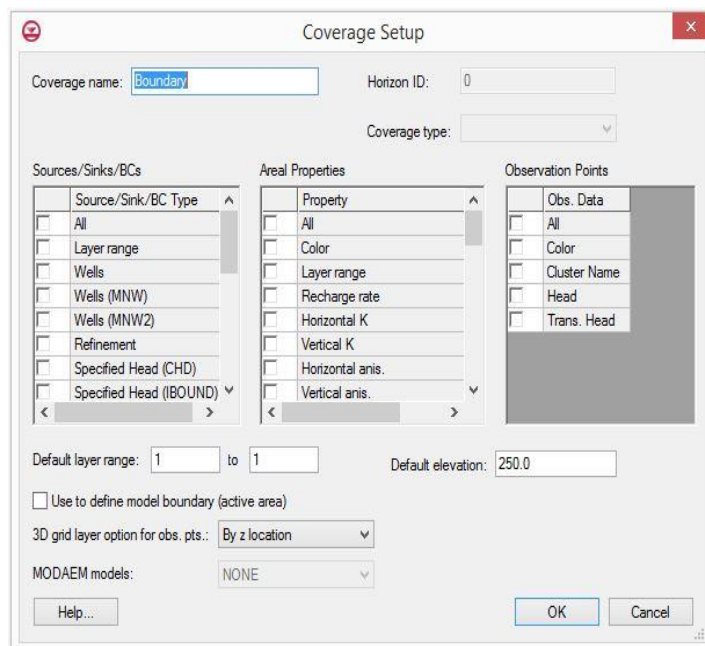


Fig.2. Set boundary coverage

3.2. Sources and Sinks coverage:-Right click on **Boundary** → **Duplicate**.

Change the name to Source and sink. Right click converge setup. Check the objects that are present in Source/Sink/BC Type and click ok. Converge defines local sources/sinks including wells, rivers, drains, and general head boundaries. After defining all source and sink *Build Polygons* macro is clicked.

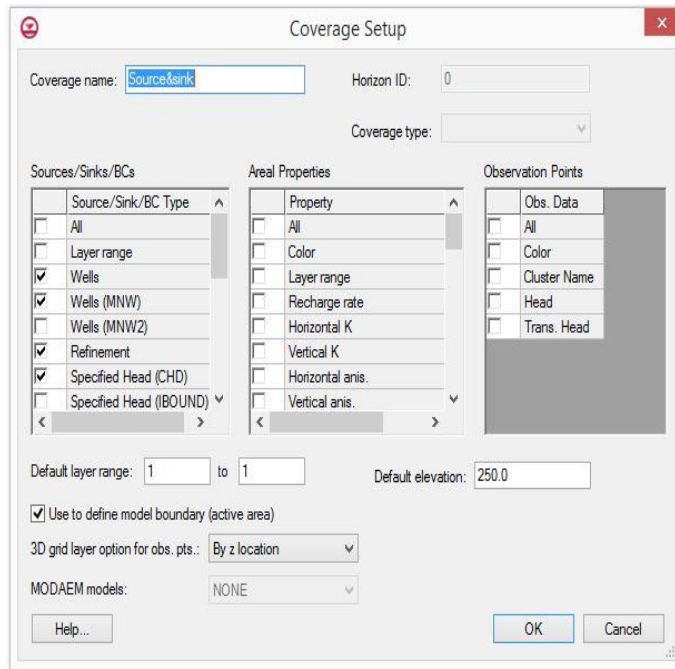


Fig.3. Set Source & sink coverage

3.3. Recharge coverage: Right click on **Boundary** → **Duplicate**. Change the name to **Recharge**. Right click converge setup. Check the Recharge rate in Areal property and click ok. Converge defines the recharge rate assigned to the model. The recharge rate can be calculated by recharge from rainfall method taking 10% of rainfall as recharge. After defining Recharge rate *Build Polygons* macro is clicked

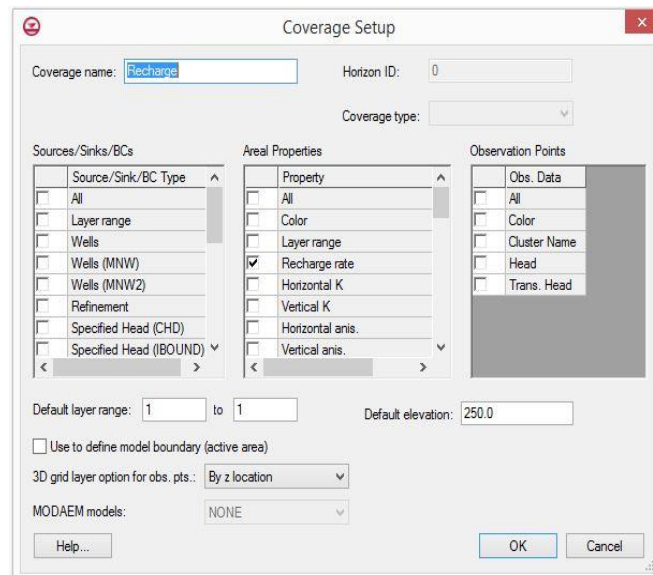


Fig.4. Set Recharge coverage

3.4. Hydraulic Conductivity:-Right click on **Boundary** →**Duplicate**. Change the name to **Hydraulic Conductivity**. Right click converge setup. Check the Horizontal K in Areal and click ok. Converge defines the recharge rate assigned to the model. Define the hydraulic conductivity of different area in the model. After defining hydraulic conductivity *Build Polygons* macro is clicked.

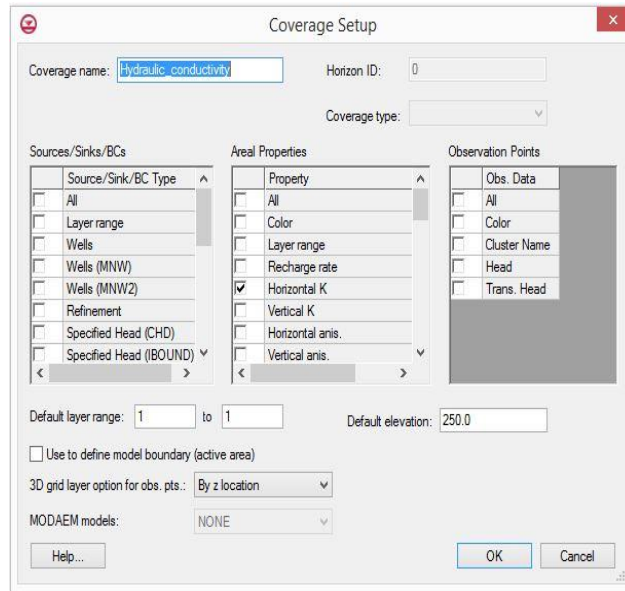


Fig.5. Set Hydraulic conductivity coverage

3.5. Observation Points:-Right click on **Boundary** →**Duplicate**. Change the name to **Observation Wells**. Right click converge setup. Check the Trans. Head in Observation point and click ok. Select create points and mark the observation points in the model. After marking the observation points on the model *Build Polygons* macro is clicked.

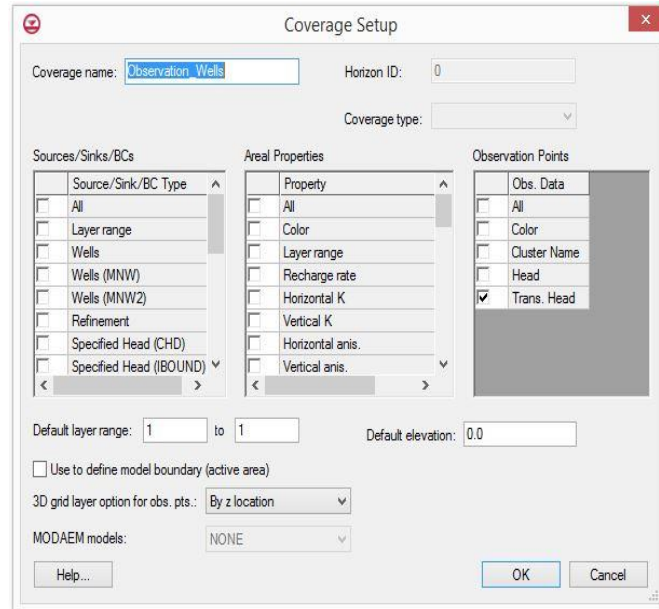


Fig.6. Set Observation Points coverage

4. Locating the grid frame to model

The coverage's are complete, and we are now ready to create the grid. First step in creating the grid is to define the location and orientation of the grid. This is done by using the Grid Frame. The Grid Frame can be positioned on top of our site map graphically and represents outline of grid.

Right-click **Project Explorer** → **New** | **Grid Frame**.

To fit the grid to correct position

Right-click on the **Grid Frame** → **Fit to Active Coverage**

5. Creating the grid – converting Map to 3D grid command.

Select the **Feature Objects** | **Map** → **3D Grid** command.

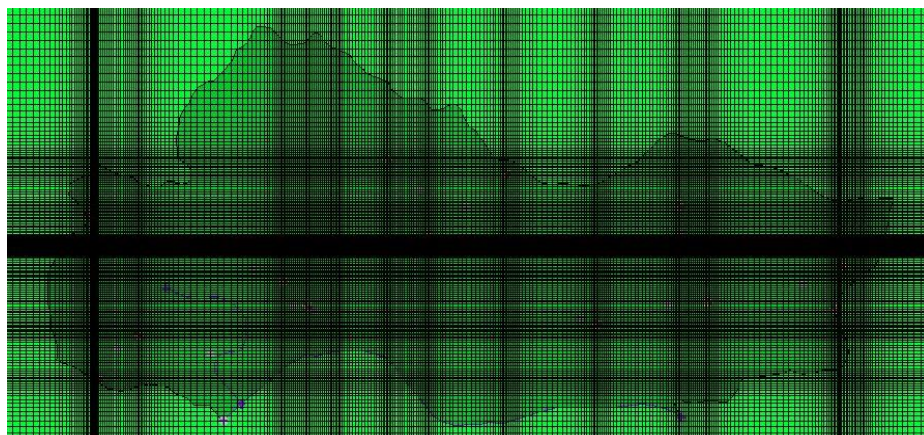



Fig.7. Creating 3D grid

6. Initializing the MODFLOW Data

The grid is constructed and the active/inactive zones are delineated, now the conceptual model will be converted to a grid-based numerical model. Before doing this, however, we must first initialize the MODFLOW data


Right click on  grid in the Project Explorer and select the New MODFLOW →OK.

7. Defining the Active/Inactive Zones

Select Sources & Sinks coverage in the Project Explorer. **Feature Objects**
→**Activate Cells in Coverage.**

8. Converting the Conceptual Model

It is now ready to convert the conceptual model from the feature object-based definition to a grid-based MODFLOW numerical model.

Right-click conceptual model created in the beginning and select the **Map To**  **MODFLOW / MODPATH** command.

All applicable coverages option is selected is to be justified and select OK

9. Define the top elevation and bottom elevation

We need to define the top elevation and the bottom elevation in the model to run the model.

For top elevation

Right click in 2D scattered data for top elevation created from Cartosat DEM version1.1. and select **Interpolate To** → **MODFLOW layer.**

For Bottom Elevation

Same procedure as of assigning Top elevation

10. Defining the Starting Head

Starting Head is needed to be defined before MODFLOW is run. This is the expected head after the MODFLOW is run.

11. Checking the Simulation

To check if there is any error in the input run the **Model Checker** to see if GMS can identify any mistakes.

MODFLOW → Check Simulation → Run Check

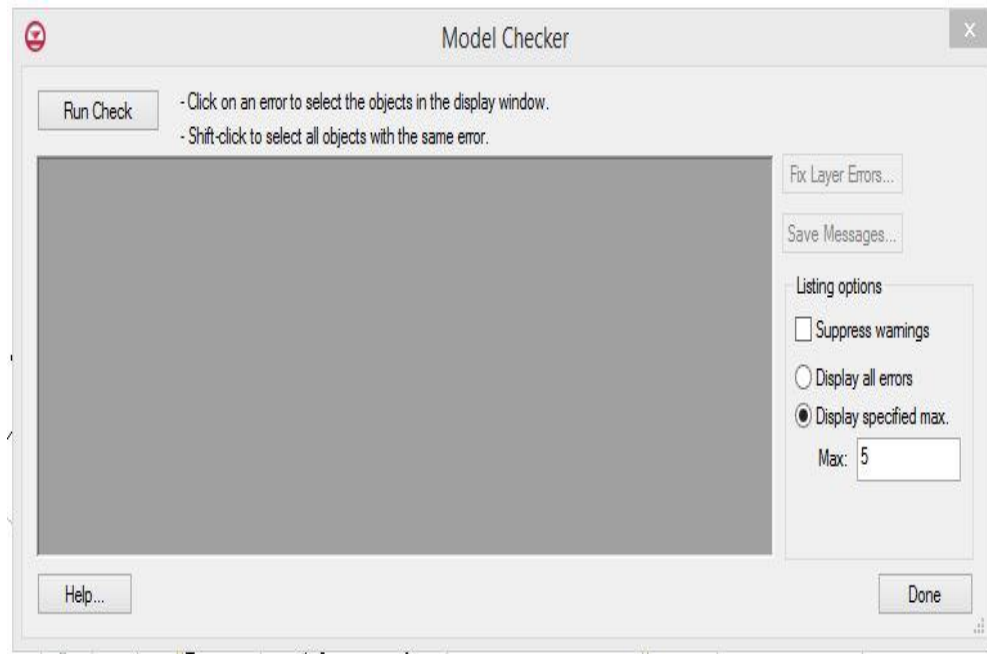


Fig.8. Check simulation

12. Saving the Project

Saving the project not saves all data associated with the project including the feature objects and scatter points including MODFLOW files.

13. Running MODFLOW

The MODFLOW is ready to run and simulate the results.

MODFLOW → Run MODFLOW. MODFLOW is launched at this point of time and the Model Wrapper appears. Select the Close button when the solution is finished. The contours that will appear are the contours of the computed head solution.

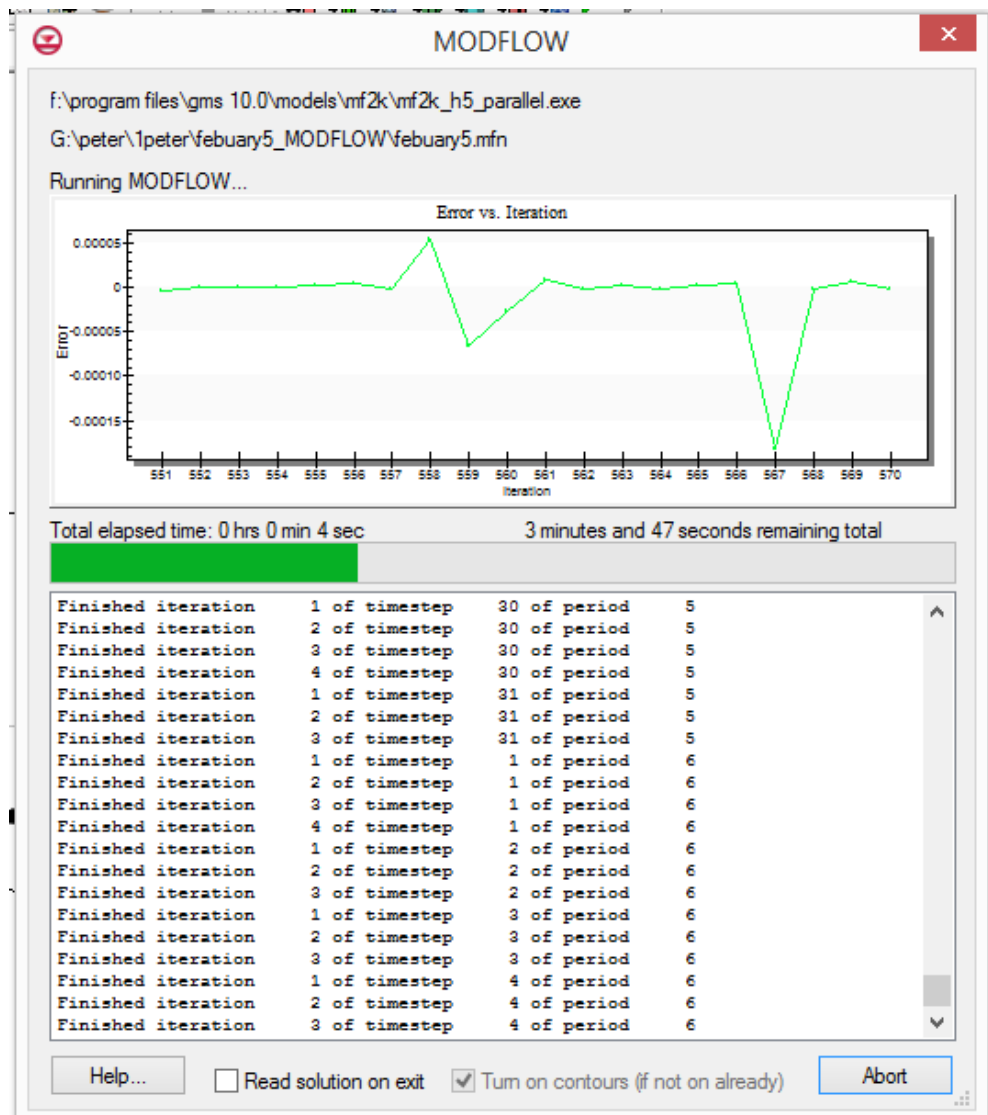
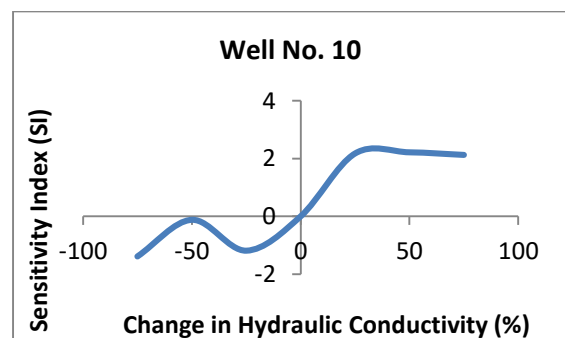
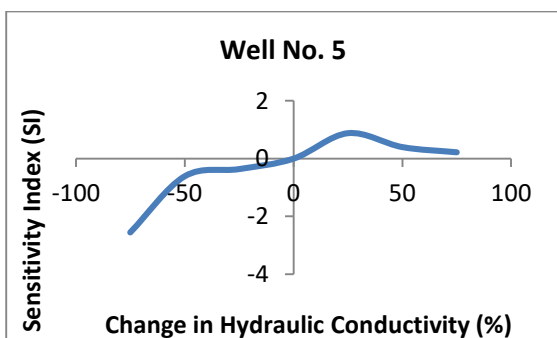
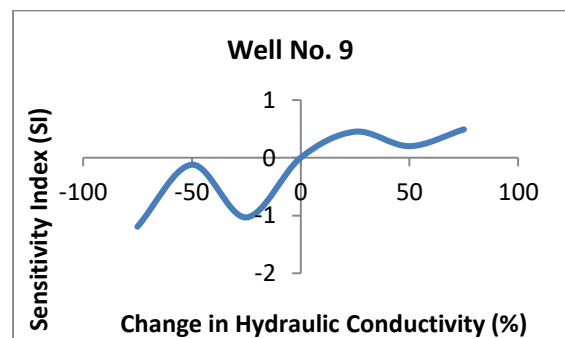
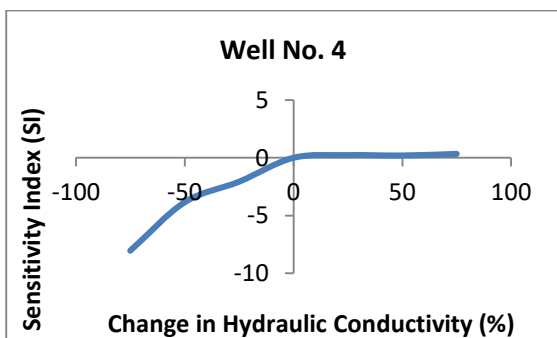
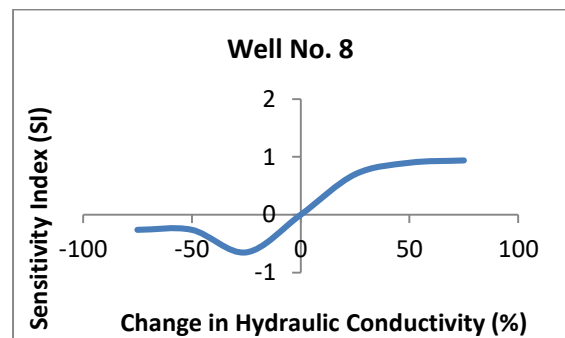
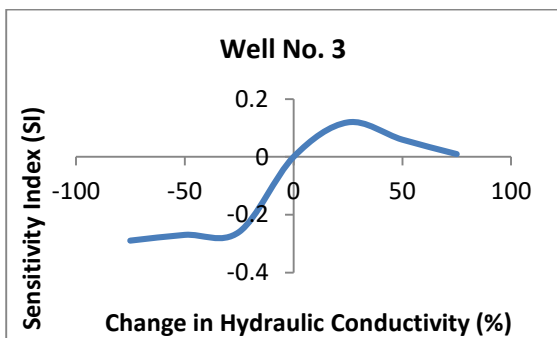
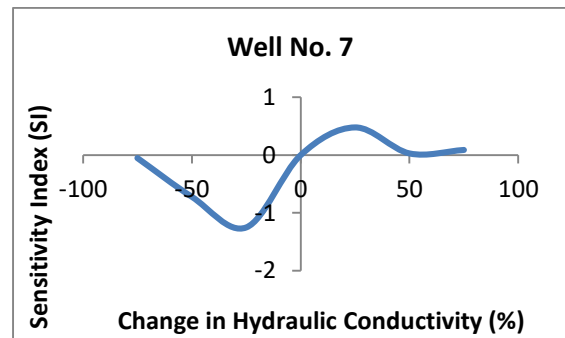
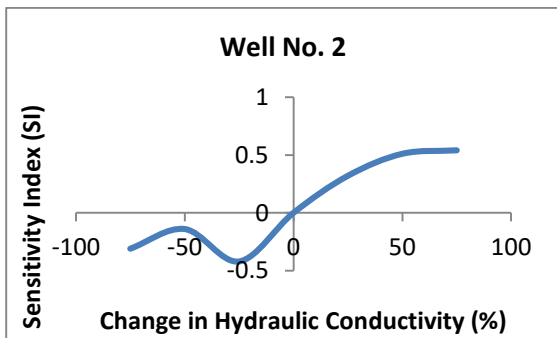
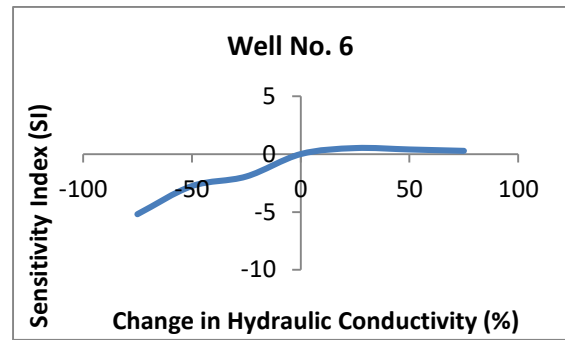
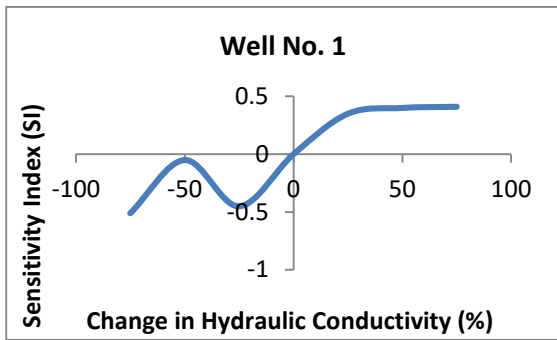
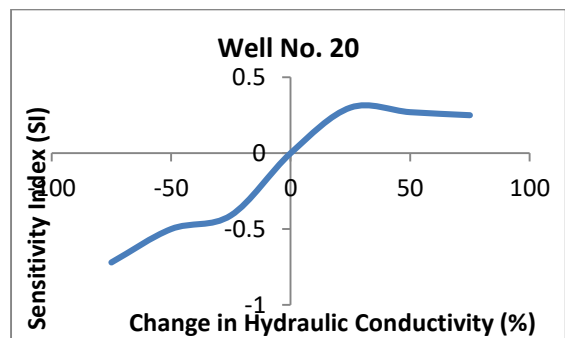
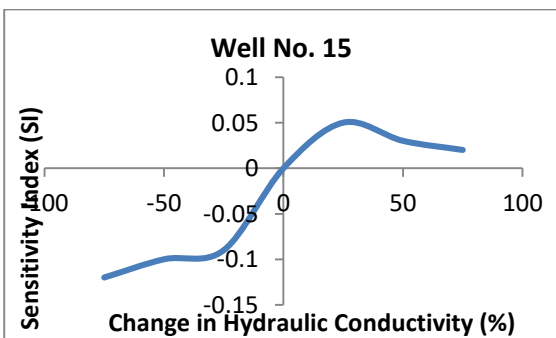
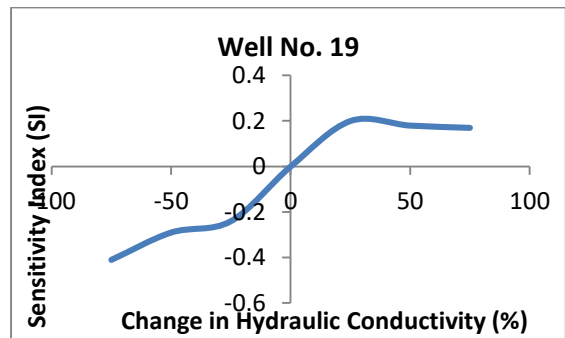
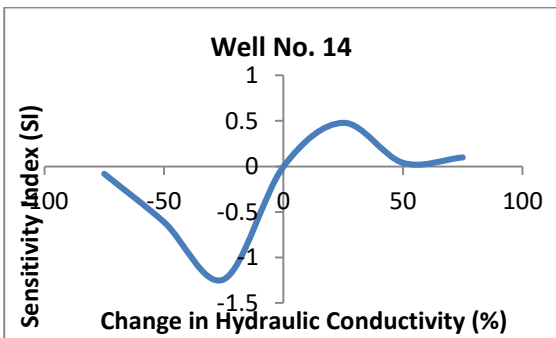
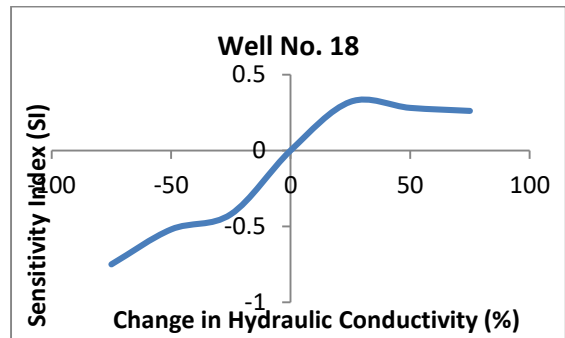
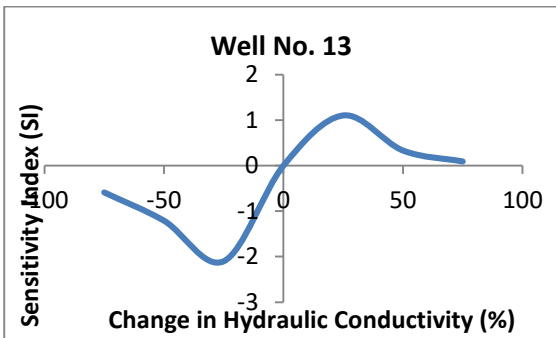
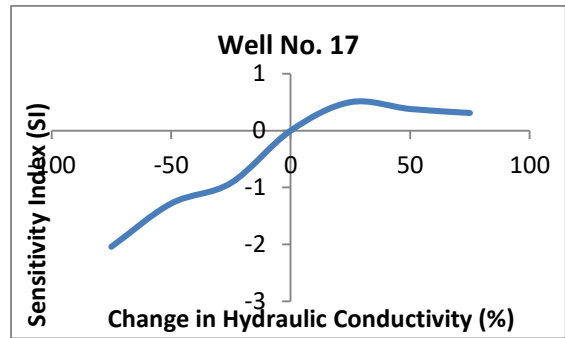
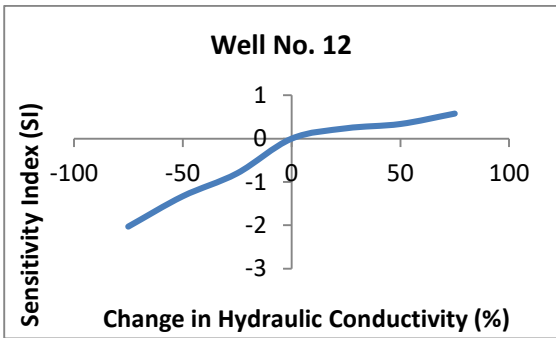
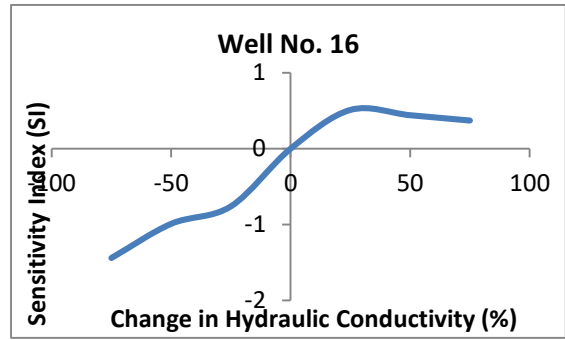
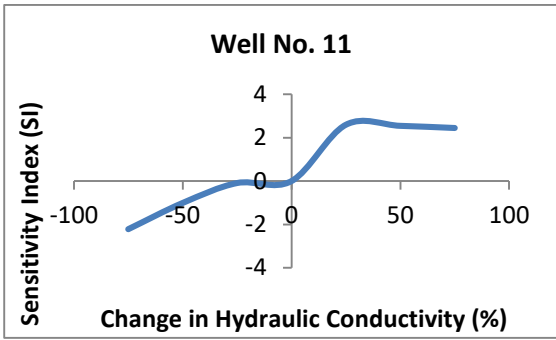


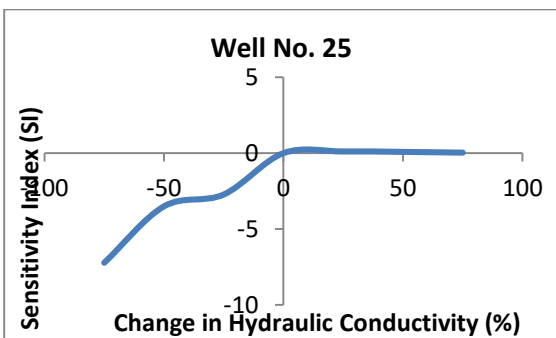
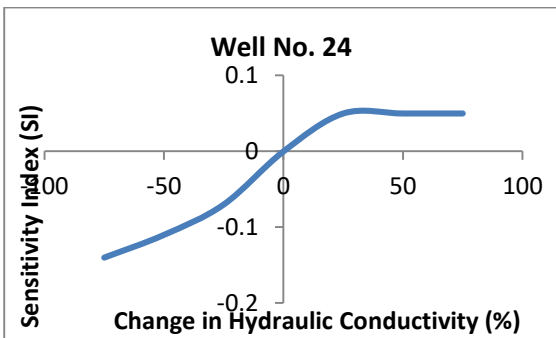
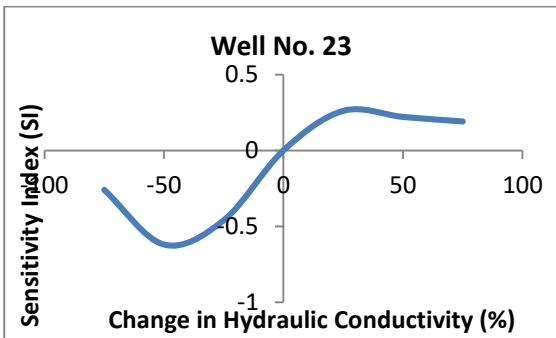
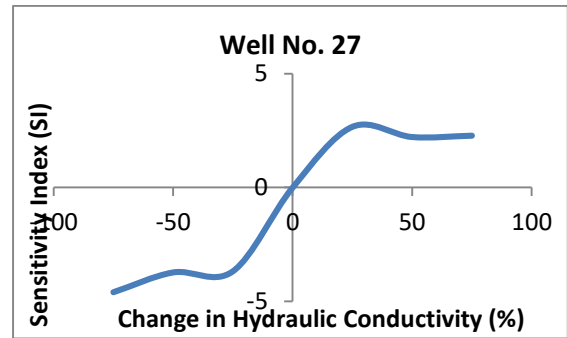
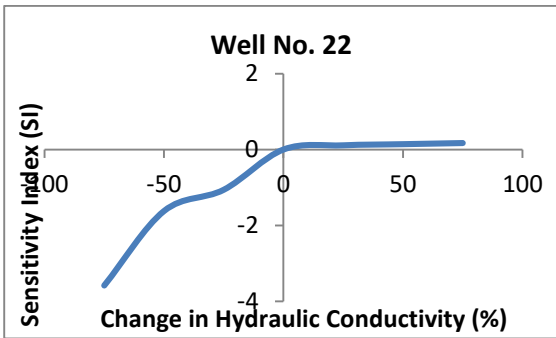
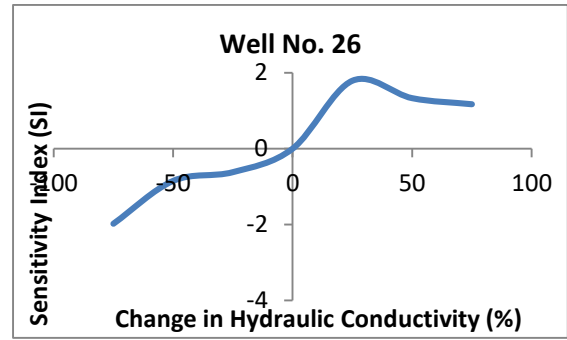
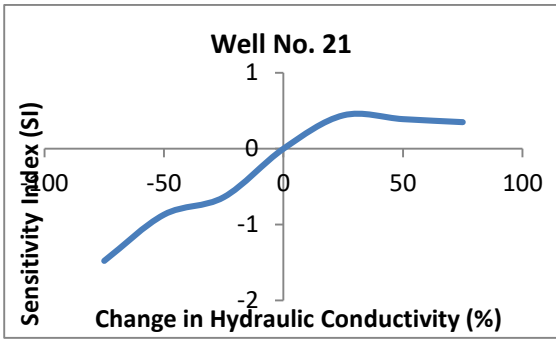
Fig.9. MODFLOW running Interface

APPENDIX IV: SENSITIVITY PLOTS :

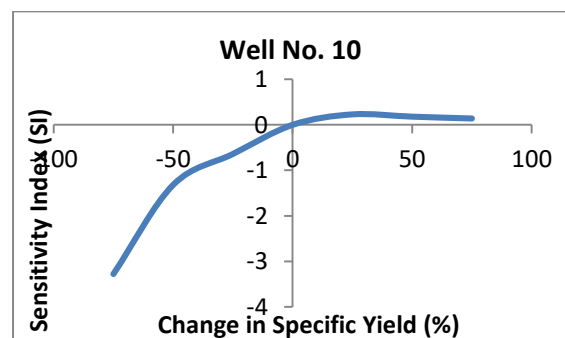
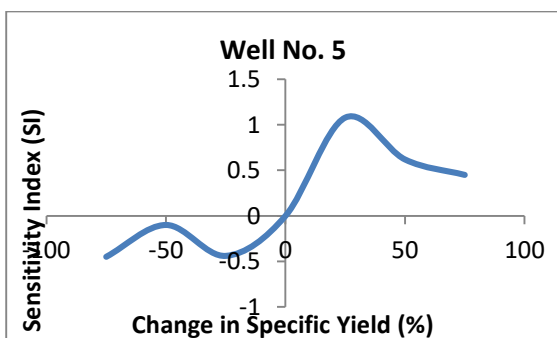
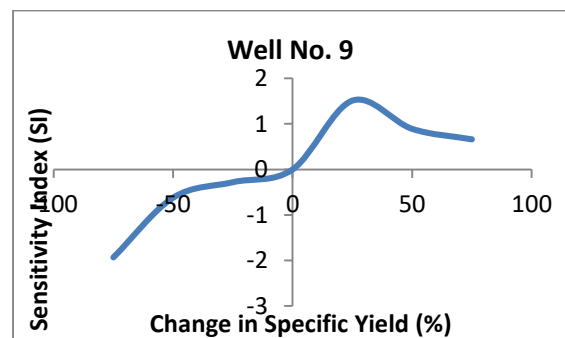
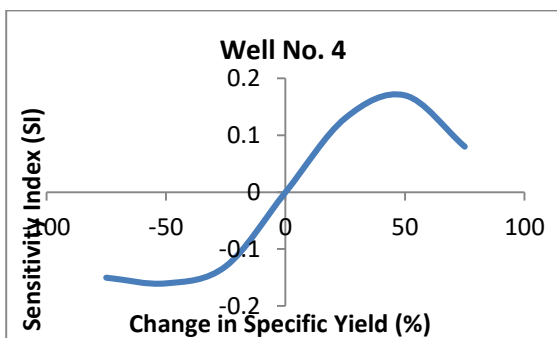
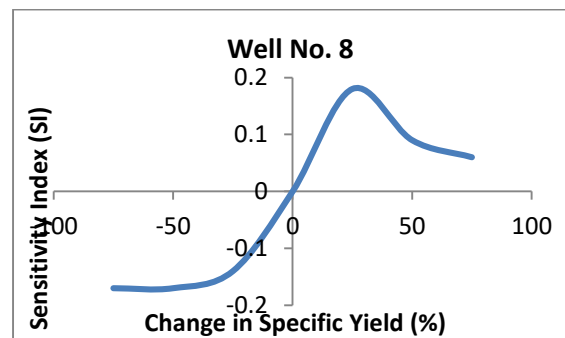
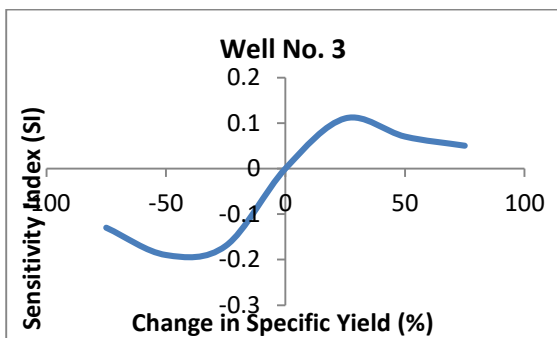
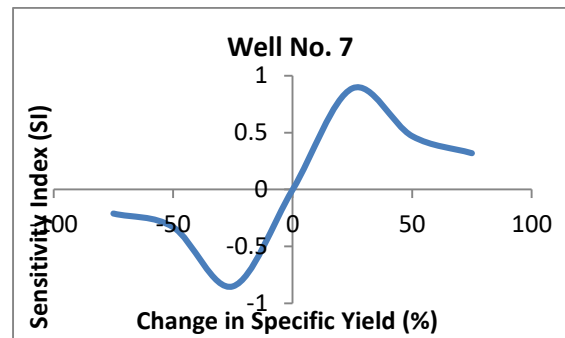
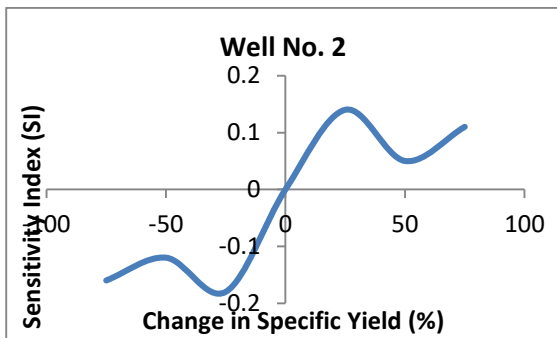
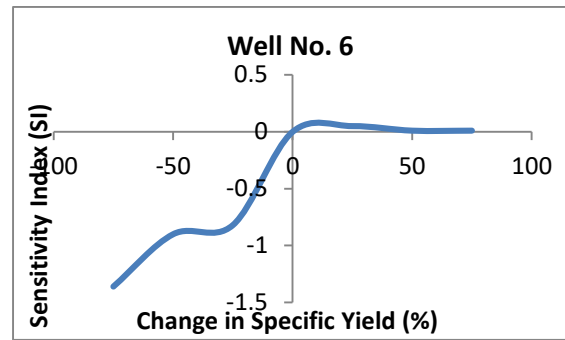
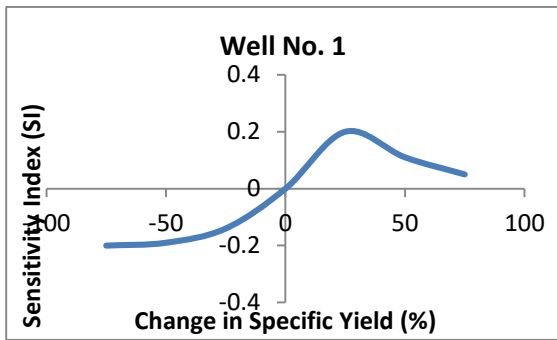
Hydraulic Conductivity

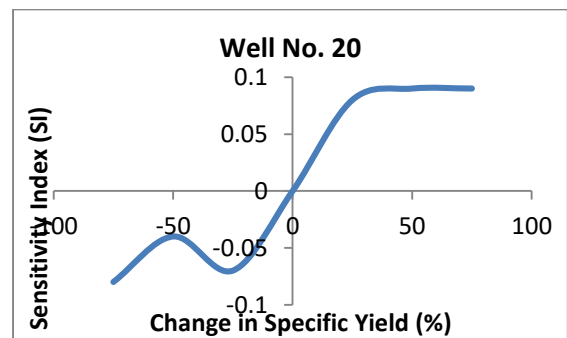
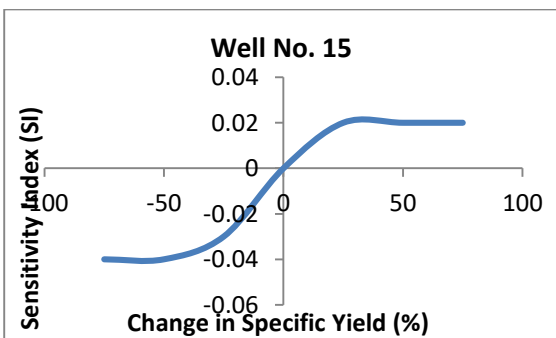
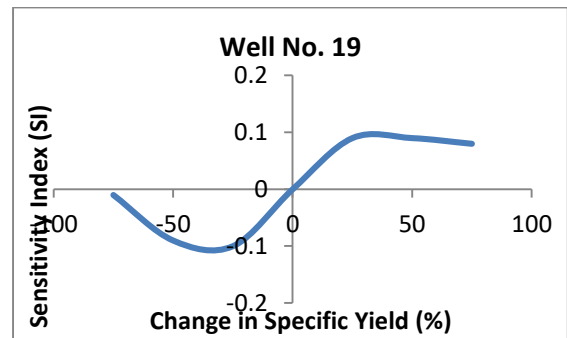
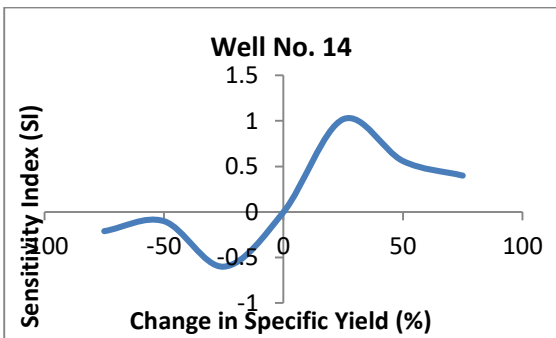
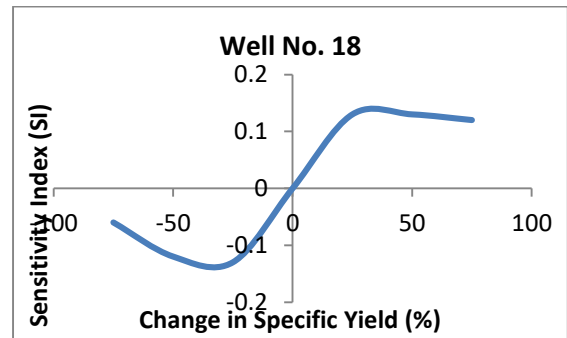
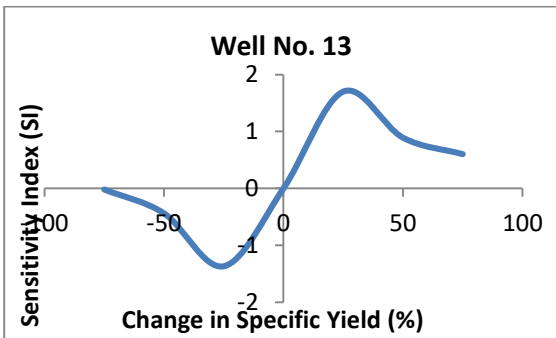
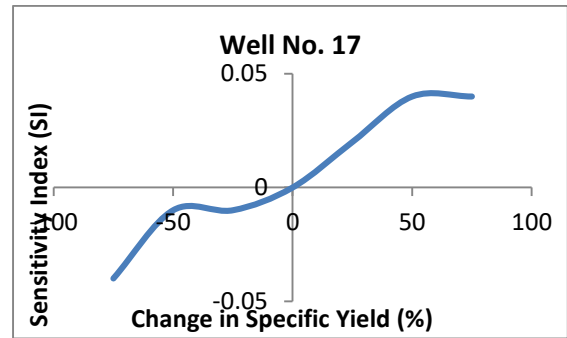
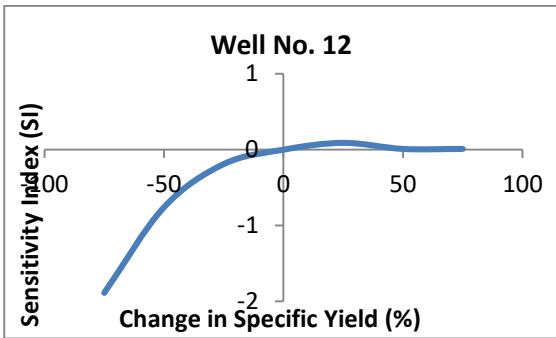
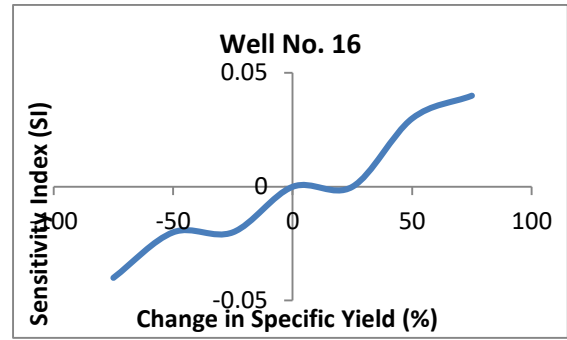
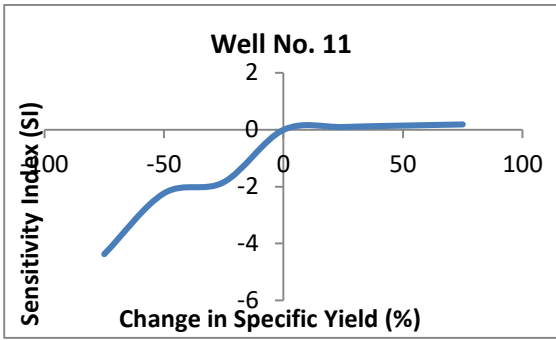


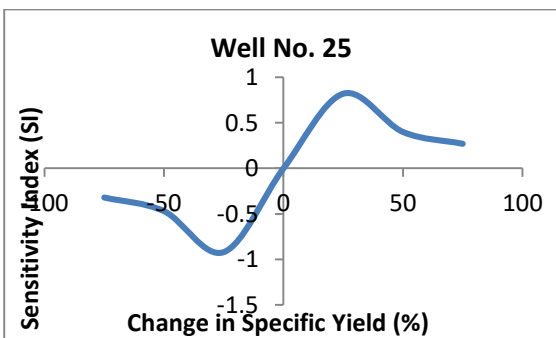
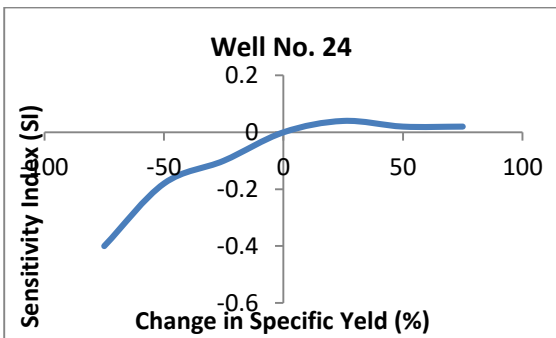
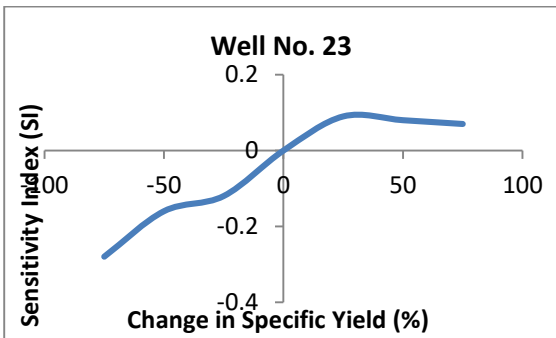
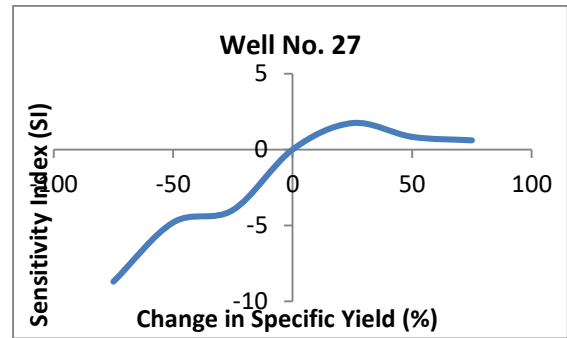
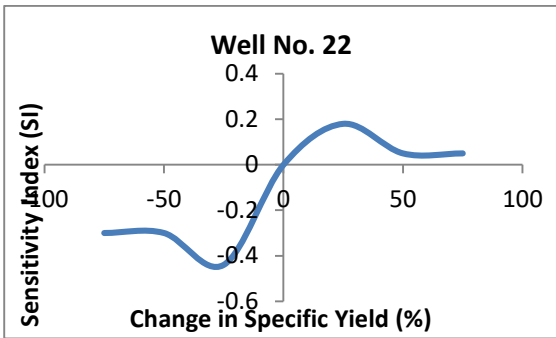
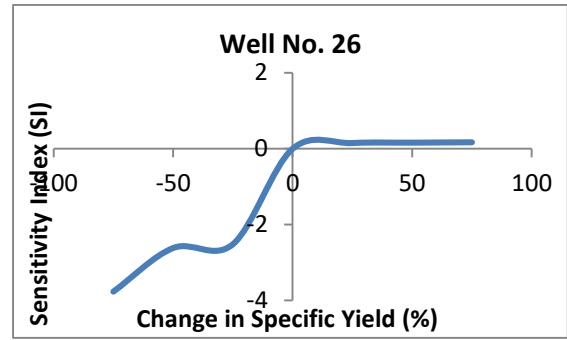
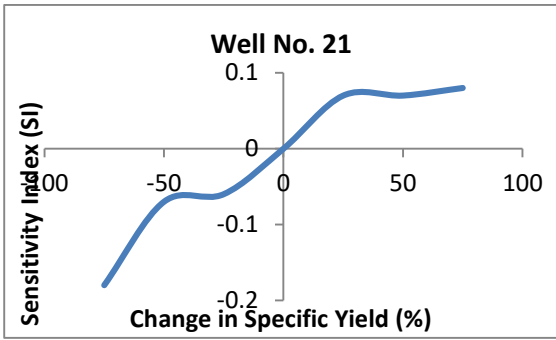




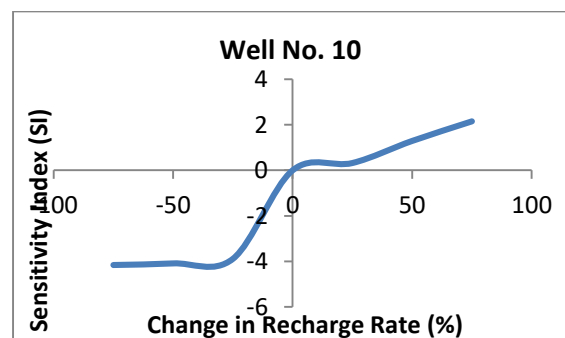
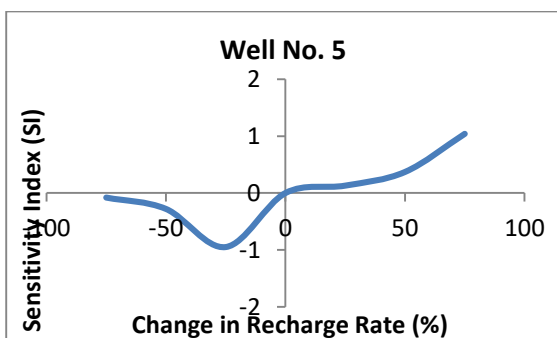
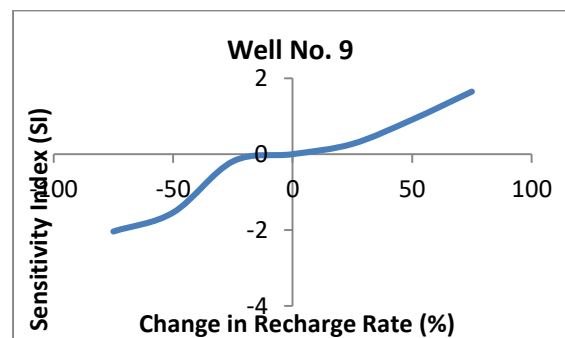
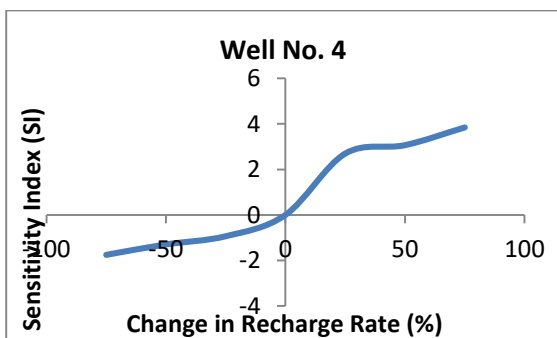
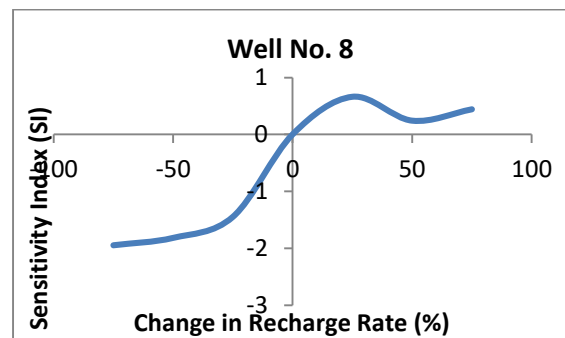
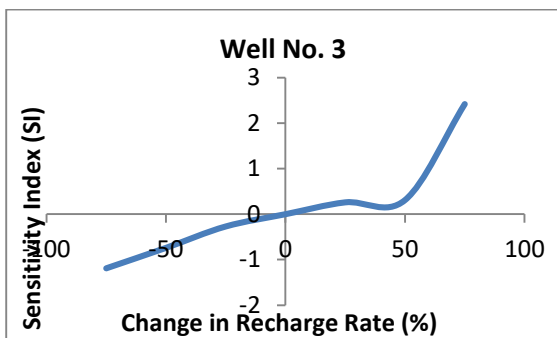
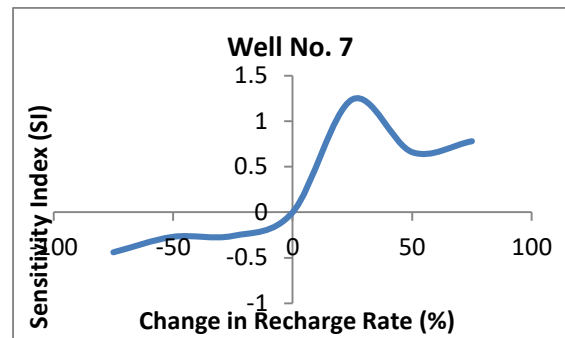
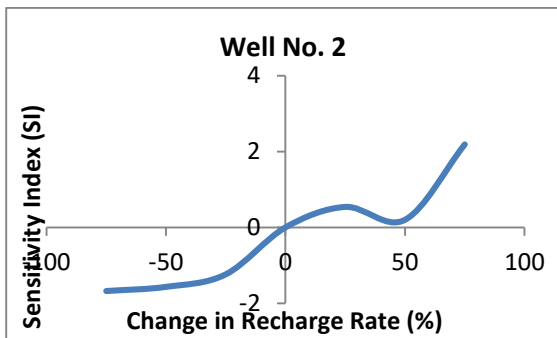
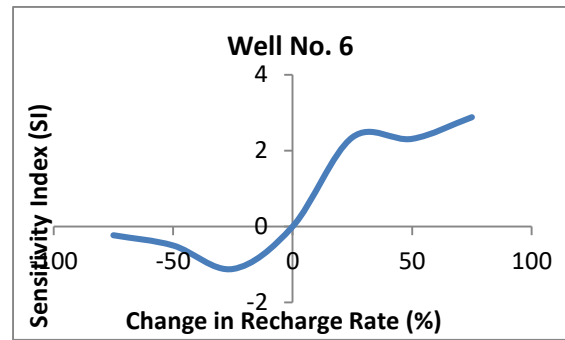
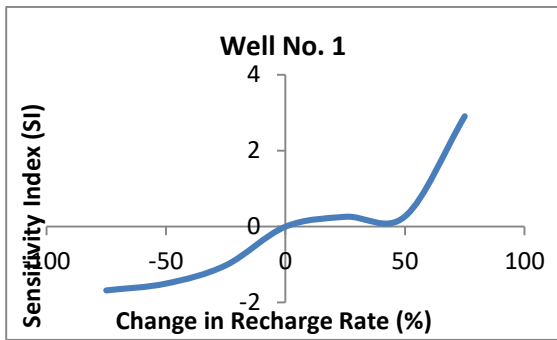
Specific Yield

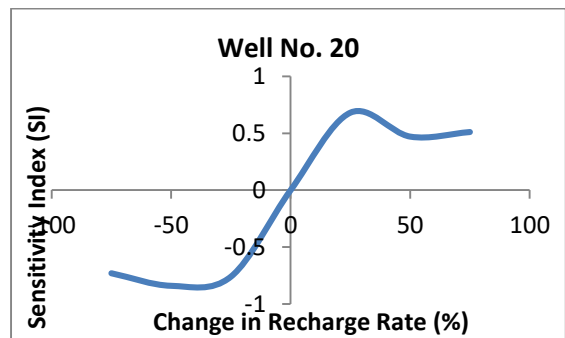
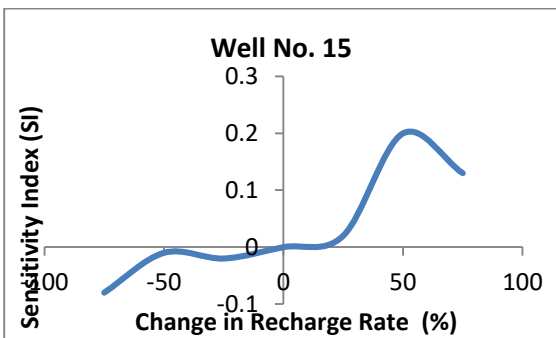
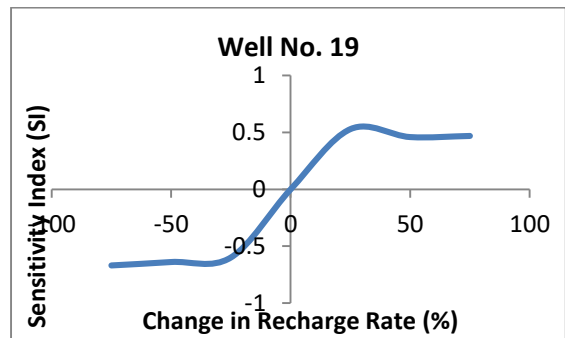
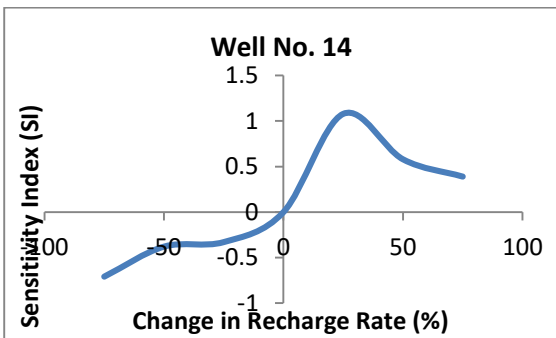
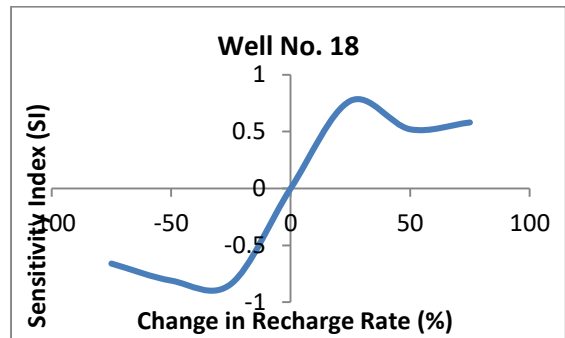
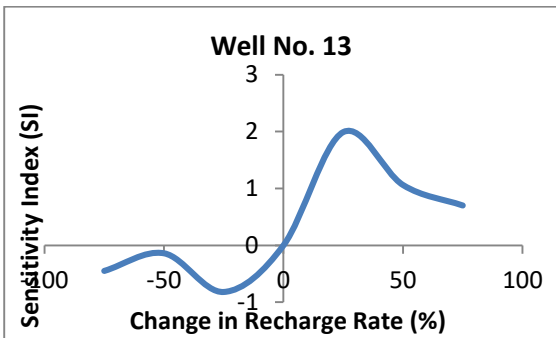
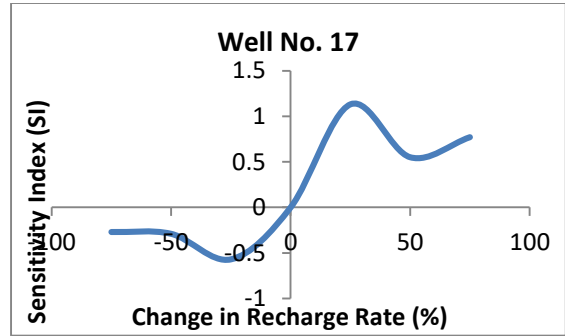
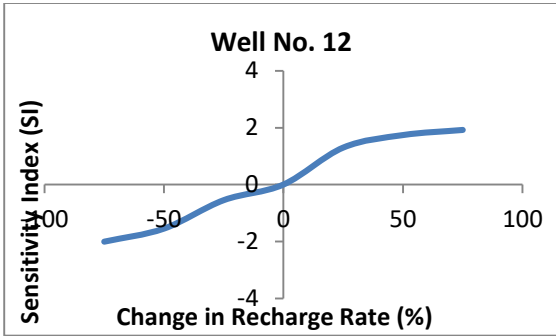
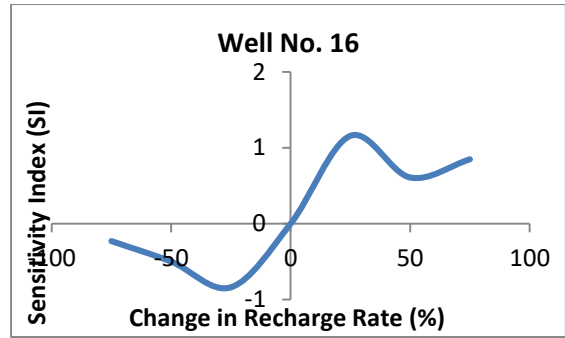
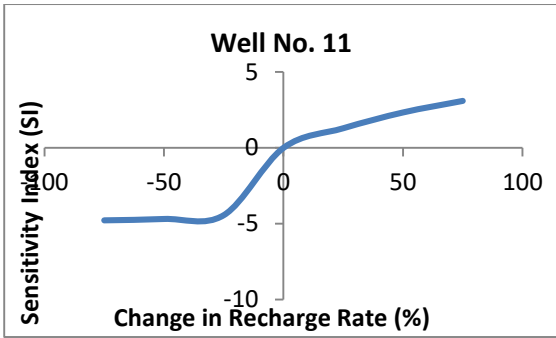


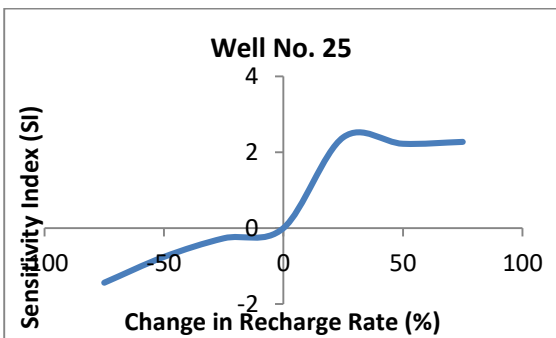
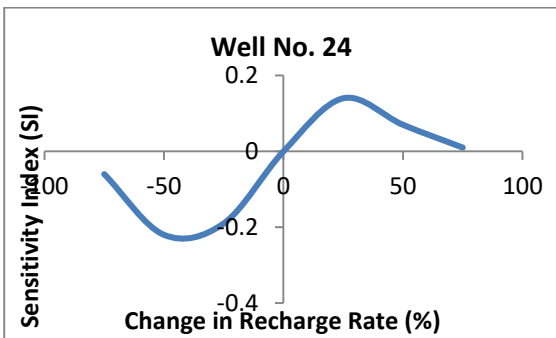
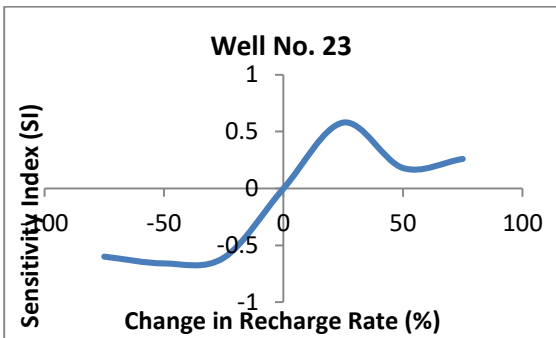
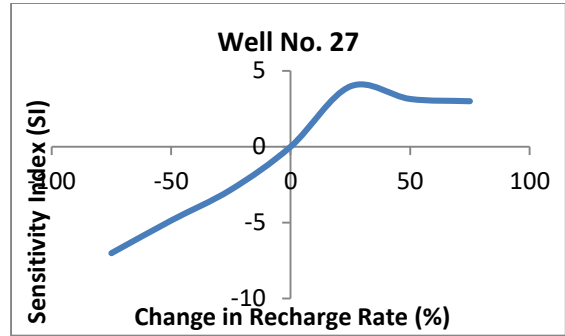
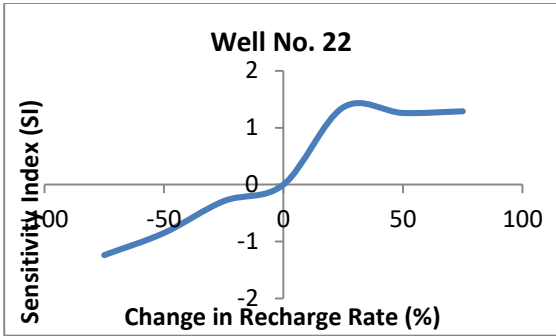
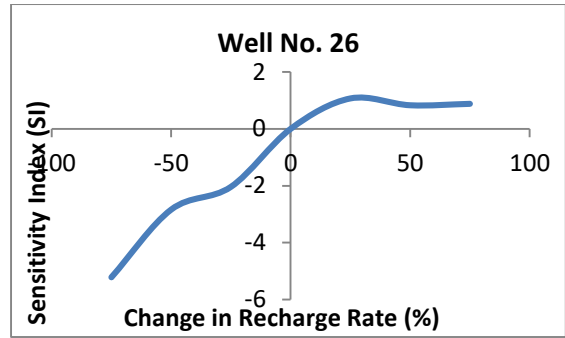
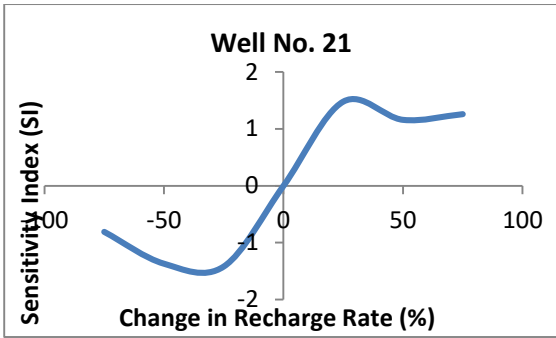




Recharge Rate







PUBLICATIONS

National Seminar

Subrahmanya K., Mahesha A. and Mohan A (2017), “Groundwater Modelling in and around Gurupura Wetlands of Dakshina Kannada District, Karnataka”,., National Seminar on “Biodiversity Conservation and Farming Systems for Wetland Ecology” (NSBC), at Regional Agricultural Research Station (RARS), Kumarakom, Kottayam, Kerala, during 22nd and 23rd February 2017, ISBN 978-81-921673-7-4, 179-180.

International Journal

Subrahmanya Kundapura and Amai Mahesha (2017), “Groundwater Flow and Transport Modelling around Gurupura Wetlands, Karnataka, India”, International Journal of Earth Sciences and Engineering (IJEE), Vol. 10 No. 3, ISSN 0974-5904, 38.

BIODATA

Name : SUBRAHMANYA KUNDAPURA

Date of birth : 28.04.1969

Address : Assistant Professor
Department of Applied Mechanics and Hydraulics
National Institute of Technology Karnataka (NITK)
Mangaluru – 575 025
Karnataka, INDIA.

Contact Number : (+91) 9448824343

Email : subrahmanyakundapura@nitk.ac.in
subrahmanyakundapura@gmail.com

Qualification : B. E. in Civil Engineering,
M. Tech. in Hydraulics and Water Resources Engg.

Publications : Journal: 1
National Seminar: 1